

# STUDIES ON CELLULOSE AND SILICA BASED SOLID ACID CATALYZED ORGANIC REACTIONS

*Thesis submitted to the Dibrugarh University for the  
award of the Degree of Doctor of Philosophy  
in Chemistry*



*Submitted by*

**Mrinaly Suri, M.Sc**

**Department of Chemistry  
Dibrugarh University  
Dibrugarh-786 004  
Assam  
2020**



**DEPARTMENT OF CHEMISTRY  
DIBRUGARH UNIVERSITY, DIBRUGARH  
ASSAM- 786004**

Date: 10/02/2021

**TO WHOM IT MAY CONCERN**

This is to certify that we have gone through the examiner's report on the Ph. D. thesis entitled "Studies on Cellulose and Silica based Solid Acid Catalyzed Organic Reactions" submitted by Mrinaly Suri, M.Sc., Department of Chemistry, Dibrugarh University along with the necessary corrections as suggested by the examiner. We also certify that Mrinaly Suri, has successfully done all necessary corrections as per suggestions of the examiner.

(Dr. Diganta Sarma)  
Chairperson, DRC  
Department of Chemistry  
Dibrugarh University  
Dibrugarh University

(Prof. Pankaj Das)  
Professor  
Supervisor  
Dept. of Chemistry  
Department of Chemistry  
Dibrugarh University  
Dibrugarh University

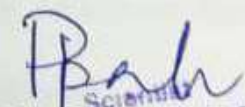
(Dr. Pallab Pahari)  
Scientist  
Supervisor  
CSIR North East Institute of Science & Technology  
Jorhat-785006, Assam  
CSIR-NEIST  
Jorhat

Date: 10/02/2021

Dr. Pallab Pahari  
Senior Scientist & Asstt. Prof. AcSIR, New Delhi  
Applied Organic Chemistry Group  
Chemical Sciences and Technology Division

### CERTIFICATE

This is to certify that the thesis entitled “**Studies on Cellulose and Silica based Solid Acid Catalyzed Organic Reactions**” submitted to the Department of Chemistry, Dibrugarh University for the degree of Doctor of Philosophy, is a record of original research work carried out by Mrinaly Suri, Chemical Sciences and Technology Division, CSIR-North East Institute of Science and Technology, Jorhat-785006, under the joint guidance of me and Prof. Pankaj Das, Department of Chemistry, Dibrugarh University. Ms. Suri is duly registered for Doctor of Philosophy degree of Dibrugarh University, w. e. f. 03-03-2016 vide Ref No. DU/DR-A/SB-SSE/16/1113 dated 30-08-2016. The thesis is an original work and had not been submitted before for any such degree anywhere. The candidate has complied with all the requirements as laid down in the regulations of the University.

  
Scientist  
(Dr. Pallab Pahari)  
CSIR-North East Institute of Science & Technology  
Jorhat-785006, Assam





DEPARTMENT OF CHEMISTRY  
Dibrugarh University, Dibrugarh- 786004  
Dibrugarh, Assam

Prof. Pankaj Das  
Professor

Ph: +91-9435394373  
Email: pankajdas@dibru.ac.in

Date: 10/02/2021

### CERTIFICATE

This is to certify that the thesis entitled “**Studies on Cellulose and Silica based Solid Acid Catalyzed Organic Reactions**” submitted to the Department of Chemistry, Dibrugarh University for the degree of Doctor of Philosophy, is a record of the original research work carried out by Ms. Mrinaly Suri, under the joint supervision and guidance of me and Dr. Pallab Pahari, Senior Scientist & Assistant Professor AcSIR, Chemical Sciences and Technology Division, CSIR-NEIST, Jorhat.

She has been duly registered for Doctor of Philosophy degree of Dibrugarh University, w. e. f. 03-03-2016 vide Ref No. DU/DR-A/SB-SSE/16/1113 dated 30-08-2016. The results embodied in this thesis had not been submitted before for any such degree anywhere. The candidate has complied with all the requirements for submitting the thesis as laid down in the regulations of Dibrugarh University. Moreover the thesis has been checked using anti-plagiarism software as per UGC guidelines.

(Prof. Pankaj Das)  
Professor  
Dept. of Chemistry  
Dibrugarh University



## Urkund Analysis Result

**Analysed Document:** Final Thesis of Mrinaly Suri2.docx (D76396930)  
**Submitted:** 7/15/2020 3:29:00 PM  
**Submitted By:** library@dibru.ac.in  
**Significance:** 0 %

Sources included in the report:

Instances where selected sources appear:

0

*LS*  
7/15/2020  
Deputy Librarian  
L. N. B. Library  
Dibrugarh University



Dibrugarh University, Dibrugarh

LNB Library, DU  
Date: 15/07/2020

Plagiarism Verification

Title of the Thesis: Studies on Cellulose and Silica based Solid Acid Catalyzed Organic Reactions.....

Page: 210.....

Researcher: Ms. Mrinaly Suri.....

Supervisors: Dr. Pankaj Das, Professor, Department of Chemistry, Dibrugarh University and Dr. Pallab Pahari, Senior Scientist, Chemical Science and Technology Division, CSIR-NEIST, Jorhat.....

Department: Department of Chemistry.....

Institution: Dibrugarh University, Dibrugarh.....

This is to report that the above thesis was scanned for similarity detection excluding bibliography and references. Process and outcome is given below:


Software used: URKUND..... Date: 15-07-2020.....

Similarity Index: 0%..... Total word count.....

The complete report is submitted for review by the Supervisor/ HOD.

Checked by

Date: 15-07-2020  
Place: Dibrugarh

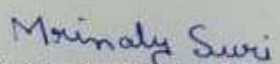
  
(Signature)  
Deputy Librarian &  
University Coordinator

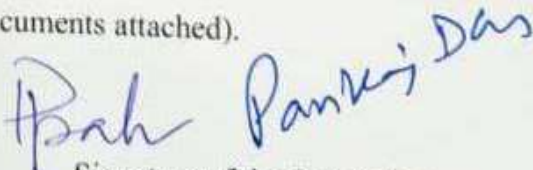
The complete report of the above thesis has been reviewed by the undersigned.  
(Tick Check Box)

- The similarity index is within the accepted norms.
- The similarity index is above accepted norms, because of the following reasons:

- 1.....
- 2.....
- 3.....
- 4.....
- 5.....

The thesis may be considered for the award of degree. (Relevant documents attached).

  
Signature of the Student

  
Signature of the Supervisor

Scientist  
CSIR-North East Institute of Science & Technology  
Jorhat-785006, Assam

Professor  
Dept. of Chemistry  
Dibrugarh University



**Dibrugarh University, Dibrugarh**

**Department of Chemistry**

Date: 10/02/2021

## **Certificate of Originality**

The research work embodied in this thesis entitled "**Studies on Cellulose and Silica based Solid Acid Catalyzed Organic Reactions**" has been carried out by me at the Department of Chemistry, Dibrugarh University, Dibrugarh, Assam, India. The manuscript has been subjected to plagiarism check by URKUND software. The work submitted for consideration of award of Ph.D. is original.

*Moinaly Sawai*

**Name and Signature of the Candidate**





## Dibrugarh University, Dibrugarh

Department of Chemistry

Date: 10/02/2021

### Student Approval Form

Name of the Author	Mrinaly Suri
Department	Chemistry
Degree	M.Sc.
University	Dibrugarh University
Guide(s)	Dr. Pallab Pahari, Prof. Pankaj Das
Thesis Title	Studies on Cellulose and Silica based Solid Acid Catalyzed Organic Reactions
Year of Submission	2020

### Agreement

1. I hereby certify that, if appropriate, I have obtained and attached hereto a written permission/statement from the owner(s) of each third party copyrighted matter to be included in my thesis/dissertation.

2. I hereby grant to Dibrugarh University and its agents the non-exclusive license to archive and make accessible my thesis/dissertation, in whole or in part in all forms of media, now or hereafter known. I retain all other ownership rights to the copyright of the thesis/dissertation. I also retain the right to use in future works (such as articles or books) all or part of this thesis, dissertation, or project report.

*Mrinaly Suri*  
Signature of the Scholar

Place: Dibrugarh University

Date: 10/02/2021

*Pankaj Das*  
Signature and seal of the Guide(s)  
Professor  
Dept. of Chemistry  
Dibrugarh University  
CSIR-North East Institute of Science & Technol  
Jorhat-785006, Assam  
Date: 10/02/2021



Dibrugarh University, Dibrugarh

Department of Chemistry

Date: 10/02/2021

Self Plagiarism Exclusion Certificate from Supervisor

The content of the chapters of the thesis entitled "Studies on Cellulose and Silica based Solid Acid Catalyzed Organic Reactions" have been published as mentioned below:

Sl. No.	Title of the Article /Chapter	Name of the Journal/Book	Publisher	Vol. & Issue No./ISSN/ SBN
1	Magnetically recoverable silica catalysed solvent-free domino Knoevenagel-hetero-Diels-Alder reaction to access divergent chromenones	Organic & Biomolecular Chemistry	Royal Society of Chemistry	18 & 1477-0539

These published works have been included in the thesis and have not been submitted for any degree to any University/Institute.

Moinaly Sui  
Signature of the Candidate  
Place: Dibrugarh University  
Date: 10/02/2021

Pankaj Das  
Professor  
Dept. of Chemistry  
Dibrugarh University  
Signature of Supervisor  
Place: Dibrugarh University  
Date: 10/02/2021  
Scientist  
East Institute of Science & Techno  
Jorhat-785006, Assam



Dibrugarh University, Dibrugarh

Department of Chemistry

Date: 10/02/2021

Self Plagiarism Co-authors Certificate

We have published the following articles/chapters jointly:

Sl. No	Title of the Article/Chapter	Name of the Journal/Book	Publisher	Vol. & Issue No./ISSN/ISBN
1	Magnetically recoverable silica catalysed solvent-free domino Knoevenagel-hetero-Diels-Alder reaction to access divergent chromenones	Organic & Biomolecular Chemistry	Royal Society of Chemistry	18 & 1477-0539

We give our consent to **Mrinaly Suri** to make use of these articles for her Ph. D. research.

The above research paper (s) has not been used by any of us for any Degree / Diploma in any other University.

We shall be responsible for any legal dispute/ case(s) for violation of any provisions of the Copy Right Act.

*Pankaj Das*

Signature of Co-author

Name: Pankaj Das

Address Dept. of Chemistry

Dibrugarh University

Phone: 9435394373

*Pallab*

Signature of Co-author

Name: Pallab Pahari

Address CSIR-NEIST

Jorhat, Assam

Phone: 8486963591

*Chinu Gogoi*

Signature of Co-author

Name: Chinu Gogoi

Address CSIR-NEIST

Jorhat, Assam

Phone: 8638260748

*F. L. Hussain*

Signature of Co-author

Name: Farhaz Liaquat Hussain

Address CSIR-NEIST

Jorhat, Assam

Phone: 8011131180

*Mrinaly Suri*  
Signature of Candidate

Name: Mrinaly Suri

Registration No. 10012962





**Dibrugarh University, Dibrugarh**

**Department of Chemistry**

Date: 10/02/2021

## **Certificate of Originality**

The research work embodied in this thesis entitled "**Studies on Cellulose and Silica based Solid Acid Catalyzed Organic Reactions**" has been carried out by me at the Department of Chemistry, Dibrugarh University, Dibrugarh, Assam, India. The manuscript has been subjected to plagiarism check by URKUND software. The work submitted for consideration of award of Ph.D. is original.

*Moinaly Sawri*

**Name and Signature of the Candidate**

## Acknowledgements

At the very outset, I would like to express my deepest gratitude and sincere thanks to my esteemed supervisors Dr. Pallab Pahari, Senior Scientist, Chemical Science and Technology Division, CSIR-NEIST, Jorhat, and Prof. Pankaj Das, Professor, Department of Chemistry, Dibrugarh University, Dibrugarh, for their constant support, guidance and encouragement throughout the course of my research work. Their positive criticism and tireless enthusiasm helped me to successfully complete my Ph. D. work without any obstruction. Words are not enough to thank them for all the concern they have bestowed upon me. I will forever remain grateful to them for their wonderful personality, friendly approach and valuable guidance.

I would like to thank the Directors of CSIR-NEIST, Jorhat, Dr. D. Ramaiah (Retd.) and Dr. G. N. Sastry, for providing all the infrastructural facilities to accomplish my research work. I wish to acknowledge the financial supports from CSIR, New Delhi.

I convey my heartfelt gratitude and special acknowledgement to Dr. Diganta Sarma, Dr. (Mrs) Geetika Borah, Dr. P. K. Gogoi, Dr. (Mrs) J. G. Handique, Dr. B. Chetia, Dr. Rahul Kar and all the other faculty members of the Chemistry Department, Dibrugarh University, Dibrugarh who inspired me and laid the foundation for me to pursue higher studies and their kind cooperation during my research tenure.

I would like to offer my sincere thanks to Dr. Amrit Goswami (Retd.), Dr. Dilip Konwar (Retd.), Dr. Tridip Goswami (Retd.), Dr. Ashutosh Namdeo and Dr. A. K. Singh for their guidance, help and constructive suggestions during my Ph. D. tenure.

My research work achieves completion by sincere analytical help from Dr. P. J. Saikia, Mr. Gaurav Kumar Rastogi, Mr. Jayanta Boruah and Dr. Ankana Phukan. I would also like to acknowledge the staff of Library section and Glass blowing section for their valuable help.

I acknowledge the suggestion and help rendered by the staff of our division, Mr. R. N. Das (Retd.), Mr. D. Borah and Mr. R. Borah.

I convey my heartiest thanks and gratitude to my labmates Dr. Ujwal Pratim Saikia, Dr. Diganta Baruah, Dr. Farhaz Liaquat Hussain, Anamika Bora, Chinu Gogoi and Trishna Saikia for their indispensable help, encouraging words and ideas which made my Ph. D. period enjoyable. My sincere thanks goes to Mr. M. J. Borah, Banani, Sateesh, Kashyap, Dr. Leema Dutta, Priyanka, Alpana, Pompei, Anup, Sumi, Dhiraj, Kashmiri, Kumud, Hemanta, Abhilash, Uma and Dhurba for their unconditional help and inspiration. I would also like to extend my heartiest appreciation to all the scientists, staff members and research scholars of CSTD, NEIST for their help and kind cooperation.

I would like to acknowledge the constant support and encouragement of my friends Dr. Manash Konwar, Munmee, Amlan, Dr. Shankar Jyoti Borah, Gyanashree, Atish, Jutika, Diganta, Dipjyoti, Apurba and Anirban.

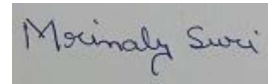


Finally, I extend my love and gratitude to my parents, brothers, sister-in-law and all the family members for their moral support, love and affection. I don't know whether it is possible to convey my deepest love and gratitude to my beloved parents in mere words, who were always there to inspire and support me, and without whose personal sacrifices, it would not have been possible for me to carry out my Ph. D. work.

Finally, I must acknowledge that this thesis has seen the light of the day only by the Grace of ALMIGHTY.

Date: 10/02/2021

Place: Dibrugarh University

A rectangular box containing a handwritten signature in cursive script that reads "Mrinaly Suri".

Mrinaly Suri

# Contents

*Acknowledgements*

*List of symbols/abbreviations/acronyms*

*Experimental remarks*

*Graphical abstract*

	<b>Page No.</b>
<b>Chapter 1: Introduction</b>	<b>1-58</b>
1.1 Overview	1-4
1.2 Solid acid catalyst	4-9
1.3 Nano-materials in solid acid catalysis	9-10
1.4 Supported solid acid catalysts	10-23
1.4.1 Silica supported solid acid catalysts	10-13
1.4.2 Alumina/silica-alumina supported solid acid catalyst	14-16
1.4.3 Zeolite supported solid acid catalyst	16-18
1.4.4 Carbon supported solid acid catalyst	18-20
1.4.5 Biopolymer supported solid acid catalyst	20-21
1.4.6 Clay supported solid acid catalyst	21-22
1.4.7 Ion-exchange resin supported solid acid catalyst	22-23
1.5 Sulfonic acid derivatives as solid acid catalyst	23-26
1.6 Magnetic solid acid catalyst	26-30
1.7 Synthesis of nanostructured solid acid catalyst	30-35
1.7.1 Co-precipitation	31-32
1.7.2 Impregnation	32-32
1.7.3 Hydrothermal	33-33

1.7.4 Sol-Gel synthesis	34-35
1.7.5 Electrochemical reduction	35-35
1.7.6 Mechanical grinding	35-35
1.8 Industrial applications of solid acid catalysts	36-41
1.9 Objective and scope of the work	41-43
1.10 References	44-58

**Chapter 2 : Synthesis of silica-supported copper oxide nanoparticles and its application in the synthesis of dihydroquinazoline and hydroxymethyl furfural (HMF) 59-114**

2.1 Introduction	59-64
2.2 Results and discussion	65-89
2.2.1 Preparation and characterization of copper oxide supported on silica (CuO@SiO <sub>2</sub> )	65-73
2.2.2 Catalytic activity of the prepared CuO@SiO <sub>2</sub> catalyst towards the synthesis of 1,2-dihydroquinazolines	73-79
2.2.3 Study of catalyst recyclability	79-82
2.2.4 Study of antibacterial activity of the synthesized dihydroquinazolines	82-83
2.2.5 Catalytic activity of the prepared CuO@SiO <sub>2</sub> towards the conversion of carbohydrates into 5-hydroxymethylfurfural (HMF)	83-88
2.2.6 Study of catalyst recyclability	88-89
2.3 Conclusion	89-90
2.4 Experimental	90-93
2.4.1 Preparation of copper oxide supported on silica (CuO@SiO <sub>2</sub> ) nanoparticles	90-91
2.4.2 General procedure for the synthesis of 1,2-dihydroquinazolines	91-91

2.4.3	General procedure for the determination of MIC of the synthesized 1,2-dihydroquinazolines	91-92
2.4.4	General procedure for the synthesis of HMF	92-93
2.5	Characterization data of the synthesized compounds	93-106
2.6	References	107-114
2.7	NMR spectra of selected compounds	

<b>Chapter 3 : Magnetically active silica catalysed solvent-free domino Knoevenagel-hetero-Diels-Alder reaction: An easy access to divergent chromenones / dihydrochromenones / spirochromenones</b>		
		<b>115-160</b>
3.1	Introduction	115-121
3.2	Results and discussion	121-134
3.2.1	Synthesis and characterization of Fe <sub>3</sub> O <sub>4</sub> @SiO <sub>2</sub> catalyst	121-127
3.2.2	Catalytic activity of the prepared Fe <sub>3</sub> O <sub>4</sub> @SiO <sub>2</sub> nanoparticles towards the synthesis of chromenones	127-133
3.2.3	Study of catalyst recyclability	133-134
3.3	Conclusion	135-135
3.4	Experimental	135-136
3.4.1	Preparation of silica-supported iron oxide (Fe <sub>3</sub> O <sub>4</sub> @SiO <sub>2</sub> ) catalyst	135-136
3.4.2	General procedure for the synthesis of chromenone/spirochromenone	136-136
3.5	Characterization data of the synthesized compounds	137-154
3.6	References	155-160
3.7	NMR spectra of selected compounds	

<b>Chapter 4 : Synthesis of cellulose-supported copper nanoparticles and its application in synthesis of 1,2,3-triazole</b>	<b>161-210</b>
4.1 Introduction	161-166
4.2 Results and discussion	166-180
4.2.1 Preparation and characterization of cellulose-supported copper (Cell-Cu(0)) nanoparticles	166-171
4.2.2 Catalytic activity of the prepared Cell-Cu(0) nanoparticles towards the azide-alkyne click reaction	171-178
4.2.3 Study of catalyst recyclability	179-180
4.3 Conclusion	181-181
4.4 Experimental	181-184
4.4.1 Preparation of cellulose-supported copper (Cell-Cu(0)) nanoparticles	181-182
4.4.1.1 Preparation of cellulose sulfuric acid	181-182
4.4.1.2 Preparation of cellulose-supported copper(0) nanoparticles (Cell-Cu(0) NPs)	182-182
4.4.2 General procedure for the synthesis of 1,2,3-triazoles <i>via</i> azide-alkyne click reaction	182-183
4.4.3 General procedure for the synthesis of 1,2,3-triazoles <i>via</i> diazo transfer click reaction	183-184
4.5 Characterization data of the synthesized compounds	184-200
4.6 References	201-210
4.7 NMR spectra of selected compounds	
<b>Chapter 5 : Conclusion and future scope</b>	<b>211-214</b>
5.1 Conclusion	211-213
5.2 Future Scope	213-214
<b>Appendix I : List of Publications</b>	
<b>Appendix II : Reprints of published paper (First page)</b>	



## List of symbols/abbreviations/acronyms

<b>AAS</b>	Atomic Absorption Spectroscopy
<b>BET</b>	Braunauer-Emmett-Teller
<b>CDCl<sub>3</sub></b>	Deuterated chloroform
<b><sup>13</sup>C</b>	Carbon-13
<b>δ</b>	Chemical shift
<b>°C</b>	Degree centigrade
<b>cm<sup>-1</sup></b>	Reciprocal centimeters
<b>d</b>	Doublet
<b>DCM</b>	1,2-Dichloromethane
<b>dd</b>	Doublets of doublet
<b>dt</b>	Doublets of triplet
<b>DMAP</b>	4-( <i>N,N</i> -Dimethylamino)pyridine
<b>DMSO</b>	Dimethylsulfoxide
<b>DMF</b>	Dimethylformamide
<b>eV</b>	Electron volt
<b>EDX</b>	Energy dispersive X-ray spectroscopy

<b>FT-IR</b>	Fourier Transform Infra-Red
<b>g</b>	Gram
<b><sup>1</sup>H</b>	Proton
<b>h</b>	Hour
<b>Hz</b>	Hertz
<b>HR-TEM</b>	High resolution transmission electron microscopy
<b>HRMS</b>	High resolution mass spectrometry
<b>HPLC</b>	High-performance liquid chromatography
<b>HMF</b>	5-Hydroxymethylfurfural
<b><i>J</i></b>	Coupling constant
<b>lit.</b>	Literature
<b>m</b>	Multiplet
<b>mg</b>	Milligram
<b>MIPK</b>	Methyl isopropyl ketone
<b>MHz</b>	Megahertz
<b>μg</b>	Microgram
<b>μL</b>	Microlitre

<b>mL</b>	Millilitre
<b>mmol</b>	Millimole
<b>MIC</b>	Minimum inhibitory concentration
<b>Mp</b>	Melting point
<b>MSA</b>	Meglumine sulfonic acid
<b>nm</b>	Nanometer
<b>NPs</b>	Nanoparticles
<b>N</b>	Normality
<b>NMR</b>	Nuclear Magnetic Resonance
<b>PPA</b>	Polyphosphoric acid
<b>q</b>	Quartet
<b>rt</b>	Room temperature
<b>s</b>	Singlet
<b>SAED</b>	Selected Area Electron Diffraction
<b>SD</b>	Standard deviation
<b>D<sub>s</sub></b>	Surface-weighted diameter
<b>SSA</b>	Specific surface area
<b>t</b>	Triplet

<b>TEM</b>	Transmission Electron Microscopy
<b>THF</b>	Tetrahydrofuran
<b>TLC</b>	Thin Layer Chromatography
<b>TOF</b>	Turn over frequency
<b>TGA</b>	Thermogravimetric analysis
<b>VSM</b>	Vibrating sample magnetometer
<b>D<sub>v</sub></b>	Volume-weighted diameter
<b>wt</b>	Weight
<b>XRD</b>	X-ray Diffraction
<b>XPS</b>	X-ray photoelectron spectroscopy



## Experimental remarks

- ❖ All the chemicals were purchased from Sigma Aldrich, Merck, SRL and Spectrochem, and used without further purification. Distilled water was used throughout the experiments.
- ❖ Progress of the reactions carried out was followed by thin-layer chromatography (TLC) with the help of aluminium-backed silica gel F<sub>254</sub> plates. Purification of the compounds was carried out using column chromatography technique with the help of silica gel 60-120.
- ❖ All the solvents like petroleum ether (60–80 °C), ethyl acetate, acetone, chloroform, acetonitrile, dichloromethane, dimethylformamide, methanol, ethanol, toluene etc. were distilled off under nitrogen atmosphere prior to use.
- ❖ Silica gel (60-120 mesh) and TLC Silica gel F<sub>254</sub> for chromatographic separation of the compounds were purchased from MERCK, Germany.
  - Visualization of spots on TLC plates were achieved either *via* treatment with KMnO<sub>4</sub> or under UV illumination.
  - Reaction products were purified by either gravity column chromatography over silica gel and radial chromatography using plates coated with silica gel.
- ❖ The powder XRD measurements were carried out by using a 2-80° 2θ on a Rigaku Ultima IV X-ray diffractometer with CuKα source ( $\lambda = 1.54056 \text{ \AA}$ ). In built program

‘XG operation RINT 2200’ associated with the XRD was used to process the data and ‘Rigaku PDXL 1.2.0.1’ library database was used for identification of the peaks.

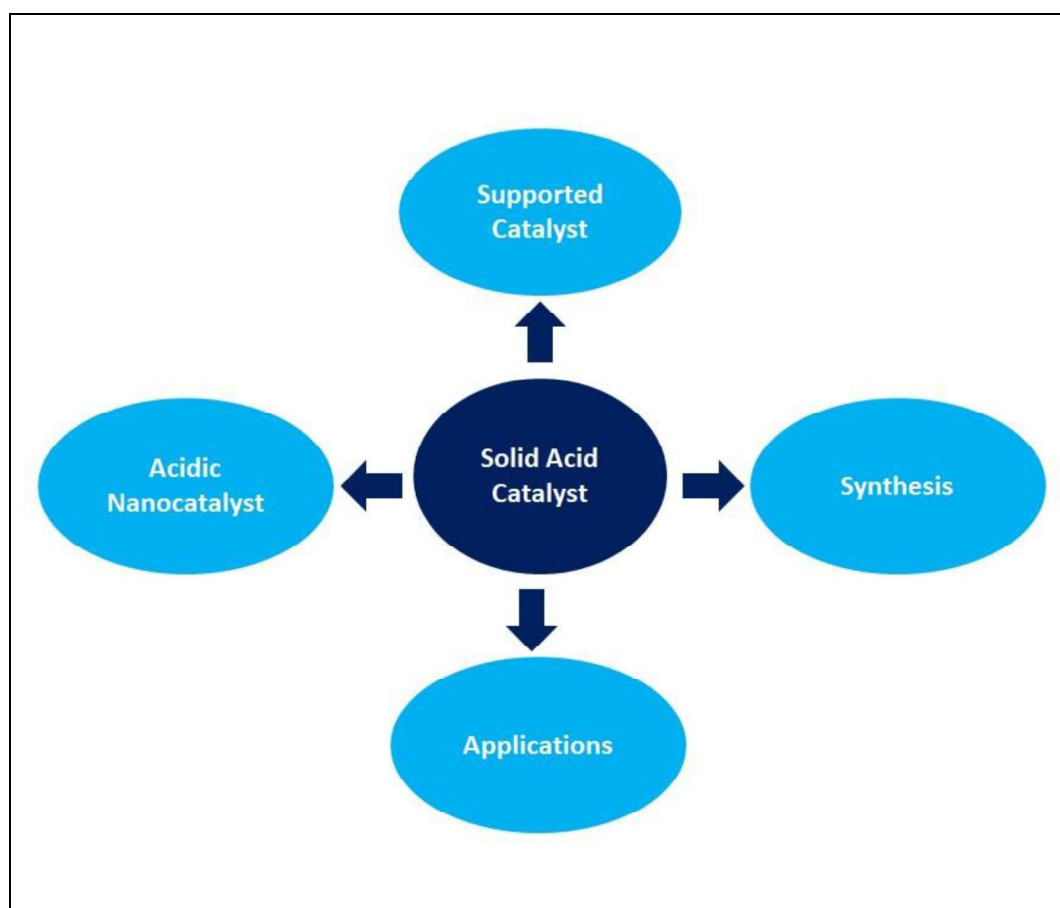
- ❖ IR spectra ( $4000\text{-}400\text{ cm}^{-1}$ ) were recorded in a Perkin Elmer Spectrum 100 machine using KBr pellete.
- ❖ Transmission electron microscopy (TEM) and high-resolution transmission electron microscopy (HR-TEM) images were recorded on a JEOL JEM-2011 electron microscope functioned at an accelerating voltage of 200 kV. Samples for the experiments were prepared by dispersing the solids in 2-propanol followed by placing them on a carbon coated copper grid and finally allowing them to dry. In built “Image J” program was used to develop TEM and HR-TEM micrographs and calculate the size of the nanoparticles.
- ❖ X-ray photoelectron spectroscopy (XPS) was carried out by Twin anode Non-Monochromated ESCALAB Xi<sup>+</sup> instrument using a monochromatized Al K $\alpha$  excitation at a pressure  $3\times 10^{-9}$  mbar, pass energy is 20 eV, electron take off angle is 55°, the full width at the half maximum of Au4f7/2 is 0.8 eV. The raw XPS data were fitted with Gauss-Lorentz curve after subtraction of Shirley background using XPS 4.1 software.
- ❖ Thermogravimetric analysis (TGA) was carried out on a SDT Q600 V20.9 Build 20 instrument at a heating rate of 10 °C/min under N<sub>2</sub> atmosphere.
- ❖ The specific surface area was recorded by using an Autosorb-iQ Station 1 (Quantachrome, USA) followed by the application of Brunauer–Emmett–Teller (BET)

calculations and the samples were degassed at 200 °C for 3 h before the experiments were carried out.

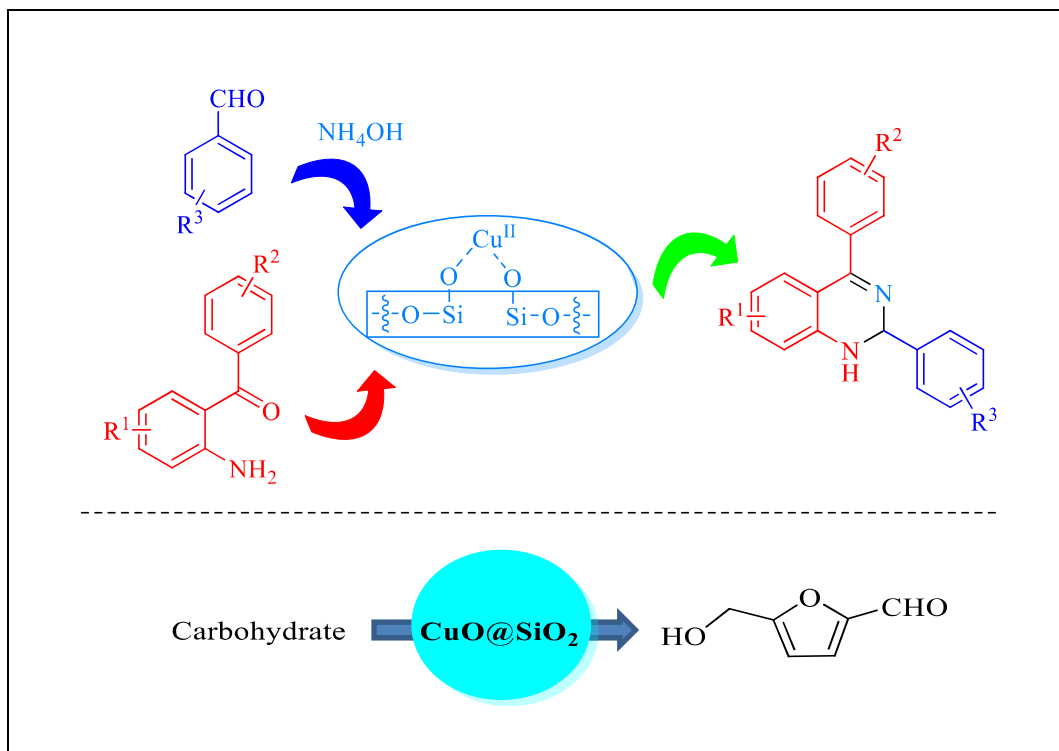
- ❖ The magnetic property was characterised by Vibrating sample magnetometer (Sigma, Model No.: 7410 series).
- ❖ High Pressure Liquid Chromatography (Waters: XEVO G2-XS QToF) was carried out in a column (waters) with mobile phase, water (0.1 % HCOOH): acetonitrile (0.1 % HCOOH). The operating condition was maintained by fixing temperature at 20°C, injection volume 10 µL, flow rate 300 µL/ min and UV absorbance 280 nm. The gradient flow of the mobile phase, water (0.1 % HCOOH): acetonitrile (0.1 % HCOOH) was 0-0.5 min 90%; 10%; at 2-3 min 10%; 90%; 4-5 min 90%; 10%.
- ❖ All Atomic Absorption Spectra were recorded by using Perkin Elmer (Model No.: AANALYST 700).
- ❖ All NMR spectra of the products were recorded by using Bruker AV500 Avance-III 500 MHz FTNMR spectrometer.
- ❖ HRMS data were recorded in a Waters XEVO G2-Xs QToF apparatus.
- ❖ Melting points were determined in open capillary tubes with a Buchi-540 micro melting point apparatus and are uncorrected.
- ❖ Chemical shifts were reported on the  $\delta$  scale (ppm) downfield from TMS ( $\delta = 0.0$  ppm) using the residual solvent signal at  $\delta = 7.26$  ppm ( $^1\text{H}$ ) or  $\delta = 77$  ppm ( $^{13}\text{C}$ ) as an internal standard.

# Graphical abstract

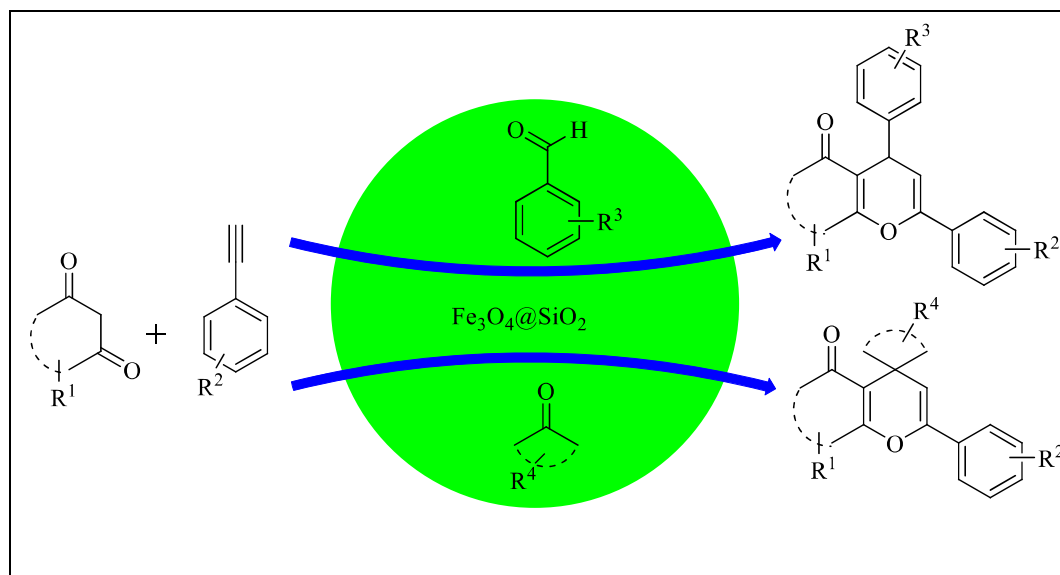
## CHAPTER 1: Introduction



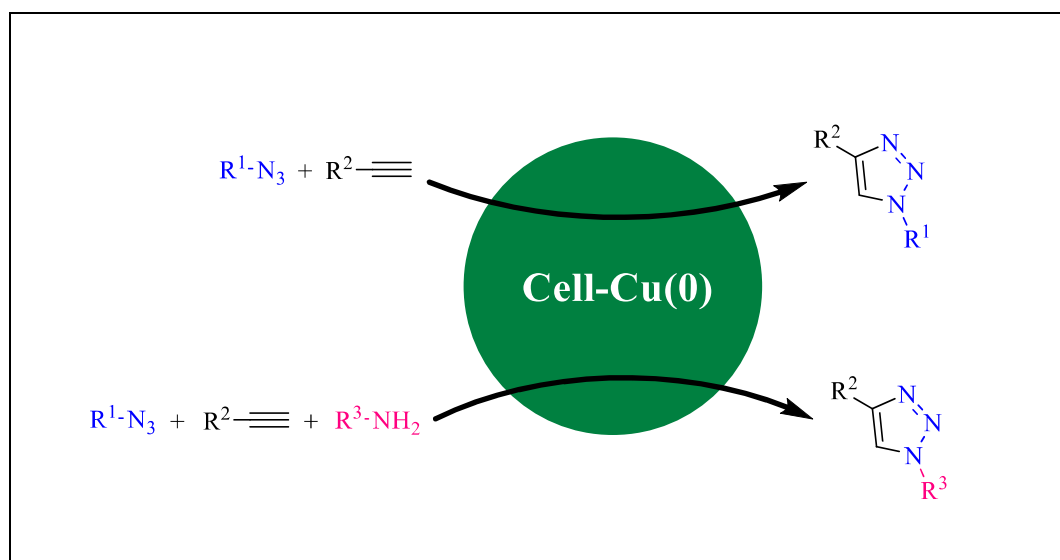
**CHAPTER 2: Synthesis of silica-supported copper oxide nanoparticles and its application in the synthesis of dihydroquinazoline and hydroxymethyl furfural (HMF)**



**CHAPTER 3: Magnetically active silica catalysed solvent-free domino Knoevenagel-hetero-Diels-Alder reaction: An easy access to divergent chromenones / dihydrochromenones / spirochromenones**



**CHAPTER 4: Synthesis of cellulose-supported copper nanoparticles and its application in synthesis of 1,2,3-triazole**





# **Chapter 1**

## **Introduction**

**1.1 Overview**

Catalytic technologies have played a vital role in the economic development of the chemical industries in the 20<sup>th</sup> century. About 90% of the chemical processes worldwide are carried out with the help of catalysts.<sup>1</sup> Catalysis occupies key positions in various chemical processes such as preparation of ammonia in Haber process, conversion of ammonia to nitric acid, production of sulfuric acid, hydrogenation and different polymerization. Different organic intermediates, necessary for the synthesis of dyes, plastics, pigments, crop-protection agents and drugs, rely only upon the use of catalysts. In 1835, J. J. Berzelius first introduced the term ‘catalysis’ to describe foreign substances which, when added in a small amount to a reaction, causes a large chemical change, without itself getting consumed during the process.<sup>2</sup> Later, in the year around 1900, W. Ostwald gave a generally accepted definition of catalysis and defined catalyst as a species which increases the rate of a chemical reaction through the formation of intermediate compounds and which is restored at the end of the reaction. In the year 1909, Ostwald was awarded the Nobel Prize in chemistry for his contribution in the field of catalysis, reaction velocities and chemical equilibrium.<sup>3</sup> Table 1 summarizes a few extremely important industrial processes that occur in the presence of catalysts.

**Table 1.** Various industrial processes that are carried out in the presence of catalysts

Chemical process	Catalysts used
Hydrogenation of coal to hydrocarbons	Sn, Mo, Fe
Sulfuric acid by lead-chamber process	NO <sub>x</sub>
Sulfuric acid by contact process	Pt, V <sub>2</sub> O <sub>5</sub>
Fat hardening	Ni
Chlorine production by HCl oxidation	CuSO <sub>4</sub>
Oxidation of ethylene to ethylene oxide	Ag
Cracking of hydrocarbons	Al <sub>2</sub> O <sub>3</sub> /SiO <sub>2</sub>
Hydroformylation of ethylene to propanal	Co
Polymerization of olefins	TiCl <sub>4</sub> /Al(C <sub>2</sub> H <sub>5</sub> ) <sub>3</sub>
Ethylene polymerization at low pressure	Pd/Cu chlorides
Methanol conversion to hydrocarbons	Ni/chelate phosphine
Hydrogenation	RhCl(PPh <sub>3</sub> ) <sub>3</sub>
Methanol conversion to acetic acid	[Rh(CO) <sub>2</sub> I <sub>2</sub> ] <sup>-</sup>
C-C cross-coupling	Pd

The increasing pressure on the chemical industries due to their negative impacts on the environment has paved the way for the introduction of efficient catalytic systems. Today catalysis is based on the development of environment

friendly and sustainable catalysts which satisfies all the goals of green chemistry. These environment friendly catalysts have become the pivotal point in modern chemical industry and applied to almost every process, including the synthesis of fine chemicals to bulk materials, pharmaceuticals and exhaust gas. Such catalysts have proved to be highly useful and selective, leading to the formation of the desired product, thereby, minimizing the side reactions. This drive towards a greener technology has further led to the replacement of conventional homogeneous catalysts with its heterogeneous counterpart.

Depending upon their physical nature, catalysis can be broadly classified into two categories, namely, homogeneous and heterogeneous. In homogeneous catalysis, the reactant as well as the catalyst exists in the same phase, namely, either in the liquid phase or in the gas phase. The homogeneous catalysts have a high degree of dispersion and selectivity. Homogeneous catalysis provides a kinetically controlled reaction and displays better activity. The major drawback associated with such catalytic systems is that they are thermally less stable and cannot be separated from the reaction medium and hence has a reusability problem.

On the other hand, in heterogeneous catalysis, solids catalyze the reactions of solution or gas phase by adsorption of the reactant molecules on its surface. Chemisorbed reactant molecules form an activated complex with the catalyst. Heterogeneous catalysts are often associated with high thermal stability, fewer disposal problems and can be readily separated from the reaction medium and can be

reused efficiently. These catalysts can also be modified in order to enhance their selectivity, activity and catalyst life. About 80% of industrial catalytic processes require the use of heterogeneous catalysts, 15% require homogeneous catalysts and the remaining 5% require biocatalysts.<sup>4</sup>

## **1.2 Solid Acid Catalyst**

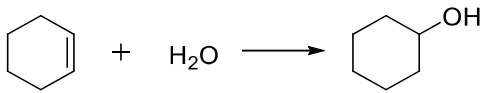
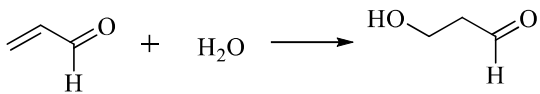
The homogeneous and heterogeneous catalysis can further be classified into acid and base catalysis. During acid catalysis, a proton is donated to the reactant while during base catalysis; a proton is abstracted from the reactant. Acids and base catalyzed processes are used in refineries, petrochemical and chemical industries for the manufacture of a wide range of specialty chemicals like agrochemicals, dyes, fragrances and pharmaceuticals. Some of the industrial applications of acid/base catalysis include isomerization, alkylation, dehydration, condensation, amination, catalytic cracking, etherification, aromatization, hydration, hydrocracking, oligomerization, polymerization as well as esterification.<sup>5-15</sup> Traditional Bronsted and Lewis acid catalysts such as  $\text{H}_2\text{SO}_4$ , HI,  $\text{H}_3\text{PO}_4$ , HCl, *p*-toluene sulfonic acid, HF,  $\text{AlCl}_3$ ,  $\text{BF}_3$  and  $\text{ZnCl}_2$  are employed in a majority of these processes. However, due to factors associated with their corrosive nature, difficulty in regeneration and reutilization, environmental hazards, storage and handling, energy consumption and waste treatment, the search for environmentally benign and recyclable catalysts which can replace the conventional Brønsted and Lewis acid catalysts has gained tremendous attention in recent years.<sup>16,17</sup> Supported catalysts as one of the classes of

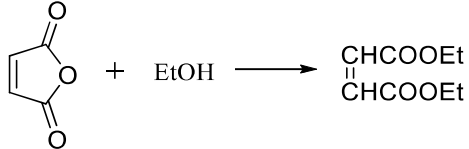
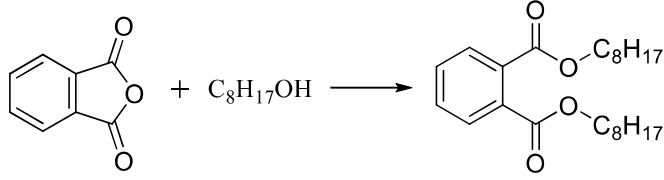
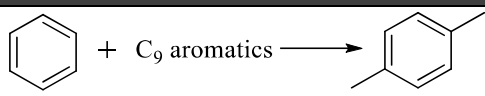
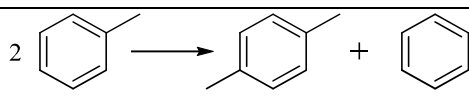
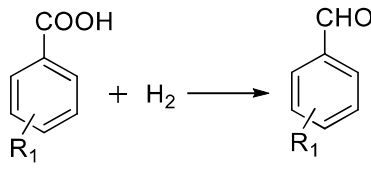
heterogeneous catalysts have emerged as a key tool in modern day synthesis. They are endowed with the combined benefits of selectivity of homogeneous catalysts as well as the added benefits of solid materials, which include high thermal stability, easy separation of the catalyst from the reaction medium, reusability of the recovered catalyst up to several consecutive cycles without any significant loss in the catalytic activity, and their application in a variety of organic reactions.<sup>18</sup> The term supported material describes a wide variety of materials containing either an organic or inorganic support onto which a chemical species can be physically or chemically adsorbed. The role of these supports is to allow uniform dispersion of the active promoter, thereby, providing a larger surface area for the reaction to occur.<sup>19</sup> Studies revealed that solids such as silica, zeolites, phosphates, metal oxides, mixed oxides, heteropolyacids, biopolymers, alumina, zirconia, activated carbon, biomass derivative, clay and other aluminosilicates can be used as efficient support.<sup>20-25</sup> These supported materials exhibit promising catalytic properties. Table 2 shows the various industrial processes which are catalyzed by solid acid/base.

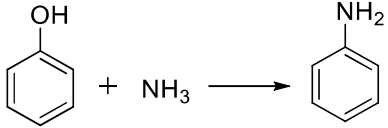
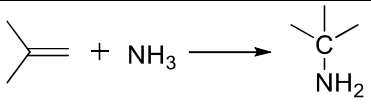
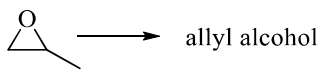
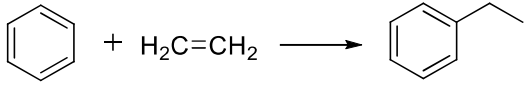
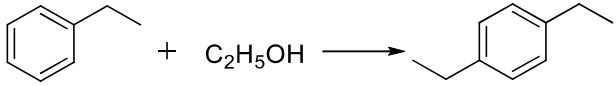
**Table 2.** Industrial processes employing solid acid/base catalysts

Sr. No.	Industrial process	Catalyst employed
<b>Cracking process</b>		
1.	Heavy oil	MgO-Al <sub>2</sub> O <sub>3</sub> -



		zeolite
2.	Cracking of straight chain paraffins and olefins	H-ZSM-5
<b>Hydrocracking process</b>		
3.	Lube dewaxing: wax oils + H <sub>2</sub> to produce lower molecular weight carbon	ZSM-5
4.	Hydrocracking of gas oils: wax oils + H <sub>2</sub> to produce gasoline	ZSM-5
<b>Etherification</b>		
5.	Olefin + MeOH to produce TAME/MTBE	Ion exchange resin
6.	<i>i</i> -C <sub>4</sub> + EtOH to produce ETBE	Ion exchange resin
<b>Hydration</b>		
7.		Highly siliceous H-ZSM-5
8.		Acid-base catalyst on TiO <sub>2</sub> /H <sub>3</sub> PO <sub>4</sub>
<b>Aromatization</b>		
9.	LPG to aromatics	Metallosilicate
10.	LPG (mainly C <sub>3</sub> , C <sub>4</sub> ) to BTX	Zeolite + promoter
<b>Esterification</b>		

11.		Ion exchange resin
12.		Mercapto functionalized sulfonated siloxane
<b>Disproportionation</b>		
13.		Zeolite
14.		ZSM-5
<b>Oligomerization and Polymerization</b>		
15.	C <sub>3</sub> to polypropylene	TiO <sub>2</sub> -MgO
16.	C <sub>4</sub> to linear octanes	H <sub>3</sub> PO <sub>4</sub> /SiO <sub>2</sub>
<b>Hydrogenation</b>		
17.		ZrO <sub>3</sub> -Cr <sub>2</sub> O <sub>3</sub> zeolite
18.	CO + H <sub>2</sub> to gasoline	zeolite
<b>Amination</b>		

19.		MgO, Al <sub>2</sub> O <sub>3</sub> or TiO <sub>2</sub> /SiO <sub>2</sub>
20.		Pentasil zeolite
<b>Isomerization</b>		
21.	$\text{H}_2\text{C}=\text{C}=\text{CH}_2 \longrightarrow \text{H}_3\text{C}-\text{C}\equiv\text{CH}$	K <sub>2</sub> O/Al <sub>2</sub> O <sub>3</sub>
22.		Li <sub>3</sub> PO <sub>4</sub>
<b>Alkylation</b>		
23.		H-ZSM-5
24.		ZSM-5

Solid acids may be defined as a substance which is capable of donating a proton or accepting an electron pair, or on which a base is chemically adsorbed. The solid acids are characterized either by the presence of protons or by the presence of coordinately unsaturated cationic centers on their surfaces. This leads to the development of Brønsted or Lewis acidity which is determined by the number of these sites and their acid strength is determined by their structure. Some of the solid

acids may possess both Brønsted and Lewis acid sites. Studies showed that more than three hundred solid acids have been developed during the recent decades.

### 1.3 Nano-materials in solid acid catalysis

Nanomaterials are extremely small particles having size less than or equal to 100 nm. The term ‘nano’ means ‘*dwarf*’ and it refers to a numerical value of  $10^{-9}$ . Though ‘nano’ is a recent concept, it was used by the people unknowingly during the ancient time. There are some examples which show the use of nanomaterials dates back to the mid-17<sup>th</sup> century, when *Purple of cassius* was discovered by the reaction of stannic acid and tetrachloroauric acid, and was used as a pigment in chinaware and glass enamel. This pigment was a mixture of gold nanoparticles and tin oxide. Another classic example is the *Lycurgus cup*, which changes color in light. This is because of the impregnation of glass with metal nanoparticles. The increased interest in the field of nanoscience aroused after the famous Physicist Richard P. Feynman delivered a lecture in 1959 describing the possibility of nanotechnology. Later in the year 1986, Binning, Rohrer and Ruska were awarded the Nobel Prize in Physics for the invention of atomic force microscope (AFM) and scanning tunneling microscope (STM) which paved the way for the development of modern nanoworld. The properties of bulk materials changes to a great extent when converted into nano-dimension. Nanomaterials have found widespread applications in recent years due to their enhanced mechanical, magnetic and electrical properties and are also used extensively in consumer products. However, in order to stabilize nanoparticles,

various stabilizing/supporting agents are used. The major role of these supports is to control the particle size and prevent agglomeration of the particles. Nanomaterials have found extensive applications in various fields due to their specific properties which include, large surface area, high thermal stability, ability of surface modification and easy isolation.<sup>26-29</sup> The use of such materials minimizes the occurrence of side reactions and hence the generation of waste, also reduces the energy requirements and use of toxic reagents. Nanosized solid acid catalysts combine the advantageous properties of solid acids and nanoparticles and thus gaining immense importance in recent decades.

#### **1.4 Supported solid acid catalysts**

The nature of the support affects the properties of the supported catalysts which, in turn, affect the catalytic behavior. Additionally, supported nanomaterials exhibit higher chemoselectivity and reactivity as compared to their bulk counterparts. Some of the most commonly employed supports used for the purpose have been described below.

##### **1.4.1 Silica supported solid acid catalysts**

Silica is one of the most abundant materials on earth. Use of silica as support has gained tremendous interest in recent years due to their wide availability, low cost, large surface area, low toxicity, highly porous structure and the lenience of tuning the morphological and compositional properties. Among the nanostructured

---

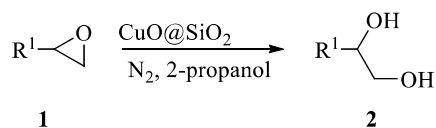
materials, mesoporous silica offers certain advantages such as high surface area and thermal stability to serve the purpose.<sup>30</sup> The surface of mesoporous silica contains hydroxyl groups which facilitate the surface of the material to be functionalized.<sup>31</sup> Some of the recently reported methods utilizing silica as a support for the preparation of solid acid catalyst have been discussed below.

In a report by Zeng et al., silica coated polycresulen (a polymer made up of formaldehyde and 2-hydroxy-4-methylbenzenesulfonic acid) was prepared and efficiently utilized as a solid acid for carrying out various organic transformations such as oxa-Pictet-Spengler reaction,  $\beta$ -alkylation of styrene and C3-alkenylation of 2- and 3-methylindoles.<sup>32</sup> Niknam and coworkers prepared silica-bonded propylpiperazine-*N*-sulfamic acid as a solid acid catalyst for the synthesis of 1,2,4,5-tetrasubstituted imidazoles.<sup>33</sup>  $\text{Bi}_2\text{O}_3@m\text{SiO}_2$  has also been reported as an environmentally friendly solid acid catalyst for Friedel-Crafts benzoylation.<sup>34</sup>

Silica phosphoric acid has been reported as an efficient solid acid catalyst for the coupling of thiols to disulfides.<sup>35</sup> The catalyst was prepared by reacting silica chloride with phosphoric acid. In another report, silica-supported sulfonic acid was prepared and used in the dihydroxylation of 1-methylcyclohexene in the presence of aqueous hydrogen peroxide.<sup>36</sup>

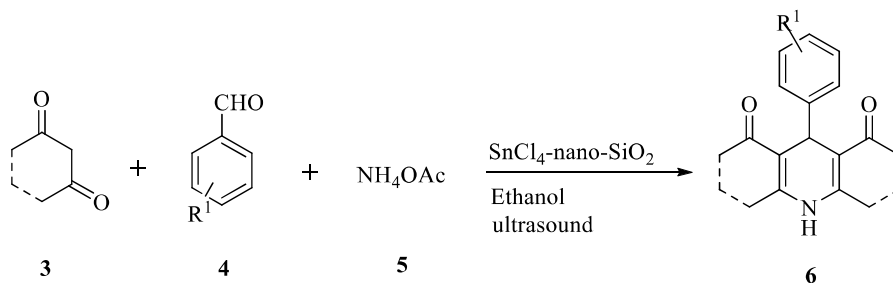


Silica-supported copper oxide ( $\text{CuO}@\text{SiO}_2$ ) has been reported as an efficient solid acid catalyst for the ring opening of epoxides **1** to form  $\beta$ -alkoxyalcohols **2** without the formation of any side product (Scheme 1).<sup>37</sup>



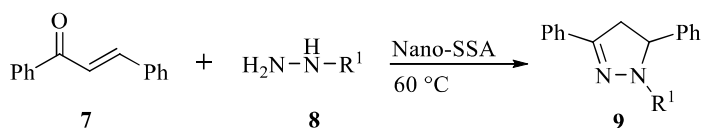
**Scheme 1.** Alcoholsis of epoxide producing  $\beta$ -alkoxyalcohol

Nano-silica supported tin chloride ( $\text{SnCl}_4\text{-nano-SiO}_2$ ) has been used in the efficient synthesis of 1,4-dihydropyridine derivatives **6** by reacting aldehydes **4** with 1,3-dicarbonyls **3** and ammonium acetate (**5**) under ultrasound irradiation (Scheme 2).<sup>38</sup> In this reaction  $\text{SnCl}_4\text{-nano-SiO}_2$  catalyst exhibited mild Lewis acid character and because of the nano-structure, the surface of contact of the material increased many fold.



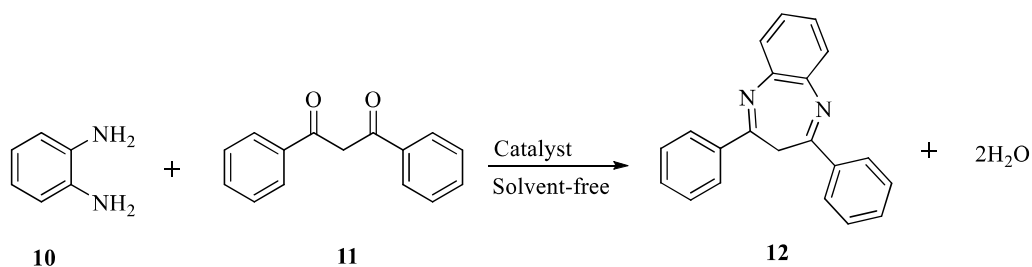
**Scheme 2.** Synthesis of 1,4-dihydropyridine *via*  $\text{SnCl}_4\text{-nano-SiO}_2$

Nano silica sulfuric acid (Nano-SSA) catalyst has been explored as an efficient solid acid catalyst for the synthesis of pyrazole derivatives **9** by treating 1,3-diketones **7** with hydrazine **8** (Scheme 3).<sup>39</sup>



**Scheme 3.** Preparation of pyrazole derivatives in the presence of nano-SSA

In a recent report by Morales, tungstophosphoric acid was incorporated onto mesoporous silica and the prepared catalyst was used for the one-pot synthesis of 1,5-benzodiazepine (**12**) by reacting 1,2-phenylenediamine (**10**) with 1,3-diphenyl-1,3-propanedione (**11**) under solvent-free condition (Scheme 4).<sup>40</sup>

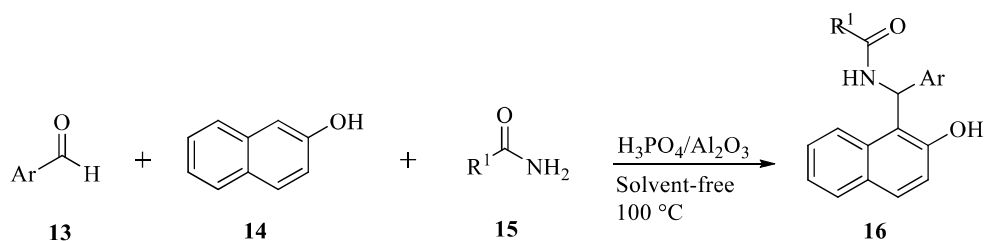


**Scheme 4.** One-pot synthesis of 1,5-benzodiazepine catalyzed by tungstophosphoric acid incorporated silica

### 1.4.2 Alumina/silica-alumina supported solid acid catalyst

Although alumina is not a naturally occurring compound, the  $\gamma$  and  $\eta$ -forms are widely employed as inert support for active metals in catalysis due to their high surface area, high stability and porous structure.<sup>41</sup> Silica and alumina are employed as solid catalysts for various industrial processes such as alkylation, polymerization, catalytic cracking, and production of fine chemical. Their activity is based upon the presence of Brønsted acidic sites which is characterized by the hydroxyl groups present on their surface. Some of the recent works displaying alumina supported solid acid catalyst have been described below.

Phosphoric acid supported on alumina ( $\text{H}_3\text{PO}_4/\text{Al}_2\text{O}_3$ ) has been found to be an effective catalyst for the synthesis of  $\alpha$ -amidoalkyl- $\beta$ -naphthols **16** by three component reactions between aromatic aldehyde **13**,  $\beta$ -naphthol (**14**), and amide **15** (Scheme 5).<sup>42</sup>

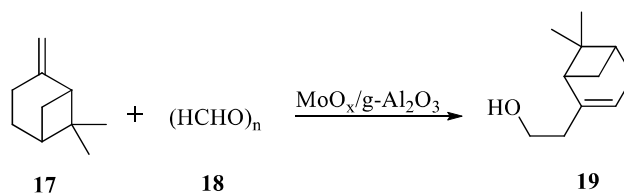


**Scheme 5.** Synthesis of  $\alpha$ -amidoalkyl- $\beta$ -naphthols in the presence of  $\text{H}_3\text{PO}_4/\text{Al}_2\text{O}_3$

Very recently, Yang et al. prepared chlorinated and fluorinated alumina support by replacing some of the hydroxyl groups of alumina with chlorine and

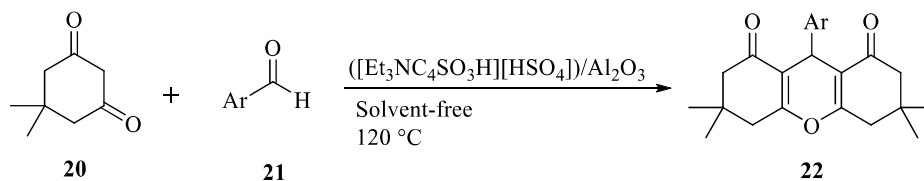
fluorine, respectively.<sup>43</sup> This affected the acidity of the other hydroxyl groups which significantly increased the acidic behavior at the surface. After incorporation of Pt nanoparticles onto the modified support, the resulting solid acid catalyst was used for the reforming reaction of *n*-hexane.

In a report by Marakatti, molybdenum oxide supported on  $\gamma$ -alumina ( $\text{MoO}_x/\gamma\text{-Al}_2\text{O}_3$ ) was used to carry out Prins condensation of  $\beta$ -pinene (**17**) with paraformaldehyde (**18**). The product of the reaction was nopol (**19**) (Scheme 6).<sup>44</sup>



**Scheme 6.**  $\text{MoO}_x/\gamma\text{-Al}_2\text{O}_3$  catalyzed Prins condensation

Alumina supported acidic ionic liquid was utilized as catalyst for the synthesis of 1,8-dioxo-octahydroxanthenes **22** by reacting dimedone (**20**) with aldehyde **21** (Scheme 7).<sup>45</sup>



**Scheme 7.** Preparation of 1,8-dioxo-octahydroxanthenes over alumina supported ionic liquid

The ionic liquid used was *N*-(4-sulfonic acid) butyl triethylammonium hydrogen sulfate ([Et<sub>3</sub>NC<sub>4</sub>SO<sub>3</sub>H][HSO<sub>4</sub>]).

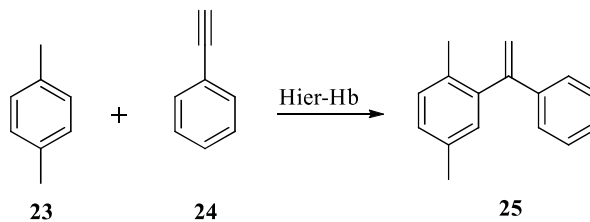
Bhatt et al. prepared 12-tungstophosphoric acid supported on alumina and carried out Friedel-Crafts alkylation reaction in the presence of that catalytic system.<sup>46</sup>

### **1.4.3 Zeolite supported solid acid catalyst**

Zeolites are highly porous three-dimensional network of aluminosilicates formed by sharing of SiO<sub>4</sub> and AlO<sub>4</sub> tetrahedra. Zeolites have occupied a pivotal position in petroleum refineries and petrochemical industries since 1960 due to their remarkable properties such as high thermal and chemical stability, enhanced acidity and high crystallinity. The Brønsted acidity of zeolites can be attributed to the presence of surface hydroxyl groups. The acidic strength and hydrophobic nature of zeolites depend upon the Si/Al ratio. Namba et al. were the first to carry out zeolite catalyzed solid acid reaction in water medium.<sup>47</sup> Zeolite supported solid acid catalysts are mainly used for the isomerization of *n*-hexane and xylene, hydrocracking, Friedel-Crafts acylation reaction, esterification, nitration of benzene, and benzylation of *o*-xylene.<sup>48-52</sup> Some of the recent reports involving zeolite supported acid catalysts have been described below.

Li et al. developed a La-doped Zr-Beta zeolite heterogeneous acid catalyst and utilized in cyclohexanone reduction *via* Meerwein-Ponndorf-Verley reaction.<sup>53</sup>

Hierarchical H $\beta$  (Hier-H $\beta$ ) zeolite was used for the alkenylation of *p*-xylene (23) with phenylacetylene (24) (Scheme 8).<sup>54</sup> It needs to be mentioned here that hierarchical zeolite combines the mesopore effect along with the properties of microporous zeolite and is considered as an excellent solid acid catalyst.

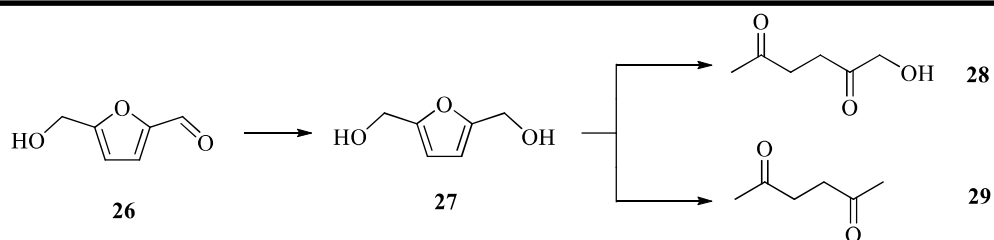


**Scheme 8.** Alkenylation of *p*-xylene over zeolites

Park et al. prepared zeolite from coal fly ash and designed Pd-Sn bimetallic catalyst on this support.<sup>55</sup> The prepared solid acid catalyst was then used for the successful reduction of NO<sub>3</sub><sup>-</sup> to N<sub>2</sub>.

In a work by Ramos and co-workers, palladium nanoparticles were prepared using Beta-zeolite support and the resulting catalyst was employed in the conversion of 5-hydroxymethylfurfural (HMF) (26) into diketone derivatives such as 1-hydroxyhexane-2,5-dione (HHD) (28) and 2,5-hexanedione (HXD) (29) (Scheme 9).<sup>56</sup> The diketone derivatives were obtained from HMF *via* furan-2,5-diylidimethanol (FDM) (27).





**Scheme 9.** Conversion of HMF into diketones over zeolites

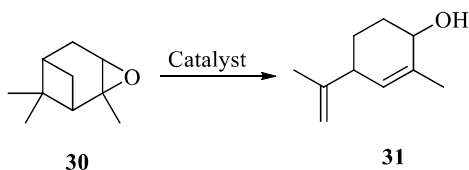
#### 1.4.4 Carbon supported solid acid catalyst

Recently, carbon-based materials have gained immense attention in solid acid chemistry due to their renewable nature, large surface area, chemical inertness, surface-containing functional groups, high abundance and low cost.<sup>57,58</sup> They can be prepared from a variety of carbon-rich waste materials of agricultural, animal and mineral origin. Activated carbon-based solid acid catalysts are widely used for the dehydration of isopropanol, esterification of fatty acids, alkylation, benzylation, condensation, and hydrolysis.<sup>59-61</sup> Below are discussed some of the recently reported methods employing the carbon-based acid catalyst.

Carbon-based sulfonic (C-SO<sub>3</sub>H) solid acid was used by Yang et al. to carry out one-pot three component reaction for the synthesis of pyrano derivatives.<sup>62</sup>

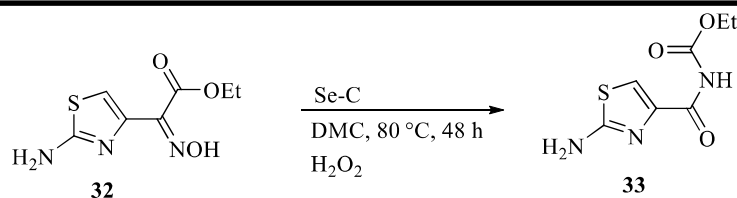
Fauziyah et al. prepared carbon aerogel from coir fiber and then sulfonated the carbon support. This solid catalyst was then used for esterification reaction.<sup>63</sup> In a recent report sulfated carbon heterogeneous catalyst was used for the efficient

isomerization of  $\alpha$ -pinene oxide (**30**) to trans-carveol (**31**) (Scheme 10).<sup>64</sup> Here chitosan was used as the source of carbon.



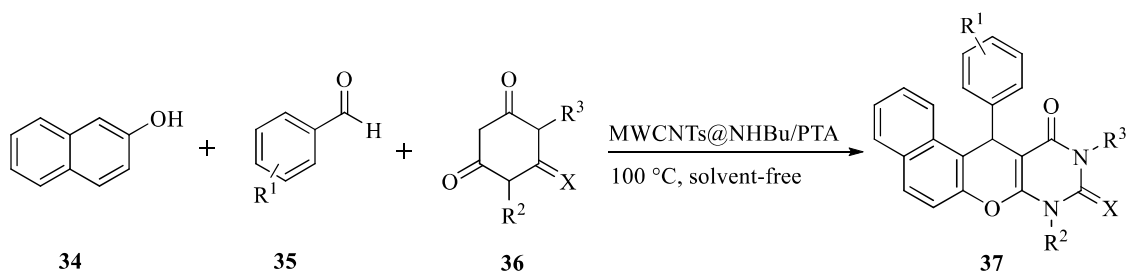
**Scheme 10.** Isomerization reaction catalyzed by sulfated carbon acid catalyst

In a report by Wang, activated carbon supported silicotungstic acid (STA/AC) was prepared and used as catalyst to synthesize isoprene from methyl *tert*-butyl ether and formaldehyde.<sup>65</sup> Zhang et al. prepared immobilized zinc on carbon nitride and then supported it with carbon fibre to form Zn-CN/C.<sup>66</sup> The catalyst was used for the cycloaddition reaction of CO<sub>2</sub> with epoxide such as styrene oxide to produce cyclic carbonates. Beckmann rearrangement of ethyl 2-(2-aminothiazole-4-yl)-2-hydroxyiminoacetate (**32**) was carried out using selenium-doped carbon (Se-C) as a solid acid catalyst (Scheme 11).<sup>67</sup> Classical Beckmann rearrangement produces oxidative deoxygenation product but in this modified Beckmann rearrangement, an amide is formed. Ethyl (2-aminothiazole-4-carbonyl)carbamate (**33**), the final product of the reaction, is an important intermediate during *Cefixime* synthesis and finds wide application in medicinal chemistry.



**Scheme 11.** Beckmann rearrangement in the presence of selenium-doped carbon

Ahmadi et al. prepared 12-tungstophosphoric acid functionalized aminated multiwalled carbon nanotubes (MWCNTs@NHBu/PTA) and employed the solid acid catalyst for the synthesis of benzochromenopyrimidine **37** under solvent-free condition (Scheme 12).<sup>68</sup>



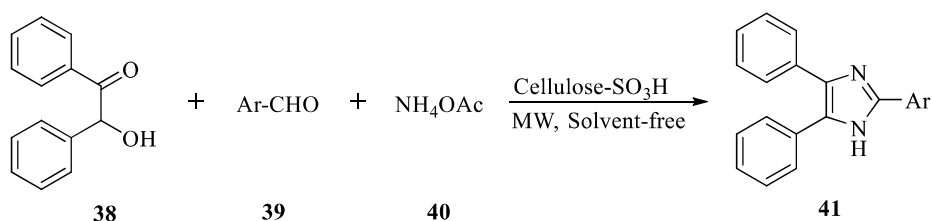
**Scheme 12.** Synthesis of benzochromenopyrimidine over carbon solid acid catalyst

### 1.4.5 Biopolymer supported solid acid catalyst

Cellulose is the most abundant natural biopolymer and possesses admirable properties such as chirality, high porosity, good mechanical property, biodegradability, thermostability, hydrophilicity, and broad chemical modifying capacity. Cellulose has an excellent capacity of metal adsorption and drug loading.<sup>69</sup>

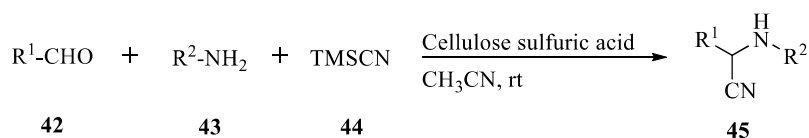
These striking properties of cellulose make it an interesting support material in catalytic applications.

Shelke and co-workers prepared cellulose sulfuric acid and used it as a highly efficient recyclable catalyst for the one-pot three component reaction of benzoin (**38**), aldehydes **39** and ammonium acetate (**40**) to produce 2,4,5-triarylimidazoles **41** under solvent-free condition (Scheme 13).<sup>70</sup>



**Scheme 13.** Synthesis of 2,4,5-triarylimidazoles over cellulose sulfuric acid

A three component reaction of amines **43** with aldehydes **42** and trimethylsilylcyanide (**44**) catalyzed by cellulose sulfuric acid to yield  $\alpha$ -amino nitriles **45** (Scheme 14) was reported by Shaabani et al..<sup>71</sup>



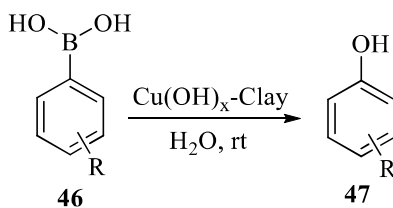
**Scheme 14.** Cellulose sulfuric acid catalyzed synthesis of  $\alpha$ -amino nitriles

#### 1.4.6 Clay supported solid acid catalyst

Clay is a naturally occurring material widely used in petrochemical industries. They possess both Brønsted and Lewis acidic sites on their surface and the negative charge of the layers are neutralized by cations occupying the inter

lamellar spaces. This paves the way for the modification of properties of clay such as surface area, pore size, acidity etc which are mainly responsible for the catalytic activity. In recent years, clay supported solid acid catalysts also are being used in different organic transformations such as Diels-Alder reaction, isomerization, Friedel-Crafts alkylation, dehydration, and esterification.<sup>72,73</sup> In a report, Fe-Mg-hydrocalcite anionic clay was used for carrying out Friedel-Crafts alkylation.<sup>74</sup>

An efficient montmorillonite clay entrapped  $\text{Cu}(\text{OH})_x$  was prepared and used as a catalyst for the ipso-hydroxylation of arylboronic acids **46** at room temperature (Scheme 15).<sup>75</sup>



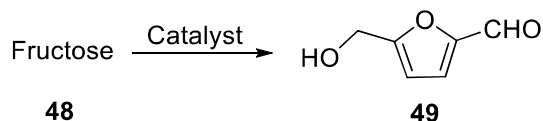
**Scheme 15.** Clay entrapped  $\text{Cu}(\text{OH})_x$  catalyzed ipso-hydroxylation of arylboronic acid

#### 1.4.7 Ion-exchange resin supported solid acid catalyst

An ion-exchange resin is a material consisting of an insoluble matrix and labile ions. These labile ions are capable of exchanging with ions in the surrounding medium without undergoing any significant physical change in the resin. The ion exchange resins can be either based on perfluorosulfonic acid or styrene sulfonic

acid. The perfluorosulfonic acid based resins such as Nafion-H (tetrafluoroethylene-perfluoro-3,6-dioxa-4-methyl-7-octansulfonic acid) are strong Brønsted acids and are capable of catalyzing a number of chemical processes such as esterification, Friedel-Crafts alkylation, acylation of anisole, condensation of ketones, trans-alkylation, alkylation of phenol, hydrolysis of ester, and synthesis of methyl *tert*-butyl ether.<sup>74-76</sup> The styrene based sulfonic acid, namely, Amberlyst, is a mild Brønsted acid and is used in a variety of organic transformations such as benzylation of arenes, Friedel-Crafts alkylation, esterification, cross-aldol condensation, halogenation, synthesis of coumarins and quinolones.<sup>77,78</sup>

In a report, Nafion-modified mesocellular silica foam catalyst was prepared and efficiently used for the conversion of fructose (**48**) to 5-Hydroxymethylfurfural (HMF) (**49**) (Scheme 16).a



**Scheme 16.** Conversion of fructose to HMF over Nafion-modified mesocellular silica foam catalyst

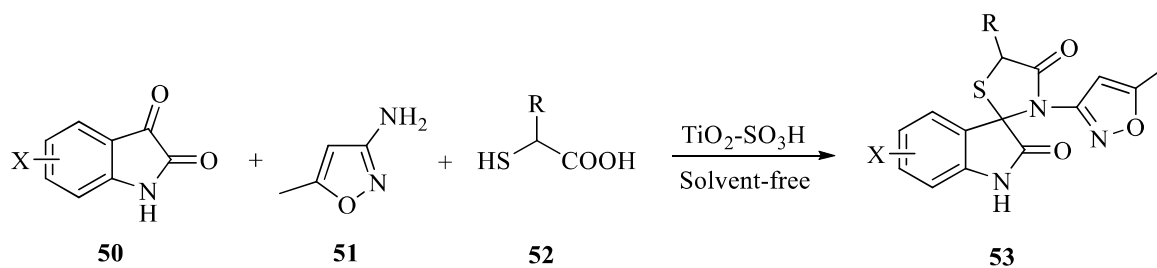
### 1.5 Sulfonic acid derivatives as solid acid catalyst

Amberlyst-15, a solid acid catalyst possessing sulfonic acid functionality exhibits high selectivity in both aqueous and non-aqueous media and has been

employed by Jeong et al. in the conversion of marine macro-algae to produce sugar.<sup>79</sup> Heydari et al. in a report exhibited the use of sulfamic acid as a recyclable solid acid catalyst for the three component reaction between aldehydes, amines and trimethylsilyl cyanide for the preparation of  $\alpha$ -amino nitriles.<sup>80</sup> Another protocol was also reported by Kamal et al. utilizing sulfamic acid for the synthesis of quinoxaline derivatives.<sup>81</sup> Kalla and co-workers used phospho sulfonic acid (PSA) as a promising solid acid catalyst for the synthesis of acylal under solvent-free conditions.<sup>82</sup> Takabatake carried out alkylation of benzene by using montmorillonite as a solid acid catalyst.<sup>83</sup> Sulfonated carboxymethyl cellulose (SCMC) was prepared by treating sodium carboxymethyl cellulose with chlorosulfonic acid and used as a solid acid for the synthesis of pyrano[2,3-*c*]pyrazole derivatives.<sup>84</sup> In a report by Agarwal et al., caffeinium hydrogen sulfate (CHS) was prepared by treating caffeine with sulfuric acid.<sup>85</sup> The prepared solid acid was used for a domino Knoevenagel-Michael reaction resulting in the formation of bis-cyclohexenones at a temperature of 30 °C. When the temperature was increased to 80 °C, 1,8-dioxooctahydroxanthenes was obtained as the sole product. A reusable tungstate sulfuric acid was prepared by Farahi et al. and used for the one-pot three component synthesis of tetrasubstituted pyrroles.<sup>86</sup> Heterocyclic nitrones was synthesized by reacting diaminoglyoxime with aromatic aldehydes in the presence of phosphate tungstate ( $\text{WO}_4(\text{OP}(\text{OH})_2)_2$ ) as an efficient solid acid catalyst.<sup>87</sup> Nitrones are versatile synthons in organic chemistry and are used as building blocks of amino acids, antibiotics and alkaloids. Nitrones

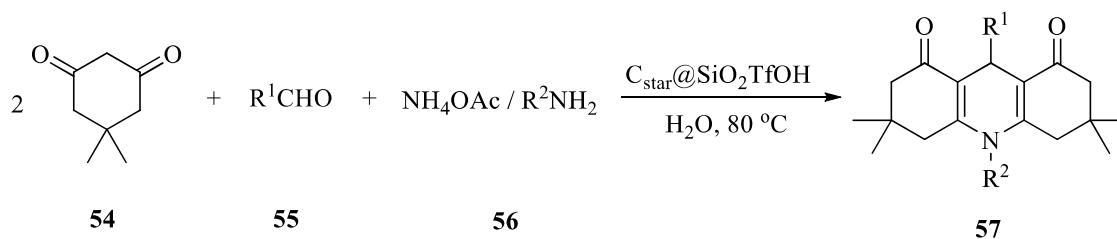
are also used as antioxidants for the treatment of age-related diseases and as spin trapping agent.

In a report by Singh et al., nano-titania supported sulfonic acid ( $\text{TiO}_2\text{-SiO}_3\text{H}$ ) was prepared and used for the synthesis of spiro derivatives **53** under solvent-free condition (Scheme 17).<sup>88</sup>



**Scheme 17.**  $\text{TiO}_2\text{-SiO}_3\text{H}$  catalyzed synthesis of spiro compounds

Sharma and co-workers prepared triflic acid immobilized on carbon@silica ( $\text{C}_{\text{star}}@\text{SiO}_2\text{TfOH}$ ) and utilized the prepared acidic catalyst for the synthesis of indeno[1,2-*b*]indoles **57** (Scheme 18).<sup>89</sup>



**Scheme 18.** Synthesis of indeno[1,2-*b*]indoles catalyzed by  $\text{C}_{\text{star}}@\text{SiO}_2\text{TfOH}$

Copper (I) oxide incorporated on sulfated zirconia ( $\text{Cu(I)}@\text{ZrO}_2\text{-SO}_4^{2-}$ ) was prepared and efficiently used for the synthesis of azo dyes.<sup>90</sup> In a recent report,

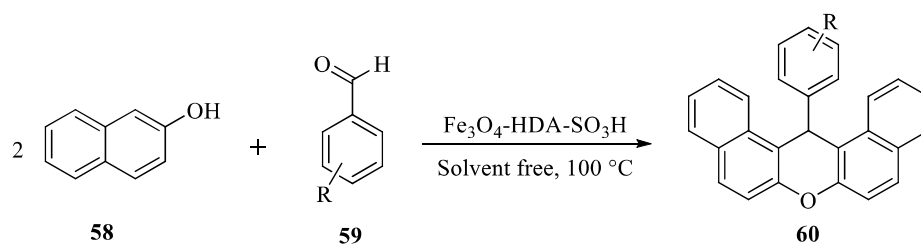


sulfoacetate modified silica supported indium (III) triflate [SiSAIn(OTf)<sub>2</sub>] was used as solid acid catalyst and screened its applicability in the synthesis of tetrasubstituted imidazole derivatives.<sup>91</sup>

### 1.6 Magnetic solid acid catalyst

Magnetic heterogeneous catalysts have gained immense interest in recent decades owing to their easy recoverability from the reaction medium, simply by using an external magnet. Magnetic solid acidic catalysts are consisting of a surface functionalized magnetic core.

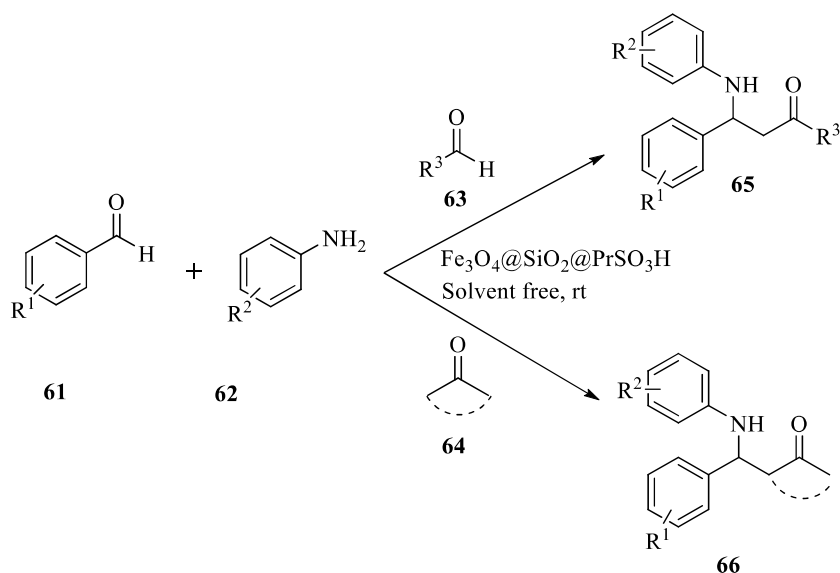
In a recent report, Naeimi et al. prepared sulfonated-functionalized magnetite nanoparticles and used for the efficient one-pot synthesis of xanthenes **60** under solvent-free condition (Scheme 19).<sup>92</sup> Xanthenes are pharmaceutically important compounds possessing various therapeutic properties such as anti-inflammatory and antibacterial.



**Scheme 19.** Synthesis of xanthenes over sulfonated magnetites

One-pot three component Mannich reaction is an important organic reaction for the construction of  $\beta$ -amino carbonyls. Sulfonated core-shell magnetic

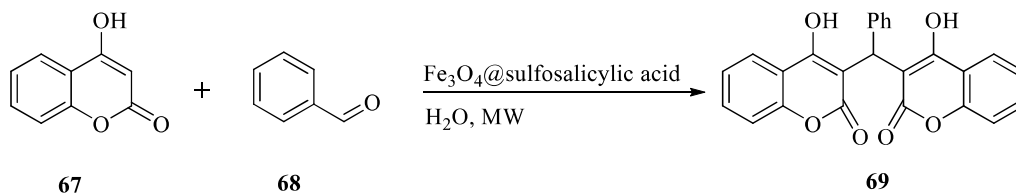
nanoparticles ( $\text{Fe}_3\text{O}_4@\text{SiO}_2@\text{PrSO}_3\text{H}$ ) was prepared and used for the three component Mannich reaction to produce  $\beta$ -amino carbonyls **65/66** under solvent-free condition (Scheme 20).<sup>93</sup>  $\beta$ -amino carbonyl is a fundamental building block of lactams and peptides, and is also used for the synthesis of amino acids and other nitrogen-containing compounds.<sup>94</sup>



**Scheme 20.** Mannich reaction catalyzed by sulfonated magnetic nanoparticles

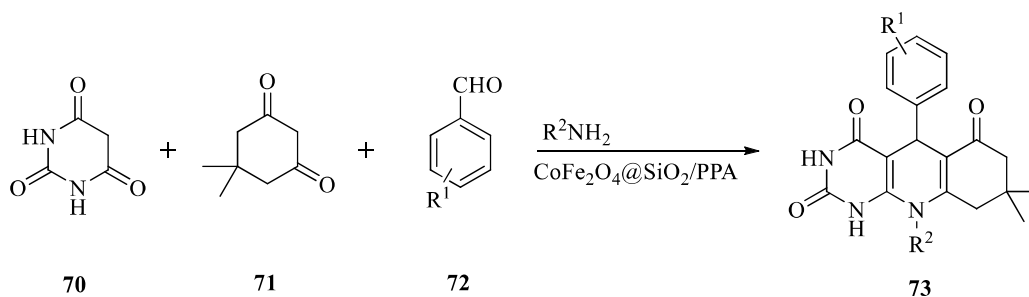
Sulfosalicylic acid functionalized iron oxide magnetic nanoparticles ( $\text{Fe}_3\text{O}_4@\text{sulfosalicylic acid MNPs}$ ) were prepared and employed as the acid catalyst in the synthesis of bis-coumarin (**69**) in aqueous medium under microwave

irradiation (Scheme 21).<sup>95</sup> Bis-coumarins are widely used as hypnotic agents, anticoagulant, antifungal, ligands and stabilizing agents.



**Scheme 21.** Synthesis of bis-coumarin over sulfosalicylic acid functionalized iron oxide

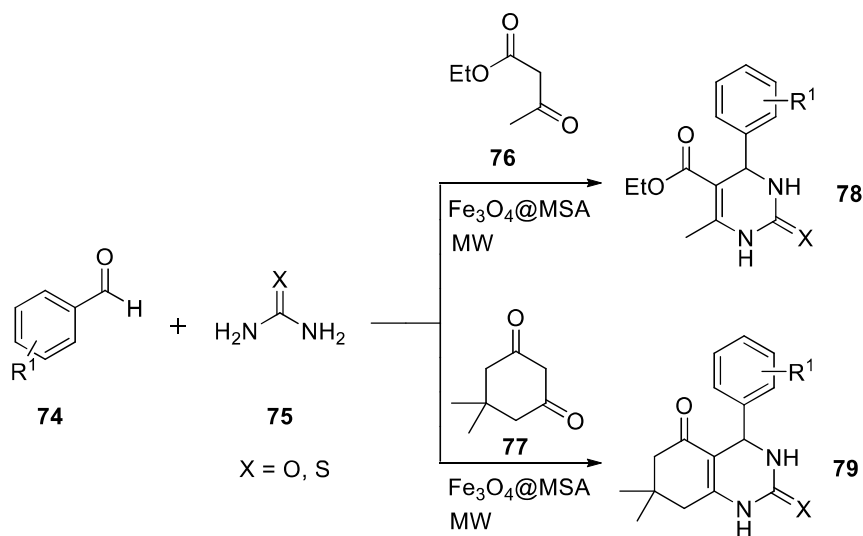
Moradi and co-workers developed an efficient phosphoric acid supported  $\text{CoFe}_2\text{O}_4$  nanoparticles ( $\text{CoFe}_2\text{O}_4@\text{SiO}_2/\text{PPA}$ ) and utilized this magnetically recoverable solid acid catalyst in the synthesis of dihydropyrimido[4,5-*b*]quinolinetriene **73** under ultrasonic irradiation (Scheme 22).<sup>96</sup>



**Scheme 22.** synthesis of dihydropyrimido[4,5-*b*]quinolinetriene over  $\text{CoFe}_2\text{O}_4@\text{SiO}_2/\text{PPA}$

The product pyrimido[4,5-*b*]quinoline derivatives are important motifs in organic chemistry as they possess different therapeutic properties such as antiviral, antioxidant and antitumor.

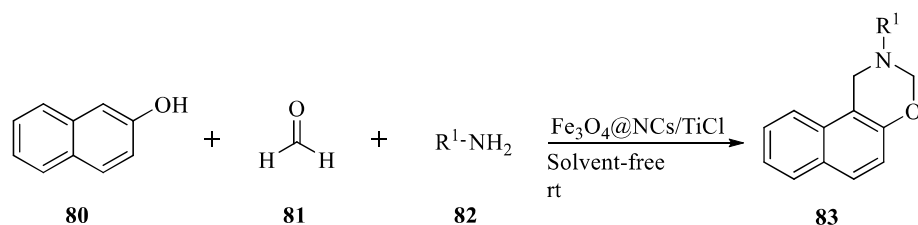
In another report, the same author prepared a sulfonated-meglumine coated  $\text{Fe}_3\text{O}_4$  ( $\text{Fe}_3\text{O}_4\text{@MSA}$ ) solid acid catalyst and studied its application in the Biginelli reaction for the synthesis of 3,4-dihydropyrimidin-2(1*H*)-ones/thiones **78/79** under microwave irradiation (Scheme 23).<sup>97</sup>



**Scheme 23.** Sulfonated-meglumine coated  $\text{Fe}_3\text{O}_4$  catalyzed Biginelli reaction

Biginelli reaction is a one-pot multicomponent reaction first studied by Pietro Biginelli in 1893 for the synthesis of 3,4-dihydropyrimidin-2(1*H*)-ones by condensation of an aldehyde,  $\beta$ -ketoester and urea catalyzed by an acid catalyst.<sup>98</sup>

Magnetic nanocellulose was synthesized by coating the nanocellulose on freshly prepared  $\text{Fe}_3\text{O}_4$  magnetic nanoparticle.<sup>99</sup> The required nanocellulose was prepared by hydrolysis of cotton with sulfuric acid. The resulting  $\text{Fe}_3\text{O}_4$ @nanocellulose ( $\text{Fe}_3\text{O}_4$ @NCs) was further used as a support for  $\text{TiCl}_4$  to prepare  $\text{Fe}_3\text{O}_4$ @nanocellulose/ $\text{TiCl}_4$  ( $\text{Fe}_3\text{O}_4$ @NCs/ $\text{TiCl}_4$ ). The prepared catalyst was then utilized for the synthesis of 2,3-dihydro-2-substituted-1*H*-naphtho[1,2-*e*][1,3]oxazine **83** by a multicomponent reaction between 2-naphthol (**80**), formaldehyde (**81**) and an amine **82** under solvent-free condition (Scheme 24).



**Scheme 24.** Multicomponent reaction catalyzed by  $\text{Fe}_3\text{O}_4$ @NCs/ $\text{TiCl}_4$

In a report by Han, magnetically recoverable cellulose microsphere supported heteropoly acid (MCM-HPW) was prepared and used for biodiesel production by transesterification of seed oil of *Pistaciachinensis*.<sup>100</sup>

### 1.7 Synthesis of nanostructured solid acid catalyst

Due to the immense importance gained by nanoparticles in recent decades, numerous approaches have been developed for their synthesis. Different processes employed for the preparation of solid acid nanoparticles are depicted in figure 1.

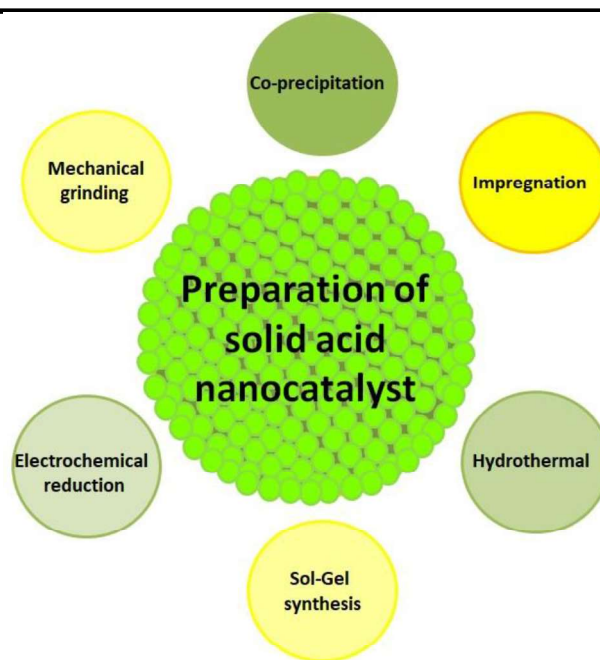


**Figure 1.** Various processes for the synthesis of nanostructured solid acid catalyst

### 1.7.1 Co-precipitation

The co-precipitation method is a convenient way of preparing nanoparticles and is widely applicable in the field of biomedicine since the materials used are usually non-toxic in nature.<sup>101</sup> The term ‘co-precipitation’ describes the phenomenon in which precipitation of usually soluble compounds occur by grain growth and nucleation, under inert nitrogen atmosphere at either room temperature or elevated temperature. This methodology also offers a way of incorporating metal nanoparticles into the porous materials.<sup>102,103</sup> In a recent report, a sulfonated magnetic solid acid catalyst was prepared via the co-precipitation method where  $\text{Fe}_3\text{O}_4$  nanoparticles was incorporated in the sulfonated cassava peel biochar.<sup>104</sup>

Another work on the synthesis of magnetically active ZnO/BiFeO<sub>3</sub> solid acid catalyst by co-precipitation method was reported and used for the production of biodiesel.<sup>105</sup>

In a recent report, a core-shell SO<sub>4</sub>/Mg-Al-Fe<sub>3</sub>O<sub>4</sub> magnetic solid acid catalyst was prepared *via* co-precipitation method and used for the efficient transesterification of waste cooking oil.<sup>106</sup>

### **1.7.2 Impregnation**

This methodology involves the filling up of porous support by metal nanoparticles. In this method, a metal salt, usually chloride or nitrate is dissolved in a suitable solvent of adequate volatility and solubility. The metal salt solution is then added dropwise onto the porous support under vigorous stirring when the metal nanoparticles fill up the pores of the support, resulting in the formation of a thick paste. The residual solvent is then removed and the solid left is then calcined or reduced by using a reducing agent.<sup>107,108</sup> Sodium/zinc oxide deposited SBA-15 catalyst was prepared *via* the one-pot impregnation method.<sup>109</sup> A study revealed that lithium/zinc can be loaded on waste chicken bones (Li/Zn-Cb) by impregnation method and the resulting solid acid displayed enhanced catalytic activity.<sup>110</sup> Another study on the synthesis of ZrO<sub>2</sub>-supported on bamboo leaf ash (ZrO<sub>2</sub>/BLA) *via* impregnation method was reported.<sup>111</sup> The prepared catalyst exhibited potent activity in biodiesel conversion.

---

### 1.7.3 Hydrothermal

The hydrothermal synthesis is a versatile chemical method for the synthesis of metal nanoparticles. This methodology provides uniform control over the shape, size and particle distribution of the metal nanoparticles, allowing tuning of the properties to generate nanoparticles of sizes varying from a few nanometers to several hundred.<sup>112,113</sup> The hydrothermal synthesis can be performed in two types of systems, namely, the batch hydrothermal, which allows to carry out with the ratio phases as desired, and the continuous hydrothermal, with the help of which a high reaction rate can be achieved within a shorter period of time.<sup>114</sup> It is an eco-friendly technique as post-treatments are not required and is able to synthesize a large amount of nanoparticles with optimized composition and morphology.<sup>115,116</sup> The particle size depends upon the time of exposure, the concentration of the precursor and the temperature of the reaction.<sup>117</sup> Silica supported zirconium catalyst was prepared by the hydrothermal method which was further sulfated to obtain sulfated Zr-KIT-6 (x) ( $x = \text{Si/Zr}$ ).<sup>118</sup> A study was conducted on the synthesis of zirconia tungstophosphoric heteropolyacid *via* hydrothermal method and the prepared heterogeneous acid catalyst demonstrated enhanced activity.<sup>119</sup> In a recent report, sulfonic acid functionalized mesoporous double-layer carbon microspheres were prepared *via* hydrothermal technique.<sup>120</sup> The prepared acidic catalyst was efficiently used in transesterification.



**1.7.4 Sol-Gel synthesis**

The sol-gel process is a method of creating a 3D network by formation of a colloidal solution i.e. sol, followed by drying or ‘gelling’ of the resulting solution to form a network.<sup>121</sup> This process consists of two components, ‘sol’ in which a solid is dispersed in a liquid to form a colloidal suspension and ‘gel’ which is a polymer containing liquid. The sol-gel process involves the use of two steps, the first step is hydrolysis where water is used to break the bonds in the precursor, and the second step involves condensation in which nanomaterial is formed after the removal of excess water. The shape and size of the nanoparticles is controlled by the sol/gel transition. The precursor used in the process for preparing colloid is usually a metal or metalloid element surrounded by various reactive ligands. The sol-gel process can be performed at room temperature and the particle size and shape is controlled by the sol/gel transition.<sup>122</sup> This method has gained immense interest because it can be used for the preparation of oxide materials and some inorganic materials such as ceramics and glass. A report exhibits the preparation of tungsten supported  $\text{TiO}_2/\text{SiO}_2$  solid acid catalyst via the sol-gel technique.<sup>123</sup> In another report, solid acid catalyst containing  $\text{TiO}_2\text{-Cu}_2\text{O}$  was prepared via the sol-gel technique.<sup>124</sup> A study revealed the preparation of mesoporous  $\text{MoO}_3/\text{SiO}_2$  solid acid catalyst by using sol-gel technique with varying amounts of  $\text{MoO}_3$ .<sup>125</sup> The catalyst with 20 mol%  $\text{MoO}_3$  exhibited enhanced activity in the acetalization of glycerol with benzaldehyde.

Another work on the synthesis of silica-alumina solid acid catalyst by sol-gel method has been reported and used for cracking of cumene.<sup>126</sup>

### **1.7.5 Electrochemical reduction**

In the year 1994, Reetz and group developed electrochemical reduction method for the synthesis of monometallic and bimetallic nanoparticles.<sup>127</sup> This method consists of six steps (i) oxidative dissolution of sacrificial metal anode, (ii) migration of cations to the cathode, (iii) formation of reduced metal species at the cathode, (iv) nucleation and grain growth leading to the formation of metal particles, (v) use of stabilising agents such as tetra alkylammonium ions, and (vi) precipitation of the formed metal nanostructured colloid. A combination of electrochemical reduction and ‘wet chemical’ methods could also be used for the synthesis of core shell nanoparticles with high surface area.<sup>128</sup>

### **1.7.6 Mechanical grinding**

Mechanical grinding is a simple and popular method for the synthesis of nanocrystalline materials. This method involves the use of inexpensive equipment and is applicable for the synthesis of practically, all types of materials. Amorphous or nanocrystalline alloy particles, elemental or compound powders can be synthesized by the application of this technique.<sup>129</sup>  $\text{Li}_2\text{TiO}_3$  was prepared by a solid state reaction through mixing of  $\text{TiO}_2$  and  $\text{Li}_2\text{CO}_3$ , followed by grinding.<sup>130</sup> After calcination at 1073.15 K, final  $\text{Li}_2\text{TiO}_3$  acid catalyst was obtained.

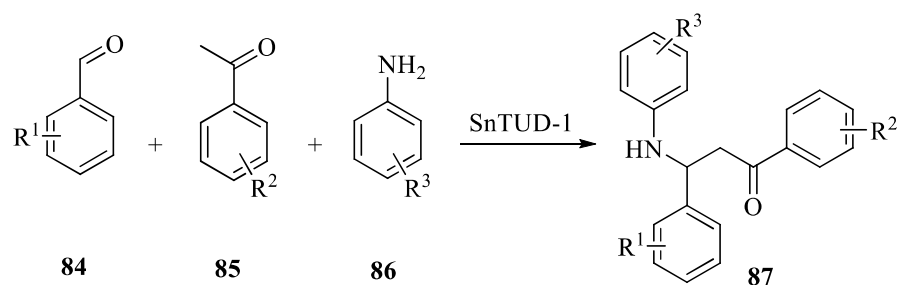
**1.8 Industrial applications of solid acid catalysts**

Heterogeneous solid acid catalysts have gained tremendous attention in recent years due to their widespread applications in the field of organic synthesis. Development of alternative methodologies employing supported catalysts for the already known organic transformations is of utmost importance at present time and this poses a challenging task to the organic chemists. Various solid acid catalysts have been developed in recent decades and their catalytic applications have been studied in a plethora of industrially important organic reactions. Solid acid catalysts are also used to catalyze diverse aspects of organic synthesis for the production of fine chemicals, pharmaceuticals, agrochemicals, and specialty chemicals.

Heterocyclic compounds are inevitable components in biological and medicinal chemistry. They are present in a wide variety of natural products and biologically active compounds, and are known to exhibit therapeutic properties ranging from anticancer, antimalarial, antibacterial, anti-HIV, antidepressant, antidiabetic, anti-inflammatory, anti-depressant and many others. Also, they have been frequently found as a key structural unit in synthetic pharmaceuticals and agrochemicals. Many of the heterocycles finds important applications in material science such as dyes, brightening agents, plastics and fluorescent sensors. Heterocycles are also of considerable interest in industrial development because of their synthetic utility as intermediates, protecting groups, catalysts and metal ligands of asymmetric catalysts.

---

Friedel-Crafts alkylation is an industrially important organic transformation used for the production of a number of different chemical compounds. Classical Friedel-Crafts reaction proceeds under strong acidic conditions. Usually, homogeneous acid catalysts such as HF and AlCl<sub>3</sub> have been widely used for the purpose. The process is associated with severe drawbacks such as corrosion and non-recyclability of the acids. To mitigate the problem several heterogeneous solid acid catalysts have been developed. Zhang et al. prepared sulfonated polystyrene confined in a benzene-silica hollow nanosphere with yolk-double-shell nanostructure and successfully applied the solid acid catalyst in Friedel-Crafts alkylation.<sup>131</sup> High yield of the desired product was obtained within a short span of time and the catalyst exhibited high thermal stability and recyclability. Tin based silicates have been employed in a number of organic transformations and industrially relevant processes.<sup>132</sup> Pachamuthu et al. prepared a nanostructured tin oxide incorporated in silica matrix (SnTUD-1) and utilized the heterogeneous solid acid catalyst in the three-component Mannich type reaction (Scheme 25).<sup>133</sup>



**Scheme 25.** SnTUD-1 catalyzed three-component Mannich type reaction

Currently, the over-exploitation of fossil fuels has generated the urgent need to search for renewable sources of energy. There are four alternatives such as natural gas, syngas, hydrogen and biofuel. Among these, biofuel is the most suitable renewable energy and can be used directly without any modification. Biofuels are liquid fuels synthesized from plants, agricultural waste products, forestry by-products and municipal waste.<sup>134</sup> Biodiesel is the only biofuel that can be used on its own or mixed with petroleum fuel without any modification in conventional engine. Biodiesel does not contain any sulfur and aromatics and so offers advantages over conventional fossil fuels such as low exhaust emission, biodegradability, non-toxicity, sustainability and renewability. The use of biodiesel leads to reduced emission of pollutant during combustion. With the advancement of technology, various routes have been developed for the production of biodiesel from renewable sources such as microorganisms, animal fat, non-edible seeds and plant oil.<sup>135</sup> However, the cost of production of biodiesel is quite high which may be attributed to the production methodologies. Strong mineral acids such as sulfuric acid and hydrochloric acid, and strong bases such as sodium hydroxide and potassium hydroxide are generally employed for the process. However, the use of these homogeneous catalytic systems poses major challenges to industry as the separation of the catalyst from the reaction mixture is quite difficult. Additionally, the liquid catalysts cause corrosion and contamination of the equipment and have to be neutralized after the completion of the reaction. Neutralization produces large

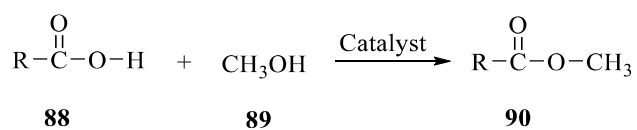
---

amount of salt which are difficult to discharge. The catalysts can also be removed by using hot water but this result in the generation of a large quantity of waste water.<sup>136</sup>

This urges the need of the time to develop a greener approach for biodiesel synthesis and lead to the application of environment friendly solid acid catalysts as alternative.

The use of solid acid catalyst minimizes the generation of waste since neutralization of the acid catalyst is not required and the catalyst can be easily separated from the product mixture. The catalyst does not cause contamination and corrosion of the metal equipment and enhances the rate of the reaction. It promotes simultaneous esterification and transesterification reactions without the formation of soap.<sup>137,138</sup>

Zirconium sulfate tetrahydrate impregnated tubular carbon membrane ((Zr(SO<sub>4</sub>)<sub>2</sub>.4H<sub>2</sub>O)/TCM) was prepared by Ma et al. by varying the surface loadings of zirconium. The high specific surface area of the heterogeneous solid acid catalyst enabled it to be used for the esterification of acidified oil with methanol.<sup>139</sup> Ballotin et al. prepared sulfonated carbon nanostructures embedded in amorphous carbon which was obtained from bio-oil.<sup>140</sup> This acidic catalyst was then used for the esterification of oleic acid **88** with methanol (**89**) (Scheme 26).



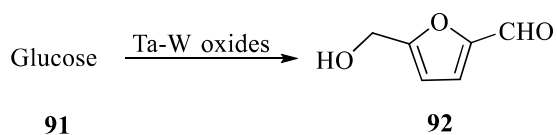
**Scheme 26.** Esterification of oleic acid with methanol catalyzed by sulfonated carbon nanostructures embedded in amorphous carbon

In a very recent report, Fe<sub>3</sub>O<sub>4</sub>/SiO<sub>2</sub> solid nanocatalyst was prepared and used for the esterification of soybean oil with methanol.<sup>141</sup>

5-Hydroxymethylfurfural (HMF) is a promising platform chemical and has gained tremendous attention in recent decades due to its versatile applications in bio-refinery.<sup>142-145</sup> HMF can be transformed into a number of value-added products such as 2,5-dimethylfuran, 1,6-hexanediol, 2,5-diformylfuran and 2,5-furandicarboxylic acid.<sup>146,147</sup> HMF has found extensive applications as a monomer in the synthesis of liquid biofuels, chemical products and other bio-based materials used in pharmaceuticals and petrochemical industries.<sup>148</sup> Due to the growing demand, various methodologies have been developed for the synthesis of this highly important chemical. However, so far, its large-scale production still remains a challenge. HMF is generally prepared by the dehydration of hexose sugars such as fructose, glucose, cellulose, cellobiose, and sucrose in acidic medium.<sup>149,150</sup> Among these, fructose is the most facile candidate for HMF production and the conversion is mainly catalyzed by Brønsted acids.<sup>151</sup> In recent years, the conversion of biomass-based carbohydrates into HMF has been studied using Lewis acids, mineral acids, and bifunctional catalysts.<sup>152</sup> Due to the drawbacks associated with the homogeneous catalytic systems, heterogeneous acid catalysts have emerged as robust alternative with stronger acidity and easy regenerability. Various solid acid catalysts have been designed for the purpose, such as carbon, tungstated zirconia, heteropoly acids, and zirconium phosphates.<sup>153-156</sup> TiO<sub>2</sub>-ZrO<sub>2</sub> mixed metal oxide catalyst was prepared and

---

employed for the efficient conversion of glucose to HMF.<sup>157</sup> Guo et al. prepared Ta-W oxides with varying ratios of Ta/W and used the catalyst for the dehydration of glucose (**91**) and fructose to HMF (**92**) (Scheme 27).<sup>158</sup>



**Scheme 27.** Conversion of glucose to HMF catalyzed by Ta-W oxides

Zhang and co-workers prepared a carbonaceous solid acid catalyst from microalgae residue and used it as for the conversion of fructose to HMF.<sup>159</sup>

## 1.9 Objective and scope of the work

In view of the literature discussed above, it is evident that there is ever increasing demand of replacement of conventional homogeneous catalysts by heterogeneous counterparts. The use of heterogeneous acid catalysts in organic transformations can meet the goals of sustainable and green chemistry. The present work is aimed at preparing solid acids, followed by its application in different organic reactions.

The objectives of my thesis are-

- Synthesis of a few cellulose and silica supported solid catalysts and their characterization through different analytical tools.



- Application of the synthesized catalysts towards different acid catalyzed reactions leading to improved synthesis of many important heterocyclic compounds.
- Characterization of the synthesized compounds by different analytical techniques and evaluation of antibacterial activity of a few selected compounds.

Taking into consideration the numerous advantages of the supports, the solid acid catalysts reported in the thesis are prepared by embedding metal oxides and metal nanoparticles on silica and cellulose supports. The prepared heterogeneous acids were then characterized by using different analytical tools like HR-TEM, EDX, FT-IR, XRD, BET, XPS and TGA in order to understand the physicochemical properties. Application of the prepared solid acids in organic transformations such as synthesis of dihydroquinazolines, synthesis of platform chemical 5-hydroxymethylfurfural, domino-Knoevenagel-Hetero-Diels-Alder reaction and diazo transfer click reaction has been studied. Some of the advantages offered by these solid catalysts involve easy work-up, enhanced product yield, environment friendliness and short reaction time. It was also observed that the catalysts were recyclable upto several consecutive cycles without any significant loss in activity. This suggested that the prepared catalysts did not undergo any deactivation during reaction. Due to the easy preparation methodologies and high thermal stability as well as good recyclability, the

prepared catalysts can find widespread applications in petrochemical, pharmaceutical and chemical industries. Additionally, they can be explored in a variety of greener organic transformations.

---

**1.10 References**

1. C. H. Bartholomew and R. J. Farrauto, Fundamentals of Industrial Catalytic Processes, *John Wiley & Sons*, 2011.
2. G. Ertl, H. Knzinger and J. Weitkamp, Handbook of Heterogeneous Catalysis, *Wiley-VCH*, 1997.
3. J. V. Houten, *J. Chem. Educ.* 2002, **79**, 146.
4. J. Hagen, Industrial Catalysis: A Practical Approach, *Wiley-VCH*, 2015.
5. A. Alsalme, E. F. Kozhevnikova and I. V. Kozhevnikov, *Appl. Catal. A-Gen.* 2010, **390**, 219.
6. S. Sahebdehfar, M. Kazemeini, F. Khorasheh and A. Badakhshan, *Chem. Eng. Sci.* 2002, **57**, 3611.
7. N. A. Khan, D. K. Mishra, I. Ahmed, J. W. Yoon, J. S. Hwang and S. H. Jhung, *Appl. Catal. A-Gen.* 2013, **452**, 34.
8. S. Bhagat, R. Sharma and A. K. Chakraborti, *J. Mol. Catal. A-Chem.* 2006, **260**, 235.
9. I. Fatimah, K. Wijaya and K. H. Setyawan, *Bull. Chem. React. Engg. Catal.* 2008, **3**, 9.
10. M. Zhu, *Catal. Lett.* 2014, **144**, 1568.
11. W. Yu, M. Wen, G. Y. Zhao, L. Yang and Z. L. Liu, *Chinese Chem. Lett.* 2006, **17**, 15.

12. C. Nicolaidis, M. S. Scurell and P. M. Semano, *Appl. Catal. A-Gen.* 2003, **245**, 43.
13. M. A. Ali, T. Kimura, Y. Suzuki, M. A. Al-saleh, H. Hamid and T. Inui, *Appl. Catal. A Gen.* 2002, **277**, 63.
14. D. Chen, Z. Xue and Z. Su, *J. Mol. Catal. A-Chem.* 2003, **203**, 307.
15. A. Patel and V. Brahmkhatri, *Fuel Process. Technol.* 2013, **113**, 141.
16. M. K. Lam, K. T. Lee and A. R. Mohamed, *Biotechnol. Adv.* 2010, **28**, 500.
17. K. Ngaosuwan, J. G. Goodwin and P. Prasertdham, *Renew. Energy.* 2016, **86**, 262.
18. C. M. A. Parlett, K. Wilson and A. F. Lee, *Chem. Soc. Rev.* 2013, **42**, 3876.
19. H. Juntgen, *Fuel* 1986, **65**, 1436.
20. G. M. Ziarani, N. Lashgari and A. Badiiei, *J. Mol. Catal. A-Chem.* 2015, **397**, 166.
21. C. Pirez, J. M. Caderon, J. P. Dacquin, A. F. Lee and K. Wilson, *ACS Catal.* 2012, **2**, 1607.
22. S. Khire, V. Bhagwat, M. Fernandes, B. Gangundi and H. Vadalía, *Indian J. Chem. Technol.* 2012, **19**, 342.
23. K. Arata, *Green Chem.* **2009**, 11, 1719.

24. L. R. V. da Conceição, C. E. R. Reis, R. de Lima, D. V. Cortez and H. F. de Castro, *RSC Adv.* 2019, **9**, 23450.
25. J. Alcañiz-Monge, B. E. Bakkali, G. Trautwein and S. Reinoso, *Appl. Catal. B-Environ.* 2018, **224**, 194.
26. M. Kazemi and L. Shiri, *Mini. Rev. Org. Chem.* 2017, **15**, 86.
27. M. Kazemi and M. Mohammadi, *Appl. Organometal. Chem.* 2020, **34**, 5400.
28. A. Ghorbani-Choghamarani, M. Mohammadi, L. Shiri and Z. Taherinia, *Res. Chem. Intermed.* 2019, **45**, 5705.
29. M. Mohammadi and A. Ghorbani-Choghamarani, *New J. Chem.* 2020, **44**, 2919.
30. (a) N. Linares, A. M. Silvestre-Albero, E. Serrano, J. Silvestre-Albero and J. Garcia-Martinez, *Chem. Soc. Rev.* 2014, **43**, 7681; (b) C. Perego and R. Millini, *Chem. Soc. Rev.* 2013, **42**, 3956; (c) Z. Zhou and M. Hartmann, *Chem. Soc. Rev.* 2013, **42**, 3894.
31. (a) L. B. Sun, X. Q. Liu and H. C. Zhou, *Chem. Soc. Rev.* 2015, **44**, 5092; (b) P. Yang, S. Gai and J. Lin, *Chem. Soc. Rev.* 2012, **41**, 3679; (c) E. Doustkhah, S. Rostamnia, H. G. Hossieni and R. Luque, *ChemistrySelect* 2017, **2**, 329; (d) M. Zarei, M. A. Zolfigol, A. R. Moosavi-Zare, E. Noroozizadeh and S. Rostamnia, *ChemistrySelect* 2018, **3**, 12144.
32. K. Zeng, Z. Huang, J. Yang and Y. Gu, *Chinese J. Catal.* 2015, **36**, 1606.
-

33. K. Niknam, A. Deris, F. Naeimi and F. Majleci, *Tetrahedron Lett.* 2011, **52**, 4642.
34. P. U. Jain and S. D. Samant, *ChemistrySelect* 2020, **5**, 4437.
35. M. A. Zolfigol, F. Shirini, K. Zamani, E. Ghofrani and S. Ebrahimi, *Phosphorus, Sulfur Silicon Relat. Elem.* 2004, **179**, 2177.
36. R. Maggi, G. Martra, C. G. Piscopo, G. Alberto and G. Sartori, *J. Catal.* 2012, **294**, 19.
37. F. Zaccheria, F. Santoro, R. Psaro and N. Ravasio, *Green Chem.* **2011**, **13**, 545.
38. A. Bamoniri, B. B. F. Mirjalili and S. Fouladgar, *J. Taiwan Inst. Chem. Eng.* 2016, **63**, 396.
39. H. Emtiazi, M. A. Amrollahi and B. B. F. Mirjalili, *Arab. J. Chem.* 2015, **8**, 793.
40. M. D. Morales, A. Infantes-Molina, J. M. Lázaro-Martínez, G. P. Romanelli, L. R. Pizzio and E. Rodríguez-Castellón, *Mol. Catal.* 2020, **485**, 110842.
41. S. N. Rashkeev, K. Sohlberg, M. V. Glazoff, J. Novak, S. J. Pennycook and S. T. Pantelides, *Phys. Rev.* 2003, **67**, 1.
42. H. R. Shaterian, K. Azizi and N. Fahimi, *Arab. J. Chem.* 2017, **10**, 42.
43. E. Yang, E. J. Jang, J. G. Lee, S. Yoon, J. Lee, N. Musselwhite, G. A. Somorjai, J. H. Kwak and K. An, *Catal. Sci. Technol.* 2018, **8**, 3295.
-

44. V. S. Marakatti, D. Mumbaraddi, G. V. Shanbhag, A. B. Halgeri and S. P. Maradur; *RSC Adv.* 2015, **5**, 93452.
45. M. Khoshnevis, A. Davoodnia, A. Zare-Bidaki and N. Tavakoli-Hoseini, *Synth. React. Inorg. M.* 2013, **43**, 1154.
46. N. Bhatt and A. Patel, *J. Taiwan Inst. Chem. Eng.* 2011, **42**, 356.
47. S. Namba, N. Hosonuma and T. Yashima, *J. Catal.* 1981, **72**, 16.
48. A. M. G. Pedrosa, M. J. B. Souza, A. O. S. Silva, D. M. A. Melo and A. S. Araujo, *Catal. Commun.* 2006, **7**, 791.
49. D. Das and S. Cheng, *Appl. Catal. A-Gen.* 2000, **201**, 159.
50. J. Bedard, H. Chiang and A. Bhan, *J. Catal.* 2012, **290**, 210.
51. V. S. P. Ganjala, C. K. P. Neeli, C. V. Promod, M. Khagga, K. S. R. Rao and D. R. Burri, *Catal. Commun.* 2014, **49**, 82.
52. V. D. Chaube, *Catal. Commun.* 2004, **5**, 321.
53. W. Li, S. Liu, H. Wang, B. Gao, C. Tu and Y. Luo, *Catal. Commun.* 2020, **133**, 105845.
54. Y. Guo and Z. Zhao, *Chem. Eng. Sci.* 2019, **201**, 25.
55. J. Park, Y. Hwang and S. Bae, *J. Hazard. Mater.* 2019, **374**, 309.
56. R. Ramos, A. Grigoropoulos, B. L. Griffiths, A. P. Katsoulidis, M. Zanella, T. D. Manning, F. Blanc, J. B. Claridge and M. J. Rosseinsky, *J. Catal.* 2019, **375**, 224.

57. S. Shen, B. Cai, C. Wang, H. Li, G. Dai and H. Qin, *Appl. Catal. A-Gen.* 2014, **473**, 70.
58. X. Qi, N. Liu and Y. Lian, *RSC Adv.* 2015, **5**, 17526.
59. M. E. Chimienti, L. R. Pizzio, C. V Cáceres and M. N. Blanco, *Appl. Catal. A- Gen.* 2001, **208**, 7.
60. A. Shokrolahi, A. Zali and H. R. Pouretedal, *Iran. J. Catal.* 2011, **1**, 37.
61. S. Kang, J. Ye and J. Chang, *Int. Rev. Chem. Eng.* 2013, **5**, 133.
62. N. Yang, D. Zhang, J. Zhou, C. Qi, C. Li and F. Zhang, *ChemistrySelect* 2020, **5**, 3613.
63. M. Fauziyah, W. Widiyastuti and H. Setyawan, *Adv. Powder Technol.* 2020, **31**, 1412.
64. J. H. Advani, A. S. Singh, N. H. Khan, H. C. Bajaj and A. V. Biradar, *Appl. Catal. B-Environ.* 2020, **268**, 118456.
65. S. S. Wang, X. Chen, Y. Tan, Z. Zhao, W. Yang, C. Huang, X. Wang, M. M. Chen, Z. Du and Y. Ding, *Mol. Catal.* 2020, **485**, 110840.
66. D. Zhang, T. Xu, C. Li, W. Xu, J. Wang and J. Bai, *J. CO<sub>2</sub> Util.* 2019, **34**, 716.
67. S. Chu, H. Cao, T. Chen, Y. Shi and L. Yu, *Catal. Commun.* 2019, **129**, 105730.
68. M. Ahmadi, L. Moradi and M. Sadeghzadeh, *Appl. Organometal. Chem.* 2019, **33**, 4980.
-



69. D. W. O'Connell, C. Birkinshaw and T. F. O'Dwyer, *Bioresour. Technol.* 2008, **99**, 6709.
70. K. F. Shelke, S. B. Sapkal, G. K. Kakade, B. B. Shingate and M. S. Shingare, *Green Chem. Lett. Rev.* 2010, **3**, 27.
71. A. Shaabani and A. Maleki, *Appl. Catal. A-Gen.* 2007, **331**, 149.
72. G. Nagendrappa, *Appl. Clay Sci.* 2011, **53**, 106.
73. V. R. Choudhary, R. Jha and P. A. Choudhari, *J. Chem. Sci.* 2005, **117**, 635.
74. G. A. Olah, J. Kaspi and J. Bukala, *J. Org. Chem.* 1977, **42**, 4187.
75. T. Jin, S. Zhang and T. Li, *Synth. Commun.* 2002, **32**, 1847.
76. M. M. Sharma, *React. Polym.* 1995, **26**, 3.
77. M. S. M. da Silva, C. L. da Costa, M. de M. Pinto and E. R. Lachter, *React. Polym.* 1995, **25**, 55.
78. R. Pal, T. Sarkar and S. Khasnobis, *Arkivoc* 2012, **1**, 570.
79. G.-T. Jeong, S.-K. Kim and D.-H. Park, *Bioresour. Technol.* 2015, **181**, 1.
80. A. Heydari, S. Khaksar, M. Pourayoubi and A. R. Mahjoub, *Tetrahedron Lett.* 2007, **48**, 4059.
81. A. Kamal, K. S. Babu, S. M. A. Hussaini, P. S. Srikanth, M. Balakrishna and A. Alarifi, *Tetrahedron Lett.* 2015, **56**, 4619.
82. R. M. N. Kalla, H. Park and T. T. K. H. Kim, *Tetrahedron Lett.* 2014, **55**, 5373.

83. M. Takabatake, M. Nambo, Y. Manaka and K. Motokura, *ChemPlusChem* 2020, **85**, 450.
84. E. Ali, M. R. Naimi-Jamal and R. Ghahramanzadeh, *ChemistrySelect* 2019, **4**, 9033.
85. S. Agarwal, R. Poddar, M. Kidwai and M. Nath, *ChemistrySelect* 2018, **3**, 10909.
86. M. Farahi, M. Davoodi and M. Tahmasebi, *Tetrahedron Lett.* 2016, **57**, 1582.
87. A. Banan, H. Valizadeh, A. Heydari and A. Moghimi, *Appl. Organometal. Chem.* 2017, **32**, 3944.
88. R. Singh, A. Singh and D. Bhardwaj, *ChemistrySelect* 2019, **4**, 9600.
89. S. Sharma, H. Sharma, S. Sharma, S. Paul, V. K. Gupta, N. Boukabcha and A. Chouaih, *ChemistrySelect* 2020, **5**, 2201.
90. L. Parashuram, S. Sreenivasa, S. R. Akshatha, V. U. Kumar and S. Kumar, *ChemistrySelect* 2019, **4**, 5097.
91. R. Vaid, M. Gupta, G. Kour and V. K. Gupta, *ChemistrySelect* 2019, **4**, 9179.
92. H. Naeimi and Z. Ansarian, *J. Taiwan Inst. Chem. Eng.* 2018, **85**, 265.
93. F. K. Esfahani, D. Zareyee, A. S. Rad and S. Taher-Bahrami, *Appl. Organometal. Chem.* 2017, **31**, 3865.

94. Z. Zhang, Y. Zhu, C. Zhou, Q. Liu, H. Lu, Y. Ge and M. Wang, *Acta Pharmacol. Sin.* 2014, **35**, 664.
95. Z. Zare-Akbari, S. Dastmalchi, L. Edjlali, L. Dinparast and M. Es'haghi, *Appl. Organometal. Chem.* 2020, **34**, 5649.
96. L. Moradi and P. Mahdipour, *Appl. Organometal. Chem.* 2019, **33**, 4996.
97. L. Moradi and M. Tadayon, *J. Saudi Chem. Soc.* 2018, **22**, 66.
98. P. Biginelli, *Gazz. Chim. Ital.* 1893, **23**, 360.
99. S. Azad and B. B. F. Mirjalili, *Mol. Divers.* 2019, **23**, 413.
100. Y. Z. Han, L. Hong, X. Q. Wang, J. Z. Liu, J. Jiao, M. Luo and Y. J. Fu, *Ind. Crops Prod.* 2016, **89**, 332.
101. M. Osial, P. Rybicka, M. Pękała, G. Cichowicz, M. K. Cyrański, P. Krysiński, *Nanomaterials* 2018, **8**, 430.
102. A. Barau, V. Budarin, A. Caragheorgheopol, R. Luque, D. J. Macquarrie, A. Prella, V. S. Teodorescu and M. Zaharescu, *Catal. Lett.* 2008, **124**, 204.
103. H. Liu, D. Ma, R. A. Blackley, W. Zhou and X. Bao, *Chem. Commun.* 2008, **23**, 2677.
104. S. Chellappan, K. Aparna, C. Chingakham, V. Sajith and V. Nair, *Fuel* 2019, **246**, 268.
105. Z. Salimi and S. A. Hosseini, *Fuel* 2019, **239**, 1204.

106. J. Gardy, E. Nourafkan, A. Osatiashtiani, A. F. Lee, K. Wilson, A. Hassanpour and X. Lai, *Appl. Catal. B-Environ.* 2019, **259**, 118093.
107. J. M. Campelo, A. F. Lee, D. Luna, R. Luque, J. M. Marinas and A. A. Romero, *Chem. Eur. J.* 2008, **14**, 5988.
108. X. Chen, H. Y. Zhu, J. C. Zhao, Z. F. Zheng and X. P. Gao, *Angew. Chem. Int. Ed.* 2008, **120**, 5433.
109. R. Malhotra and A. Ali, *Renew. Energy* 2019, **133**, 606.
110. M. AlSharifi and H. Znad, *Renew. Energy* 2019, **136**, 856.
111. I. Fatimah, D. Rubiyanto, A. Taushiyah, F. B. Najah, U. Azmi and Y.-L. Sim, *Sustain. Chem. Pharm.* 2019, **12**, 100129.
112. K. Nejati and R. Zabihi, *Chem. Cent. J.* 2012, **6**, 394.
113. A. Lassoued, M. S. Lassoued, B. Dkhil, S. Ammar and A. Gadri, *Phys. E Low-Dimens. Syst. Nanostruct.* 2018, **101**, 212.
114. H. Hayashi and Y. Hakuta, *Materials* 2010, **3**, 3794.
115. M. Wegmann and M. Scharr, Synthesis of iron oxide magnetic nanoparticles, *Elsevier Inc.* 2018.
116. A. Abedini, A. R. Daud, M. A. A. Hamid, N. K. Othman and E. Saion, *Nanoscale Res. Lett.* 2013, **8**, 1.
117. S. Gyergyek, D. Makovec, M. Jagodič, M. Drogenik, K. Schenk, O. Jordan, J. Kovač, G. Dražič and H. Hofmann, *J. Alloys Compd.* 2017, **694**, 261.
-

118. S. Gopinath, P. S. M. Kumar, K. A. Y. Arafath, K. V. Thiruvengadaravi, S. Sivanesan and P. Baskaralingam, *Fuel* 2017, **203**, 488.
119. J. Alcañiz-Monge, B. E. Bakkali, G. Trautwein and S. Reinoso, *Appl. Catal. B-Environ.* 2018, **224**, 194.
120. L. Yang, S. Wang, H. Yuan and H. Liu, *J. Chem. Technol. Biot.* 2019, **94**, 3538.
121. S. F. Hasany, I. Ahmed, J. Rajan and A. Rehman, *Nanosci. Nanotechnol.* 2013, **2**, 148.
122. K. Raja, M. M. Jacqueline, M. Jose, S. Verma, A. A. M. Prince, K. Ilangovan, K. Sethusankar and S. J. Das, *Superlattices Microstruct.* 2015, **86**, 306.
123. M. Kaur, R. Malhotra and A. Ali, *Renew. Energy* 2018, **116**, 109.
124. A. Patil, S. S. Baral, P. Dhanke and V. Kore, *Mater. Today Proc.* 2020, **27**, 198.
125. S. B. Umbarkar, T. V. Kotbagi, A. V. Biradar, R. Pasricha, J. Chanale, M. K. Dongare, A.-S. Mamede, C. Lancelot and E. Payen, *J. Mol. Catal. A-Chem.* 2009, **310**, 150.
126. R. Takahashi, S. Sato, T. Sodesawa and M. Yabuki, *J. Catal.* 2001, **200**, 197.
127. M. T. Reetz and W. Helbig, *J. Am. Chem. Soc.* 1994, **116**, 7401.
-

128. L. D. Pachon, M. B. Thathagar, F. Hartl and G. Rothenberg, *Phys. Chem. Chem. Phys.* 2006, **8**, 151.
129. A. Alagarasi, Introduction to nanomaterials, *Narosa Publishing House*, 2009.
130. Y. M. Dai, I. H. Kao and C. C. Chen, *J. Taiwan Inst. Chem. Eng.* 2017, **70**, 260.
131. X. Zhang, Y. Zhao and Q. Yang, *J. Catal.* 2014, **320**, 180.
132. M. Boronat, P. Concepcion, A. Corma and M. Renz, *Catal. Today*, 2007, **121**, 39.
133. M. P. Pachamuthu, K. Shanthi, R. Luque and A. Ramanathan, *Green Chem.* **2013**, 15, 2158.
134. M. Balat and H. Balat, *Appl. Energy* 2009, **86**, 2273.
135. K. Y. Wong, J.-H. Ng, C. T. Chong, S. S. Lam and W. T. Chong, *Renew. Sustain. Energy Rev.* 2019, **116**, 109399.
136. N. Diamantopoulos, D. Panagiotaras and D. Nikolopoulos, *J. Thermodyn. Catal.* 2015, **6**, 1.
137. C. Descorme, P. Gallezot, C. Geantet and C. George, *ChemCatChem* 2012, **4**, 1897.
138. A. Sivasamy, K.Y. Cheah, P. Fornasiero, F. Kemausuor and S. Zinoviev, S. Miertus, *ChemSusChem* 2009, **2**, 278.

139. L. Ma, E. Lv, L. Du, Y. Han, J. Lu and J. Ding, *J. Energy Inst.* 2017, **90**, 875.
140. F. C. Ballotin, M. J. da Silva, R. M. Lago and A. P. C Teixeira, *J. Environ. Chem. Eng.* 2020, **8**, 103674.
141. W. Xie and H. Wang, *Renew. Energy* 2020, **145**, 1709.
142. Y. L. Zhang, P. Jin, M. Liu, J. M. Pan, Y. S. Yan, Y. Chen and Q. G. Xiong, *AIChE J.* 2017, **63**, 4920.
143. A. A. Rosatella, S. P. Simeonov, R. F. M. Frade and C. A. M. Afonso, *Green Chem.* 2011, **13**, 754.
144. J. Z. Chen, K. Q. Li, L. M. Chen, R. L. Liu, X. Huang and D. Q. Ye, *Green Chem.* 2014, **16**, 2490.
145. Y. L. Zhang, P. Jin, M. Liu, J. M. Pan, Y. S. Yan, Y. Chen and Q. G. Xiong, *AIChE J.* 2017, **63**, 4920.
146. G. Y. Li, N. Li, Z. Q. Wang, C. Z. Li, A. Q. Wang, X. D. Wang, Y. Cong and T. Zhang, *ChemSusChem.* 2012, **5**, 1958.
147. Y. L. Zhang, J. M. Pan, Y. Chen, W. D. Shi, Y. S. Yan and L. B. Yu, *Chem. Eng. J.* 2016, **283**, 956.
148. I. Elsayed, M. Mashaly, F. Eltaweel, M. A. Jackson and E. B. Hassan, *Fuel* 2018, **221**, 407.
149. Q. D. Hou, M. N. Zhen, L. Liu, Y. Chen, F. Huang, S. Q. Zhang, W. Z. Li and M. T. Ju, *Appl. Catal. B-Environ.* 2018, **224**, 183.
-

150. P. Bhanja, A. Modak, S. Chatterjee and A. Bhaumik, *ACS Sustain. Chem. Eng.* 2017, **5**, 2763.
151. J. M. Wang, Z. H. Zhang, S. W. Jin and X. Z. Shen, *Fuel* 2017, **192**, 102.
152. V. Choudhary, S. H. Mushrif, C. Ho, A. Anderko, V. Nikolakis, N. S. Marinkovic, A. I. Frenkel, S. I. Sandler and D. G. Vlachos, *J. Am. Chem. Soc.* 2013, **135**, 3997.
153. P. Wataniyakul, P. Boonnoun, A. T. Quitain, M. Sasaki, T. Kida, N. Laosiripojana and A. Shotipruk, *Catal. Commun.* 2018, **104**, 41.
154. R. Kourieh, V. Rakic, S. Bennici and A. Auroux, *Catal. Commun.* 2013, **30**, 5.
155. G. Raveendra, M. Surendar and P. S. S. Prasad, *New J. Chem.* 2017, **41**, 8520.
156. C. Antonetti, M. Melloni, D. Licursi, S. Fulignati, E. Ribechini, S. Rivas, J. C. Parajó, F. Cavani and A. M. R. Galletti, *Appl. Catal. B-Environ.* 2017, **206**, 364.
157. A. A. Silahua-Pavón, C. G. Espinosa-González, F. Ortiz-Chi, J. G. Pacheco-Sosa, H. Pérez-Vidal, J. C. Arévalo-Pérez, S. Godavarthi and J. G. Torres-Torres, *Catal. Commun.* 2019, **129**, 105723.
158. B. Guo, L. He, G. Tang, L. Zhang, L. Ye, B. Yue, S. C. E. Tsang and H. He, *Chinese J. Catal.* 2020, **41**, 1248.
-



159. J. Zhang, S. Yang, Z. Zhang, L. Cui, J. Jia, D. Zhou and B. Zhu,  
*ChemistrySelect* 2019, 4, 1259.

# **Chapter 2**

**Synthesis of silica-supported copper oxide nanoparticles and its application in the synthesis of dihydroquinazoline and hydroxymethyl furfural (HMF)**

---

## 2.1 Introduction

Metal oxide nanoparticles have been widely explored in recent decades due to their valuable contribution in the field of nanoscience and nanotechnology.<sup>1</sup> Owing to their high surface to volume ratio, photocatalytic activity, and low cost these materials are extensively employed as catalysts, antibacterial agents and energy storage devices.<sup>2</sup> Especially, transition metal oxides deserve special mention because of their wide application in electronics, sensors, and catalysis. Among the various transition metal oxides, the copper oxide nanoparticles occupies an integral position due to its novel physiochemical properties.<sup>3</sup> Copper oxide nanoparticles are used in lithium ion batteries, solar cell technology, magnetic resonance imaging, and drug delivery devices.<sup>4</sup> Copper oxide is also known as p-type semiconductors and have found extensive use as heterogeneous catalysts in the complete conversion of hydrocarbon to carbon dioxide and water, photoelectrochemical water splitting, steam reforming, and oxidation of carbon monoxide.<sup>5</sup>

The metal oxide nanoparticles dispersed homogeneously on the surface of a mesoporous material have gained immense interest because they exhibit the combined advantages of the nano-sized particles as well as the matrix support.<sup>6-10</sup> The nano-sized particles allow the applications at the interface of the material by a high exposure of active sites while the matrix support ensures processes such as separation and device fabrication. The nature of interaction between the metal oxide nanoparticles and support is affected by the methods of preparation, application and

regeneration of the catalyst. The interaction between nanoparticles and support leads to proper dispersion of the particles. This results in decrease in particle size and an increase in surface coverage by nanoparticles.<sup>11</sup> The catalytic activity of the supported nanomaterials depends not only upon the dispersion of active metal on the support but also on the extent of accessibility of the pore openings present on the support by the reactant molecules. Additionally, the structure of the pores also determines the dispersion within and the catalytic activity of the supported catalyst. Silica is a nontoxic, biocompatible material with tunable pore diameter, high surface area, high thermal stability and uniform pore channels.<sup>12</sup> This mesoporous material has found widespread applications both as individual catalyst and support of nano sized metal catalysts as well as adsorbent and drug delivery systems.<sup>13-16</sup> Copper oxide nanoparticles embedded on silica support is a widely studied material as the use of silica as a support renders significant increase in different surface characteristics of copper including acidic properties. In recent years, various works have been reported for the efficient synthesis of this nanomaterial and its application in different facets of chemical science. Ghorbanpour et al. prepared silica-supported copper oxide nanoleaf (CuO/SGn) *via* molten salt method.<sup>17</sup> In this report, silica gel was added to CuSO<sub>4</sub> and heated to the melting point temperature of the salt when CuO/SGn was obtained. The prepared catalyst displayed potent antibacterial activity against gram-negative *Escherichia Coli*. Parida and co-worker prepared mesoporous silica impregnated with copper oxide and utilized it for the oxidation of benzene to

phenol.<sup>18</sup> In a report by Kadam and group, hexagonal mesoporous silica-supported copper oxide (CuO/HMS) was prepared by sol-gel technique, and used in the conversion of aldehydes into amines.<sup>19</sup> In a report by Li and co-workers, copper oxide supported on silica matrix (CuO/SiO<sub>2</sub>) was prepared by three different methods, namely, impregnation, deposition-precipitation and ammonia evaporation.<sup>20</sup> Among these, CuO/SiO<sub>2</sub> prepared by ammonia evaporation exhibited better activity towards the ethynylation of formaldehyde. Qiu and co-workers prepared copper oxide supported on mesoporous silica (SBA/CuO) and studied its antibacterial activity against *E. coli* and *S. aureus*.<sup>21</sup> Patel and co-workers prepared copper oxide supported mesoporous silica by wet impregnation method and utilized it for the efficient reduction of NO with CO.<sup>22</sup> Samadi and co-workers reported the preparation of copper oxide nanoparticles encapsulated in mesoporous silica and described its application in the oxidation of allylic C-H bond of cyclic olefins.<sup>23</sup> Barrera-Calva and team prepared silica supported copper oxide thin films by using sol-gel technique and evaluated its application as a solar selective coating.<sup>24</sup> Wang and co-workers, in a report, displayed the preparation of silica supported copper oxide quantum dots (SiO<sub>2</sub>/CuO) by hydrothermal technique and the prepared material showed enhanced photocatalytic activity.<sup>25</sup>

Dihydroquinazolines present a pharmaceutically integral class of a range of functional molecules, alkaloids, therapeutics and agrochemicals.<sup>27,28</sup> This privileged moiety is endowed with significant bioactivity such as antibacterial, antiparasitic,

antifungal, anti-obesity, anti-alzheimer, antidiuretic, antihypertensive, antiviral and antitumor.<sup>29-37</sup> Ispinesib (**1**), a selective kinesin spindle protein (KSP) inhibitor, aquamox (**2**), an antihypertensive agent and antidiuretic, evodiamine (**3**), a natural product with anti-obese activity, prevymis (**4**), a FDA approved drug for the treatment of HIV, and vasicine (**5**), a butyrylcholinesterase inhibitor, contains dihydroquinazoline in their skeleton (Figure 1).<sup>33,35-39</sup>

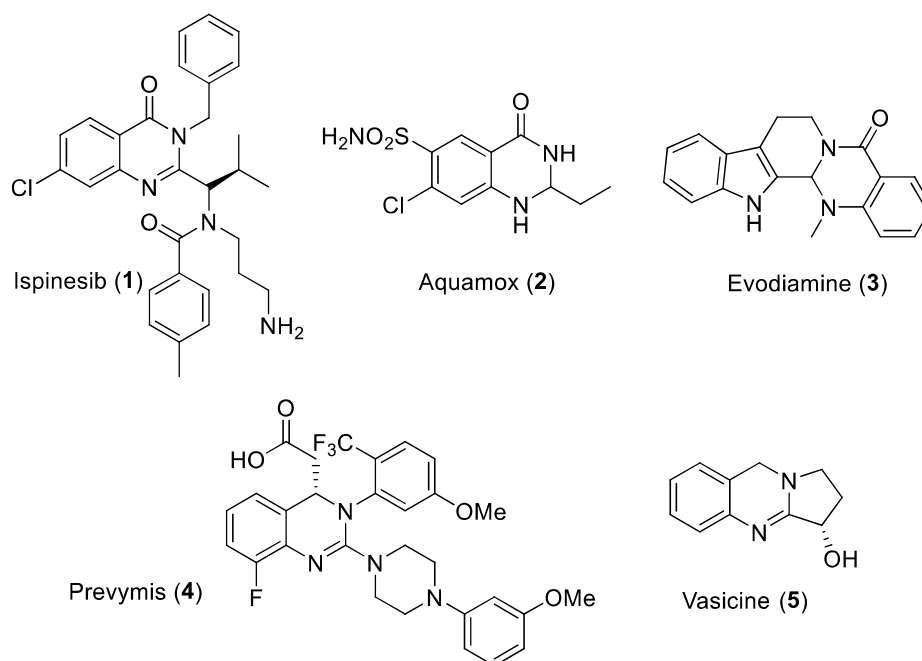


**Figure 1.** Example of a few biologically active compounds containing dihydroquinazoline and quinazolinone backbone

Because of their importance, a number of different methods have been developed for the efficient synthesis of dihydroquinazolines. In a report, Sarma and co-worker described microwave promoted synthesis of 1,2-dihydroquinazolines by

treating 2-aminobenzophenone with aldehydes under solvent-free condition in the presence of urea as the nitrogen source at a temperature of 130 °C.<sup>40</sup> In a recent report, Gudimella et al. carried out one-pot synthesis of 1,2-dihydroquinazoline analogues by reacting benzylamine with 2-bromobenzophenone.<sup>41</sup> The synthesized compounds were then evaluated for anticancer activity and among the various analogues; two compounds were found to exhibit acute anticancer activity. Rohlmann and co-workers reported the synthesis of dihydroquinazolines *via* an iron catalyzed process using TEMPO oxoammonium salt as an oxidant.<sup>42</sup> In a recent report, Chen and group described the synthesis of 1,2-dihydroquinazolines by the treatment of indazolium halides with K<sub>2</sub>CO<sub>3</sub> using toluene as the solvent.<sup>43</sup> Kamal and group reported the synthesis of 1,2-dihydroquinazolines by a three-component reaction catalyzed by sulfamic acid.<sup>44</sup> In a very recent report, Azizi and co-workers prepared dihydroquinazolines by using sulfuric acid functionalized nano-silica (KCC-1/Pr-SO<sub>3</sub>H).<sup>45</sup> Derabli et al. carried out DMAP catalyzed synthesis of dihydroquinazolines *via* a three-component reaction.<sup>46</sup> Srivastava employed ionic liquid immobilized hydrotalcite clay as a catalyst for the synthesis of 1,2-dihydroquinazoline derivatives.<sup>47</sup> Despite these notable advances, most of the existing methods suffer from the burdens of prolonged reaction time, high catalyst loading, difficulty in catalyst recyclability, limited functional group tolerance, and requirement of high reaction temperature. Moreover, most of the reactions suffer from the problem of poor selectivity and produce a mixture of both

dihydroquinazoline as well as quinazoline. It is to be noted that there are a few heterogeneous catalysts containing copper/copper oxide reported for the synthesis of quinazoline. For example, Baghbanian and Farhang reported magnetically active  $\text{CuFe}_2\text{O}_4$  nanoparticles for the synthesis of quinoline and quinazoline.<sup>48</sup> Zhang and co-workers described the synthesis of quinazoline using kaolin supported copper oxide nanoparticle. Both the reported studies were carried out at 80 °C and 90 °C, respectively.<sup>49</sup> Another study by Zhang and group members reported the use of supported CuO nanoparticles for the synthesis of quinazoline from amidine and alcohol.<sup>50</sup> In this case, they have refluxed the reaction in toluene for 24 h. None of the methods described above are used for the selective synthesis of dihydroquinazolines alone. Due to the increase in environmental awareness the development of mild and recyclable catalytic strategies along with simple, rapid and high atom economic reactions are actually need of the time. The use of a suitable heterogeneous catalyst over homogeneous catalysts not only reduces dissipation, but also makes it easier for the separation process and scale-up. Herein, we present synthesis and detailed characterization of copper oxide supported on silica ( $\text{CuO@SiO}_2$ ) nanoparticles and its further application in the construction of pharmaceutically significant phenyl-1,2-dihydroquinazolines from 2-aminoketones, benzaldehydes and ammonium hydroxide at room temperature. To the best of our knowledge, the catalytic performance of  $\text{CuO@SiO}_2$  in the synthesis of dihydroquinazolines at ambient temperature has not been examined so far.



---

## 2.2 Results and discussion

### 2.2.1 Preparation and characterization of copper oxide supported on silica (CuO@SiO<sub>2</sub>)

The CuO@SiO<sub>2</sub> nanoparticles were prepared in two steps using a reduction precipitation technique starting from copper acetate and silicic acid. Initially, the prepared material is characterized by powder XRD to determine the crystallinity of the solid (Figure 2b). The powder XRD pattern shows a broad diffraction peak at  $2\theta = 22.3^\circ$  corresponding to (002) plane of support SiO<sub>2</sub>. The diffraction peaks at  $2\theta = 35.4^\circ$ ,  $38.8^\circ$ ,  $48.5^\circ$ ,  $57.7^\circ$  and  $62.2^\circ$  can be assigned to the (002), (111), (-202), (202) and (-113) planes of the monoclinic structure of CuO nanoparticles (JCPDS Card No. 03-065-2309). No other secondary peaks corresponding to metallic Cu, Cu(OH)<sub>2</sub> or Cu<sub>2</sub>O phases are observed. This confirms the formation of CuO in the nanomaterial. The XRD pattern of parent silicic acid shows a diffraction peak at  $2\theta = 22.6^\circ$  (Figure 2a). After the formation of nanoparticles, the intensity of basal reflection of parent support decreases considerably with the simultaneous appearances of diffraction peaks for CuO phase.

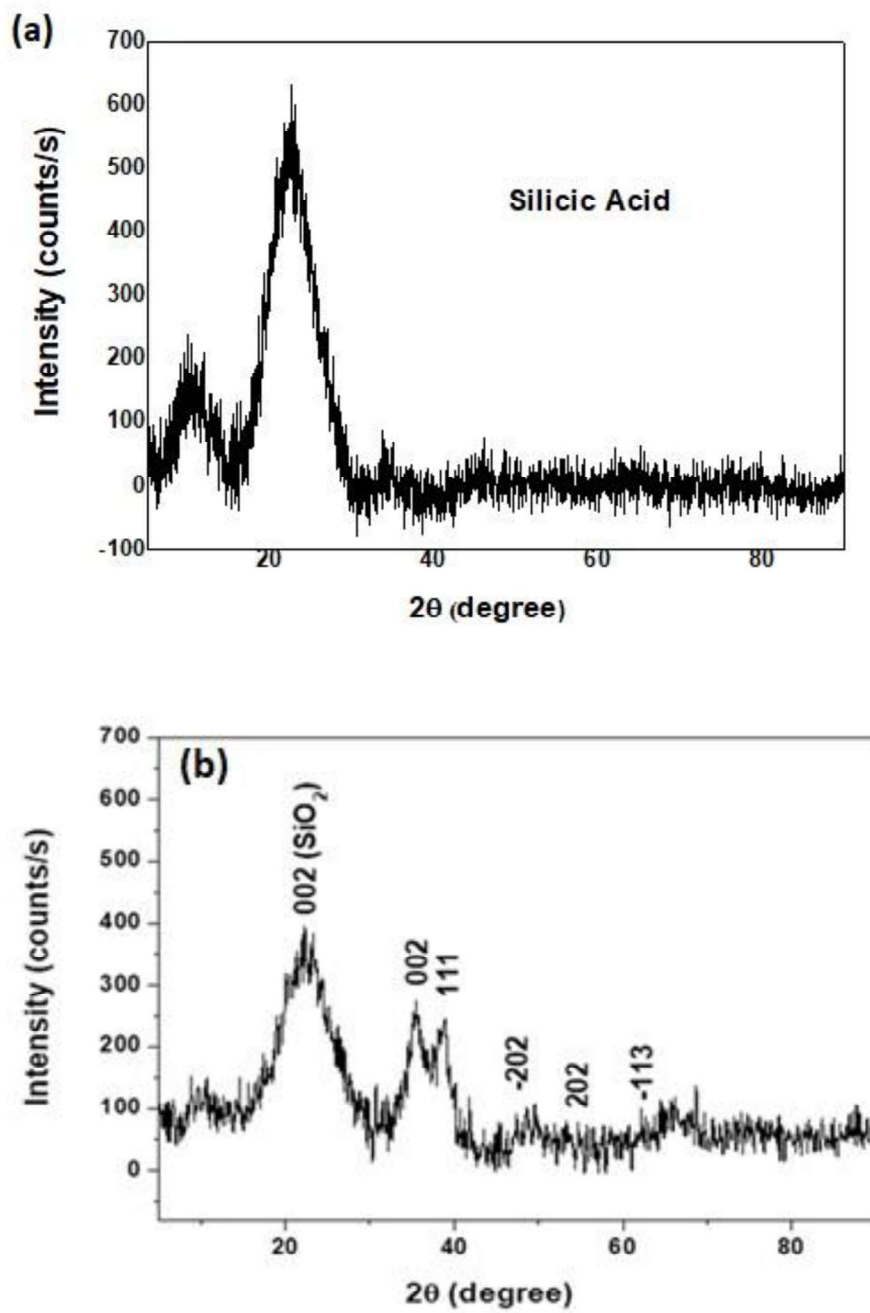


**Figure 2.** Powder XRD pattern of (a) Silicic acid support and (b) CuO@SiO<sub>2</sub> catalyst

The functional groups present and the bonding in the CuO@SiO<sub>2</sub> catalyst are determined by FT-IR analysis in the range of 400-4000 cm<sup>-1</sup> (Figure 3). The absorption bands observed at 3421 and 1628 cm<sup>-1</sup> correspond to the stretching vibration of -OH group and the bending vibration of H-O-H group, respectively. The peak positioned at 1013 cm<sup>-1</sup> corresponds to the Si-O-Cu bond due to the adsorption of CuO on SiO<sub>2</sub>.<sup>51</sup> Also, the peak at 510 cm<sup>-1</sup> can be attributed to the stretching vibration of Cu-O bond.<sup>52</sup>

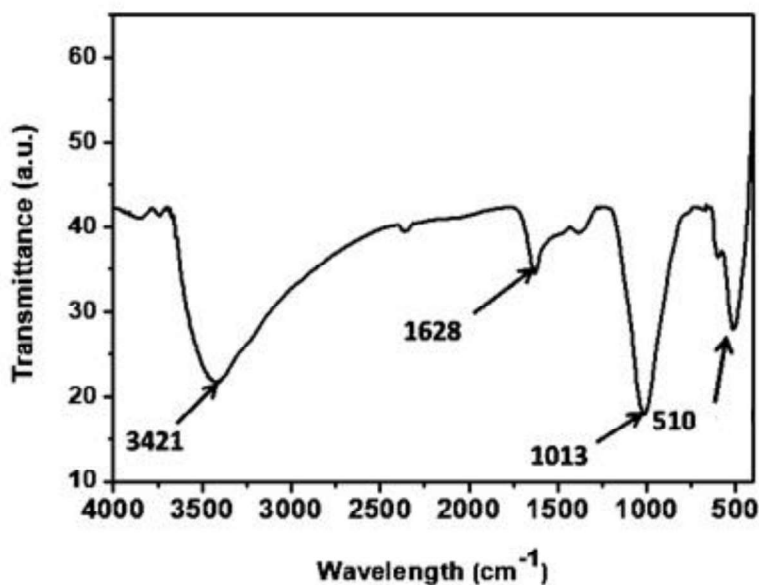


**Figure 3.** FT-IR spectrum of CuO@SiO<sub>2</sub> catalyst

The microstructure of the synthesized CuO@SiO<sub>2</sub> catalyst is characterized by TEM and HR-TEM analyses (Figure 4 and 5). The low resolution TEM image reveals the homogeneous distribution of nearly spherical CuO nanoparticles on the support with particle size distribution in the range of 2-5 nm (Figure 4a and 4b). The

number average diameter has been calculated to be 3 nm with standard deviation (SD) of 0.57 using ImageJ software.<sup>53</sup>

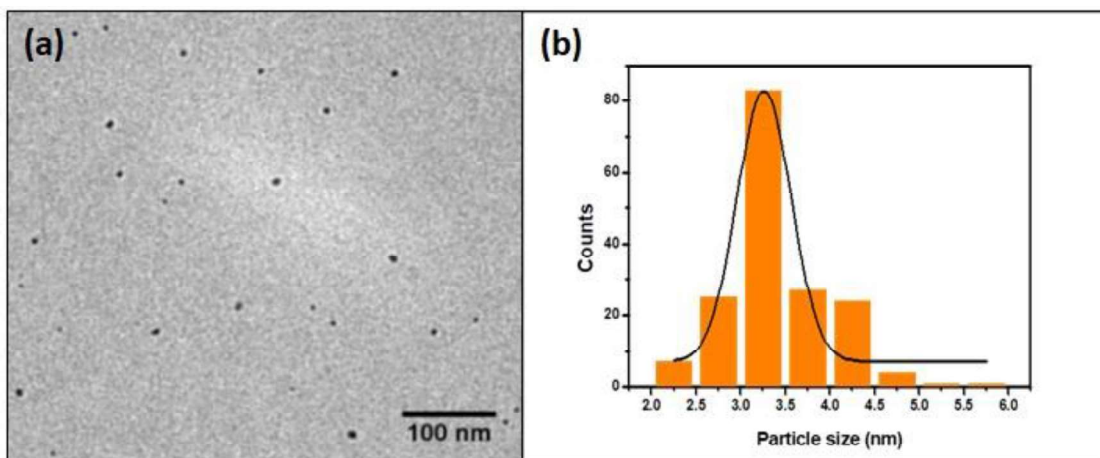


**Figure 4.** (a) TEM image of CuO@SiO<sub>2</sub> and (b) Particle size distribution histogram

This suggests the narrow crystallite size distribution of CuO nanoparticles onto catalyst's support. The surface-weighted diameter ( $D_s$ ), calculated from the number average diameter, was found to be 3.5 nm.<sup>54</sup> The HR-TEM image indicates the formation of highly crystalline structure and the inter-planar lattice fringe spacing of 0.25 nm agrees with the (002) plane of monoclinic structure of CuO nanoparticles (Figure 5a). The selected area electron diffraction (SAED) pattern confirms the crystalline nature of the sample as indicated by the (002) and (111) crystalline planes (Figure 5b).

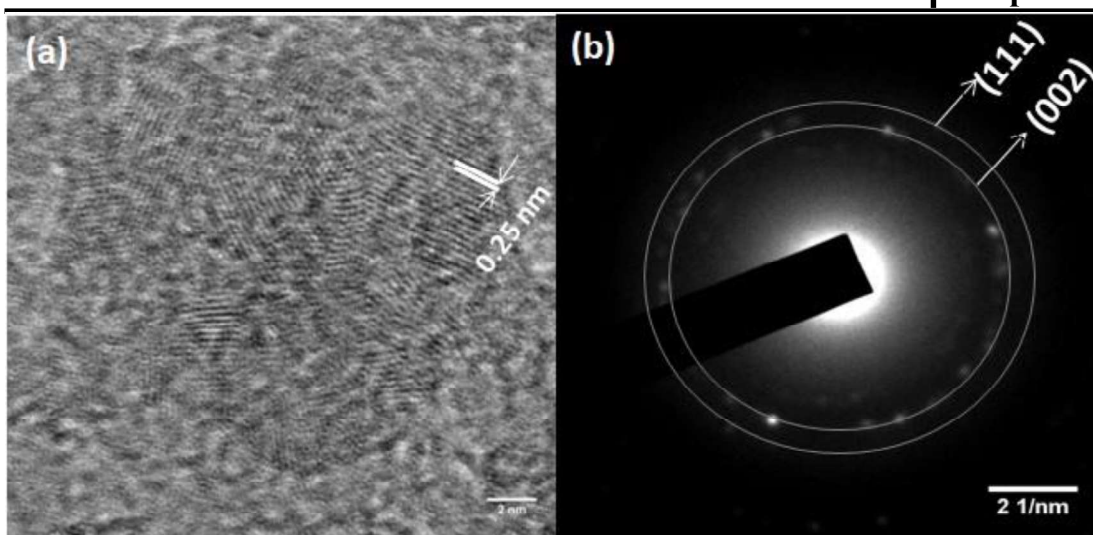


**Figure 5.** (a) HR-TEM image with fringe spacing and (b) SAED pattern of  $\text{CuO}@\text{SiO}_2$  catalyst

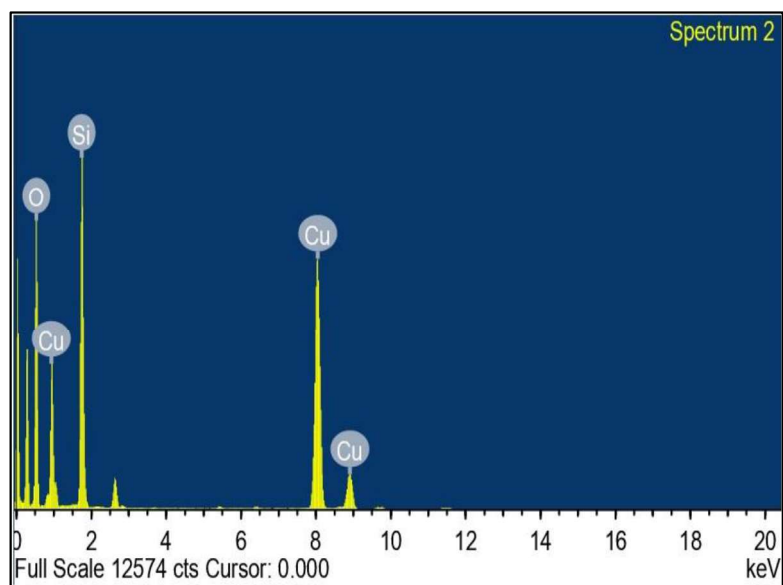


**Figure 6.** EDX analysis of  $\text{CuO}@\text{SiO}_2$  catalyst showing the presence of Cu, O and Si

Energy Dispersive X-ray (EDX) analysis of the prepared nanoparticles indicates the presence of Cu, Si and O signals (Figure 6).

More information about the chemical composition and the electronic state of the metal atom at the catalyst surface has been obtained from X-ray Photoelectron Spectroscopy (XPS) analysis. The Cu 2p<sub>3/2</sub> peak at 934.09 eV and the Cu 2p<sub>1/2</sub> peak at 953.84 eV are characteristic peaks for the copper(II).<sup>3,55</sup> Additionally, the presence of copper(II) can also be supported by the strong shake-up-peak observed at around ~943 eV for Cu2p<sub>3/2</sub> (Figure 8a).<sup>3,55</sup> The raw data of full Cu 2p XPS profile is presented in Figure 7.

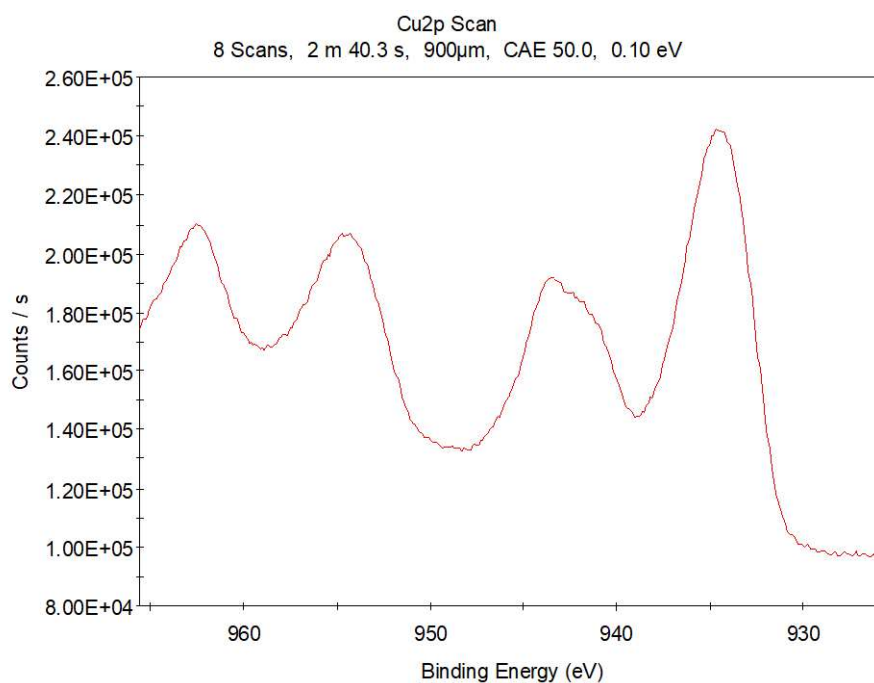


**Figure 7.** Full spectrum of XPS Cu2p

The raw data of Cu2p<sub>3/2</sub> corresponds to three peaks; 933.6 eV, 935.4 eV and fitted shake-up peak at 942.6 eV. The shifting of Cu 2p<sub>3/2</sub> peak to higher binding energy (933.6 eV) in the prepared CuO@SiO<sub>2</sub> can be assigned to the formation of Cu-O-Si surface structures.<sup>55,56</sup> It is to be noted here that a similar inference of formation of Cu-O-Si is indicated in the FT-IR spectra (Figure 3). Similarly, the O1s spectrum exhibits three distinct peaks at 529.75 eV, 532.24 eV and 531.12 eV (Figure 8b). The peak at 529.75 eV is a characteristic of metal-oxygen bond and the peak at 532.24 eV can be attributed to the presence of SiO<sub>2</sub>. The peak at 531.12 eV may again be attributed to the presence of Cu-O-Si kind of structure.<sup>56,57</sup> The Cu2p<sub>3/2</sub> and O1s were fitted using XPS.4.1 software.

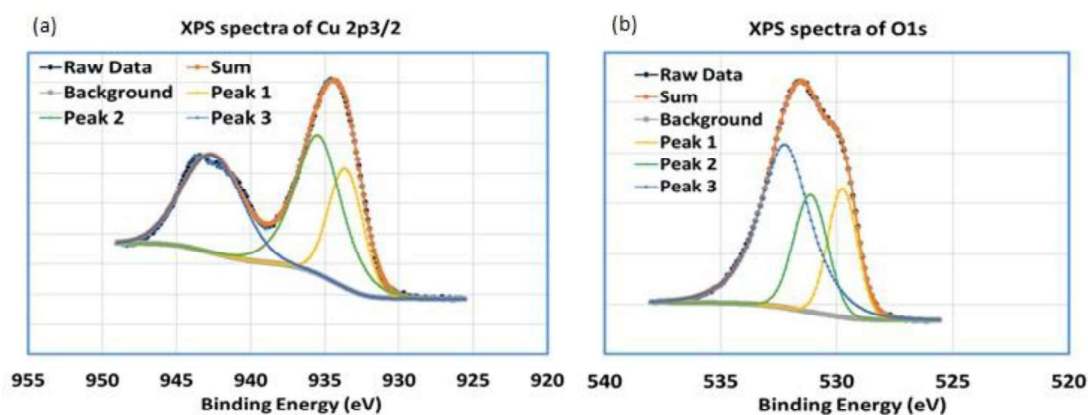


**Figure 8.** High resolution XPS spectra of CuO@SiO<sub>2</sub>: (a) Cu2p and (b) O1s regions

An analysis through Atomic Absorption Spectroscopy (AAS) shows the presence of 7.2 wt% of copper metal in the prepared catalyst.

The specific surface area (SSA) of the synthesized CuO@SiO<sub>2</sub> has been determined by the nitrogen gas adsorption study in the Brunauer-Emmett-Teller

(BET) analyser (Figure 9). The adsorption-desorption isotherm obtained for the samples indicates a type IV isotherm (based on Brunauer et al. classification) pointing towards meso-porous nature of the materials.<sup>58(a,b)</sup> Further, hysteresis loop signifies the meso-porosity which is attributed by the presence of ink-bottle shaped pores or else by the packing of spheroidal particles in each cases.<sup>54a,58(c,d)</sup> We observed a decrease in BET surface area and pore volume of the synthesized nanoparticle as compared to that of the support (Table 1). Since, the catalyst is synthesized by calcination at 300 °C, there are possibility of the collapse of microporous structure of the support. This results in the overall enhancement of pore size of the CuO@SiO<sub>2</sub> catalyst, thereby, causing reduction in the pore volume and surface area. Other possibility of this reduction may be attributed to the filling of the pores by active metal oxide.<sup>55</sup>

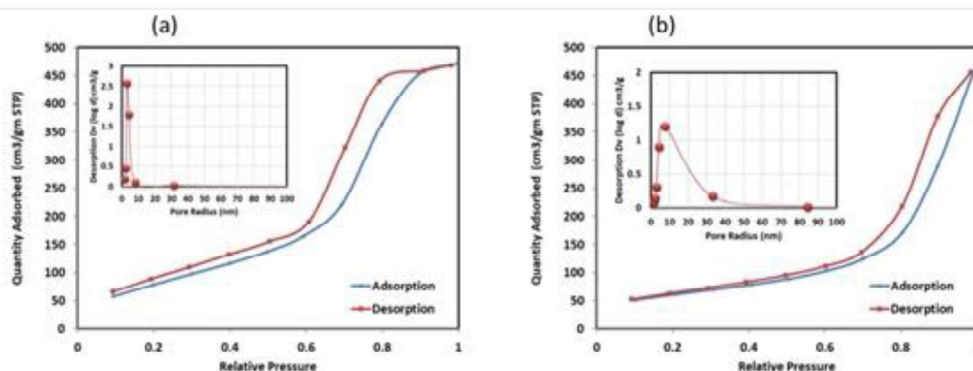


**Figure 9.** (a) BET analysis with pore size distribution (stacked inset plot) of support and (b) CuO@SiO<sub>2</sub> catalyst



**Table 1.** Comparison of surface area, pore radius and pore volume of support and freshly prepared catalyst

Sample	BET Surface Area (m <sup>2</sup> /g)	Pore Radius (nm)	Pore Volume (cm <sup>3</sup> /g)
Support	416.42	3.10	0.74
Fresh CuO@SiO <sub>2</sub>	217.47	4.43	0.69

### 2.2.2 Catalytic activity of the prepared CuO@SiO<sub>2</sub> catalyst towards the synthesis of 1,2-Dihydroquinazolines

After the preparation and extensive characterization, the activity of the material was studied in the synthesis of dihydroquinazolines. For this purpose, a reaction was carried out using 2-aminobenzophenone (**6a**) and benzaldehyde (**7a**) in the presence of ammonium hydroxide as nitrogen source at room temperature (Table 2). It was observed that the CuO@SiO<sub>2</sub> could efficiently catalyze the three-component reaction leading to the synthesis of dihydroquinazoline **8a** as the only product. The reaction was selective and no formation of quinazoline by-product was observed. To find out the optimized reaction condition different parameters like, solvent, catalyst loading, and reaction time was studied (Table 2). Acetonitrile was found to be the most suitable solvent and the reaction was complete within 1 hour (Table 2, entry 11). A blank reaction, with only silicic acid, was performed which did not produce any product (Table 2, entry 13). SiO<sub>2</sub>, prepared separately following the

identical procedure without addition of copper salt, also failed to produce any product (Table 2, entry 14). These two reactions confirmed the role of the metal in the reaction. The reaction was also carried out with individual copper salts which produced the dihydroquinazoline in much less yield (Table 2, entries 15-16). The finding confirms that the Cu-O-Si interface formation is responsible for the enhanced catalytic activity. Rate of reaction in terms of turn over frequency (TOF) has been calculated and found to be  $\sim 0.1 \text{ s}^{-1}$  based on 40% conversion in 10 min.

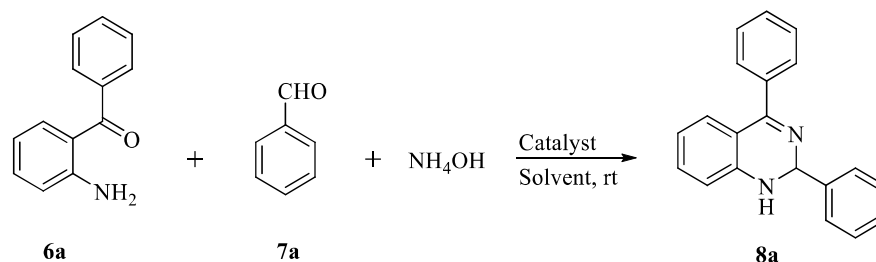
Turn over frequency (TOF) has been calculated following the formula-

$$TOF = \frac{\text{moles of reactant consumed}}{\text{moles of catalytic active sites} \times \text{time}}$$

Moles of catalytic active site = total mole of copper in the catalyst  $\times$  Dispersion

The % dispersion (Ds) has been calculated as 31% using surface-weighted average diameter calculated from TEM.<sup>54a,59</sup>

**Table 2.** Synthesis of 1,2-Dihydroquinazolines and optimization of the reaction condition<sup>a</sup>

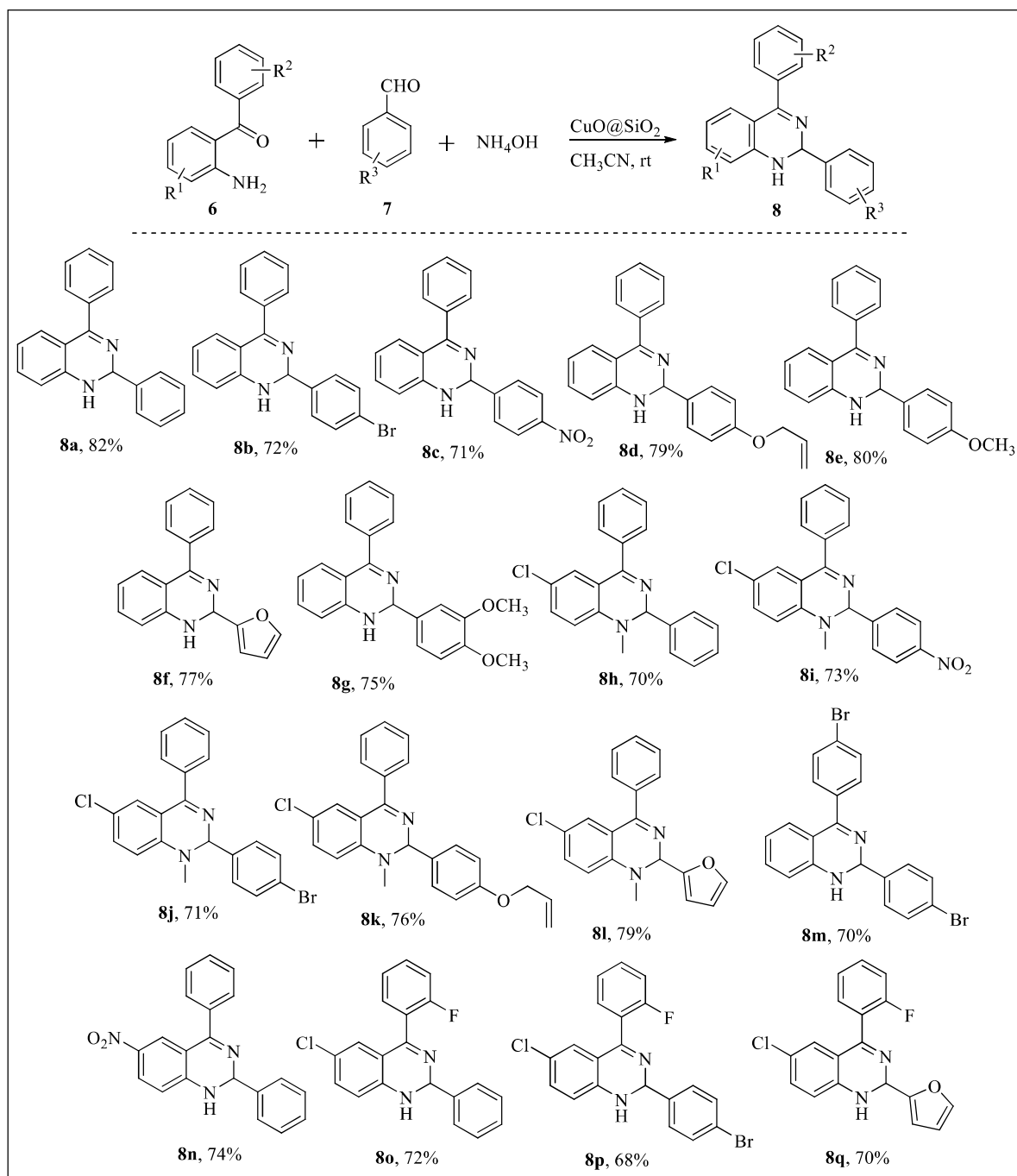


Entry	Catalyst	Solvent	Time (h)	Catalyst loading (wt%)	Yield (%) <sup>b</sup>
1	CuO@SiO <sub>2</sub>	CH <sub>3</sub> OH	10	20	42
2	CuO@SiO <sub>2</sub>	C <sub>2</sub> H <sub>5</sub> OH	10	20	22
3	CuO@SiO <sub>2</sub>	DMSO	10	20	20
4	CuO@SiO <sub>2</sub>	H <sub>2</sub> O	10	20	55
5	CuO@SiO <sub>2</sub>	1,4-Dioxane	10	20	51
6	CuO@SiO <sub>2</sub>	Toluene	10	20	33
7	CuO@SiO <sub>2</sub>	THF	10	20	52
8	CuO@SiO <sub>2</sub>	CH <sub>3</sub> CN	10	20	82
9	CuO@SiO <sub>2</sub>	CH <sub>3</sub> CN	1	20	82
10	CuO@SiO <sub>2</sub>	CH <sub>3</sub> CN	0.5	20	80
11	CuO@SiO <sub>2</sub>	CH <sub>3</sub> CN	1	15	82
<b>12</b>	<b>CuO@SiO<sub>2</sub></b>	<b>CH<sub>3</sub>CN</b>	<b>1</b>	<b>10</b>	<b>82</b>
13	CuO@SiO <sub>2</sub>	CH <sub>3</sub> CN	1	5	78
14	CuO@SiO <sub>2</sub>	CH <sub>3</sub> CN	1	2	74
15	No catalyst (only silicic acid)	CH <sub>3</sub> CN	1	10	0
16	SiO <sub>2</sub> without Cu (prepared using identical condition)	CH <sub>3</sub> CN	1	10	0
17	Cu(OAc) <sub>2</sub>	CH <sub>3</sub> CN	10	10	35
18	CuBr	CH <sub>3</sub> CN	10	10	28
19	CuI	CH <sub>3</sub> CN	10	10	23

Bold values indicate the best experimental result. <sup>a</sup>All the reactions were carried out using 2-aminobenzophenone **6a** (0.5 mmol), benzaldehyde **7a** (0.5 mmol), ammonium hydroxide (0.5 mL), solvent (3 mL) at room temperature. <sup>b</sup>Yield refers to the isolated product after column chromatographic purification.

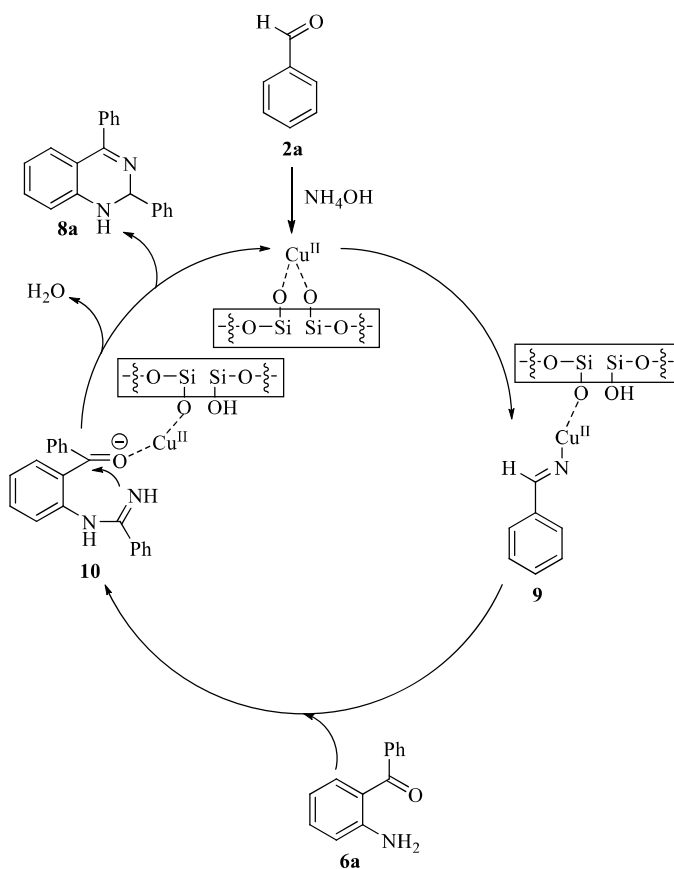
With the optimal reaction conditions in hand, we next investigated the scope of the process where different substituted aromatic aldehydes were tested with the 2-aminobenzophenone **6a** (Table 3). All the reactions worked well to produce the corresponding dihydroquinazolines in good to excellent yields **8(a-g)**. The halogenated substrates were well-tolerated in this reaction, producing the corresponding dihydroquinazoline **8b**. Both the electron donating and electron withdrawing functional groups such as nitro and methoxy also produced the desired dihydroquinazolines **8(c-e)** and **8g** with 71-79% yield. To our delight, the optimized conditions were mild enough for the reaction of heteroaryl aldehydes such as furan-2-carbaldehyde which produced the corresponding product **8f**. A variety of substituted 2-aminoketones were also investigated **8(h-q)**. 2-aminoketones bearing both electron-withdrawing and electron-donating groups at different positions of the phenyl ring coupled smoothly with the benzaldehyde **7a** to produce the desired dihydroquinazolines with very good yield.

**Table 3.** Synthesis of 1,2-dihydroquinazolines from 2-aminocarbonyls, aldehydes and ammonium hydroxide



The reaction has also been carried out with phenylacetaldehyde and other aliphatic aldehydes like, butyraldehyde and octanal. Unfortunately, there was no reaction in all the cases. This may be due to the problem in imine formation with aliphatic aldehydes in the very first step of the reaction. All the prepared compounds were duly characterized with the help of NMR and Mass spectral data.

Based on the reports available in the literature, a tentative mechanism of the reaction has been proposed (scheme 1).<sup>60</sup>



**Scheme 1.** A plausible mechanism for the synthesis of dihydroquinazoline catalyzed by  $\text{CuO}@\text{SiO}_2$

The imine, formed by the reaction between aldehyde **7a** and ammonia, gets activated by the surface stabilized Cu(II) and forms the intermediate **9**. Reaction between **9** and 2-aminobenzophenone (**6a**) produces the amidine intermediate **10**. Finally, Cu(II) catalyzed removal of water produces the dihydroquinazoline **8a**.

An alternative pathway is also possible where intramolecular condensation of ketimine, formed by the reaction between benzophenone and ammonium hydroxide, and aldoxime, formed by the condensation of amine with aldehyde, leads to the product. Based on the earlier literature report, the former one looks more feasible.<sup>60</sup> As described earlier, the improved catalytic performance may be attributed to the enhanced electronegativity of Cu(II) due to the formation of Cu-O-Si which facilitates facile attack of aromatic amine into imine centre leading to formation of amidine **10**. The same phenomena also explain facile dehydration of **10** leading to the product **8a**.

### 2.2.3 Study of catalyst recyclability

To study the recyclability of the catalyst, we investigated its recovery and reusability under the optimized reaction condition. After the completion of the reaction, the solid catalyst was recovered by simple filtration followed by washing with distilled water. After drying, the recovered CuO@SiO<sub>2</sub> catalyst was reused directly in the next reaction. It was observed that the recovered catalyst could be reused up to five consecutive catalytic cycles without any significant loss in the activity (Figure 10). However, loss in catalytic activity was observed after 5<sup>th</sup> run.

The physical characteristics of the catalyst recovered after 5<sup>th</sup> run were also investigated through TEM, BET and XPS analysis. In the TEM image of the recovered catalyst, any significant morphological change was not observed (Figure 11a). In the BET analysis the specific surface area (214.46 m<sup>2</sup>/g), pore radius (4.47 nm), and pore volume (0.68 cm<sup>3</sup>/g) of the recovered catalyst after a single run was found to be almost similar to that of the freshly prepared catalyst (Figure 11b). Furthermore, the recovered catalyst was also subjected to the XPS analysis and the fitted values of XPS binding energies for Cu 2p 3/2 and O1s of recovered catalyst appeared almost similar to that of the original catalyst (Figure 12a and 12b). This signifies that oxidation state and structure of the catalyst was intact even after the reaction.

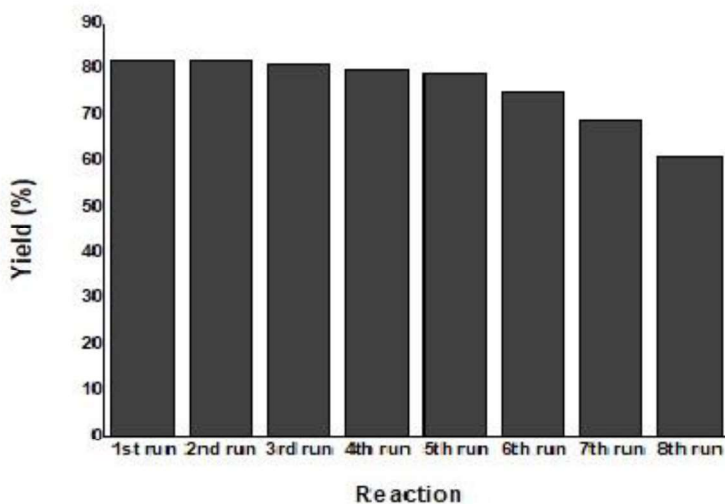


**Figure 10.** Study of recyclability of the catalyst



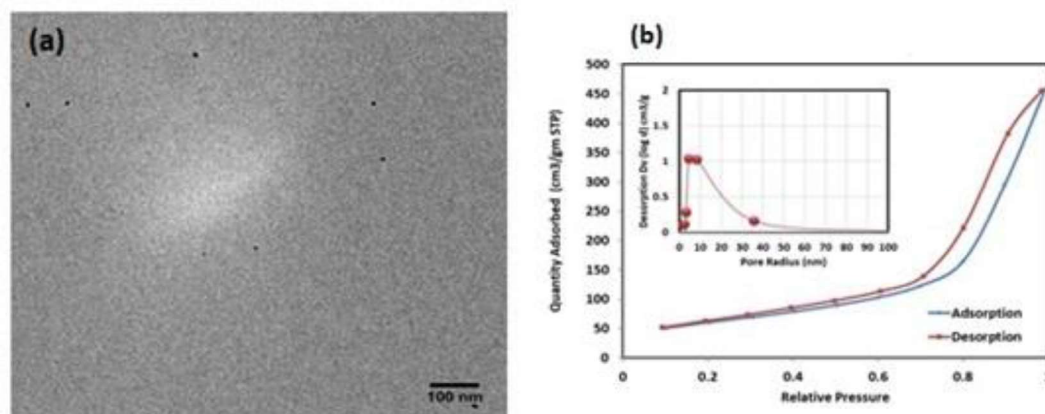


**Figure 11.** (a) TEM image of the recovered CuO@SiO<sub>2</sub> catalyst after 5<sup>th</sup> run and (b) BET analysis with the pore size distribution of the CuO@SiO<sub>2</sub> catalyst recovered after 5<sup>th</sup> run.

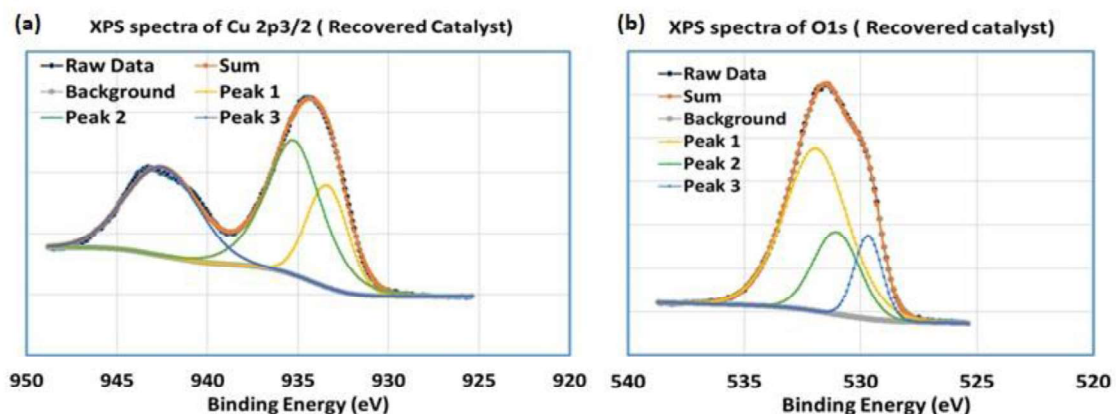


**Figure 12.** High resolution XPS spectra of recovered CuO@SiO<sub>2</sub>: (a) Cu2p and (b) O1s

After the catalyst recovery, the metal content of the filtrate was estimated using AAS and negligible trace of copper was found. The recovered catalyst was also

subjected to AAS experiment after the 5<sup>th</sup> run and the metal content was found to be similar to that of the original.

#### 2.2.4 Study of antibacterial activity of the synthesized dihydroquinazolines

Inspired by the reports on the biological activities of 1,2-dihydroquinazolines, we investigated the antibacterial properties of the synthesized compounds against two different gram-positive bacterial strains namely, *Mycobacterium abscessus* and *Staphylococcus aureus* and a gram-negative strain *Escheria fergusonii* (Table 4). Unfortunately, most of the compounds did not show any activity against the selected strains. Only, eight analogues **8a**, **8g-k**, **8m** and **8q** showed some inhibitory activity although in very low level. The experiments were performed using ampicillin and tetracycline as positive control. Cell cytotoxicity test of these eight compounds were also carried out and except compound **8g**, all others were almost non-toxic. Further extension of this work suggested that a few of these compounds act as efflux pump modulator against multidrug resistant *Staphylococcus aureus* 1199B, a fluoroquinolone resistant strain, when administered along with norfloxacin or ethidium bromide. More detailed and in-depth study in this line is going on.

**Table 4.** Minimum inhibitory concentration (MIC,  $\mu\text{g/mL}$ ) of the synthesized 1,2-dihydroquinazoline derivatives against selected bacterial strains

Compounds	<i>M. abscessus</i>	<i>E. fergusonii</i>	<i>S. aureus</i>
<b>8a</b>	>1000	>1000	125

<b>8g</b>	>1000	>1000	250
<b>8h</b>	250	500	125
<b>8i</b>	500	500	125
<b>8j</b>	500	1000	125
<b>8k</b>	250	500	62
<b>8m</b>	>1000	>1000	250
<b>8q</b>	>1000	>1000	250
<b>Ampicilin</b>	-	32	60
<b>Tetracycline</b>	64	-	-

### 2.2.5 Catalytic activity of the prepared CuO@SiO<sub>2</sub> towards the conversion of carbohydrates into 5-hydroxymethylfurfural (HMF)

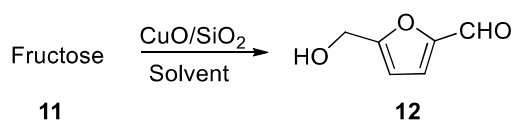
5-Hydroxymethylfurfural (HMF) is a versatile platform chemical and act as precursor of different fine chemicals, liquid fuels, and building blocks for the synthesis of a number of different polymeric materials including 2,5-furandicarboxylic, 2,5-diformylfuran, and 1,6-hexanediol.<sup>61(a-c)</sup> 2,5-Furandicarboxylic acid finds wide application in the petrochemical and nylon industries.<sup>61(d,e)</sup> HMF is generally produced by acid-catalyzed dehydration of carbohydrates such as fructose, glucose, sucrose, and cellulose.<sup>62</sup> Several acid catalysts have been employed for the production of HMF such as H<sub>2</sub>SO<sub>4</sub>, HCl, CrCl<sub>3</sub>, AlCl<sub>3</sub>, SnCl<sub>4</sub>, GeCl<sub>4</sub>, maleic acid, and LiCl.<sup>63</sup> The use of these catalytic systems

usually suffers from drawbacks such as corrosiveness, high toxicity, non-recyclability of catalyst, and problem of product purification. For this reason, the use of acidic heterogeneous catalysts is getting popularity in recent years. Various solid acid catalysts such as metal oxides, immobilized ionic liquids, zeolites, acid resins, lignosulfonic acid, mesocellular silica foam, and niobic acid have been developed for the synthesis of HMF.<sup>61b,64</sup> Wang et al. performed the conversion of cellulose to HMF using N-doped mesoporous carbon materials (MCNs) as catalyst.<sup>65a</sup> The yield of HMF from cellulose was ~52% while a considerable amount (~30%) of reducing sugar and levulinic acid was formed as side product. In a report by Liu and co-workers, functionalized halloysite nanotubes were prepared which worked as a solid acid for the dehydration of carbohydrates to HMF.<sup>65b</sup> In this case, a very high conversion (up to 92%) of fructose to HMF was observed. Zhang and co-workers reported bimetallic aluminium-molybdenum mixed oxide solid acid catalyzed conversion of fructose to HMF where a moderate yield (~49%) of the product was observed.<sup>65c</sup> Herbst and group utilized metal-organic frameworks (MOFs) based solid acid catalysts for the efficient conversion of biomass to HMF.<sup>65d</sup> In this example high fructose conversion up to 79% could be observed although toxic chromium metal was used in the MOF framework.

However, there are only a very few reports on the conversion of carbohydrates to HMF using copper catalyst is available in the literature.<sup>66</sup> Due to the acidic nature of our CuO@SiO<sub>2</sub> catalyst, we decided to investigate the possibility of

its application in the conversion of carbohydrates such as fructose, glucose and sucrose to HMF. For initial study fructose **11** was chosen as the model substrate and it was observed that the catalyst could produce HMF from fructose in a moderate yield. For optimization of the reaction condition, different reaction parameters such as solvent, temperature and catalyst loading were studied (Table 5). DMSO was found to be the best solvent for the conversion (Table 5, entry 4). The highest yield of HMF (35%) was observed at a temperature of 120 °C with a catalyst loading of 15 wt% (Table 5, entry 7). A blank reaction was also performed in the absence of copper by using silicic acid and silica. Expectedly, under such condition, product formation was not observed (Table 5, entries 9-10). The reaction with simple copper salts such as copper acetate and copper sulphate failed to produce any product (Table 5, entries 11-12). The experiments confirmed the role of the metal oxide and silica support in the production of HMF.

**Table 5.** Synthesis of HMF from fructose and optimization of the reaction condition<sup>a</sup>



Entry	Catalyst	Solvent	Temperature (°C)	Catalyst loading (wt%)	Yield (%) <sup>b</sup>
1	CuO@SiO <sub>2</sub>	H <sub>2</sub> O	100	20	12
2	CuO@SiO <sub>2</sub>	DMF	100	20	19

3	CuO@SiO <sub>2</sub>	MIPK	100	20	7
4	CuO@SiO <sub>2</sub>	DMSO	100	20	25
5	CuO@SiO <sub>2</sub>	DMSO	130	20	31
6	CuO@SiO <sub>2</sub>	DMSO	120	20	35
7	<b>CuO@SiO<sub>2</sub></b>	<b>DMSO</b>	<b>120</b>	<b>15</b>	<b>35</b>
8	CuO@SiO <sub>2</sub>	DMSO	120	10	29
9	No catalyst (only silicic acid)	DMSO	120	15	0
10	SiO <sub>2</sub> without Cu prepared using identical condition	DMSO	120	15	0
11	Cu(OAc) <sub>2</sub>	DMSO	120	15	0
12	CuSO <sub>4</sub>	DMSO	120	15	0
Bold values indicate the best experimental result. <sup>a</sup> All the reactions were carried out using fructose <b>11</b> (0.27 mmol), solvent (1 mL). <sup>b</sup> Yield refers to isolated yields.					

With optimized reaction condition in hand, scope of the catalytic reaction was further extended to other sugars like, glucose, sucrose, cellulose, cellobiose, sorbitol and mannitol (Figure 13). The study revealed that the catalytic system could convert carbohydrates into HMF with moderate yield.

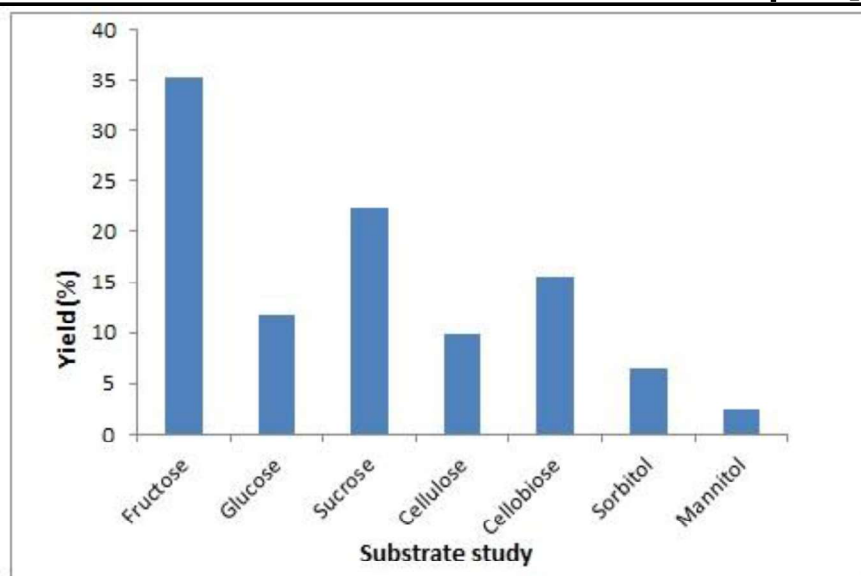
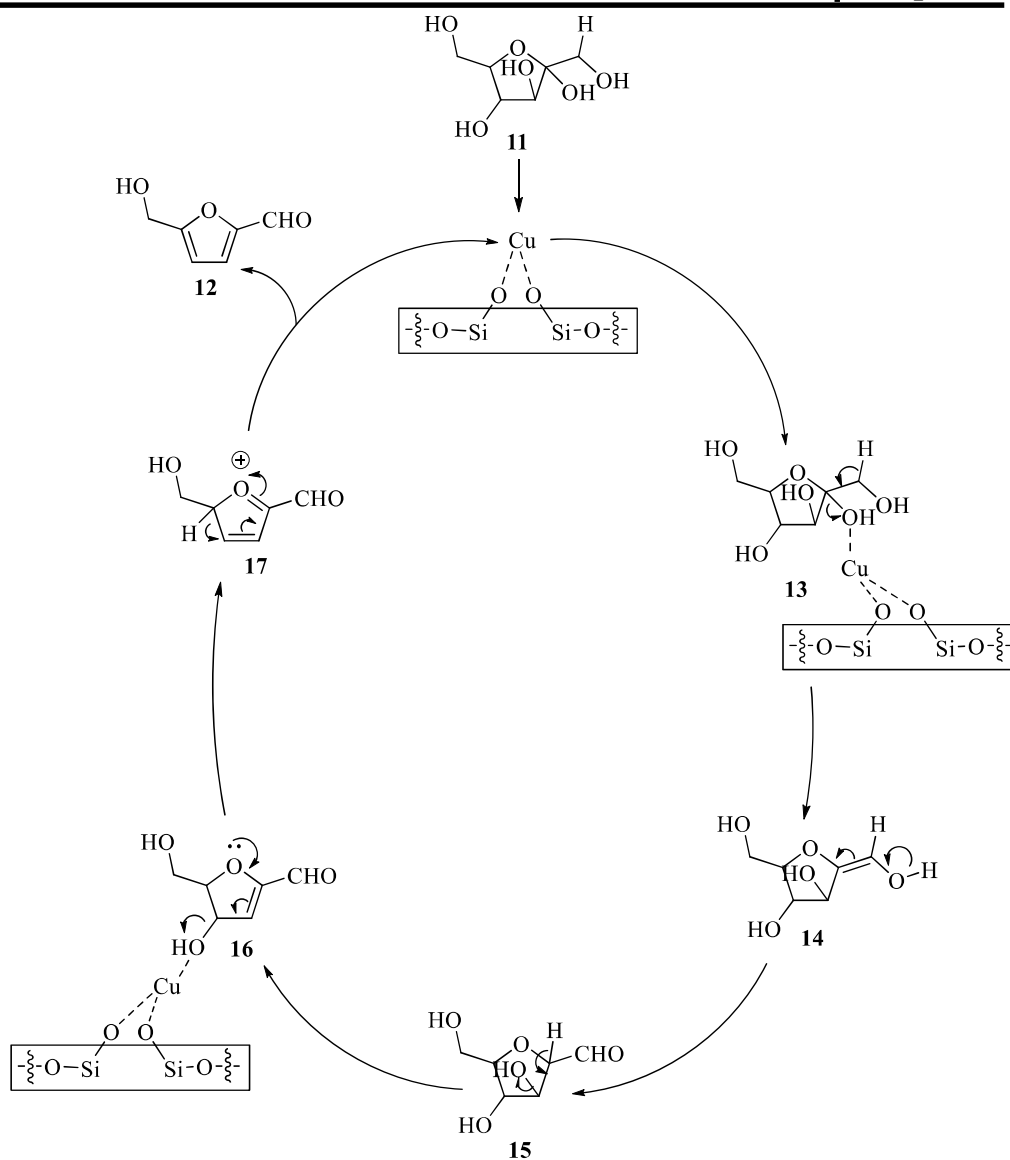


**Figure 13.** Substrate study for the conversion of carbohydrate into HMF

Based on the experimental findings and literature report, a plausible mechanism has been proposed (Scheme 2). Initially, CuO@SiO<sub>2</sub> catalyst activates the hydroxyl group at C-4 of D-fructose (**11**) forming an intermediate **13** which on dehydration produces the second intermediate **14**. Tautomerization of **14** produces intermediate **15** which further undergo dehydration to give the final product HMF (**12**) *via* the formation of the intermediates **16** and **17**.



**Scheme 2.** Proposed mechanism for the dehydration of fructose to HMF

### 2.2.6 Study of catalyst recyclability

The recoverability and reusability of the CuO@SiO<sub>2</sub> catalyst after the conversion of carbohydrates into HMF was also studied. The catalyst was recovered by simple filtration, followed by washing with distilled water and drying in an oven.



It was observed that the recovered catalyst could be reused upto five consecutive cycles without any significant loss in the activity (Figure 14). However, after the 5<sup>th</sup> run, the catalytic activity of CuO@SiO<sub>2</sub> started decreasing gradually.

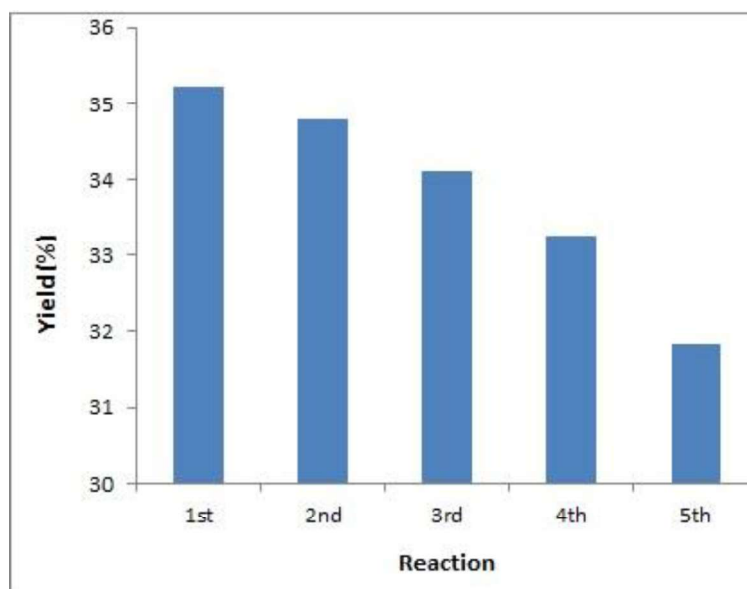


**Figure 14.** Study of the recyclability of CuO@SiO<sub>2</sub> catalyst

### 2.3 Conclusion

In summary, we have synthesized a copper oxide supported on silica catalyst and thoroughly characterized its physical and catalytic properties. The efficiency of the prepared catalyst has been studied for a three-component reaction between 2-aminobenzophenone, aldehyde, and ammonia leading to a convenient synthesis of 1,2-dihydroquinazoline. The synthesis was carried out at room temperature with high atom efficiency. Seventeen different 1,2-dihydroquinazoline derivatives with various

substituents were prepared using the simple reaction condition thereby making the process useful for multipurpose application. The synthesized 1,2-dihydroquinazolines were examined for antibacterial activity and four derivatives were found to display antibacterial property against the multidrug resistant *Staphylococcus aureus* bacterial strain. The activity of the catalyst was further screened towards the conversion of carbohydrates into HMF. The study was conducted using fructose, glucose, sucrose, cellulose, cellobiose, sorbitol and mannitol as substrates and a moderate yield of the product was obtained. The recovery and reusability of the catalyst was also studied. Based on the earlier literature report tentative mechanisms of both the reaction has been proposed.

## **2.4 Experimental**

### **2.4.1 Preparation of copper oxide supported on silica (CuO@SiO<sub>2</sub>) nanoparticles**

In the first step of the catalyst preparation, 0.6 g (3.0 mmol) of copper(II) acetate monohydrate {Cu(CH<sub>3</sub>COO)<sub>2</sub>·H<sub>2</sub>O} was dissolved in 40 mL of distilled water in a round-bottomed flask to form a homogeneous solution. Similarly, 2 g of silicic acid was homogeneously dispersed in 60 mL of distilled water in another round-bottomed flask. The copper acetate solution was then added dropwise into the silicic acid solution with stirring. This was followed by the dropwise addition of 5 mL of 10 N NaOH solutions into the mixture and stirring was continued for 2 h. The precipitate thus obtained was washed with distilled water until neutral and then dried

at 100 °C for 10 h in an oven. After calcination at 300°C for 3 h, CuO@SiO<sub>2</sub> catalyst was obtained as black powder.

#### **2.4.2 General procedure for the synthesis of 1,2-dihydroquinazolines**

To a solution of 2-aminobenzophenone (0.5 mmol, 100 mg), benzaldehyde (0.5 mmol, 54 mg) and ammonium hydroxide (0.5 mL) in acetonitrile (3 mL), CuO@SiO<sub>2</sub> catalyst (10 wt%, 10 mg) was added. The mixture was allowed to stir at room temperature and the progress of the reaction was followed using thin layer chromatography (TLC). After the completion of the reaction, the catalyst was filtered off and washed with acetonitrile. Combined acetonitrile was removed under reduced pressure. Organics were extracted with ethyl acetate (2 x 20 mL) and the combined organic fraction was washed with water (2 x 10 mL) and brine (10 mL). Drying over Na<sub>2</sub>SO<sub>4</sub> and removal of the solvent under reduced pressure, produced the crude mixture which was purified by column chromatography using ethyl acetate /hexane (10%-30% ethyl acetate in hexane) as eluent. For further recyclability experiments, the catalyst was oven-dried (at 100 °C for 10 h) before the next run.

#### **2.4.3 General procedure for the determination of MIC of the synthesized 1,2-dihydroquinazolines**

MIC determination assay was performed for test compounds as well as standard compounds using a reported method.<sup>67</sup> Briefly the compounds were dissolved in DMSO to prepare stock solutions of 5 mg/ml. Further to determine the MIC, the compounds were diluted in MHB (Muller Hinton broth) to give the starting

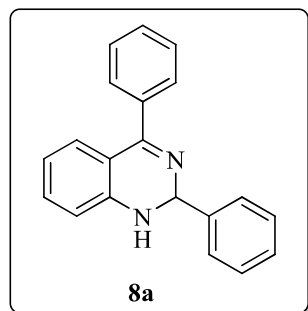
concentration of 1000  $\mu\text{g/mL}$ . Further dilutions were carried out throughout the plate to a range of 0.95  $\mu\text{g/mL}$ . Bacteria inocula was grown to 1 OD at 600 nm, equivalent to McFarland standards, and added to all the wells of the 96 well microtiter plate (10  $\mu\text{L}$ ) from a final density of  $0.5 \times 10^5$  cfu/ml. The plate was incubated at 37 °C for 72 hours. The MIC was recorded as the lowest concentration at which no bacterial growth was observed which was further confirmed by the addition of 20  $\mu\text{L}$  of MTT (3-(4,5-Dimethylthiazol-2-yl)-2,5-Diphenyltetrazolium Bromide) dissolved in MeOH to each well and incubation at 37 °C for 20 min. Purple coloration indicated bacterial growth. The experiment was performed in triplicates with appropriate DMSO. Safety standards were strictly maintained and the experiments were performed in a BSL-2 facility.

#### **2.4.4 General procedure for the synthesis of HMF**

To a solution of fructose (0.27 mmol, 50 mg) in DMSO solvent (3 mL), CuO@SiO<sub>2</sub> catalyst (15 wt%, 15 mg) was added and the mixture was allowed to stir at 120 °C for 5 h. The progress of the reaction was monitored by using thin layer chromatography (TLC). After the conversion, 10 mL ethyl acetate was added to the reaction mixture followed by filtration to recover the catalyst. Organics were extracted with ethyl acetate (2 x 30 mL) and the combined organic fraction was washed with water (2 x 20 mL) and brine (20 mL). Drying over Na<sub>2</sub>SO<sub>4</sub> and removal of the solvent under reduced pressure, produced the final product which was then analysed in a High-Pressure Liquid Chromatography (HPLC) for purity. The HPLC

experiment was carried out in a Waters UHPLC system having C<sub>18</sub> column (2.1 mm x 100 mm, particle size < 2 micron) with mobile phase, water (0.1 % HCOOH): acetonitrile (0.1 % HCOOH). The operating condition was maintained by fixing temperature at 20 °C, injection volume 10 μL, flow rate 300 μL/min and UV absorbance 280 nm. The gradient flow of the mobile phase, water (0.1 % HCOOH): acetonitrile (0.1 % HCOOH) was 0-0.5 min 90%; 10%; at 2-3 min 10%; 90%; 4-5 min 90%; 10%. Finally, the structure of the compound was confirmed using NMR and HRMS.

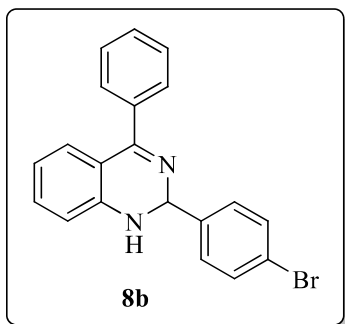
## 2.5 Characterization data of the synthesized compounds



### 2,4-Diphenyl-1,2-dihydroquinazoline (8a)

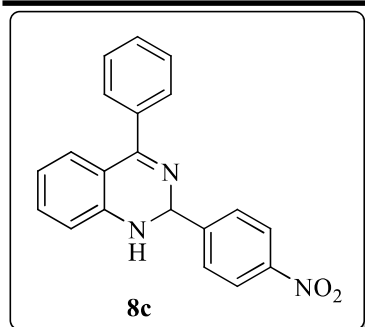
Yellow solid; Mp: 49-50 °C (lit.<sup>2</sup> 51-53 °C); Yield: 82%; <sup>1</sup>H NMR (500 MHz, CDCl<sub>3</sub>): δ 7.62 – 7.56 (m, 4H), 7.44 – 7.34 (m, 6H), 7.29 – 7.24 (m, 1H), 7.17 (d, 1H, *J* = 8.0 Hz), 6.73 (t, 1H, *J* = 7.5 Hz), 6.67 (d, 1H, *J* = 8.0 Hz), 5.94 (s, 1H), 4.29 (s, 1H); <sup>13</sup>C NMR (125 MHz, CDCl<sub>3</sub>): δ 165.7 (C), 146.7 (C), 142.4 (C), 138.0 (C), 132.7 (CH), 129.3 (CH), 129.1 (CH), 128.8 (CH), 128.6 (CH), 128.3 (CH), 128.0

(CH), 127.2 (CH), 118.2 (CH), 117.8 (C), 114.1 (CH), 72.5 (CH); HRMS (ESI)  $m/z$  285.1389 ( $[M+H]^+$  C<sub>20</sub>H<sub>17</sub>N<sub>2</sub>, requires 285.1392).



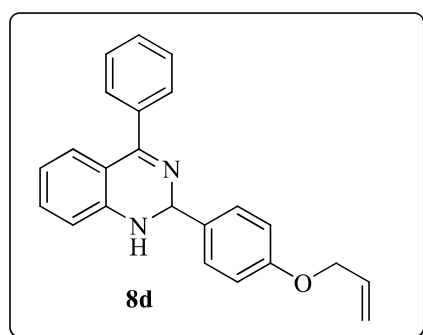
### 2-(4-Bromophenyl)-4-phenyl-1,2-dihydroquinazoline (8b)

Yellow solid; Mp: 118-120 °C; Yield: 72%; <sup>1</sup>H NMR (500 MHz, CDCl<sub>3</sub>): δ 7.50 – 7.33 (m, 9H), 7.22 – 7.17 (m, 1H), 7.10 (d, 1H,  $J = 8.0$  Hz), 6.67 (t, 1H,  $J = 7.5$  Hz), 6.61 (d, 1H,  $J = 8.0$  Hz), 5.83 (s, 1H), 4.19 (s, 1H); <sup>13</sup>C NMR (125 MHz, CDCl<sub>3</sub>): δ 166.2 (C), 146.7 (C), 141.7 (C), 138.1 (C), 133.1 (CH), 132.0 (CH), 129.7 (CH), 129.4 (CH), 129.3 (CH), 129.1 (CH), 128.3 (CH), 122.5 (C), 118.7 (CH), 118.1 (C), 114.5 (CH), 72.2 (CH); HRMS (ESI)  $m/z$  363.0501 ( $[M+H]^+$  C<sub>20</sub>H<sub>16</sub>N<sub>2</sub>Br, requires 363.0497).



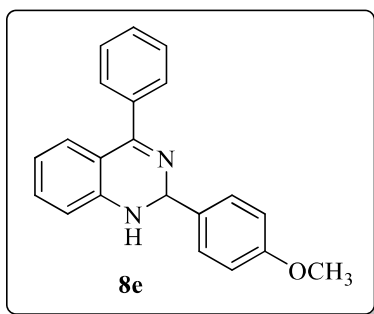
### 2-(4-Nitrophenyl)-4-phenyl-1,2-dihydroquinazoline (8c)

Yellow solid; Mp: 126-128 °C; Yield: 71%;  $^1\text{H}$  NMR (500 MHz,  $\text{CDCl}_3$ ):  $\delta$  8.22 (d, 2H,  $J = 8.5$  Hz), 7.78 (d, 2H,  $J = 8.5$  Hz), 7.57 – 7.54 (m, 2H), 7.47 – 7.42 (m, 3H), 7.30 (dt, 1H,  $J = 8.0, 1.0$  Hz), 7.18 (dd, 1H,  $J = 8.0, 1.0$  Hz), 6.77 (t, 1H,  $J = 7.5$  Hz), 6.74 (d, 1H,  $J = 7.5$  Hz), 6.07 (s, 1H), 4.41 (s, 1H);  $^{13}\text{C}$  NMR (125 MHz,  $\text{CDCl}_3$ ):  $\delta$  166.4 (C), 149.3 (C), 147.7 (C), 146.0 (C), 137.5 (C), 133.1 (CH), 129.6 (CH), 129.0 (CH), 129.0 (CH), 128.2 (CH), 128.1 (CH), 123.7 (CH), 118.8 (CH), 117.8 (C), 114.5 (CH), 71.4 (CH); HRMS (ESI)  $m/z$  330.1239 ( $[\text{M}+\text{H}]^+$   $\text{C}_{20}\text{H}_{16}\text{N}_3\text{O}_2$ , requires 330.1243).



**2-(4-(Allyloxy)phenyl)-4-phenyl-1,2-dihydroquinazoline (8d)**

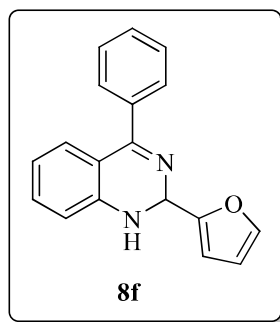
Yellow semi-solid; Yield: 79%;  $^1\text{H}$  NMR (500 MHz,  $\text{CDCl}_3$ ):  $\delta$  7.59 (d, 2H,  $J = 6.5$  Hz), 7.52 (d, 2H,  $J = 8.5$  Hz), 7.49 – 7.42 (m, 3H), 7.29 – 7.25 (m, 1H), 7.19 (d, 1H,  $J = 8.0$  Hz), 6.95 (d, 2H,  $J = 8.5$  Hz), 6.74 (t, 1H,  $J = 7.5$  Hz), 6.67 (d, 1H,  $J = 8.0$  Hz), 6.11 – 6.04 (m, 1H), 5.88 (s, 1H), 5.46 – 5.41 (m, 1H), 5.31 (d, 1H,  $J = 10.5$  Hz), 4.56 (d, 2H,  $J = 5.0$  Hz), 4.31 (s, 1H);  $^{13}\text{C}$  NMR (125 MHz,  $\text{CDCl}_3$ ):  $\delta$  165.6 (C), 158.5 (C), 146.8 (C), 138.0 (C), 134.9 (C), 133.1 (CH), 132.7 (CH), 129.3 (CH), 129.1 (CH), 128.8 (CH), 128.4 (CH), 128.0 (CH), 118.1 (CH), 117.7 (C), 117.6 ( $\text{CH}_2$ ), 114.7 (CH), 114.1 (CH), 72.1 (CH), 68.7 ( $\text{CH}_2$ ); HRMS (ESI)  $m/z$  341.1635 ( $[\text{M}+\text{H}]^+$   $\text{C}_{23}\text{H}_{21}\text{N}_2\text{O}$ , requires 341.1654).

**2-(4-Methoxyphenyl)-4-phenyl-1,2-dihydroquinazoline (8e)**

Yellow solid; Mp: 101-103 °C, Yield: 80%,  $^1\text{H}$  NMR (500 MHz,  $\text{CDCl}_3$ ):  $\delta$  7.55 (dd, 2H,  $J = 7.5, 2.0$  Hz), 7.49 (d, 2H,  $J = 8.5$  Hz), 7.45 – 7.37 (m, 3H), 7.25 – 7.19 (m, 1H), 7.14 (d, 1H,  $J = 8.0$  Hz), 6.89 (d, 2H,  $J = 8.0$  Hz), 6.69 (t, 1H,  $J = 8.0$  Hz), 6.63 (d, 1H,  $J = 8.0$  Hz), 5.86 (s, 1H), 4.24 (s, 1H), 3.78 (s, 3H);  $^{13}\text{C}$  NMR (125 MHz,

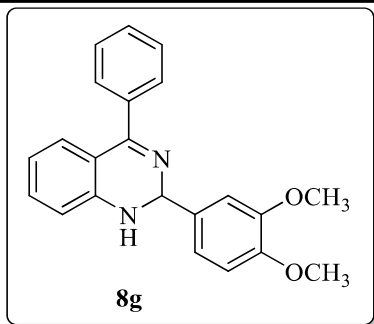


CDCl<sub>3</sub>):  $\delta$  166.0 (C), 160.0 (C), 147.1 (C), 138.3 (C), 135.1 (C), 133.0 (CH), 129.5 (CH), 129.4 (CH), 129.1 (CH), 129.0 (CH), 128.3 (CH), 118.3 (CH), 118.0 (C), 114.4 (CH), 114.2 (CH), 72.4(CH), 55.5 (CH<sub>3</sub>); HRMS (ESI)  $m/z$  315.1515 ([M+H]<sup>+</sup> C<sub>21</sub>H<sub>19</sub>N<sub>2</sub>O, requires 315.1497).



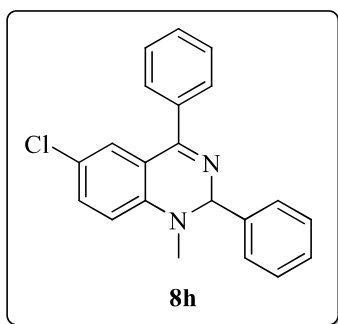
### 2-(Furan-2-yl)-4-phenyl-1,2-dihydroquinazoline (8f)

Yellowish-orange low melting solid; Yield: 77%; <sup>1</sup>H NMR (500 MHz, CDCl<sub>3</sub>):  $\delta$  7.59 (dd, 2H,  $J = 7.5, 1.5$  Hz), 7.48 – 7.41 (m, 4H), 7.28 – 7.25 (m, 1H), 7.18 (d, 1H,  $J = 8.0$  Hz), 6.74 (t, 1H,  $J = 7.5$  Hz), 6.69 (d, 1H,  $J = 8.0$  Hz), 6.40 (d, 1H,  $J = 3.0$  Hz), 6.36 – 6.33 (m, 1H), 6.11 (s, 1H), 4.56 (s, 1H); <sup>13</sup>C NMR (125 MHz, CDCl<sub>3</sub>):  $\delta$  167.0 (C), 154.4 (C), 146.4 (C), 142.6 (CH), 138.1 (C), 133.0 (CH), 129.7 (CH), 129.4 (CH), 129.1 (CH), 128.3 (CH), 118.7 (CH), 118.1 (C), 114.8 (CH), 110.5 (CH), 107.7 (CH), 66.3 (CH); HRMS (ESI)  $m/z$  275.1186 ([M+H]<sup>+</sup> C<sub>18</sub>H<sub>15</sub>N<sub>2</sub>O, requires 275.1184).



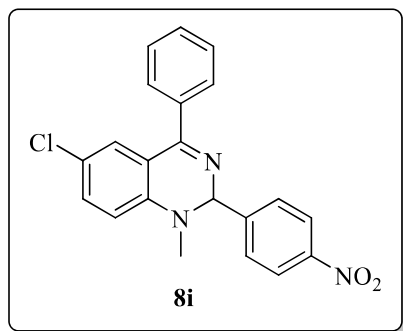
### 2-(3,4-Dimethoxyphenyl)-4-phenyl-1,2-dihydroquinazoline (8g)

Yellowish-orange low melting solid; Yield: 75%;  $^1\text{H}$  NMR (500 MHz,  $\text{CDCl}_3$ ):  $\delta$  7.59 (d, 2H,  $J = 7.0$  Hz), 7.46 – 7.42 (m, 3H), 7.29 – 7.27 (m, 1H), 7.22 – 7.17 (m, 1H), 7.11 (d, 1H,  $J = 7.5$  Hz), 6.89 (d, 1H,  $J = 8.5$  Hz), 6.76 (t, 1H,  $J = 7.5$  Hz), 6.71 (d, 1H,  $J = 8.0$  Hz), 5.86 (s, 1H), 4.28 (s, 1H), 3.90 (s, 6H);  $^{13}\text{C}$  NMR (125 MHz,  $\text{CDCl}_3$ ):  $\delta$  165.7 (C), 149.0 (C), 149.0 (C), 146.9 (C), 138.0 (C), 135.1 (C), 132.6 (CH), 129.3 (CH), 129.1 (CH), 128.8 (CH), 128.0 (CH), 119.5 (CH), 118.2 (CH), 117.8 (C), 114.1 (CH), 110.8 (CH), 110.2 (CH), 72.6 (CH), 55.9 ( $\text{CH}_3$ ), 55.8 ( $\text{CH}_3$ ); HRMS (ESI)  $m/z$  345.1587 ( $[\text{M}+\text{H}]^+$   $\text{C}_{22}\text{H}_{21}\text{N}_2\text{O}_2$ , requires 345.1603).

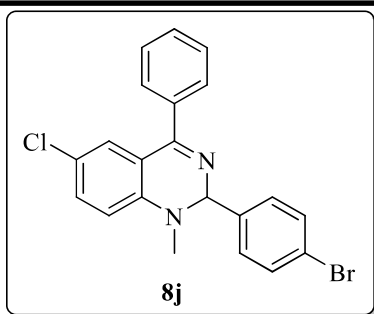


**6-Chloro-1-methyl-2,4-diphenyl-1,2-dihydroquinazoline (8h)**

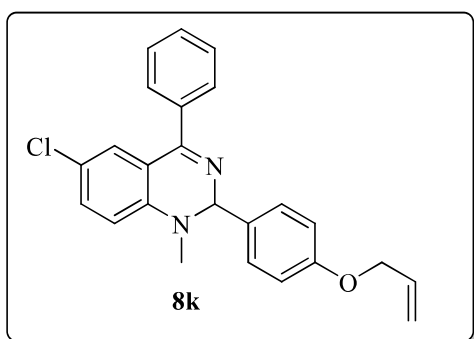
Yellow solid; Mp: 131-132 °C; Yield: 70%;  $^1\text{H}$  NMR (500 MHz,  $\text{CDCl}_3$ ):  $\delta$  7.50 – 7.39 (m, 5H), 7.32 – 7.23 (m, 6H), 7.08 (d, 1H,  $J = 2.5$  Hz), 6.53 (d, 1H,  $J = 8.5$  Hz), 6.20 (s, 1H), 2.85 (s, 3H);  $^{13}\text{C}$  NMR (125 MHz,  $\text{CDCl}_3$ ):  $\delta$  163.6 (C), 145.7 (C), 139.7 (C), 137.7 (C), 133.3 (CH), 129.7 (CH), 129.0 (CH), 128.8 (CH), 128.6 (CH), 128.5 (CH), 128.5 (CH), 126.6 (CH), 121.2 (C), 118.3 (C), 112.7 (CH), 79.6 (CH), 35.2 ( $\text{CH}_3$ ); HRMS (ESI)  $m/z$  333.1161 ( $[\text{M}+\text{H}]^+$   $\text{C}_{21}\text{H}_{18}\text{N}_2\text{Cl}$ , requires 333.1159).

**6-Chloro-1-methyl-2-(4-nitrophenyl)-4-phenyl-1,2-dihydroquinazoline (8i)**

Yellow solid; Mp: 50-52 °C; Yield: 73%;  $^1\text{H}$  NMR (500 MHz,  $\text{CDCl}_3$ ):  $\delta$  8.16 (dd, 2H,  $J = 7.0, 2.0$  Hz), 7.49 (d, 2H,  $J = 8.5$  Hz), 7.45 – 7.42 (m, 5H), 7.30 (dd, 1H,  $J = 9.0, 2.5$  Hz), 7.08 (d, 1H,  $J = 2.5$  Hz), 6.62 (d, 1H,  $J = 9.0$  Hz), 6.30 (s, 1H), 2.92 (s, 3H);  $^{13}\text{C}$  NMR (125 MHz,  $\text{CDCl}_3$ ):  $\delta$  164.7 (C), 148.0 (C), 146.8 (C), 145.2 (C), 137.2 (C), 133.9 (CH), 130.1 (CH), 129.0 (CH), 128.8 (CH), 128.6 (CH), 127.9 (CH), 124.2 (CH), 122.1 (C), 118.3 (C), 113.1 (CH), 78.6 (CH), 35.7 ( $\text{CH}_3$ ); HRMS (ESI)  $m/z$  378.1001 ( $[\text{M}+\text{H}]^+$   $\text{C}_{21}\text{H}_{17}\text{N}_3\text{O}_2\text{Cl}$ , requires 378.1009).

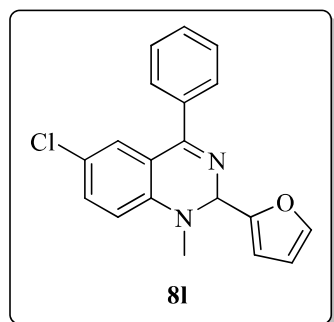
**2-(4-Bromophenyl)-6-chloro-1-methyl-4-phenyl-1,2-dihydroquinazoline (8j)**

Brown low melting solid; Yield: 71%;  $^1\text{H}$  NMR (500 MHz,  $\text{CDCl}_3$ ):  $\delta$  7.48 – 7.39 (m, 7H), 7.27 (dd, 1H,  $J = 8.5, 2.5$  Hz), 7.18 (dd, 2H,  $J = 8.5, 2.5$  Hz), 7.07 (d, 1H,  $J = 2.5$  Hz), 6.55 (d, 1H,  $J = 8.5$  Hz), 6.15 (s, 1H), 2.85 (s, 3H);  $^{13}\text{C}$  NMR (125 MHz,  $\text{CDCl}_3$ ):  $\delta$  164.0 (C), 145.5 (C), 138.7 (C), 138.0 (C), 133.6 (CH), 132.0 (CH), 130.0 (CH), 129.0 (CH), 128.6 (CH), 128.6 (CH), 128.4 (CH), 122.6 (C), 121.6 (C), 118.3 (C), 112.9 (CH), 79.0 (CH), 35.3 ( $\text{CH}_3$ ); HRMS (ESI)  $m/z$  411.0271 ( $[\text{M}+\text{H}]^+$   $\text{C}_{21}\text{H}_{17}\text{N}_2\text{ClBr}$ , requires 411.0264).



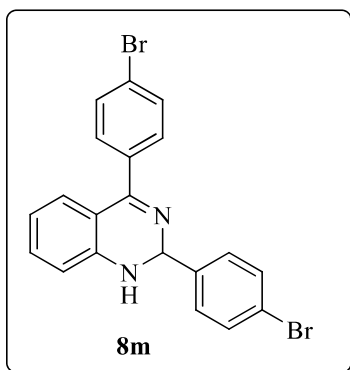
**2-(4-(Allyloxy)phenyl)-6-chloro-1-methyl-4-phenyl-1,2-dihydroquinazoline (8k)**

Yellow solid; Mp: 115-118 °C; Yield: 76%; <sup>1</sup>H NMR (500 MHz, CDCl<sub>3</sub>): δ 7.45 – 7.41 (m, 2H), 7.39 – 7.34 (m, 3H), 7.16 (d, 2H, *J* = 9.0 Hz), 7.02 (d, 1H, *J* = 2.5 Hz), 6.77 (d, 2H, *J* = 8.5 Hz), 6.46 (d, 1H, *J* = 9.0 Hz), 6.08 (s, 1H), 6.00 – 5.92 (m, 1H), 5.32 (dd, 1H, *J* = 17.0, 1.5 Hz), 5.20 (dd, 1H, *J* = 10.5, 1.5 Hz), 4.43 (d, 2H, *J* = 5.0 Hz), 2.77 (s, 3H); <sup>13</sup>C NMR (125 MHz, CDCl<sub>3</sub>): δ 163.1 (C), 158.6 (C), 145.4 (C), 137.4 (C), 133.0 (CH), 133.0 (CH), 131.7 (C), 129.4 (CH), 128.7 (CH), 128.2 (CH), 128.1 (CH), 127.6 (CH<sub>2</sub>), 120.9 (C), 118.0 (C), 117.7 (CH), 114.6 (CH), 112.5 (CH), 78.8 (CH), 68.7 (CH), 34.7 (CH<sub>2</sub>), 29.6 (CH<sub>3</sub>); HRMS (ESI) *m/z* 389.1410 ([M+H]<sup>+</sup> C<sub>24</sub>H<sub>22</sub>N<sub>2</sub>OCl, requires 389.1421).

**6-Chloro-2-(furan-2-yl)-1-methyl-4-phenyl-1,2-dihydroquinazoline (8l)**

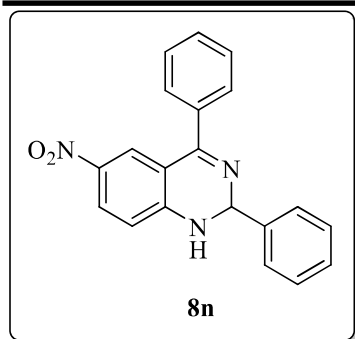
Yellow low melting solid; Yield: 79%; <sup>1</sup>H NMR (500 MHz, CDCl<sub>3</sub>): δ 7.56 (dd, 2H, *J* = 7.5, 1.0 Hz), 7.49 – 7.44 (m, 3H), 7.34 – 7.32 (m, 1H), 7.28 – 7.26 (m, 1H), 7.14 (d, 1H, *J* = 2.0 Hz), 6.57 (d, 1H, *J* = 9.0 Hz), 6.25 (t, 1H, *J* = 2.0 Hz), 6.21 (s, 1H), 6.14 (d, 1H, *J* = 2.0 Hz), 2.98 (s, 3H); <sup>13</sup>C NMR (125 MHz, CDCl<sub>3</sub>): δ 165.4 (C),

151.7 (C), 145.1 (C), 142.5 (CH), 137.3 (C), 132.8 (CH), 129.7 (CH), 128.9 (CH), 128.2 (CH), 128.2 (CH), 121.6 (C), 118.6 (C), 113.1 (CH), 109.9 (CH), 108.1 (CH), 72.4 (CH), 34.9 (CH<sub>3</sub>); HRMS (ESI)  $m/z$  323.0943 ([M+H]<sup>+</sup> C<sub>19</sub>H<sub>16</sub>N<sub>2</sub>OCl, requires 323.0951).



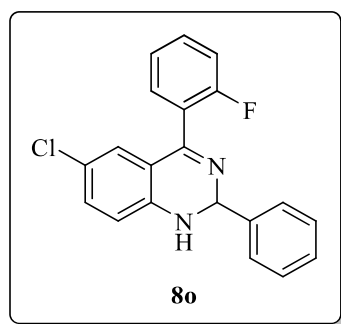
#### 4-(4-Bromophenyl)-2-(4-nitrophenyl)-1,2-dihydroquinazoline (8m)

Yellow low melting solid; Yield: 70%; <sup>1</sup>H NMR (500 MHz, CDCl<sub>3</sub>): δ 8.26 (d, 2H,  $J$  = 9.0 Hz), 7.80 (d, 2H,  $J$  = 9.0 Hz), 7.59 (d, 2H,  $J$  = 8.5 Hz), 7.47 (d, 2H,  $J$  = 8.5 Hz), 7.34 (t, 1H,  $J$  = 8.0 Hz), 7.17 (d, 1H,  $J$  = 8.0 Hz), 6.81 (t, 1H,  $J$  = 8.0 Hz), 6.77 (d, 1H,  $J$  = 8.0 Hz), 6.05 (s, 1H), 4.37 (s, 1H); <sup>13</sup>C NMR (125 MHz, CDCl<sub>3</sub>): δ 165.4 (C), 149.0 (C), 147.8 (C), 146.1 (C), 136.4 (C), 133.3 (CH), 131.3 (CH), 130.7 (CH), 128.6 (CH), 128.2 (CH), 124.1 (C), 123.8 (CH), 119.0 (CH), 117.5 (C), 114.6 (CH), 71.5 (CH); HRMS (ESI)  $m/z$  408.0333 ([M+H]<sup>+</sup> C<sub>20</sub>H<sub>15</sub>N<sub>3</sub>O<sub>2</sub>Br, requires 408.0348).



### 6-Nitro-2,4-diphenyl-1,2-dihydroquinazoline (8n)

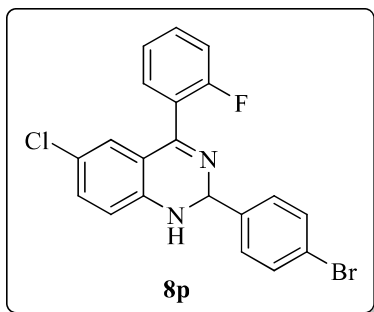
Brown solid; Mp: 196-197 °C; Yield: 74%;  $^1\text{H}$  NMR (500 MHz,  $\text{CDCl}_3$ ):  $\delta$  8.14 – 8.08 (m, 2H), 7.57 – 7.35 (m, 10H), 6.60 (d, 1H,  $J = 9.0$  Hz), 6.30 (s, 1H), 5.08 (s, 1H);  $^{13}\text{C}$  NMR (125 MHz,  $\text{CDCl}_3$ ):  $\delta$  164.1 (C), 151.1 (C), 141.7 (C), 138.6 (C), 136.8 (C), 130.3 (CH), 129.3 (CH), 129.2 (CH), 129.2 (CH), 129.0 (CH), 128.8 (CH), 127.1 (CH), 125.6 (CH), 115.0 (C), 113.6 (CH), 72.9 (CH); HRMS (ESI)  $m/z$  330.1239 ( $[\text{M}+\text{H}]^+$   $\text{C}_{20}\text{H}_{16}\text{N}_3\text{O}_2$ , requires 330.1243).



### 6-Chloro-4-(2-fluorophenyl)-2-phenyl-1,2-dihydroquinazoline (8o)

Yellow solid; Mp: 223-225 °C; Yield: 72%;  $^1\text{H}$  NMR (500 MHz,  $\text{CDCl}_3$ ):  $\delta$  7.54 (d, 2H,  $J = 7.0$  Hz), 7.42 – 7.32 (m, 5H), 7.20 (t, 1H,  $J = 7.0$  Hz), 7.16 – 7.10 (m, 2H),

6.89 (t, 1H,  $J = 2.0$  Hz), 6.52 (d, 1H,  $J = 8.5$  Hz), 6.06 (s, 1H), 4.29 (s, 1H);  $^{13}\text{C}$  NMR (125 MHz,  $\text{CDCl}_3$ ):  $\delta$  161.4 (C), 160.1 (C, d,  $J = 247.5$  Hz), 144.2 (C), 142.2 (C), 133.2 (CH), 131.3 (CH), 131.1 (CH, d,  $J = 3.75$  Hz), 128.9 (CH), 128.8 (CH), 127.8 (CH, d,  $J = 1.25$  Hz), 127.3 (CH), 125.7 (C, d,  $J = 16.25$  Hz), 124.6 (CH, d,  $J = 3.7$  Hz), 123.1 (C), 118.6 (C), 116.2 (d, CH,  $J = 22.5$  Hz), 115.5 (CH), 73.0 (CH); HRMS (ESI)  $m/z$  337.0902 ( $[\text{M}+\text{H}]^+$   $\text{C}_{20}\text{H}_{15}\text{N}_2\text{FCl}$ , requires 337.0908).



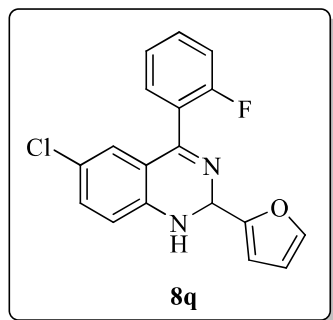
### 2-(4-Bromophenyl)-6-chloro-4-(2-fluorophenyl)-1,2-dihydroquinazoline (8p)

Yellow solid; Mp: 192-193 °C; Yield: 68%;  $^1\text{H}$  NMR (500 MHz,  $\text{CDCl}_3$ ):  $\delta$  7.50 (d, 2H,  $J = 7.5$  Hz), 7.43 (d, 2H,  $J = 7.5$  Hz), 7.42 – 7.38 (m, 2H), 7.23 – 7.15 (m, 2H), 7.13 (t, 1H,  $J = 9.0$  Hz), 6.89 (s, 1H), 6.56 (d, 1H,  $J = 9.0$  Hz), 6.05 (s, 1H), 4.23 (s, 1H);  $^{13}\text{C}$  NMR (125 MHz,  $\text{CDCl}_3$ ):  $\delta$  161.7 (C), 160.1 (d, C,  $J = 247.75$  Hz), 144.0 (C), 141.2 (C), 133.4 (CH), 132.1 (CH), 131.5 (d, C,  $J = 8.0$  Hz), 131.0 (C), 129.1 (CH), 128.0 (CH), 125.5 (d, C,  $J = 15.4$  Hz), 124.7 (d, CH,  $J = 3.5$  Hz), 123.5 (CH),



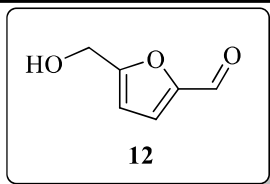
122.8 (CH), 118.7 (C), 116.3 (d, CH,  $J = 21.25$  Hz), 115.7 (CH), 72.4 (CH); HRMS

(ESI)  $m/z$  415.0025 ( $[M+H]^+$  C<sub>20</sub>H<sub>14</sub>N<sub>2</sub>FClBr, requires 415.0013).



### 6-Chloro-4-(2-fluorophenyl)-2-(furan-2-yl)-1,2-dihydroquinazoline (8q)

Yellow low melting solid; Yield: 70%; <sup>1</sup>H NMR (500 MHz, CDCl<sub>3</sub>):  $\delta$  7.44 – 7.37 (3H, m), 7.21 (dd, 1H,  $J = 7.5, 1.0$  Hz), 7.17 – 7.11 (2H, m), 6.89 (1H, m), 6.57 (d, 1H,  $J = 9.0$  Hz), 6.39 (1H, d,  $J = 3.0$  Hz), 6.34 – 6.31 (1H, m), 6.23 (1H, s), 4.50 (1H, s); <sup>13</sup>C NMR (125 MHz, CDCl<sub>3</sub>):  $\delta$  162.6 (C), 160.2 (d, C,  $J = 247.5$  Hz), 153.6 (C), 143.6 (C), 142.9 (CH), 133.3 (CH), 131.5 (d, CH,  $J = 8.75$  Hz), 131.0 (d, CH,  $J = 2.5$  Hz), 127.9 (CH), 125.6 (d, C,  $J = 15.0$  Hz), 124.6 (d, CH,  $J = 3.75$  Hz), 123.5 (C), 118.9 (C), 116.3 (d, CH,  $J = 21.25$  Hz), 116.0 (CH), 110.6 (CH), 108.0 (CH), 66.5 (CH); HRMS (ESI)  $m/z$  327.0713 ( $[M+H]^+$  C<sub>18</sub>H<sub>13</sub>N<sub>2</sub>OFCl, requires 327.0700).

**5-(Hydroxymethyl)furan-2-carbaldehyde (12)**

Yellow low melting solid; Yield: 70%;  $^1\text{H}$  NMR (500 MHz,  $\text{CDCl}_3$ ):  $\delta$  9.53 (s, 1H), 7.19 (d, 1H,  $J = 4.5$  Hz), 6.49 (d, 1H,  $J = 4.5$  Hz), 4.68 (s, 2H), 2.82 (s, 1H);  $^{13}\text{C}$  NMR (125 MHz,  $\text{CDCl}_3$ ):  $\delta$  177.9 (CH), 160.9 (C), 152.3 (CH), 123.4 (C), 110.1 (CH), 57.6 ( $\text{CH}_2$ ); HRMS (ESI)  $m/z$  127.0392 ( $[\text{M}+\text{H}]^+$   $\text{C}_6\text{H}_7\text{O}_3$ , requires 127.0395).

---

**2.6 References**

1. (a) P. Lignier, R. Bellabarba and R. P. Tooze, *Chem. Soc. Rev.* 2012, **41**, 1708; (b) M. Alavi and M. Rai, *Expert Rev. Anti-Infect. Ther.* 2019, **217**, 419.
2. (a) X. He, D. -P. Yang, X. Zhang, M. Liu, Z. Kang, C. Lin, N. Jia and R. Luque, *Chem. Eng. J.* 2019, **369**, 621; (b) D. Malwal and P. Gopinath, *J. Hazard. Mater.* 2017, **321**, 611; (c) J. Huang, L. Lin, D. Sun, H. Chen, D. Yang and Q. Li, *Chem. Soc. Rev.* 2015, **44**, 6330.
3. S. M. Lomnicki, H. Wu, S. N. Osborne, J. M. Pruett, R. L. McCarley, E. Poliakoff and B. Dellinger, *Mater. Sci. Eng. B.* 2010, **175**, 136.
4. N. Zhang, Y. L. Du, Y. Zhang and C. M. Wang, *J. Mater. Chem.* 2011, **21**, 5408.
5. (a) J. B. Reitz and E. I. Solomon, *J. Am. Chem. Soc.* 1998, **120**, 11467; (b) C. Y. Chiang, K. Aroh, N. Franson, V. R. Satsangi, S. Dass and S. Ehrman, *Int. J. Hydrogen Energy* 2011, **36**, 15519; (c) P. Udani, P. Gunawardana, H. C. Lee and D. H. Kim, *Int. J. Hydrogen Energy* 2009, **34**, 7648; (d) J. -L. Cao, G.-S. Shao, Y. Wang, Y. Liu and Z. -Y. Yuan, *Catal. Commun.* 2008, **9**, 2555.
6. F. Shi, M. K. Tse, M.-M. Pohl, A. Brückner, S. Zhang and M. Beller, *Angew. Chem. Int. Ed.* 2007, **46**, 8866.

- 
7. D. Astruc, F. Lu and J. R. Aranzaes, *Angew. Chem. Int. Ed.* 2005, **44**, 7852.
  8. A. Corma and P. Serna, *Science* 2006, **313**, 332.
  9. Z. W. Huang, F. Cui, H. X. Kang, J. Chen, X. Z. Zhang and C. G. Xia, *Chem. Mater.* 2008, **20**, 5090.
  10. M. L. Kantam, J. Yadav, S. Laha, P. Srinivas, B. Sreedhar and F. Figueras, *J. Org. Chem.* 2009, **74**, 4608.
  11. (a) S. J. Tauster, *Acc. Chem. Res.* 1987, **20**, 389; (b) J. J. Liu, *ChemCatChem* 2011, **3**, 934; (c) S. Bernal, J. Calvino, M. Cauqui, J. Gatica, C. Larese, J. Pérez Omil and J. Pintado, *Catal. Today* 1999, **50**, 175.
  12. F. Hoffmann, M. Cornelius, J. Morell and M. Fröba, *Angew. Chem. Int. Ed.* 2006, **45**, 3216.
  13. K. Y. Ho, G. McKay and K. L. Yeung, *Langmuir* 2003, **19**, 3019.
  14. M.S. Morey, A. Davidson and G.D. Stucky, *J. Porous Mater.* 1998, **5**, 195.
  15. F. Schüth and W. Schmidt, *Adv. Mater.* 2002, **14**, 629.
  16. D. M. Antonelli and J. Y. Ying, *Curr. Opin. Colloid Interface Sci.* 1996, **1**, 523.
  17. M. Ghorbanpour, M. Moghimi and S. Lotfiman, *J. Water Environ. Nanotechnol.* 2017, **2**, 112.

- 
18. K. M. Parida and D. Rath, *Appl. Catal. A-Gen.* 2007, **321**, 101.
  19. R. G. Kadam, A. K. Rathi, K. Cepe, R. Zboril, R. S. Varma, M. B. Gawande and R. V. Jayaram, *ChemPlusChem* 2017, **82**, 467.
  20. H. Li, L. Ban, Z. Wang, P. Meng, Y. Zhang, R. Wu and Y. Zhao, *Nanomaterials* 2019, **9**, 842.
  21. S. Qiu, H. Zhou, Z. Shen, L. Hao, H. Chen and X. Zhou, *RSC Adv.* 2020, **10**, 2767.
  22. A. Patel, P. Shukla, T. Rufford, S. Wang, J. Chen, V. Rudolph and Z. Zhu, *Appl. Catal. A-Gen.* 2011, **409**, 55.
  23. S. Samadi, A. Ashouria and M. Ghambarian, *RSC Adv.* 2017, **7**, 19330.
  24. E. Barrera-Calva, J. Méndez-Vivar, M. Ortega-López, L. Huerta-Arcos, J. Morales-Corona and R. Olayo-González, *Adv. Mater. Sci. Eng.* 2008, 190920.
  25. K. Wang, G. -Y. Zhu and Q. Xiao, *Surf. Innov.* 2019, **7**, 44.
  26. M. Dixit, M. Mishra, P. A. Joshi and D. O. Shah, *Procedia Eng.* 2013, **51**, 467.
  27. J. P. Michael, *Nat. Prod. Rep.* 2008, **25**, 166.
  28. I. Khan, A. Ibrar, W. Ahmed and A. Saeed, *Eur. J. Med. Chem.* 2015, **90**, 124.
  29. E. Jafari, M. R. Khajouei, F. Hassanzadeh, G. H. Hakimelahi and G. A. Khodarahmi, *Res. Pharm. Sci.* 2016, **11**, 1.

- 
30. R. Los, M. Trojanowska-Wesolowska, A. Malm, M. M. Karpinska, J. Matysiak, A. Niewiadomy and U. Glaszcz, *Heteroat. Chem.* 2012, **23**, 265.
31. S. Patterson, M. S. Alphey, D. C. Jones, E. J. Shanks, I. P. Street, J. A. Frearson, P. G. Wyatt, I. H. Gilbert and A. H. Fairlamb, *J. Med. Chem.* 2011, **54**, 6514.
32. W. J. Li, Q. Li, D. L. Liu and M. W. Ding, *J. Agric. Food Chem.* 2013, **61**, 1419.
33. Y. Kobayashi, Y. Nakano, M. Kizaki, K. Hoshikuma, Y. Yokoo and T. Kamiya, *Planta Med.* 2001, **67**, 628.
34. B. Park, J. H. Nam, J. H. Kim, H. J. Kim, V. Onnis, G. Balboni, K. -T. Lee, J. H. Park, M. Catto, A. Carotti and J. Y. Lee, *Bioorg. Med. Chem. Lett.* 2017, **27**, 1179.
35. B. M. Verdel, P. C. Souverein, A. C. G. Egberts and H. G. M. Leufkens, *Ann. Pharmacother.* 2006, **40**, 1040.
36. M. Marschall, T. Stamminger, A. Urban, S. Wildum, H. Ruebsamen-Schaeff, H. Zimmermann and P. Lischka, *Antimicrob. Agents Chemother.* 2012, **56**, 1135.
37. L. Lad, L. Luo, J. D. Carson, K. W. Wood, J. J. Hartman, R. A. Copeland and R. Sakowicz, *Biochemistry.* 2008, **47**, 3576.
38. M. Rosini, A. Antonello, A. Cavalli, M. L. Bolognesi, A. Minarini, G.

- 
- Marucci, E. Poggesi, A. Leonardi and C. Melchiorre, *J. Med. Chem.* 2003, **46**, 4895.
39. K. Nepali, S. Sharma, R. Ojha and K. L. Dhar, *Med. Chem. Res.* 2013, **22**, 1.
40. R. Sarma and D. Prajapati, *Green Chem.* 2011, **13**, 718.
41. K. K. Gudimella, K. B. Bonige, R. Gundla, N. K. Katari, B. Yamajala and V. R. Battula, *ChemistrySelect* 2019, **4**, 12528.
42. R. Rohlmann, T. Stopka, H. Richter and O. G. Mancheño, *J. Org. Chem.* 2013, **78**, 6050.
43. Q. Chen, Z. Mao, K. Gao, F. Guo, L. Sheng and Z. Chen, *J. Org. Chem.* 2018, **83**, 8750.
44. A. Kamal, K. S. Babu, Y. Poornachandra, B. Nagaraju, S. M. A. Hussaini, S. P. Shaik, C. G. Kumar and Abdullah Alarifi, *Arab. J. Chem.* 2019, **12**, 3546.
45. S. Azizi, J. Soleymani and M. Hasanzadeh, *Nanocomposites* 2020, **6**, 31.
46. C. Derabli, R. Boulcina, G. Kirsch, B. Carboni and A. Debache, *Tetrahedron Lett.* 2014, **55**, 200.
47. V. Srivastava, *Curr. Organocatal.* 2019, **6**, 44.
48. S. M. Baghbanian and M. Farhang, *RSC Adv.* 2014, **4**, 11624.
49. J. Zhang, C. Yu, S. Wang, C. Wan and Z. Wang, *Chem. Commun.* 2010, **46**, 5244.

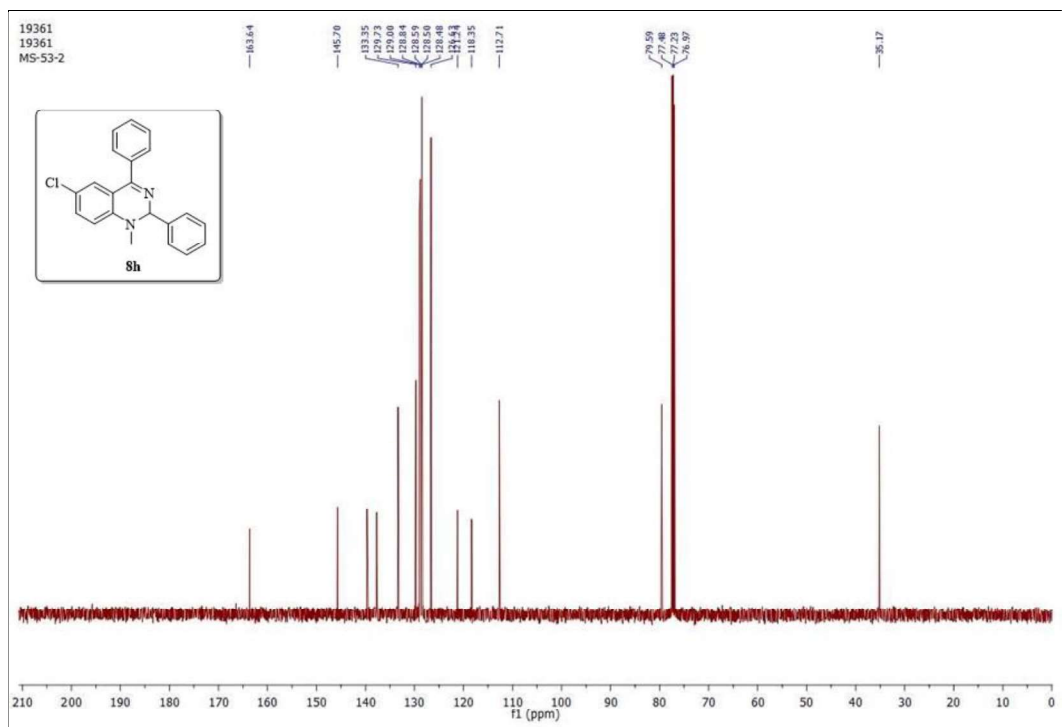
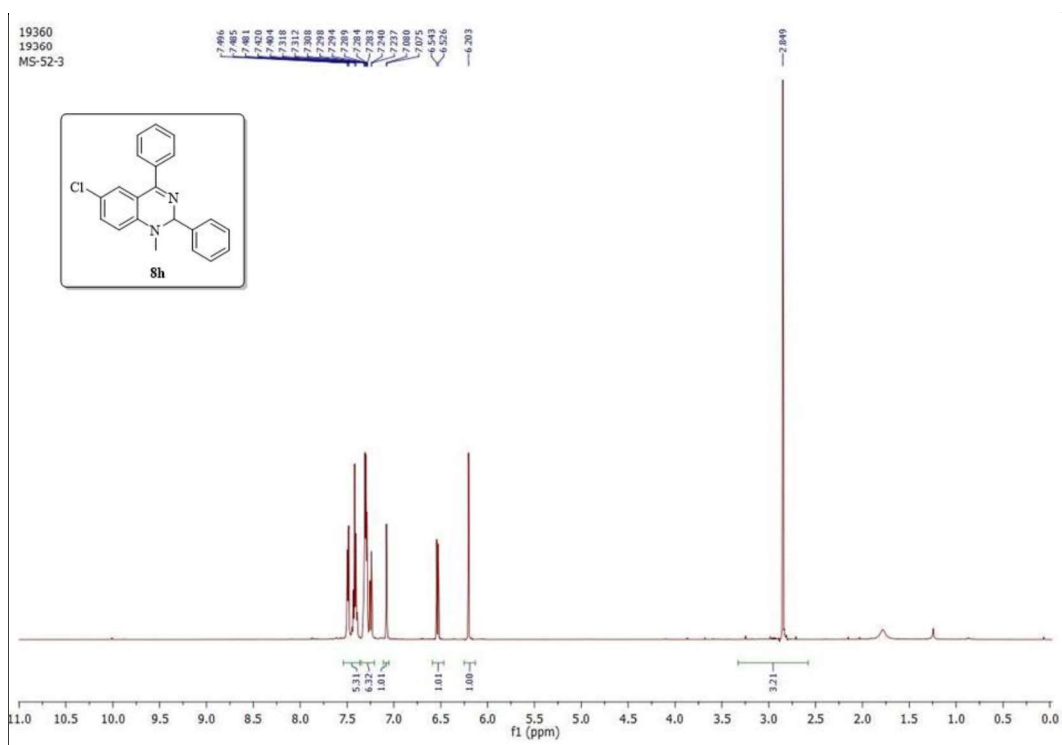
- 
50. W. Zhang, F. Guo, F. Wang, N. Zhao, L. Liu, J. Li and Z. Wang, *Org. Biomol. Chem.* 2014, **12**, 5752.
51. M. Dai, J. Kwon, Y. J. Chabal, M. D. Halls and R. G. Gordon, *Mater. Res. Soc. Symp. Proc.* 2009, **1155**, 11.
52. P. Deka, R. C. Deka and P. Bharali, *New J. Chem.* 2014, **38**, 1789.
53. C. A. Schneider, W. S. Rasband and K. W. Eliceiri, *Nat. Methods.* 2012, **9**, 671.
54. F. L. Hussain, M. Suri, A. Namdeo, G. Borah, D. Dutta, T. Goswami and P. Pahari, *Catal. Commun.* 2019, **124**, 76.
55. T. Tsoncheva, G. Issa, T. Blasco, M. Dimitrov, M. Popova, S. Hernández, D. Kovacheva, G. Atanasova and J. M. L. Nieto, *Appl. Catal. A Gen.* 2013, **453**, 1.
56. N. Benito and M. Flores, *J. Phys. Chem. C.* 2017, **121**, 18771.
57. Q. T. Trinh, K. Bholá, P. N. Amaniampong, F. Jérôme and S. H. Mushrif, *J. Phys. Chem. C.* 2018, **122**, 22397.
58. (a) S. Brunauer, L. S. Deming, W. E. Deming and E. Teller, *J. Am. Chem. Soc.* 1940, **62**, 1723; (b) S. Brunauer, P. H. Emmett and E. Teller, *J. Am. Chem. Soc.* 1938, **60**, 309.
59. A. Borodziński and M. Bonarowska, *Langmuir* 1997, **13**, 5613.
60. K. N. V. Sastry, B. Prasad, B. Nagaraju, V. G. Reddy, A. Alarifi, B. N. Babu and A. Kamal, *ChemistrySelect* 2017, **2**, 5378.



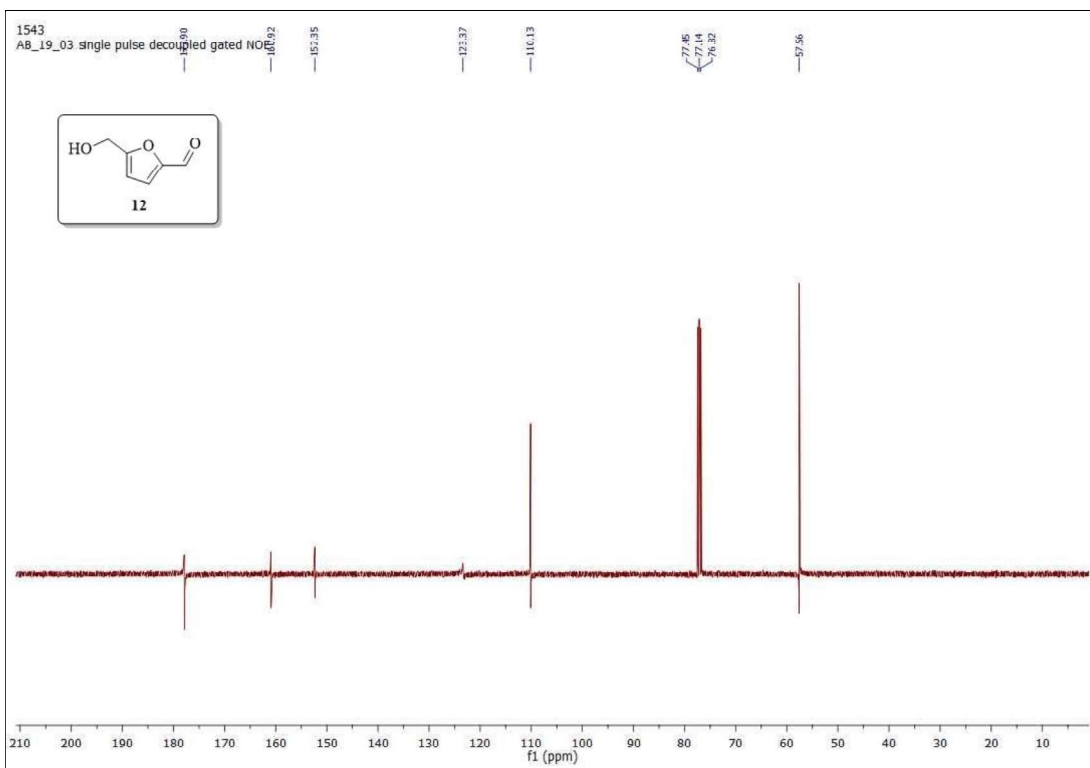
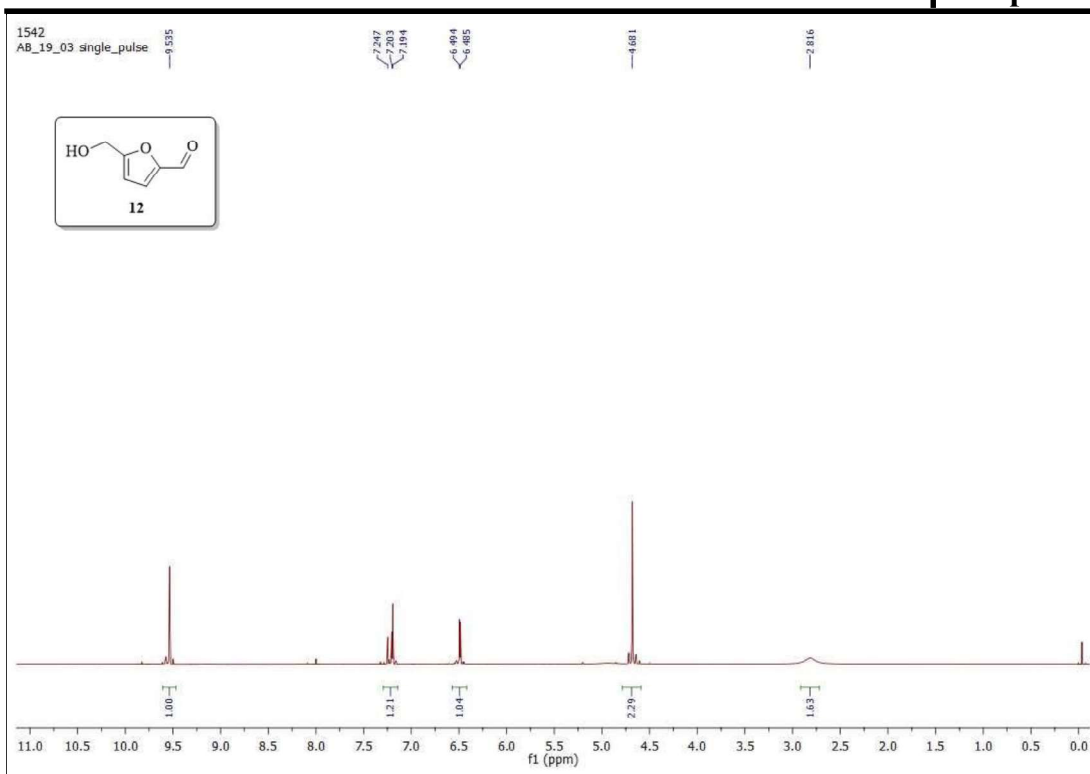
61. (a) R. -J. V. Putten, J. C. van der Waal, E. de Jong, C. B. Rasrendra, H. J. Heeres, J. G. de Vries, *Chem. Rev.* 2013, **113**, 1499; (b) J. Chen, K. Li, L. Chen, R. Liu, X. Huang and D. Ye, *Green Chem.* 2014, **16**, 2490; (c) Y. Zhang, P. Jin, M. Liu, J. Pan, Y. Yan, Y. Chen and Q. Xiong, *AIChE J.* 2017, **63**, 4920; (d) T. Buntara, S. Noel, P. H. Phua, I. Melián-Cabrera, J. G. de Vries and H. J. Heeres, *Angew. Chem. Int. Ed.* 2011, **50**, 7083; (e) A. D. Patel, J. C. Serrano-Ruiz, J. A. Dumesic and R. P. Anex, *Chem. Eng. J.* 2010, **160**, 311.
62. (a) Q. Hou, M. Zhen, L. Liu, Y. Chen, F. Huang, S. Zhang, W. Li and M. Ju, *Appl. Catal. B-Environ.* 2018, **224**, 183; (b) P. Bhanja, A. Modak, S. Chatterjee and A. Bhaumik, *ACS Sustain. Chem. Eng.* 2017, **5**, 2763; (c) F. Delbecq and C. Len, *Molecules* 2018, **23**, 1973; (d) F. Menegazzo, E. Ghedini and M. Signoretto, *Molecules* 2018, **23**, 2201.
63. (a) M. J. da Silva and C. M. de Oliveira, *Curr. Catal.* 2018, **7**, 26; (b) G. -T. Jeong, C. H. Ra, Y. -K. Hong, J. K. Kim, I. -S. Kong, S. -K. Kim and D. -H. Park, *Bioprocess Biosyst. Eng.* 2015, **38**, 207; (c) S. Peleteiro, A. M. C. Lopes, G. Garrote, J. C. Parajó and R. Bogel-Lukasik, *Ind. Eng. Chem. Res.* 2015, **54**, 8368; (d) M. G. Mazzotta, D. Gupta, B. Saha, A. K. Patra, A. Bhaumik and M. M. Abu-Omar, *ChemSusChem* 2014, **7**, 2342.
64. (a) G. Gliozzi, A. Innorta, A. Mancini, R. Bortolo, C. Perego, M. Ricci and F. Cavani, *Appl. Catal. B-Environ.* 2014, **145**, 24; (b) Z. Chao, Z. Fu,

- 
- B. Dai, S. Zen, Y. Liu, Q. Xu, S. R. Kirk and D. Yin, *Cellulose* 2014, **21**, 1227; (c) L. Atanda, M. Konarova, Q. Ma, S. Mukundan, A. Shrotri and J. Beltramini, *Catal. Sci. Technol.* 2016, **6**, 6257; (d) P. Lanzafame, D. M. Temi, S. Perathoner, A. N. Spadaro and G. Centi, *Catal. Today* 2012, **179**, 178.
65. (a) Y. Wang, Y. Zhang, C. Li, M. Wang, H. Cui, W. Yi, F. Song, X. Sun and Q. Fu, *ChemistrySelect* 2020, **5**, 4136; (b) M. Liu, Y. Zhang, E. Zhu, P. Jin, K. Wang, J. Zhao, C. Li and Y. Yan, *ChemistrySelect* 2017, **2**, 10413; (c) Q. Zhang, X. Liu, T. Yang, Q. Pu, C. Yue, S. Zhang and Y. Zhang, *Int. J. Chem. Eng.* 2019, 3890298; (d) A. Herbst and C. Janiak, *CrystEngComm.* 2017, **19**, 4092; (e) A. Herbst and C. Janiak, *New J. Chem.* 2016, **40**, 7958;
66. X. Lu, H. Zhao, W. Feng and P. Ji, *Catalysts* 2017, **7**, 330.
67. (a) G. W. Kaatz and S. M. Seo, *Antimicrob. Agents Chemother.* 1997, **41**, 2733; (b) L. Rodrigues, D. Wagner, M. Viveiros, D. Sampaio, I. Couto, M. Vavra, W. V. Kern and L. Amaral, *J. Antimicrob. Chemother.* 2008, **61**, 1076.

2.7 NMR spectra of selected compounds



# Chapter 2



# **Chapter 3**

**Magnetically active silica catalysed solvent-free domino Knoevenagel-hetero-Diels-Alder reaction: An easy access to divergent chromenones / dihydrochromenones / spirochromenones**

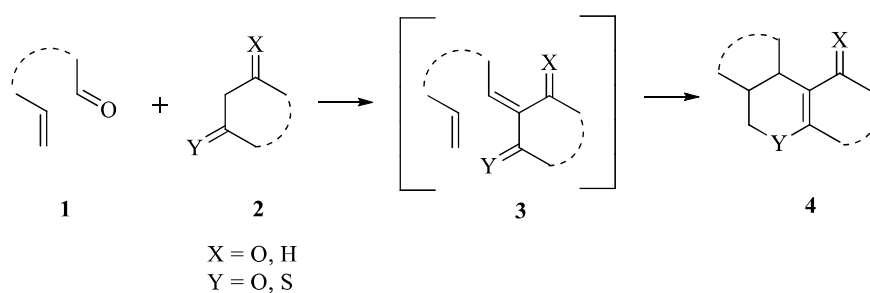
---

### 3.1 Introduction

Domino reactions can be defined as a process in which two or more bond formation takes place under similar conditions and the subsequent transformation occurs at the functionalities generated in the former transformation.<sup>1</sup> These reactions are important tools of particular interest as they meet the criteria of green chemistry with their ability to construct molecular complexity from simple substrates, while simultaneously minimizing the generation of waste. Domino reactions can involve one-, two- or multi-components and can be classified into homo domino and hetero domino reactions depending upon the mechanism of the first step. The sequence of reactions involving same mechanism is called homo-domino reactions while those with different mechanisms are called hetero-domino reactions. The commonly studied domino reactions are homo-domino reactions involving two or more anionic, cationic or radical transformations, while hetero-domino reactions involve anionic-pericyclic processes such as the domino-Knoevenagel-ene reaction, the domino-Knoevenagel-hetero-Diels-Alder reaction and the domino-Sakurai-ene reaction.

In recent years, the domino-Knoevenagel-hetero-Diels-Alder (DKHDA) reaction has emerged as a powerful tool for the construction of complex molecules with important therapeutic properties. The DKHDA reaction allows the construction of highly diverse structures such as natural products, synthetic drugs and poly-heterocyclic compounds, incorporating a number of pyran-based frameworks with high atom economy.<sup>2-4</sup> Following the pioneering work by Tietze, several methods

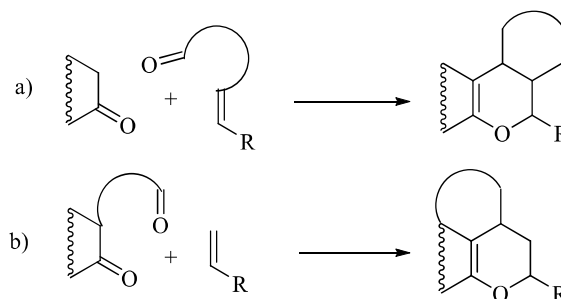
employing the DKHDA strategy have been reported, leading to a diaspora of significantly diverse pyran and pyrano-fused carbocycles.<sup>4(a-c),5</sup> These pyrano-fused carbocycles are important motifs distributed over a broad range of natural products and bio-active molecules.<sup>6</sup> The DKHDA reaction involves an initial Knoevenagel condensation of an aldehyde **1** with either a 1,3-dicarbonyl compound or an active methylene group **2** to produce 1,3-heterodiene intermediate **3**, which further undergoes hetero-Diels-Alder reaction to give the corresponding heterocyclic product **4** (Scheme 1).



**Scheme 1.** Schematic diagram representing domino-Knoevenagel-hetero-Diels-Alder reaction

The DKHDA reaction can be carried out as a two-, three- or four- component reaction. The commonly explored aldehyde substrates include coumarin, quinoline, naphthaldehyde, salicylaldehyde etc. while dienophiles such as enol ethers and alkenes are commonly used. Unlike aldehyde, ketones are seldom studied as a substrate in DKHDA reaction. While intramolecular or two component DKHDA reaction between various aromatic and aliphatic aldehydes with 1,3-dicarbonyl compounds has been widely reported, examples involving intermolecular three

component reaction between 1,3-dicarbonyl, aldehyde/ketone, and alkenes/alkynes is comparatively less (Scheme 2).<sup>2-5,7</sup> Moreover, reaction with non-activated terminal alkynes as dienophile is limited as compared to alkenes due to its poor reactivity.



**Scheme 2.** Literature reported two-component DKHDA reaction

The DKHDA reaction is a straightforward approach for the synthesis of pyran-fused heterocycles. The chromene core (i.e. benzopyran) is exemplified as a privileged moiety in a variety of synthetic and natural products such as alkaloids, flavonoids, anthocyanins and is known to exhibit fascinating pharmacological properties.<sup>8</sup> For example, calanolide B (**5**) have prominent HIV-1 inhibitory activity, while ethuliacoumarion A (**6**) and its derivatives show anticancer, molluscicidal and anthelmintic properties (Figure 1).<sup>9,10</sup> Ferprenin (**7**) is a specific inhibitor of enzyme VKORC1 which is responsible for the recycling of vitamin K, a vitamin essential for blood clotting, and trigolutes (**8**) displays acuteAChE inhibitory activity (Figure 1).<sup>11,12</sup> Synthetic chromene derivatives are also known to exhibit potent anticancer, antioxidant, molluscicidal and antimicrobial activities.<sup>13-16</sup>



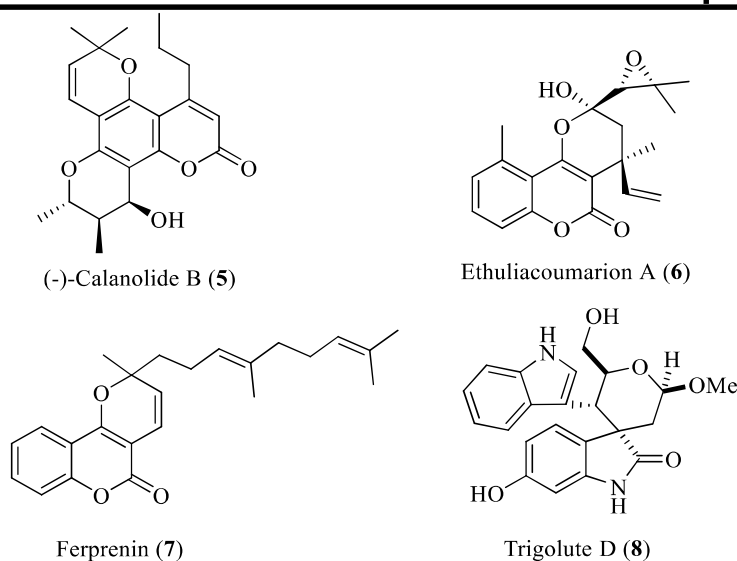


**Figure 1.** A few biologically active natural products containing chromenone moiety

To date, variety of catalytic systems has been employed for the synthesis of chromene core *via* DKHDA strategy. These include copper (I) iodide, EDDA (ethylenediammonium diacetate), zirconium oxide NPs-[bmim] [NO<sub>3</sub>], tetrabutylammonium hydrogen sulfate (TBA-HS) etc.<sup>17-20</sup> The first report on intramolecular DKHDA reaction involving non-terminal alkyne for the efficient synthesis of embelin derivatives was carried out by Martín-Acosta and group.<sup>21</sup> Embelin is a promising skeletal framework in a number of drug candidates. In a report by Khan and group, molecular iodine was used for the synthesis of chromene by the reaction between 3-aminocoumarin, 1,3-diketone and aromatic aldehyde.<sup>22</sup> In another report, Li and co-workers prepared chromenone *via* L-proline catalyzed three component reaction between an aromatic aldehyde, an activated methylene and a nucleophile.<sup>23</sup> Suatiya and co-workers reported the use of ionic liquid [DBU][Ac] for

the synthesis of chromeno-fused pyrano[2,3-*c*]pyrazoles *via* an efficient DKHDA reaction.<sup>24</sup> Maddila and group prepared arylsulfonyl-4*H*-pyrans *via* ruthenia doped fluorapatite (RuO<sub>2</sub>/FAp) catalyzed three component reaction between an aldehyde, dimedone and phenylsulphonyl acetonitrile.<sup>25</sup> Bakthadoss et al. carried out a DKHDA reaction for the synthesis of chromeno-fused phenazinone by a solid-state melt reaction between 2-hydroxynaphthalene-1,4-dione, *o*-phenylenediamine and *o*-allylated/vinylated salicylaldehyde.<sup>26</sup> Ramesh and co-workers used erbium triflate [Er(OTf)<sub>3</sub>] as a Lewis acid for the synthesis of 3,4-dihydro-2*H*-pyrans *via* three component hetero-Diels-Alder reaction between a 1,3-diketone, an aldehyde and an alkene.<sup>27</sup> A Fe(III)/caffeine-based ionic liquid supported on graphene oxide was prepared by Zand and co-workers and was efficiently used as a Lewis acid catalyst for the synthesis of 2-amino-2-cyano-4*H*-pyrans.<sup>28</sup> Kiamehr et al. used DKHDA strategy to prepare tetrahydropyrazolo[4',3':5,6]-pyrano[3,4-*c*]quinolones by the reaction of *N*-acrylatedanthranilic aldehyde with pyrazolone in the presence of ZnBr<sub>2</sub> as Lewis acid catalyst.<sup>29</sup> Although the methods mentioned above are highly efficient, most of them are associated with certain drawbacks such as prolonged reaction time, use of solvent, use of non-recyclable catalysts, high reaction temperature, and requirement of a base. To our knowledge, so far, there is no report of DKHDA reaction involving 1,3-dicarbonyl, ketone, and alkynes producing spirocyclicpyranone derivatives.

Use of silica as a catalyst for organic reactions is a relatively less explored area.<sup>30</sup> Because of its non-toxicity, large specific area, porous structure, high stability, low cost and wide availability, there is a wide scope of utilization of silica as recyclable heterogeneous catalyst. Utilization of silica as a coating material of iron oxide nanoparticles leads to the formation of magnetic silica which acts as a mild solid acid. The silica coating reduces toxicity and enhances stability of iron oxide nanoparticles.<sup>31</sup> One of the important advantages of using magnetic silica is that they can easily be recovered from the reaction medium through magnetic filtration.<sup>32</sup> On the other hand, transformation of conventional chemical processes into environmentally viable one is an important requirement of modern organic chemistry. One of the growing consensus is carrying out reactions under solvent-free conditions and thus making the process safer and cleaner. Solvent free reactions are associated with certain advantages such as decreased energy requirement, shorter reaction time and less waste generation. R. A. Sheldon stated that “the best solvent is no solvent and if a solvent (diluent) is needed it should preferably be water”.<sup>33</sup>

In view of the above, it appears quite interesting to explore the role of solid acid catalyst in the synthesis of chromenone scaffold *via* DKHDA reaction. Herein, we report the preparation and detailed characterization of a magnetically recoverable silica catalyst which has been used as a solid acid catalyst in the three component DKHDA reaction for the efficient synthesis of highly substituted chromenones, dihydrochromenones, and spirochromenones. The reaction has been performed under

solvent-free condition which meets the recent green chemistry trends of developing green and sustainable chemical processes.

## 3.2 Results and discussion

### 3.2.1 Synthesis and characterization of $\text{Fe}_3\text{O}_4@\text{SiO}_2$ catalyst

A magnetic silica catalyst ( $\text{Fe}_3\text{O}_4@\text{SiO}_2$ ) was prepared using co-precipitation technique by modification of a literature reported method.<sup>34</sup> Initially, the crystalline structure of the synthesized material was monitored by powder XRD analysis (Figure 2). The diffraction peaks at  $2\theta = 35.7^\circ$ ,  $53.2^\circ$  and  $65.8^\circ$  could be ascribed to the (311), (422) and (440) planes of cubic spinel phase of  $\text{Fe}_3\text{O}_4$  crystal. These values are in good agreement with the JCPDS card no. 19-629 for magnetite. The broad, low intensity diffraction peaks observed at  $2\theta$  from  $20^\circ$  to  $27^\circ$  are due to the presence of  $\text{SiO}_2$  in the sample.<sup>34,35</sup> The crystallite size of the prepared material was calculated from XRD pattern at  $2\theta$  value of  $35.7^\circ$  by means of Scherer equation and found to be in the range of 3.5 nm.

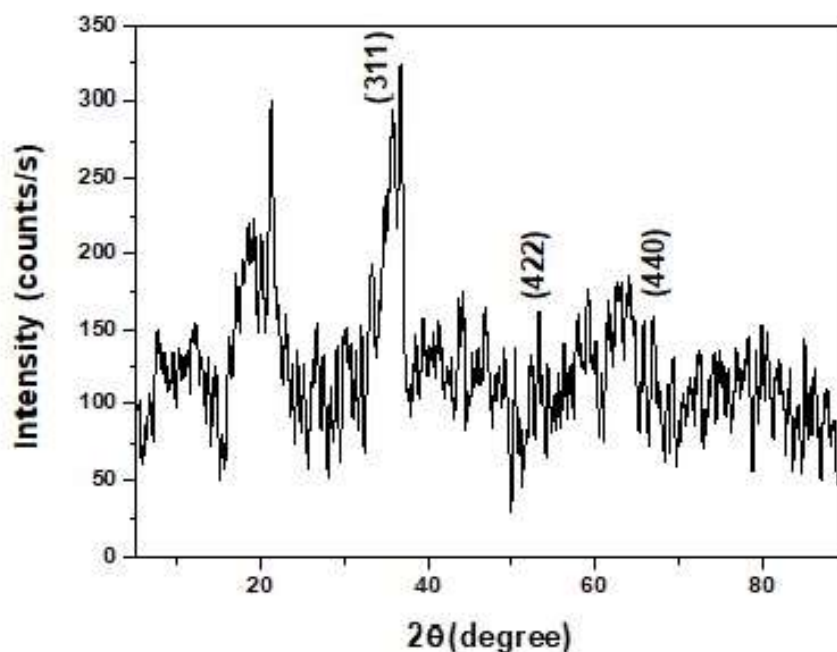


**Figure 2.** Powder XRD pattern of  $\text{Fe}_3\text{O}_4@\text{SiO}_2$

The functional groups present and the mode of bonding in the  $\text{Fe}_3\text{O}_4@\text{SiO}_2$  nanoparticles were examined through FT-IR spectroscopy recorded in the 4000-400  $\text{cm}^{-1}$  range (Figure 3). The bands observed in the regions of 3391 and 1631  $\text{cm}^{-1}$  could be assigned to the  $-\text{OH}$  stretching and  $\text{H}-\text{O}-\text{H}$  bond vibrations of the surface adsorbed water molecules, respectively. The absorption peaks at 583 and 619  $\text{cm}^{-1}$  is due to  $\text{Fe}-\text{O}$  stretching vibration. The absorption peaks at 795 and 1054  $\text{cm}^{-1}$  may be attributed to symmetric and non-symmetric stretching vibration of  $\text{Si}-\text{O}-\text{Si}$ , respectively.<sup>36</sup> These IR peaks confirm the presence of silica and  $\text{Fe}_3\text{O}_4$  in the sample.

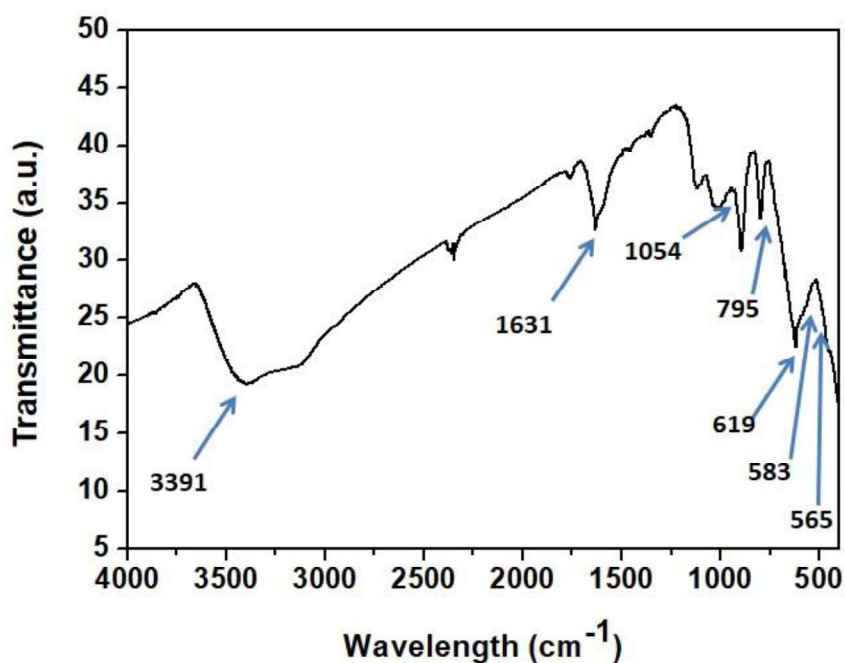


**Figure 3.** FT-IR spectrum of Fe<sub>3</sub>O<sub>4</sub>@SiO<sub>2</sub>

The particle size and microstructure of the prepared Fe<sub>3</sub>O<sub>4</sub>@SiO<sub>2</sub> catalyst was determined by TEM and HR-TEM analysis. The low resolution TEM image revealed homogeneous distribution of the particles with nearly spherical shape (Figure 4a). The particle size distribution was found to be in the range 2-3 nm with number-average diameter of 2.5 nm (standard deviation (SD) = 0.22) (Figure 4b). The close relation between surface-weighted diameter ( $D_s = 2.58$  nm) and volume-weighted diameter ( $D_v = 2.59$  nm) revealed narrow-size distribution of the prepared nanoparticles.

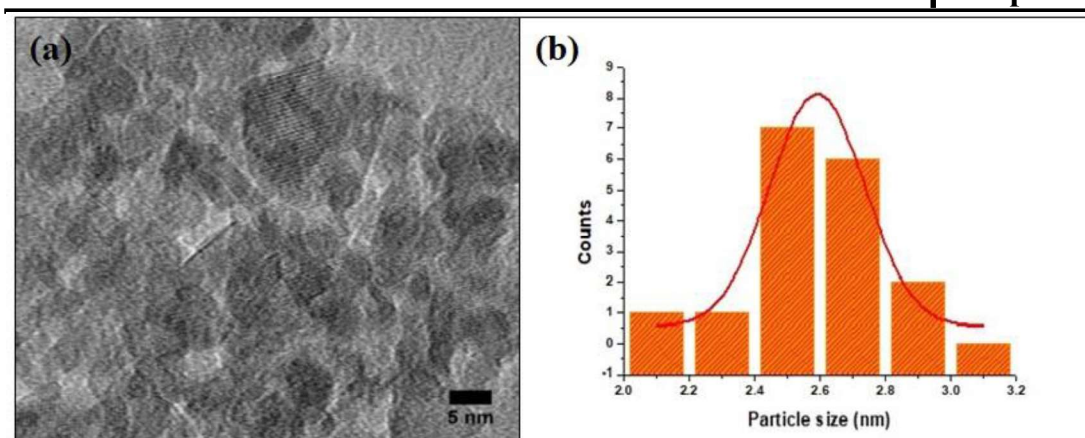


**Figure 4.** (a) TEM image of  $\text{Fe}_3\text{O}_4@\text{SiO}_2$  and (b) Particle size distribution histogram of  $\text{Fe}_3\text{O}_4@\text{SiO}_2$  nanoparticles

The HR-TEM image indicated that silica shell was coated on the surface of  $\text{Fe}_3\text{O}_4$  nanoparticle and the inter-planar lattice-fringe spacing of the  $\text{Fe}_3\text{O}_4$  core was 0.25 nm, corresponding to the (311) spinel phase of  $\text{Fe}_3\text{O}_4$  crystal (Figure 5a).

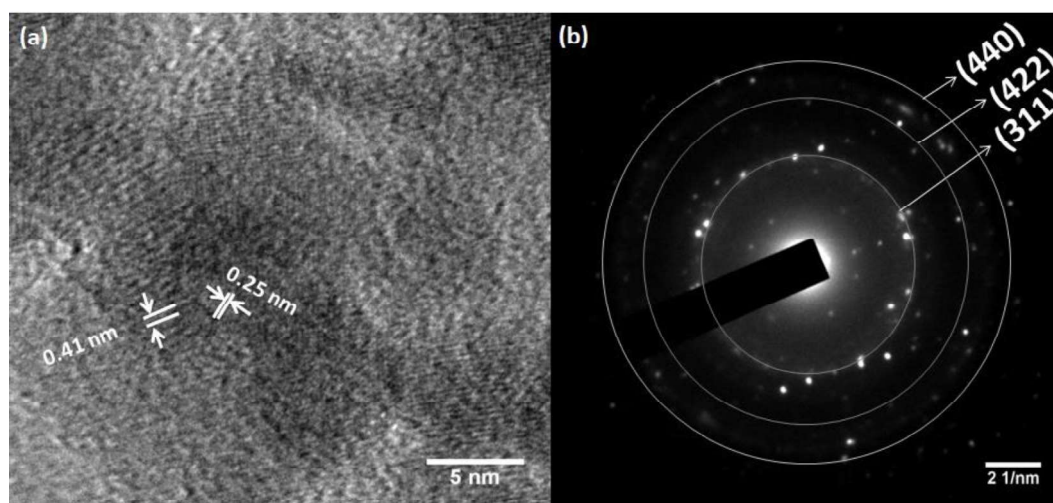


**Figure 5.** (a) HRTEM image with fringe spacing and (b) SAED pattern of  $\text{Fe}_3\text{O}_4$  nanoparticles

The selected area electron diffraction (SAED) pattern further confirmed the crystalline nature of the sample as indicated by the (311), (422) and (440) crystalline planes (Figure 5b).

Energy Dispersive X-ray (EDX) analysis of the prepared nanoparticles indicates the presence of Fe, Si and O signals, devoid of the presence of any other metal or impurity (Figure 6).

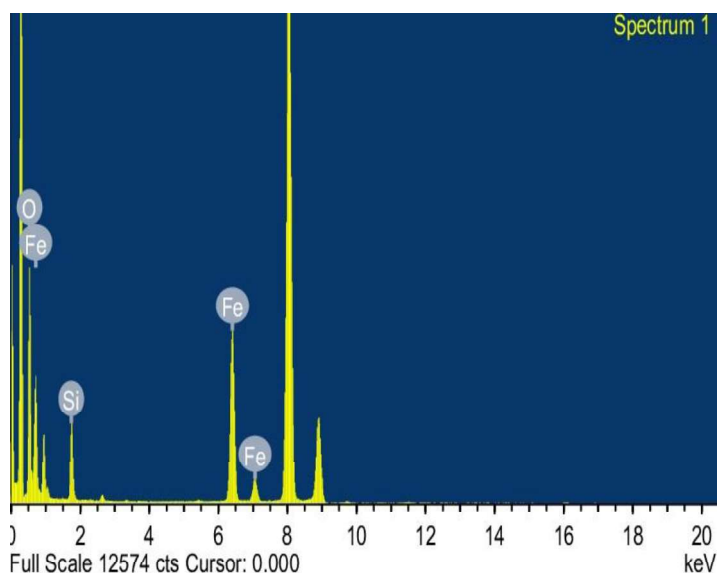


**Figure 6.** EDX spectra of Fe<sub>3</sub>O<sub>4</sub>@SiO<sub>2</sub> nanoparticles showing the presence of Fe, O and Si

The magnetic property of the synthesized Fe<sub>3</sub>O<sub>4</sub>@SiO<sub>2</sub> nanoparticles was studied by Vibrating Sample Magnetometer (VSM) at room temperature (Figure 7). Saturation magnetization value of 13.24 emu/g was obtained for the synthesized nanoparticles, which was quite lower than that reported for bare Fe<sub>3</sub>O<sub>4</sub> nanoparticles.<sup>35</sup> This reduction in saturation magnetization value can be attributed to



the coating of  $\text{Fe}_3\text{O}_4$  nanoparticles by an amorphous silica shell.<sup>35</sup> However, the decrease in saturation magnetization value did not affect the magnetic property of the nanoparticles and they could be magnetically separated by the application of an external magnet.

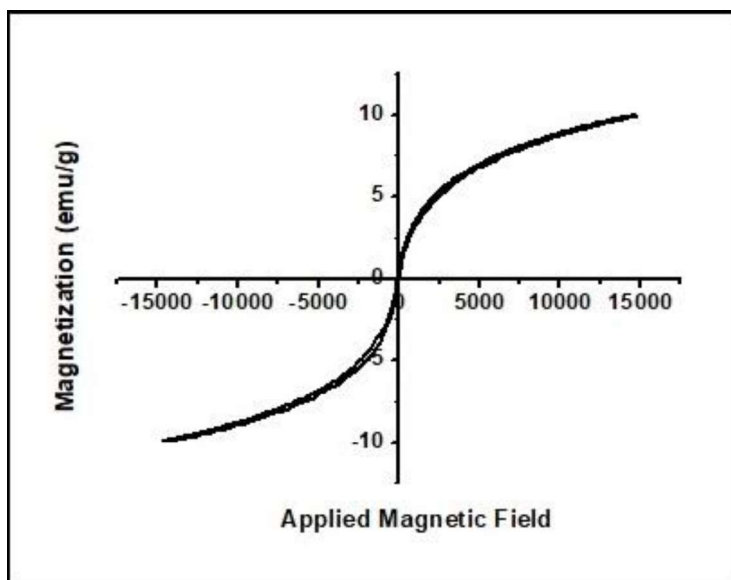


**Figure 7.** Magnetization curve of  $\text{Fe}_3\text{O}_4@\text{SiO}_2$

The thermal stability of the catalyst was analyzed by thermogravimetric analysis (TGA) (Figure 8). The TGA curve didn't show any major weight loss upto  $\sim 800^\circ\text{C}$  confirming the high thermal stability of the prepared  $\text{Fe}_3\text{O}_4@\text{SiO}_2$  nanoparticles. There was an initial weight loss of 9.73% below  $200^\circ\text{C}$  which can be attributed to the release of adsorbed water molecules from the catalyst surface.

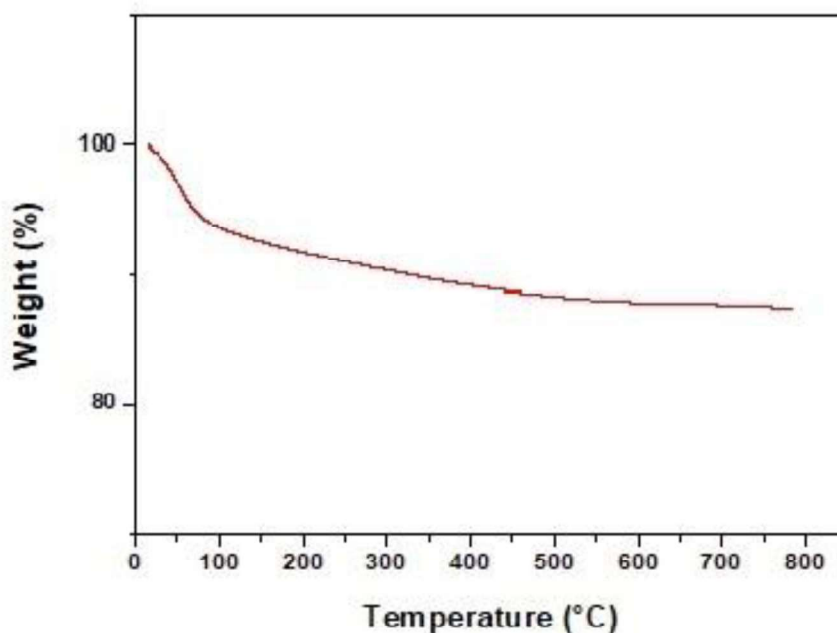


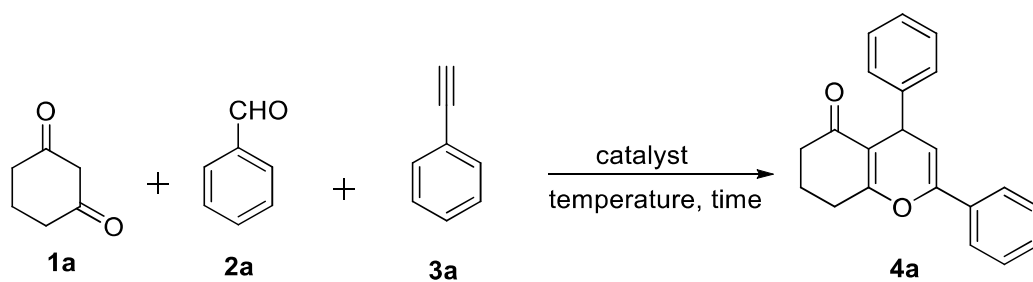
**Figure 8.** TGA curve of Fe<sub>3</sub>O<sub>4</sub>@SiO<sub>2</sub> nanoparticles

### 3.2.2 Catalytic activity of the prepared Fe<sub>3</sub>O<sub>4</sub>@SiO<sub>2</sub> nanoparticles towards the synthesis of chromenones

After the preparation and characterization, activity of the prepared Fe<sub>3</sub>O<sub>4</sub>@SiO<sub>2</sub> nanomaterial as catalyst for the synthesis of chromenone derivatives via DKHDA reaction was studied. For the purpose, we initiated our study by using 1,3-cyclohexanedione (**1a**), benzaldehyde (**2a**), and phenylacetylene (**3a**) as model substrate. Using acetonitrile as solvent the reaction mixture was refluxed for 3 h and the chromenone product was obtained in 50% yield (Table 1, entry 1). While the yield could not be improved significantly by variation of solvents (Table 1, entries 2-5), the reaction provided significantly good yield (82%) of the product under solvent

free condition (Table 1, entry 6). Optimal temperature was found to be 100 °C and the reaction was completed in 2 h (Table 1, entries 6-11). The ideal catalyst amount was 10 wt% with respect to **1a**. The role of the catalyst was confirmed by performing the reaction in the absence of the catalyst when no product formation could be observed (Table 1, entry 12). The reaction did not produce any product when performed in the presence of Fe<sub>3</sub>O<sub>4</sub>, FeCl<sub>2</sub> or FeCl<sub>3</sub> (Table 1, entries 14-16). The observation confirmed the role of the silica as active catalyst. For further confirmation, a catalyst was prepared from silicic acid without addition of iron salt. The newly formed silica catalyst showed identical activity compared to the original Fe<sub>3</sub>O<sub>4</sub>@SiO<sub>2</sub> (Table 1, entry 11).

**Table 1.** Synthesis of chromenone and optimization of the reaction condition<sup>a</sup>



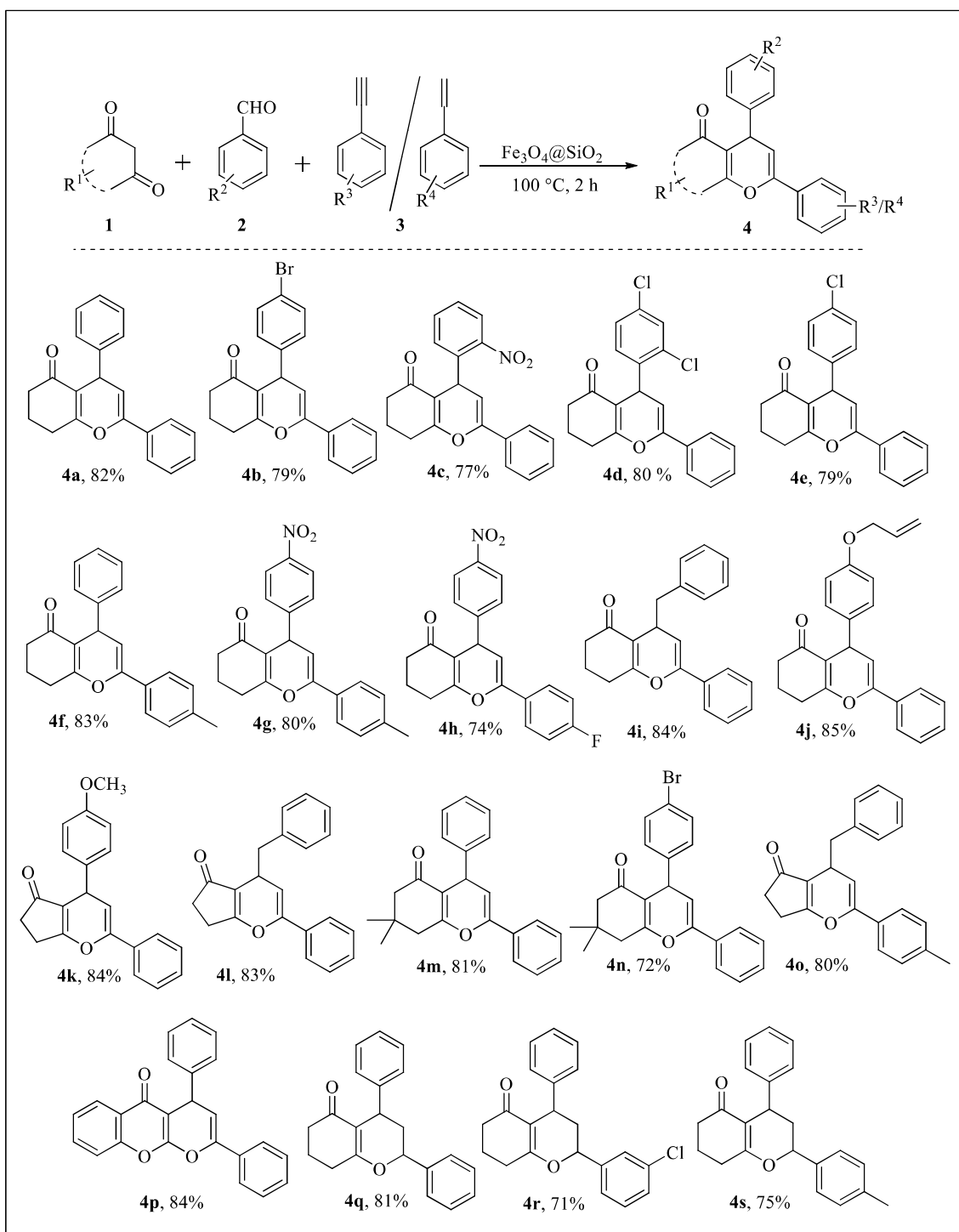
Entry	Catalyst	Solvent	Temperature (°C)	Catalyst amount (wt%)	Yield (%) <sup>b</sup>
1	Fe <sub>3</sub> O <sub>4</sub> @SiO <sub>2</sub>	CH <sub>3</sub> CN	80	20	50
2	Fe <sub>3</sub> O <sub>4</sub> @SiO <sub>2</sub>	DMSO	110	20	52
3	Fe <sub>3</sub> O <sub>4</sub> @SiO <sub>2</sub>	H <sub>2</sub> O	100	20	38
4	Fe <sub>3</sub> O <sub>4</sub> @SiO <sub>2</sub>	C <sub>2</sub> H <sub>5</sub> OH	80	20	45
5	Fe <sub>3</sub> O <sub>4</sub> @SiO <sub>2</sub>	Toluene	110	20	18

6	Fe <sub>3</sub> O <sub>4</sub> @SiO <sub>2</sub>	None	80	20	73
7	Fe <sub>3</sub> O <sub>4</sub> @SiO <sub>2</sub>	None	100	20	82
8	Fe <sub>3</sub> O <sub>4</sub> @SiO <sub>2</sub>	None	120	20	79
9	Fe <sub>3</sub> O <sub>4</sub> @SiO <sub>2</sub>	None	100	15	82
10	Fe <sub>3</sub> O <sub>4</sub> @SiO <sub>2</sub>	None	100	5	79
<b>11</b>	<b>Fe<sub>3</sub>O<sub>4</sub>@SiO<sub>2</sub></b>	<b>None</b>	<b>100</b>	<b>10</b>	<b>82</b>
12	No catalyst (only silicic acid)	None	100	10	0
13	SiO <sub>2</sub> without Fe <sub>3</sub> O <sub>4</sub> (prepared using identical condition)	None	100	10	82
14	Fe <sub>3</sub> O <sub>4</sub>	None	100	10	0
15	FeCl <sub>3</sub>	None	100	10	0
16	FeCl <sub>2</sub> ·H <sub>2</sub> O	None	100	10	0

Bold values indicate the best experimental result. <sup>a</sup>All the reactions were carried out using 1,3-cyclohexanedione **1a** (0.9 mmol), benzaldehyde **2a** (0.9 mmol), phenylacetylene **3a** (0.9 mmol). <sup>b</sup>Isolated yield.

With the optimized reaction condition in hand, we further examined the substrate scope by reacting 1,3-cyclohexanedione with different aromatic aldehydes and terminal alkyne/alkene (Table 2). It was observed that aldehydes and alkynes containing electron withdrawing as well as electron donating groups provided the corresponding tetrahydro-5*H*-chromen-5-one **4(a-s)** in a very good yield. Phenylacetaldehyde also participated in the reaction and yielded the desired product **4i** and **4l**. 4-Allyloxybenzaldehyde reacted well to give the corresponding tetrahydro-5*H*-chromen-5-one **4j** without any side reaction.

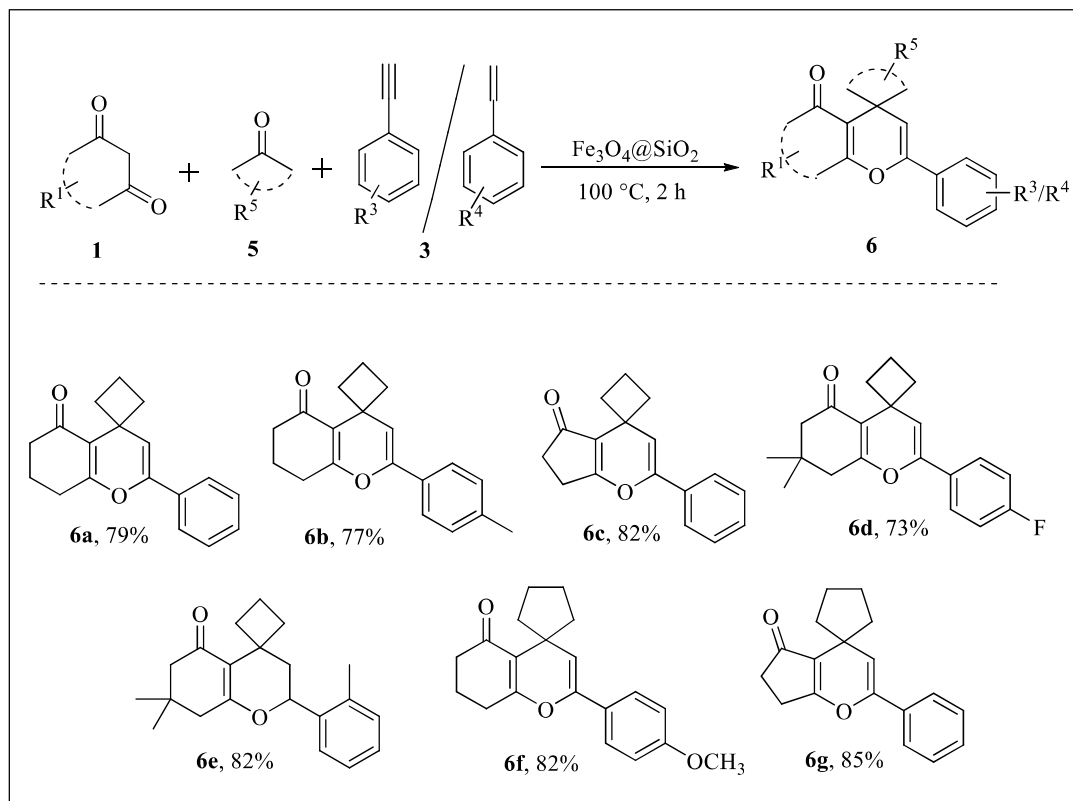
Table 2. Synthesis of chromenone from 1,3-diketone, aldehyde, and alkyne or alkene



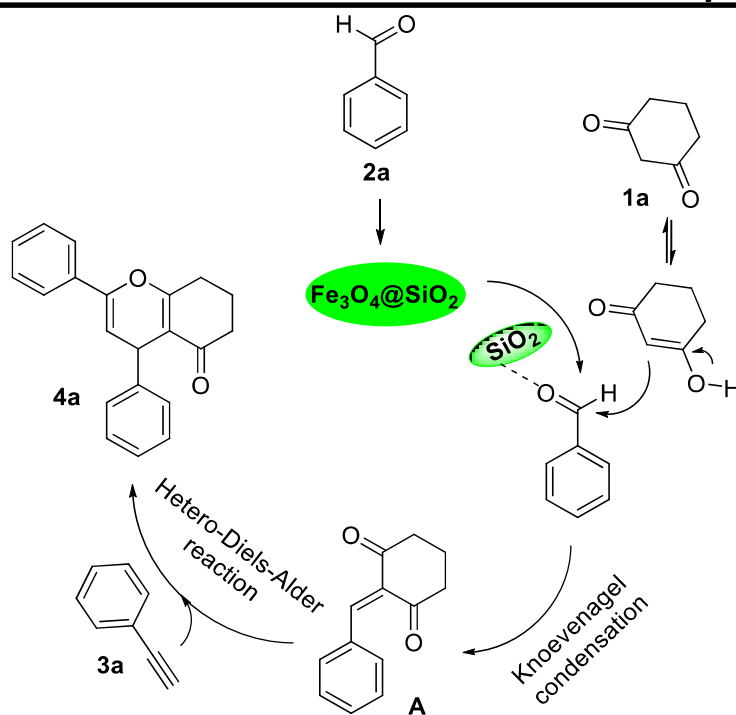
Unfortunately, aliphatic aldehydes like, butyraldehyde and octanal did not participate in the reaction. This may be due to the problem in formation of Knoevenagel adduct between these aliphatic aldehydes and 1,3-diketone. Other 1,3-diones like, cyclopentane-1,3-dione, dimedone, and chromane-2,4-dione was coupled with aldehydes and alkynes to give the corresponding chromenones **4(k-p)** with very good yield. Styrene derivatives also participated in the same reaction producing the corresponding hexahydro-5*H*-chromen-5-one **4(q-s)**. All the compounds were characterized with the help of <sup>1</sup>H NMR and <sup>13</sup>C NMR. The molecular formula was confirmed from HRMS data. The melting point data of the reported compounds were matched with the literature.

After the successful exploration of Fe<sub>3</sub>O<sub>4</sub>@SiO<sub>2</sub> towards the synthesis of chromenone, we further extended our study towards cyclic ketones. It was observed that the reaction between 1,3-diketone, alkyne or alkene and cyclic ketones provided corresponding spirocyclicchromenones in good to excellent yield (Table 3). Both the cyclobutanone and cyclopentanone provided corresponding spirochromenes **6(a-g)** in good yield. Unfortunately, cyclohexanone and larger cyclic ketones did not participate in the reaction. The fact may be explained by the difficulty in formation of Knoevenagel product with cyclohexanone and larger counterparts. For the same reason, simple acyclic ketones also didn't take part in the given reaction condition. All the prepared compounds were duly characterized with the help of NMR and Mass spectral data.

**Table 3.** Synthesis of spirochromenone from 1,3-diketone, ketone, and alkyne or alkene



Based on the earlier report of participation of silica as catalyst in Knoevenagel reaction, a plausible mechanism is proposed (Scheme 3).<sup>30c</sup> Firstly, a  $\text{SiO}_2$  catalyzed Knoevenagel condensation between 1,3-dicarbonyl **1a** and aldehyde **2a** produces enone intermediate **A**. In the second step, the 1,3-heterodiene undergoes subsequent thermal [4+2] cycloaddition with alkyne **3a** to produce the chromenone **4a**. It is to be noted that this type of thermal hetero-Diels-Alder reaction is also known in the literature.<sup>5a</sup>



**Scheme 3.** A plausible mechanism for the  $\text{Fe}_3\text{O}_4@\text{SiO}_2$  catalyzed domino-Knoevenagel-hetero-Diels–Alder reaction

### 3.2.3 Study of catalyst recyclability

To study the recyclability of the catalyst, after the completion of the reaction, the solid catalyst was recovered by magnetic filtration using an external magnet which was then washed with distilled water and dried at 100 °C. It was observed that the catalyst could be reused up to five consecutive catalytic cycles without any significant loss in the activity (Figure 9). However, after the 5<sup>th</sup> run, the catalytic activity of the recovered catalyst decreased gradually.



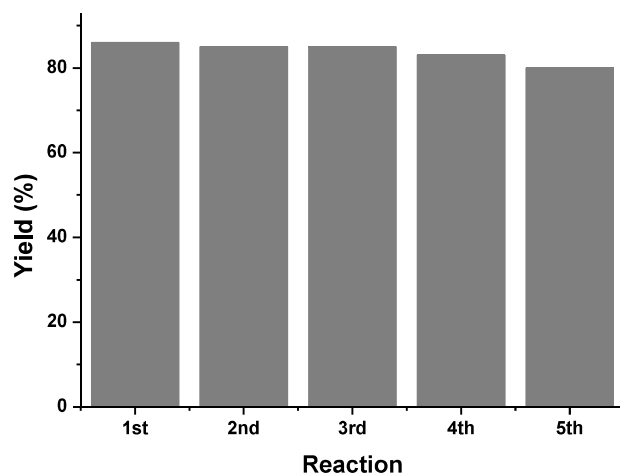


**Figure 9.** Study of recyclability of the catalyst

The physical characteristics of the recovered catalyst were also investigated through TEM analysis (Figure 10). In the TEM image any significant morphological change was not observed.

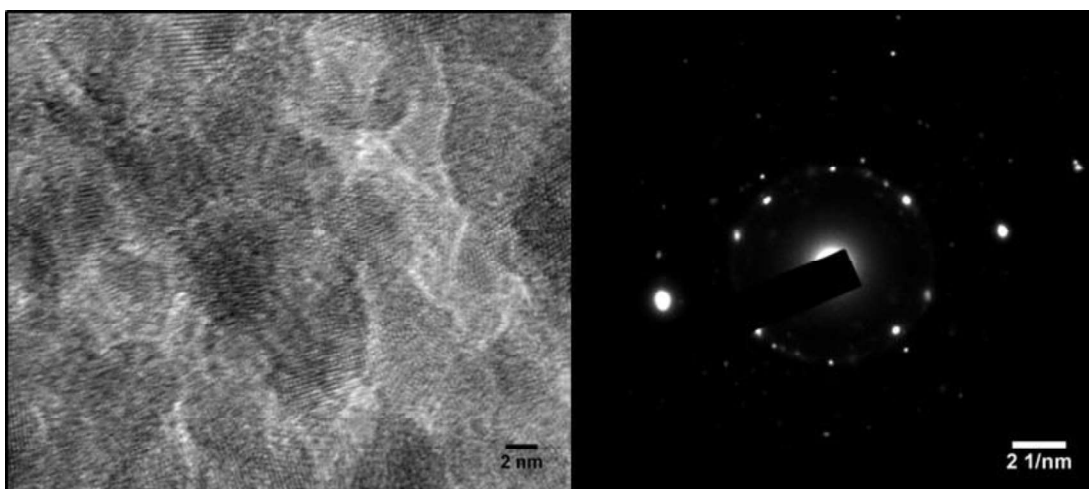


**Figure 10.** HRTEM and SAED images of the recovered catalyst after 5<sup>th</sup> run

### 3.3 Conclusion

In summary, we have developed a simple, one-step three component DKHDA reaction between 1,3-cycloalkanedione, aldehyde/ketone and terminal alkyne/alkene to produce chromenone derivatives. A simple magnetically active silica, prepared from silicic acid, iron(II) chloride and iron(III) chloride, acted as solid acid catalyst for the reaction. The shape, size, structure, thermal stability, and magnetic property of the catalyst were determined by XRD, HR-TEM, FT-IR, TGA, and VSM, respectively. One of the major advantages of the process is the ability to carry out the reactions under solvent free condition, thereby creating the scope of waste reduction and energy efficiency. Nineteen different chromenone/dihydrochromenone and seven different spirochromeone derivatives have been prepared using the methodology. Unfortunately, the reaction was not suitable for acyclic ketones, cyclohexanone and larger cyclic ketones. A tentative mechanism has been discussed where silica acts as acidic catalyst for initial Knoevenagel reaction. Recyclability of the catalyst has also been studied.

### 3.4 Experimental

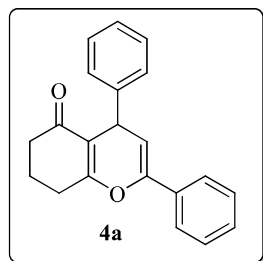
#### 3.4.1 Preparation of silica-supported iron oxide ( $\text{Fe}_3\text{O}_4@SiO_2$ ) catalyst

Iron(III) chloride hexahydrate  $\{\text{FeCl}_3 \cdot 6\text{H}_2\text{O}\}$  (1.2 g) and iron(II) chloride tetrahydrate  $\{\text{FeCl}_2 \cdot 4\text{H}_2\text{O}\}$  (0.47 g) was dissolved in 100 mL of distilled water to form a homogeneous solution. Under  $\text{N}_2$  atmosphere 10 mL of 10 N NaOH solutions was added drop wise into the mixture with vigorous stirring and the resulting

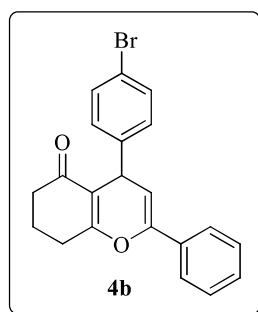
solution was heated at 80 °C for 1 h when a black precipitate of Fe<sub>3</sub>O<sub>4</sub> appeared. Silicic acid (2 g) was homogeneously dispersed separately in 40 mL of distilled water. The silicic acid solution was then added drop wise into the iron oxide solution with stirring under N<sub>2</sub> atmosphere. The mixture was further allowed to stir at room temperature for 16 h. The precipitate obtained was separated by magnetic decantation and washed with distilled water and ethanol until neutral and then dehydrated at 200 °C for 4 h in a vacuum oven. A brownish-black powder of Fe<sub>3</sub>O<sub>4</sub>@SiO<sub>2</sub> was obtained.

### **3.4.2 General procedure for the synthesis of chromenone/spirochromenone**

To a mixture of 1,3-cyclohexanedione (0.9 mmol, 100 mg), benzaldehyde (0.9 mmol, 95 mg) and phenylacetylene (0.9 mmol, 91 mg), Fe<sub>3</sub>O<sub>4</sub>@SiO<sub>2</sub> (10 wt%, 10 mg) was added and the mixture was heated at 100 °C for 2 h under solvent-free condition. The progress of the reaction was followed using thin layer chromatography (TLC). After the completion of the reaction, 5 mL ethyl acetate was added to the reaction mixture and the catalyst was removed by magnetic filtration. Organics were extracted with ethyl acetate (2 x 20 mL) and the combined organic fraction was washed with water (2 x 10 mL) and brine (10 mL). Drying over Na<sub>2</sub>SO<sub>4</sub> and removal of the solvent under reduced pressure, produced the crude mixture which was purified by column chromatography using ethyl acetate/hexane as eluent. For further recyclability experiments, the recovered catalyst was oven-dried (at 100 °C for 2 h) under vacuum before the next run.

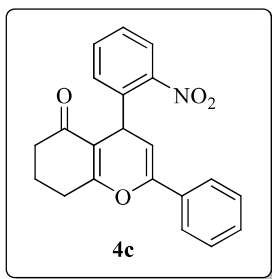
**3.5 Characterization data of the synthesized compounds****2,4-Diphenyl-4,6,7,8-tetrahydro-5H-chromen-5-one (4a)**

Orange solid; Mp: 169-171 °C (Lit.<sup>11</sup> 171-173 °C); Yield: 86%; <sup>1</sup>H NMR (500 MHz, CDCl<sub>3</sub>): δ 7.60 – 7.58 (m, 2H), 7.38 – 7.31 (m, 5H), 7.30 – 7.25 (m, 2H), 7.20 – 7.15 (m, 1H), 5.71 (d, 1H, *J* = 5.0 Hz), 4.52 (d, 1H, *J* = 5.0 Hz), 2.75 – 2.64 (m, 2H), 2.40 – 2.35 (m, 2H), 2.08 – 2.02 (m, 2H); <sup>13</sup>C NMR (125 MHz, CDCl<sub>3</sub>): δ 197.7 (C), 166.6 (C), 147.0 (C), 145.4 (C), 133.1 (C), 128.9 (CH), 128.6 (CH), 128.6 (CH), 128.4 (CH), 126.8 (CH), 124.7 (CH), 114.0 (C), 104.7 (CH), 37.3 (CH<sub>2</sub>), 35.5 (CH), 27.9 (CH<sub>2</sub>), 20.6 (CH<sub>2</sub>); HRMS (ESI) *m/z* 303.1394 ([M+H]<sup>+</sup> C<sub>21</sub>H<sub>19</sub>O<sub>2</sub>, requires 303.1385).



**4-(4-Bromophenyl)-2-phenyl-4,6,7,8-tetrahydro-5H-chromen-5-one (4b)**

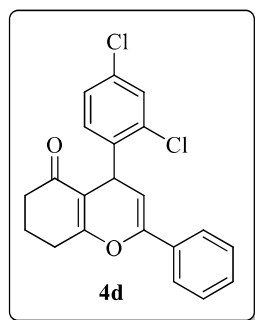
White solid; Mp: 110-112 °C; Yield: 79%; <sup>1</sup>H NMR (500 MHz, CDCl<sub>3</sub>): δ 7.60 – 7.56 (m, 2H), 7.41 – 7.35 (m, 5H), 7.21 (d, 2H, *J* = 8.5 Hz), 5.66 (d, 1H, *J* = 5.0 Hz), 4.49 (d, 1H, *J* = 5.0 Hz), 2.71 – 2.64 (m, 2H), 2.41 – 2.35 (m, 2H), 2.09 – 2.01 (m, 2H); <sup>13</sup>C NMR (125 MHz, CDCl<sub>3</sub>): δ 197.3 (C), 166.4 (C), 147.0 (C), 144.1 (C), 132.6 (C), 131.3 (CH), 129.9 (CH), 128.8 (CH), 128.4 (CH), 124.4 (CH), 120.3 (C), 113.3 (C), 103.7 (CH), 36.9 (CH<sub>2</sub>), 34.7 (CH), 27.6 (CH<sub>2</sub>), 20.3 (CH<sub>2</sub>); HRMS (ESI) *m/z* 381.0497 ([M+H]<sup>+</sup> C<sub>21</sub>H<sub>18</sub>O<sub>2</sub>Br, requires 381.0490).

**4-(2-Nitrophenyl)-2-phenyl-4,6,7,8-tetrahydro-5H-chromen-5-one (4c)**

Yellow solid; Mp: 160-162 °C; Yield: 77%; <sup>1</sup>H NMR (500 MHz, CDCl<sub>3</sub>): δ 7.82 (d, 1H, *J* = 8.0 Hz), 7.62 – 7.58 (dd, 2H, *J* = 8.0 Hz, 1.5 Hz), 7.49 (t, 1H, *J* = 7.5 Hz), 7.40 – 7.33 (m, 4H), 7.29 (t, 1H, *J* = 7.5 Hz), 5.88 (d, 1H, *J* = 4.5 Hz), 5.09 (d, 1H, *J* = 4.5 Hz), 2.76 – 2.68 (m, 2H), 2.38 – 2.34 (m, 2H), 2.11 – 2.04 (m, 2H); <sup>13</sup>C NMR (125 MHz, CDCl<sub>3</sub>): δ 197.1 (C), 167.5 (C), 149.4 (C), 147.7 (C), 139.9 (C), 133.1 (CH), 132.8 (C), 130.7 (CH), 129.2 (CH), 128.7 (CH), 127.4 (CH), 124.7 (CH),

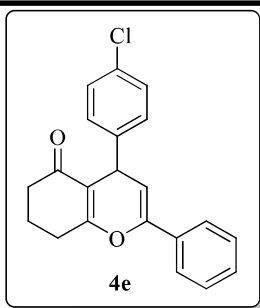
124.3 (CH), 112.9 (C), 102.9 (CH), 36.9 (CH<sub>2</sub>), 31.1 (CH), 27.8 (CH<sub>2</sub>), 20.7 (CH<sub>2</sub>);

HRMS (ESI)  $m/z$  348.1238 ( $[M+H]^+$  C<sub>21</sub>H<sub>18</sub>NO<sub>4</sub>, requires 348.1236).



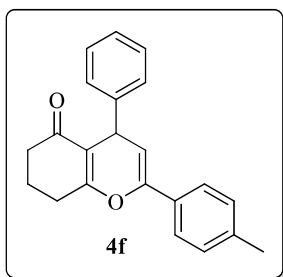
#### 4-(2,4-Dichlorophenyl)-2-phenyl-4,6,7,8-tetrahydro-5H-chromen-5-one (4d)

Pale yellow solid; Mp: 85-87 °C; Yield: 80 %; <sup>1</sup>H NMR (500 MHz, CDCl<sub>3</sub>): δ 7.57 – 7.54 (m, 2H), 7.38 – 7.33 (m, 4H), 7.15 (dd, 1H,  $J = 8.5$  Hz, 2.5 Hz), 7.09 (d, 1H,  $J = 8.5$  Hz), 5.68 (d, 1H,  $J = 4.5$  Hz), 4.93 (d, 1H,  $J = 4.5$  Hz), 2.80 – 2.69 (m, 2H), 2.46 – 2.40 (m, 2H), 2.18 – 2.07 (m, 2H); <sup>13</sup>C NMR (125 MHz, CDCl<sub>3</sub>): δ 197.2 (C), 168.1 (C), 147.3 (C), 140.9 (C), 133.7 (C), 132.8 (CH), 130.4 (C), 129.6 (CH), 129.2 (CH), 128.8 (C), 128.6 (CH), 127.7 (CH), 124.7 (CH), 112.1 (C), 102.4 (CH), 37.2 (CH<sub>2</sub>), 32.5 (CH), 28.0 (CH<sub>2</sub>), 20.7 (CH<sub>2</sub>); HRMS (ESI)  $m/z$  371.0591 ( $[M+H]^+$  C<sub>21</sub>H<sub>17</sub>O<sub>2</sub>Cl<sub>2</sub>, requires 371.0606).



#### 4-(4-Chlorophenyl)-2-phenyl-4,6,7,8-tetrahydro-5H-chromen-5-one (4e)

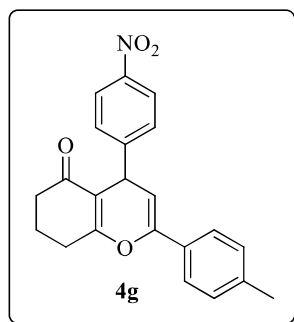
White solid; Mp: 117-119 °C (Lit.<sup>11</sup> 117-118 °C); Yield: 79%; <sup>1</sup>H NMR (500 MHz, CDCl<sub>3</sub>): δ 7.61 – 7.57 (m, 2H), 7.40 – 7.34 (m, 3H), 7.29 – 7.22 (m, 4H), 5.66 (d, 1H, *J* = 5.0 Hz), 4.50 (d, 1H, *J* = 5.0 Hz), 2.74 – 2.64 (m, 2H), 2.42 – 2.36 (m, 2H), 2.09 – 2.00 (m, 2H); <sup>13</sup>C NMR (125 MHz, CDCl<sub>3</sub>): δ 197.6 (C), 166.7 (C), 147.3 (C), 143.9 (C), 132.9 (C), 132.5 (C), 129.8 (CH), 129.1 (CH), 128.7 (CH), 128.7 (CH), 124.7 (CH), 113.7 (C), 104.1 (CH), 37.2 (CH<sub>2</sub>), 34.9 (CH), 27.9 (CH<sub>2</sub>), 20.6 (CH<sub>2</sub>); HRMS (ESI) *m/z* 337.0996 ([M+H]<sup>+</sup> C<sub>21</sub>H<sub>18</sub>O<sub>2</sub>Cl, requires 337.0995).



#### 4-Phenyl-2-(*p*-tolyl)-4,6,7,8-tetrahydro-5H-chromen-5-one (4f)

White solid; Mp: 130-132 °C (lit.<sup>13</sup> 130-131 °C); Yield: 83%; <sup>1</sup>H NMR (500 MHz, CDCl<sub>3</sub>): δ 7.46 (d, 2H, *J* = 8.0 Hz), 7.33 – 7.29 (m, 2H), 7.26 (d, 2H, *J* = 8.0 Hz), 7.17 – 7.13 (m, 3H), 5.64 (d, 1H, *J* = 5.0 Hz), 4.49 (d, 1H, *J* = 5.0 Hz), 2.72 – 2.61

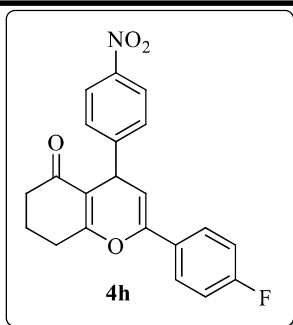
(m, 2H), 2.39 - 2.35 (m, 2H), 2.34 (s, 2H), 2.07 - 1.97 (m, 2H);  $^{13}\text{C}$  NMR (125 MHz,  $\text{CDCl}_3$ ):  $\delta$  197.7 (C), 166.6 (C), 147.1 (C), 145.6 (C), 138.9 (C), 130.2 (C), 129.3 (CH), 128.6 (CH), 128.4 (CH), 126.7 (CH), 124.6 (CH), 114.1 (C), 103.8 (CH), 37.3 (CH<sub>2</sub>), 35.4 (CH), 28.0 (CH<sub>2</sub>), 21.4 (CH<sub>2</sub>), 20.6 (CH<sub>3</sub>); HRMS (ESI)  $m/z$  317.1554 ( $[\text{M}+\text{H}]^+$  C<sub>22</sub>H<sub>21</sub>O<sub>2</sub>, requires 317.1542).



#### 4-(4-Nitrophenyl)-2-(*p*-tolyl)-4,6,7,8-tetrahydro-5*H*-chromen-5-one (4g)

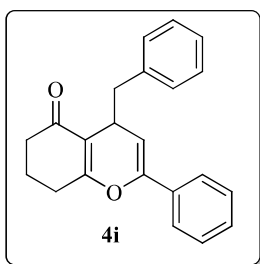
Pale yellow solid; Mp: 144-145 °C; Yield: 80%;  $^1\text{H}$  NMR (500 MHz,  $\text{CDCl}_3$ ):  $\delta$  8.11(d, 2H,  $J = 8.5$  Hz), 7.49 - 7.43 (m, 4H), 7.17 (d, 2H,  $J = 8.5$  Hz), 5.57 (d, 1H,  $J = 4.5$  Hz), 4.60 (d, 1H,  $J = 4.5$  Hz), 2.74 - 2.65 (m, 2H), 2.39 - 2.35 (m, 2H), 2.35 (s, 3H), 2.11 - 2.00 (m, 2H);  $^{13}\text{C}$  NMR (125 MHz,  $\text{CDCl}_3$ ):  $\delta$  196.9 (C), 167.3 (C), 152.8 (C), 148.0 (C), 146.8 (C), 139.5 (C), 129.8 (C), 129.4 (CH), 129.3 (CH), 124.7 (CH), 123.9 (CH), 113.0 (C), 102.1 (CH), 37.1 (CH<sub>2</sub>), 35.7 (CH), 28.0 (CH<sub>2</sub>), 21.5 (CH<sub>2</sub>), 20.6 (CH<sub>3</sub>); HRMS (ESI)  $m/z$  362.1390 ( $[\text{M}+\text{H}]^+$  C<sub>22</sub>H<sub>20</sub>NO<sub>4</sub>, requires 362.1392).





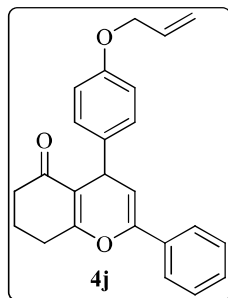
**2-(4-Fluorophenyl)-4-(4-nitrophenyl)-4,6,7,8-tetrahydro-5H-chromen-5-one (4h)**

Yellow solid; Mp: 55-57 °C; Yield: 74%;  $^1\text{H}$  NMR (500 MHz,  $\text{CDCl}_3$ ):  $\delta$  8.12 (d, 2H,  $J = 8.5\text{ Hz}$ ), 7.57 – 7.52 (m, 2H), 7.47 (d, 2H,  $J = 8.5\text{ Hz}$ ), 7.08 – 7.02 (m, 2H), 5.56 (d, 1H,  $J = 4.5\text{ Hz}$ ), 4.61 (d, 1H,  $J = 4.5\text{ Hz}$ ), 2.72 – 2.64 (m, 2H), 2.40 – 2.36 (m, 2H), 2.12 – 1.90 (m, 2H);  $^{13}\text{C}$  NMR (125 MHz,  $\text{CDCl}_3$ ):  $\delta$  197.4 (C), 167.1 (C), 163.4 (C, d,  $J = 247.5\text{ Hz}$ ), 152.5 (C), 147.1 (C), 146.9 (C), 129.3 (CH), 128.8 (C), 126.7 (d, CH,  $J = 8.7\text{ Hz}$ ), 124.0 (CH), 115.8 (d, CH,  $J = 21.2\text{ Hz}$ ), 113.0 (C), 102.7 (CH), 37.1 ( $\text{CH}_2$ ), 35.7 (CH), 27.9 ( $\text{CH}_2$ ), 20.5 ( $\text{CH}_2$ ); HRMS (ESI)  $m/z$  366.1136 ( $[\text{M}+\text{H}]^+$   $\text{C}_{21}\text{H}_{17}\text{NO}_4\text{F}$ , requires 366.1142).



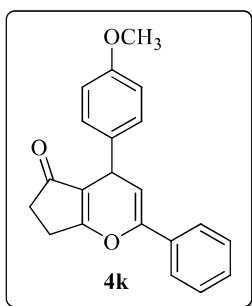
**4-Benzyl-2-phenyl-4,6,7,8-tetrahydro-5H-chromen-5-one (4i)**

Yellow solid; Mp: 55-57 °C; Yield: 84%; <sup>1</sup>H NMR (500 MHz, CDCl<sub>3</sub>): δ 7.49 – 7.45 (m, 2H), 7.35 – 7.30 (m, 4H), 7.28 – 7.23 (m, 4H), 5.47 (d, 1H, *J* = 5.0 Hz), 3.71 – 3.63 (m, 1H), 3.06 – 3.01 (m, 1H), 2.69 – 2.63 (m, 1H), 2.51 – 2.40 (m, 4H), 2.06 – 2.01 (m, 2H); <sup>13</sup>C NMR (125 MHz, CDCl<sub>3</sub>): δ 198.4 (C), 167.9 (C), 147.9 (C), 139.1 (C), 133.4 (C), 129.9 (CH), 128.8 (CH), 128.6 (CH), 128.1 (CH), 126.3 (CH), 124.6 (CH), 113.4 (C), 103.9 (CH), 42.9 (CH<sub>2</sub>), 37.4 (CH<sub>2</sub>), 31.2 (CH), 27.8 (CH<sub>2</sub>), 20.7 (CH<sub>2</sub>); HRMS (ESI) *m/z* 317.1554 ([M+H]<sup>+</sup> C<sub>22</sub>H<sub>21</sub>O<sub>2</sub>, requires 317.1542).

**4-(4-(Allyloxy)phenyl)-2-phenyl-4,6,7,8-tetrahydro-5H-chromen-5-one (4j)**

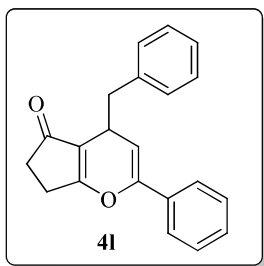
Yellow solid; Mp: 92-94 °C; Yield: 85%; <sup>1</sup>H NMR (500 MHz, CDCl<sub>3</sub>): δ 7.63 – 7.59 (m, 2H), 7.41 – 7.32 (m, 3H), 7.26 (d, 2H, *J* = 9.0 Hz), 6.85 (d, 2H, *J* = 9.0 Hz), 6.10 – 6.0 (m, 1H), 5.72 (d, 1H, *J* = 5.0 Hz), 5.42 (dd, 1H, *J* = 17.0, 1.5 Hz), 5.39 (dd, 1H, *J* = 11.0, 1.5 Hz), 4.52 – 4.48 (m, 3H), 2.75 – 2.65 (m, 2H), 2.43 – 2.37 (m, 2H), 2.09 – 2.02 (m, 2H); <sup>13</sup>C NMR (125 MHz, CDCl<sub>3</sub>): δ 197.8 (C), 166.3 (C), 157.5 (C), 146.9 (C), 137.9 (C), 133.6 (CH), 133.2 (C), 129.4 (CH), 128.9 (CH), 128.6 (CH),

124.6 (CH), 117.8 (CH<sub>2</sub>), 114.8 (CH), 114.3 (C), 104.8 (CH), 69.0 (CH<sub>2</sub>), 37.3 (CH<sub>2</sub>), 34.5 (CH), 27.9 (CH<sub>2</sub>), 20.6 (CH<sub>2</sub>); HRMS (ESI)  $m/z$  359.1665 ([M+H]<sup>+</sup> C<sub>24</sub>H<sub>23</sub>O<sub>3</sub>, requires 359.1647).



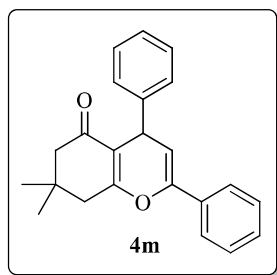
#### 4-(4-Methoxyphenyl)-2-phenyl-6,7-dihydrocyclopenta[b]pyran-5(4H)-one (4k)

Brown solid; Mp: 60-62 °C; Yield: 84%; <sup>1</sup>H NMR (500 MHz, CDCl<sub>3</sub>): δ 7.66 (d, 2H,  $J = 7.0$  Hz), 7.44 – 7.38 (m, 3H), 7.29 – 7.27 (m, 2H), 6.87 (d, 2H,  $J = 8.5$  Hz), 5.68 (d, 1H,  $J = 4.5$  Hz), 4.44 (d, 1H,  $J = 3.5$  Hz), 3.80 (s, 3H), 2.83 – 2.78 (m, 2H), 2.52 – 2.48 (m, 2H); <sup>13</sup>C NMR (125 MHz, CDCl<sub>3</sub>): δ 203.4 (C), 178.7 (C), 158.7 (C), 148.5 (C), 135.6 (C), 133.0 (C), 129.4 (CH), 129.2 (CH), 128.7 (CH), 124.9 (CH), 117.5 (C), 114.1 (CH), 104.3 (CH), 55.5 (CH<sub>3</sub>), 35.0 (CH), 33.6 (CH<sub>2</sub>), 25.8 (CH<sub>2</sub>); HRMS (ESI)  $m/z$  319.1346 ([M+H]<sup>+</sup> C<sub>21</sub>H<sub>19</sub>O<sub>3</sub>, requires 319.1334).



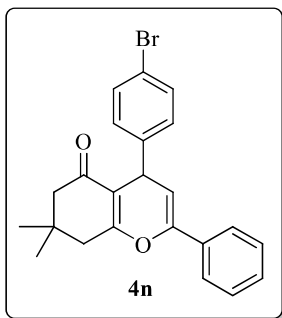
**4-Benzyl-2-phenyl-6,7-dihydrocyclopenta[b]pyran-5(4H)-one (4l)**

Orange solid; Mp: 88-90 °C; Yield: 83%; <sup>1</sup>H NMR (500 MHz, CDCl<sub>3</sub>): δ 7.52 – 7.48 (m, 2H), 7.41 – 7.33 (m, 3H), 7.30 – 7.16 (m, 5H), 5.42 (d, 1H, *J* = 4.0 Hz), 3.62 – 3.58 (m, 1H), 3.33 – 3.28 (m, 1H), 2.75 – 2.63 (m, 3H), 2.54 – 2.50 (m, 2H); <sup>13</sup>C NMR (125 MHz, CDCl<sub>3</sub>): δ 204.3 (C), 180.2 (C), 149.0 (C), 138.6 (C), 133.2 (C), 129.8 (CH), 129.1 (CH), 128.7 (CH), 128.4 (CH), 126.4 (CH), 124.9 (CH), 117.0 (C), 103.6 (CH), 41.2 (CH<sub>2</sub>), 33.6 (CH), 31.8 (CH<sub>2</sub>), 25.7 (CH<sub>2</sub>); HRMS (ESI) *m/z* 303.1394 ([M+H]<sup>+</sup> C<sub>21</sub>H<sub>19</sub>O<sub>2</sub>, requires 303.1385).

**7,7-Dimethyl-2,4-diphenyl-4,6,7,8-tetrahydro-5H-chromen-5-one (4m)**

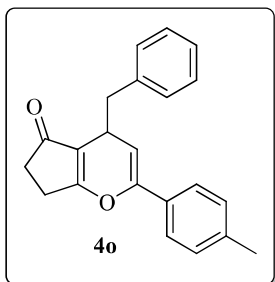
Yellow solid; Mp: 141-143 °C (lit.<sup>13</sup> 142-143 °C); Yield: 81%; <sup>1</sup>H NMR (500 MHz, CDCl<sub>3</sub>): δ 7.63 – 7.59 (m, 2H), 7.40 – 7.27 (m, 7H), 7.19 (t, 1H, *J* = 7 Hz), 5.74 (d, 1H, *J* = 5.0 Hz), 4.52 (d, 1H, *J* = 5.0 Hz), 2.58 (s, 2H), 2.27 (ABq, 2H, *J* = 16.5 Hz), 1.16 (s, 3H), 1.09 (s, 3H); <sup>13</sup>C NMR (125 MHz, CDCl<sub>3</sub>): δ 197.5 (C), 164.8 (C), 146.9 (C), 145.4 (C), 133.2 (C), 128.9 (CH), 128.6 (CH), 128.6 (CH), 128.4 (CH), 126.8 (CH), 124.7 (CH), 112.7 (C), 104.7 (CH), 51.1 (CH<sub>2</sub>), 41.7 (CH), 35.6 (CH<sub>2</sub>),

32.3 (C), 29.4 (CH<sub>3</sub>), 27.9 (CH<sub>3</sub>); HRMS (ESI)  $m/z$  331.1716 ([M+H]<sup>+</sup> C<sub>23</sub>H<sub>23</sub>O<sub>2</sub>, requires 331.1698).



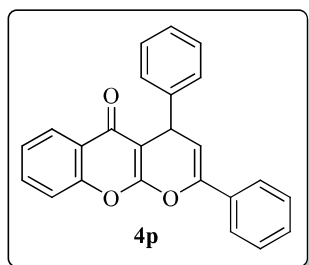
**4-(4-Bromophenyl)-7,7-dimethyl-2-phenyl-4,6,7,8-tetrahydro-5H-chromen-5-one (4n)**

Pale yellow solid; Mp: 93-94 °C; Yield: 72%; <sup>1</sup>H NMR (500 MHz, CDCl<sub>3</sub>): δ 7.62 – 7.58 (m, 2H), 7.43 – 7.35 (m, 5H), 7.23 (d, 2H,  $J = 8.5$  Hz), 5.68 (d, 1H,  $J = 5.0$  Hz), 4.49 (d, 1H,  $J = 5.0$  Hz), 2.57 (s, 2H), 2.26 (ABq, 2H,  $J = 16.0$  Hz), 1.15 (s, 3H), 1.07 (s, 3H); <sup>13</sup>C NMR (125 MHz, CDCl<sub>3</sub>): δ 197.4 (C), 164.9 (C), 147.3 (C), 144.5 (C), 132.9 (C), 131.7 (CH), 130.2 (CH), 129.1 (CH), 128.7 (CH), 124.7 (CH), 120.6 (C), 112.4 (C), 103.9 (CH), 51.1 (CH<sub>2</sub>), 41.6 (CH<sub>2</sub>), 35.2 (CH), 32.4 (C), 29.4 (CH<sub>3</sub>), 27.8 (CH<sub>3</sub>); HRMS (ESI)  $m/z$  425.0768 ([M+H]<sup>+</sup> C<sub>23</sub>H<sub>22</sub>O<sub>3</sub>Br, requires 425.0752)



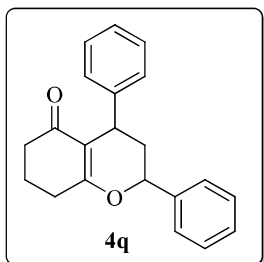
**4-Benzyl-2-(*p*-tolyl)-6,7-dihydrocyclopenta[*b*]pyran-5(4*H*)-one (4o)**

Yellow solid; Mp: 125-126 °C; Yield: 80%; <sup>1</sup>H NMR (500 MHz, CDCl<sub>3</sub>): δ 7.39 (d, 2H, *J* = 8.5 Hz), 7.30 – 7.25 (m, 2H), 7.23 – 7.20 (m, 1H), 7.20 – 7.15 (m, 4H), 5.37 (d, 1H, *J* = 4.0 Hz), 3.62 – 3.55 (m, 1H), 3.30 (dd, 1H, *J* = 13.0, 3.5 Hz), 2.71 (dd, 1H, *J* = 13.0, 9.0 Hz), 2.67 – 2.63 (m, 2H), 2.54 – 2.50 (m, 2H), 2.36 (s, 3H); <sup>13</sup>C NMR (125 MHz, CDCl<sub>3</sub>): δ 204.3 (C), 180.2(C), 149.0(C), 139.1 (C), 138.6 (C), 130.3 (C), 129.8 (CH), 129.3 (CH), 128.3 (CH), 126.4 (CH), 124.8 (CH), 117.0 (C), 102.7 (CH), 41.2 (CH<sub>2</sub>), 33.6 (CH), 31.8 (CH<sub>2</sub>), 25.7 (CH<sub>2</sub>), 21.4 (CH<sub>3</sub>); HRMS (ESI) *m/z* 317.1554 ([M+H]<sup>+</sup> C<sub>22</sub>H<sub>21</sub>O<sub>2</sub>, requires 317.1542)

**2,4-Diphenyl-4*H*,5*H*-pyrano[2,3-*b*]chromen-5-one (4p)**

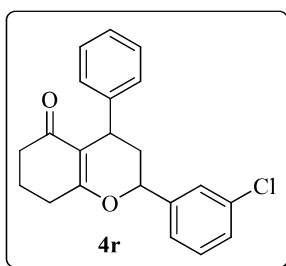
Yellow solid; Mp: 158-159 °C; Yield: 84%; <sup>1</sup>H NMR (500 MHz, CDCl<sub>3</sub>): δ 8.07 – 8.03 (m, 1H), 7.79 – 7.74 (m, 2H), 7.62 – 7.57 (m, 1H), 7.50 – 7.41 (m, 5H), 7.40 – 7.32 (m, 4H), 7.28 – 7.23 (m, 1H), 5.87 (d, 1H, *J* = 4.5 Hz), 4.74 (d, 1H, *J* = 4.5 Hz); <sup>13</sup>C NMR (125 MHz, CDCl<sub>3</sub>): δ 161.7 (C), 156.0 (C), 153.0 (C), 147.1(C), 143.7 (C), 132.8 (C), 132.2 (CH), 129.5 (CH), 128.9 (CH), 128.8 (CH), 128.7 (CH), 127.4 (CH), 124.9 (CH), 124.0 (CH), 123.0 (CH), 117.1 (CH), 114.8 (C), 104.0 (CH),

103.9 (C), 36.8 (CH); HRMS (ESI)  $m/z$  353.1198 ( $[M+H]^+$   $C_{24}H_{17}O_3$ , requires 353.1178)



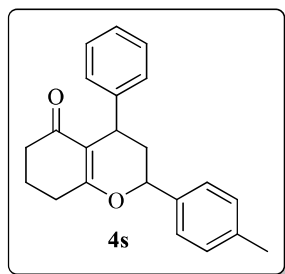
**2,4-Diphenyl-2,3,4,6,7,8-hexahydro-5H-chromen-5-one (4q)**

White solid; Mp: 127-129 °C (lit.<sup>7</sup> 129-130 °C); Yield: 81%;  $^1H$  NMR (500 MHz,  $CDCl_3$ ):  $\delta$  7.37 – 7.36 (m, 4H), 7.34 – 7.31 (m, 1H), 7.26 – 7.23 (m, 2H), 7.19 – 7.13 (m, 3H), 4.97 (dd, 1H,  $J = 11.5, 1.5$  Hz), 3.97 – 3.93 (m, 1H), 2.64 – 2.24 (m, 5H), 2.05 – 1.96 (m, 3H);  $^{13}C$  NMR (125 MHz,  $CDCl_3$ ):  $\delta$  196.8 (C), 173.1 (C), 145.0 (C), 139.3 (C), 128.6 (CH), 128.3 (CH), 128.3 (CH), 126.4 (CH), 126.0 (CH), 125.9 (CH), 115.6 (C), 79.0 (CH), 41.7 ( $CH_2$ ), 37.1 ( $CH_2$ ), 36.9 (CH), 29.2 ( $CH_2$ ), 20.2 ( $CH_2$ ); HRMS (ESI)  $m/z$  305.1555 ( $[M+H]^+$   $C_{21}H_{21}O_2$ , requires 305.1542)



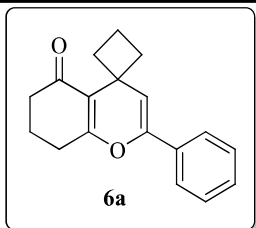
**2-(3-Chlorophenyl)-4-phenyl-2,3,4,6,7,8-hexahydro-5H-chromen-5-one (4r)**

White solid; Mp: 150-151 °C; Yield: 71%; <sup>1</sup>H NMR (500 MHz, CDCl<sub>3</sub>): δ 7.38 (s, 1H), 7.30 – 7.28 (m, 2H), 7.26 – 7.23 (m, 3H), 7.17– 7.13 (m, 3H), 4.96 (dd, 1H, *J* = 11.5, 1.5 Hz), 3.96 – 3.92 (m, 1H), 2.67 – 2.36 (m, 5H), 2.07 – 1.91 (m, 3H); <sup>13</sup>C NMR (125 MHz, CDCl<sub>3</sub>): δ 196.4 (C), 172.8 (C), 144.6 (C), 141.5 (C), 134.4 (C), 130.0 (CH), 128.5 (CH), 128.5 (CH), 126.3 (CH), 126.1 (CH), 126.0 (CH), 124.1 (CH), 115.6 (C), 78.1 (CH), 41.7 (CH<sub>2</sub>), 37.7 (CH<sub>2</sub>), 36.8 (CH), 29.0 (CH<sub>2</sub>), 20.1 (CH<sub>2</sub>); HRMS (ESI) *m/z* 339.1162 ([M+H]<sup>+</sup> C<sub>21</sub>H<sub>20</sub>O<sub>2</sub>Cl, requires 339.1152).

**4-Phenyl-2-(*p*-tolyl)-2,3,4,6,7,8-hexahydro-5H-chromen-5-one (4s)**

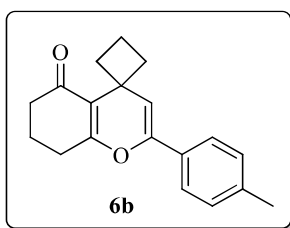
White solid; Mp: 121-123 °C; Yield: 75%; <sup>1</sup>H NMR (500 MHz, CDCl<sub>3</sub>): δ 7.28 – 7.23 (m, 5H), 7.21 – 7.14 (m, 4H), 4.94 (d, 1H, *J* = 10.5 Hz), 3.96 – 3.91 (m, 1H), 2.64 – 2.39 (m, 3H), 2.35 (s, 3H), 2.36 – 2.17 (m, 2H), 2.05 – 1.97 (m, 3H); <sup>13</sup>C NMR (125 MHz, CDCl<sub>3</sub>): δ 196.7 (C), 173.2 (C), 145.0 (C), 138.2 (C), 136.3 (C), 129.2 (CH), 128.3 (CH), 126.3 (CH), 126.1 (CH), 125.8 (CH), 115.5 (C), 79.0 (CH), 41.6 (CH<sub>2</sub>), 38.0 (CH<sub>2</sub>), 36.9 (CH), 29.1 (CH<sub>2</sub>), 21.1 (CH<sub>2</sub>), 20.0 (CH<sub>3</sub>); HRMS (ESI) *m/z* 319.1708 ([M+H]<sup>+</sup> C<sub>22</sub>H<sub>23</sub>O<sub>2</sub>, requires 319.1698)





### 2-Phenyl-7,8-dihydrospiro[chromene-4,1'-cyclobutan]-5(6*H*)-one (6a)

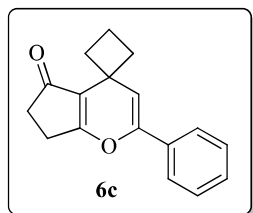
Yellow solid; Mp: 77-78 °C; Yield: 79%; <sup>1</sup>H NMR (500 MHz, CDCl<sub>3</sub>): δ 7.61 (d, 2H, *J* = 7.0 Hz), 7.40 (t, 1H, *J* = 7.0 Hz), 7.37 (d, 2H, *J* = 7.0 Hz), 5.87 (s, 1H), 3.16 – 3.07 (m, 2H), 2.56 (t, 2H, *J* = 6.5 Hz), 2.47 (t, 2H, *J* = 6.5 Hz), 2.14 – 2.0 (m, 4H), 1.88 – 1.82 (m, 2H); <sup>13</sup>C NMR (125 MHz, CDCl<sub>3</sub>): δ 199.2 (C), 166.3 (C), 143.8 (C), 133.3 (C), 128.6 (CH), 128.6 (CH), 124.4 (CH), 115.7 (C), 111.3 (CH), 39.0 (CH<sub>2</sub>), 36.6 (CH<sub>2</sub>), 35.9 (CH<sub>2</sub>), 29.9 (C), 28.4 (CH<sub>2</sub>), 20.7 (CH<sub>2</sub>), 14.2 (CH<sub>2</sub>); HRMS (ESI) *m/z* 267.1389 ([M+H]<sup>+</sup> C<sub>18</sub>H<sub>19</sub>O<sub>2</sub>, requires 267.1385)



### 2-(*p*-Tolyl)-7,8-dihydrospiro[chromene-4,1'-cyclobutan]-5(6*H*)-one (6b)

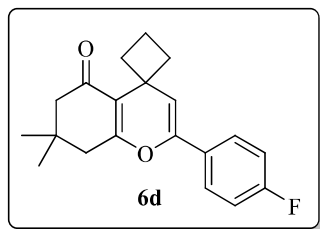
White solid; Mp: 128-129 °C; Yield: 77%; <sup>1</sup>H NMR (500 MHz, CDCl<sub>3</sub>): δ 7.47 (d, 2H, *J* = 8.0 Hz), 7.17 (d, 2H, *J* = 8.0 Hz), 5.79 (s, 1H), 3.11-3.05 (m, 2H), 2.53 (t, 2H, *J* = 6.0 Hz), 2.44 (t, 2H, *J* = 6.0 Hz), 2.36 (s, 3H), 2.10 – 1.95 (m, 4H), 1.85 – 1.78 (m, 2H); <sup>13</sup>C NMR (125 MHz, CDCl<sub>3</sub>): δ 198.9 (C), 166.1 (C), 143.5 (C), 138.3 (C),

130.2 (C), 129.0 (CH), 124.0 (CH), 115.4 (C), 110.2 (CH), 38.7 (CH<sub>2</sub>), 36.3 (CH<sub>2</sub>), 35.6 (CH<sub>2</sub>), 29.6 (C), 28.1 (CH<sub>2</sub>), 21.1 (CH<sub>2</sub>), 20.4 (CH<sub>3</sub>), 13.9 (CH<sub>2</sub>); HRMS (ESI)  $m/z$  281.1563 ([M+H]<sup>+</sup> C<sub>19</sub>H<sub>21</sub>O<sub>2</sub>, requires 281.1542).



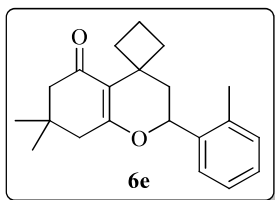
**2'-Phenyl-6',7'-dihydro-5'*H*-spiro[cyclobutane-1,4'-cyclopenta[b]pyran]-5'-one  
(6c)**

White solid; Mp: 100-101 °C; Yield: 82%; <sup>1</sup>H NMR (500 MHz, CDCl<sub>3</sub>): δ 7.57 – 7.53 (m, 2H), 7.35 – 7.27 (m, 3H), 5.79 (s, 1H), 2.85 – 2.77 (m, 2H), 2.61 – 2.57 (m, 2H), 2.45 – 2.41 (m, 2H), 2.09 – 1.82 (m, 4H); <sup>13</sup>C NMR (125 MHz, CDCl<sub>3</sub>): δ 204.4 (C), 178.3 (C), 146.5 (C), 133.1 (C), 129.0 (CH), 128.7 (CH), 124.8 (CH), 119.7 (C), 110.5 (CH), 35.8 (CH<sub>2</sub>), 35.6 (CH<sub>2</sub>), 34.0 (CH<sub>2</sub>), 29.9 (C), 25.2 (CH<sub>2</sub>), 15.2 (CH<sub>2</sub>); HRMS (ESI)  $m/z$  253.1218 ([M+H]<sup>+</sup> C<sub>17</sub>H<sub>17</sub>O<sub>2</sub>, requires 253.1229).



**2-(4-Fluorophenyl)-7,7-dimethyl-7,8-dihydrospiro[chromene-4,1'-cyclobutan]-5(6H)-one (6d)**

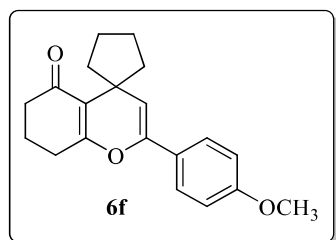
White solid; Mp: 124-125 °C; Yield: 73%;  $^1\text{H}$  NMR (500 MHz,  $\text{CDCl}_3$ ):  $\delta$  7.58 – 7.53 (m, 2H), 7.10 – 7.03 (m, 2H), 5.78 (s, 1H), 3.11 – 3.03 (m, 2H), 2.40 (s, 2H), 2.31 (s, 2H), 2.12 – 2.01 (m, 2H), 1.87 – 1.79 (m, 2H), 1.11 (s, 6H);  $^{13}\text{C}$  NMR (125 MHz,  $\text{CDCl}_3$ ):  $\delta$  199.0 (C), 164.3 (C), 162.9 (d, C,  $J = 246.5$  Hz), 143.1 (C), 129.4 (C), 126.3 (d, CH,  $J = 8.75$  Hz), 115.5 (d, CH,  $J = 21.25$  Hz), 114.5 (C), 111.0 (CH), 52.7 ( $\text{CH}_2$ ), 42.0 ( $\text{CH}_2$ ), 36.6 ( $\text{CH}_2$ ), 35.7 ( $\text{CH}_2$ ), 31.8 (C), 29.9 (C), 28.4 ( $\text{CH}_3$ ), 28.4 ( $\text{CH}_3$ ), 14.2 ( $\text{CH}_2$ ); HRMS (ESI)  $m/z$  313.1599 ( $[\text{M}+\text{H}]^+$   $\text{C}_{20}\text{H}_{22}\text{O}_2\text{F}$ , requires 313.1604).



**7,7-Dimethyl-2-(*o*-tolyl)-2,3,7,8-tetrahydrospiro[chromene-4,1'-cyclobutan]-5(6H)-one (6e)**

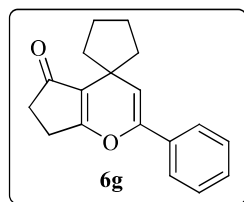
White solid; Mp: 110-111 °C; Yield: 80%;  $^1\text{H}$  NMR (500 MHz,  $\text{CDCl}_3$ ):  $\delta$  7.31 (d, 1H,  $J = 7.5$  Hz), 7.16 – 7.02 (m, 3H), 4.83 (d, 1H,  $J = 10.5$  Hz), 3.10 (q, 1H,  $J = 10.5$  Hz), 2.6 (q, 1H,  $J = 10.5$  Hz), 2.24 (s, 3H), 2.19-2.15 (m, 4H), 2.02 - 1.79 (m, 4H), 1.75 – 1.51 (m, 2H), 0.95 (s, 3H), 0.94 (s, 3H);  $^{13}\text{C}$  NMR (125 MHz,  $\text{CDCl}_3$ ):  $\delta$  197.9 (C), 169.4 (C), 137.8 (C), 134.4 (C), 130.4 (CH), 127.8 (CH), 126.2 (CH), 125.4

(CH), 115.9 (C), 73.7 (CH), 51.9 (CH<sub>2</sub>), 44.0 (CH<sub>2</sub>), 42.6 (CH<sub>2</sub>), 36.2 (CH<sub>2</sub>), 33.4 (C), 31.2 (CH<sub>2</sub>), 30.3 (C), 29.1 (CH<sub>3</sub>), 27.1 (CH<sub>3</sub>), 18.8 (CH<sub>3</sub>), 14.3 (CH<sub>2</sub>); HRMS (ESI)  $m/z$  311.2017 ( $[M+H]^+$  C<sub>21</sub>H<sub>27</sub>O<sub>2</sub>, requires 311.2011).



**2-(4-Methoxyphenyl)-7,8-dihydrospiro[chromene-4,1'-cyclopentan]-5(6H)-one  
(6f)**

Yellow low melting solid; Yield: 83%; <sup>1</sup>H NMR (500 MHz, CDCl<sub>3</sub>):  $\delta$  7.41 (d, 2H,  $J$  = 9.0 Hz), 6.82 (d, 2H,  $J$  = 9.0 Hz), 5.24 (s, 1H), 3.76 (s, 3H), 2.49 (t, 2H,  $J$  = 6.5 Hz), 2.34 (t, 2H,  $J$  = 6.5 Hz), 2.25 – 2.17 (m, 2H), 1.99 – 1.92 (m, 4H), 1.89 – 1.84 (m, 2H), 1.66 – 1.63 (m, 2H); <sup>13</sup>C NMR (125 MHz, CDCl<sub>3</sub>):  $\delta$  198.4 (C), 166.4 (C), 159.6 (C), 141.8 (C), 135.1 (C), 125.5 (CH), 116.2 (C), 113.6 (CH), 109.6 (C), 55.2 (CH<sub>3</sub>), 42.2 (CH<sub>2</sub>), 38.8 (CH<sub>2</sub>), 38.8 (CH<sub>2</sub>), 32.1 (C), 28.3 (CH<sub>2</sub>), 26.2 (CH<sub>2</sub>), 20.5 (CH<sub>2</sub>), 14.0 (CH<sub>2</sub>); HRMS (ESI)  $m/z$  311.2939 ( $[M+H]^+$  C<sub>21</sub>H<sub>23</sub>O<sub>3</sub>, requires 311.1647).



**2'-Phenyl-6',7'-dihydro-5'*H*-spiro[cyclopentane-1,4'-cyclopenta[b]pyran]-5'-one****(6g)**

Yellow solid; Mp: 191-192 °C; Yield: 85%; <sup>1</sup>H NMR (500 MHz, CDCl<sub>3</sub>): δ 7.62 – 7.58 (m, 2H), 7.41 – 7.33 (m, 3H), 5.49 (s, 1H), 2.70 – 2.66 (m, 2H), 2.50 – 2.46 (m, 2H), 2.25 – 2.13 (m, 2H), 1.94 – 1.88 (m, 2H), 1.78 – 1.73 (m, 2H), 1.58-1.51 (m, 2H); <sup>13</sup>C NMR (125 MHz, CDCl<sub>3</sub>): δ 203.7 (C), 178.4 (C), 145.1 (C), 133.0 (C), 128.5 (CH<sub>2</sub>), 128.3 (CH<sub>2</sub>), 124.5 (CH<sub>2</sub>), 120.1 (C), 110.2 (CH), 40.8 (CH<sub>2</sub>), 39.7 (CH<sub>2</sub>), 33.6 (CH<sub>2</sub>), 29.6 (C), 25.3 (CH<sub>2</sub>), 25.0 (CH<sub>2</sub>), 14.0 (CH<sub>2</sub>); HRMS (ESI) *m/z* 267.1630 ([M+H]<sup>+</sup> C<sub>18</sub>H<sub>19</sub>O<sub>2</sub>, requires 267.1385).

---

**3.6 References**

1. (a) L. F. Tietze and A. Modi, *Med. Res. Rev.* 2000, **20**, 304; (b) G. Poli, G. Giambastiani and A. Heumann, *Tetrahedron* 2000, **56**, 5959; (c) T. Hudlicky, *Chem. Rev.* 1996, **96**, 3.
2. (a) S. Jiménez-Alonso, A. L. Pérez-Lomas, A. Estévez-Braun, F. M. Martínez, H. C. Orellana, A. G. Ravelo, F. Gamarro, S. Castanys and M. López, *J. Med. Chem.* 2008, **51**, 7132.
3. R. Peña, P. Martín, G. E. Feresin, A. Tapia, F. Machín and A. Estévez-Braun, *J. Nat. Prod.* 2016, **79**, 970.
4. (a) L. F. Tietze, *J. Heterocycl. Chem.* 1990, **27**, 47; (b) L. F. Tietze, *Chem. Rev.* 1996, **96**, 115; (c) L. F. Tietze and N. Rackelman; *Pure Appl. Chem.* 2004, **76**, 1967; (d) J. S. Yadav, B. V. S. Reddy, D. Narsimhaswamy, P. N. Lakahmi, K. Narsimulu, G. Srinivasulu and A. C. Kunwar, *Tetrahedron Lett.* 2004, **45**, 3493; (e) J. Jayashankaran, R. D. R. S. Manian and R. Raghunathan, *Tetrahedron Lett.* 2006, **47**, 2265.
5. (a) M. Wu, J. Yang, F. Luo, C. Cheng and G. Zhu, *Org. Biomol. Chem.* 2019, **17**, 5684; (b) P. Biswas, J. Ghosh, S. Maiti and C. Bandyopadhyay, *Tetrahedron Lett.* 2014, **55**, 6882; (c) K. C. Majumdar, A. Taher and R. K. Nandi, *Tetrahedron* 2012, **68**, 5693; (d) Y. Ren, W. Zhang, J. Lu, K. Gao, X. Liao and X. Chen, *RSC Adv.* 2015, **5**, 79405; (e) Q. Yang, L. -H. Zhou, W. -X. Wu, W. Zhang, N. Wang and X. -Q. Yu, *RSC Adv.* 2015, **5**,

- 78927; (f) M. Baghernejad, S. Khodabakhshi and S. Tajik, *New. J. Chem.* 2016, **40**, 2704; (g) A. Khazaei, M. A. Zolfigol, F. Karimitabar, I. Nikokar and A. R. Moosavi-Zare, *RSC Adv.* 2015, **5**, 71402; (h) F. Tufail, M. Saquib, S. Singh, J. Tiwari, P. Dixit, J. Singh and J. Singh, *New. J. Chem.* 2018, **42**, 17279; (i) R. Jamatia, A. Gupta and A. K. Pal, *RSC Adv.* 2016, **6**, 20994; (j) S. Bagchi, A. S. Hussien, Deeksha and A. Sharma, *ChemistrySelect* 2019, **4**, 6593; (k) M. -M. Li, C. -S. Duan, Y. -Q. Yu and D. -Z. Xu, *Dyes Pigm.* 2018, **150**, 202; (l) A. Hasaninejad, F. Mandegani, M. Beyrati, A. Maryamabadi and G. Mohebbi, *ChemistrySelect* 2017, **2**, 6784.
6. (a) S. Jiménez-Alonso, H. C. Orellana, A. Estévez-Braun, A. G. Ravelo, E. Pérez-Sacau, F. Machín, *J. Med. Chem.* 2008, **51**, 6761; (b) R. Peña, P. Martín, G. E. Feresin, A. Tapia, F. Machín, A. Estévez-Braun, *J. Nat. Prod.* 2016, **79**, 970.
7. F. C. da Silva, S. B. Ferreira, C. R. Kaiser, A. C. Pinto and V. F. Ferreira, *J. Braz. Chem. Soc.* 2009, **20**, 1478.
8. A. Gaspar, M. J. Motos, J. Garrido, E. Uriarte and F. Borges, *Chem. Rev.* 2014, **114**, 4960.
9. D. L. Galinis, R. W. Fuller, T. C. McKee, J. H. Cardellina, R. J. Gulakowski, J. B. McMahon and M. R. Boyd, *J. Med. Chem.* 1996, **39**, 4507.

- 
10. P. Panda, S. Nayak, S. Ku. Sahoo, S. Mohapatra, D. Nayak, R. Pradhan and C. N. Kundu, *RSC Adv.* 2018, **8**, 16802.
11. G. Gault, S. Lefebvre, E. Benoit, V. Lattard and D. Grancher, *Toxicon* 2019, **165**, 47.
12. S. -S. Ma, W. -L Mei, Z. -K. Guo, S. -B. Liu, Y. -X. Zhao, D. -L. Yang, Y. -B. Zeng, B. Jiang and H. -F. Dai, *Org. Lett.* 2013, **15**, 1492.
13. P. Vats, V. Hadjimitova, K. Yoncheva, A. Kathuria, A. Sharma, K. Chand, A. J. Duraisamy, A. K. Sharma, A. K. Sharma, L. Saso and S. K. Sharma, *Med. Chem. Res.* 2014, **23**, 4907.
14. (a) Z. Huang, *Oncogene* 2000, **19**, 6627; (b) W. Zhu, C. Chen, C. Sun, S. Xu, C. Wu, F. Lei, H. Xia, Q. Tu and P. Zheng, *Eur. J. Med. Chem.* 2015, **93**, 64.
15. K. Kushwaha, N. Kaushik, Lata and S. C. Jain, *Bioorg. Med. Chem. Lett.* 2014, **24**, 1795.
16. F. M. Abdelrazek, P. Metz and E. K. Farrag, *Arch. Pharm.* 2004, **337**, 482.
17. (a) J. S. Yadav, B. V. S. Reddy, A. V. H. Gopal, R. N. Rao, R. Somaiah, P. P. Reddy and A. C. Kunwar, *Tetrahedron Lett.* 2010, **51**, 2305; (b) M. Mollazadeh, M. J. Khoshkholgh, S. Balalaie, F. Rominger, H. R. Bijanzadeh, *J. Heterocycl. Chem.* 2010, **47**, 1200; (c) M. J. Khoshkholgh, S. Balalaie, H. R. Bijanzadeh, J. H. Gross, *Arkivoc* 2009, **9**, 114; (d) M. J.



- 
- Khoshkholgh, M. Lotfi, S. Balalaie and F. Rominger, *Tetrahedron* 2009, **65**, 4228.
18. (a) Y. R. Lee, Y. M. Kim, *Tetrahedron* 2009, **65**, 101; (b) Y. R. Lee, T. V. Hung, *Tetrahedron* 2008, **64**, 7338.
19. S. Balalaie, A. Poursaeed, M. J. Khoshkholgh, H. R. Bijanzadeh and E. Wolf, *C. R. Chimie* 2012, **15**, 283.
20. (a) N. J. Parmar, S. B. Teraiya, R. A. Patel and N. P. Talpada, *Tetrahedron Lett.* 2011, **52**, 2853; (b) N. J. Parmar, B. R. Pansuriya, B. M. Labana, T. R. Sutariya, R. Kant and V. K. Gupta, *Eur. J. Org. Chem.* 2012, **30**, 5953.
21. P. Martín-Acosta, G. Feresin, A. Tapia and A. Estévez-Braun, *J. Org. Chem.* 2016, **81**, 9738.
22. (a) M. M. Khan, Saigal, S. Khan, S. Shareef and S. Hussain, *ChemistrySelect* 2018, **3**, 2261; (b) N. J. Parmar, B. R. Pansuriya, H. A. Barad, B. D. Parmar, R. Kant and V. K. Gupta, *Monatsh Chem.* 2013, **144**, 865.
23. M. Li, A. Taheri, M. Liu, S. Sun and Y. Gua, *Adv. Synth. Catal.* 2014, **356**, 537.
24. T. R. Suatiya, B. M. Labana, B. D. Parmar, N. J. Parmar, R. Kant and V. K. Gupta, *RSC Adv.* 2015, **5**, 23519.

- 
25. S. N. Maddila, S. Maddila, N. Kerru, S. V. H. S. Bhaskaruni, and S. B. Jonnalagadda, *ChemistrySelect* 2020, **5**, 1786.
26. M. Bakthadoss, J. Srinivasan, M. A. Hussain and D. S. Sharada, *RSC Adv.* 2019, **9**, 24314.
27. V. Ramesh, S. Shanmugam and N. S. Devi, *ChemistrySelect* 2018, **3**, 3652.
28. H. R. E. Zand, H. Ghafuri and N. Ghanbari, *ChemistrySelect* 2018, **3**, 8229.
29. M. Kiamehr, L. Mohammadkhani, M. R. Khodabakhshi, B. Jafari, P. Langer, *Synlett* 2019, **30**, 1782.
30. (a) Y. Jin, J. Li, L. Peng and C. Gao, *Chem. Commun.* 2015, **51**, 15390; (b) C.-Y. Lai, *J. Thermodyn. Catal.* 2013, **5**, 1; (c) H. V. Farahani, M. Bayat and S. Nasri, *Silicon* 2020, **12**, 41; (d) M. G. Shioorkar and M. B. Ubale, *Asian J. Chem.* 2017, **29**, 1249; (e) P. Pathak, P. K. Shukla, V. Naumovich, M. Grishina, V. Potemkin and A. Verma, *Synth. Commun.* 2019, **49**, 2725.
31. L. S. Arias, J. P. Pessan, A. P. M. Vieira, T. M. T. de Lima, A. C. B. Delbem and D. R. Monteiro, *Antibiotics* 2018, **7**, 46.
32. (a) B. Karimi, F. Mansouri and H. M. Mirzaei, *ChemCatChem* 2015, **7**, 1736; (b) D. Wang and D. Astruc, *Chem. Rev.* 2014, **114**, 6949; (c) J. Lee, Y. Lee, J. K. Youn, H. B. Na, T. Yu, H. Kim, S. M. Lee, Y. M. Koo, J. H.

Kwak, H. G. Park, H. N. Chang, M. Hwang, J. G. Park, J. Kim and T.

Hyeon, *Small* 2008, **4**, 143.

33. R. A. Sheldon, *J. Mol. Catal. A*. 1996, **107**, 75.

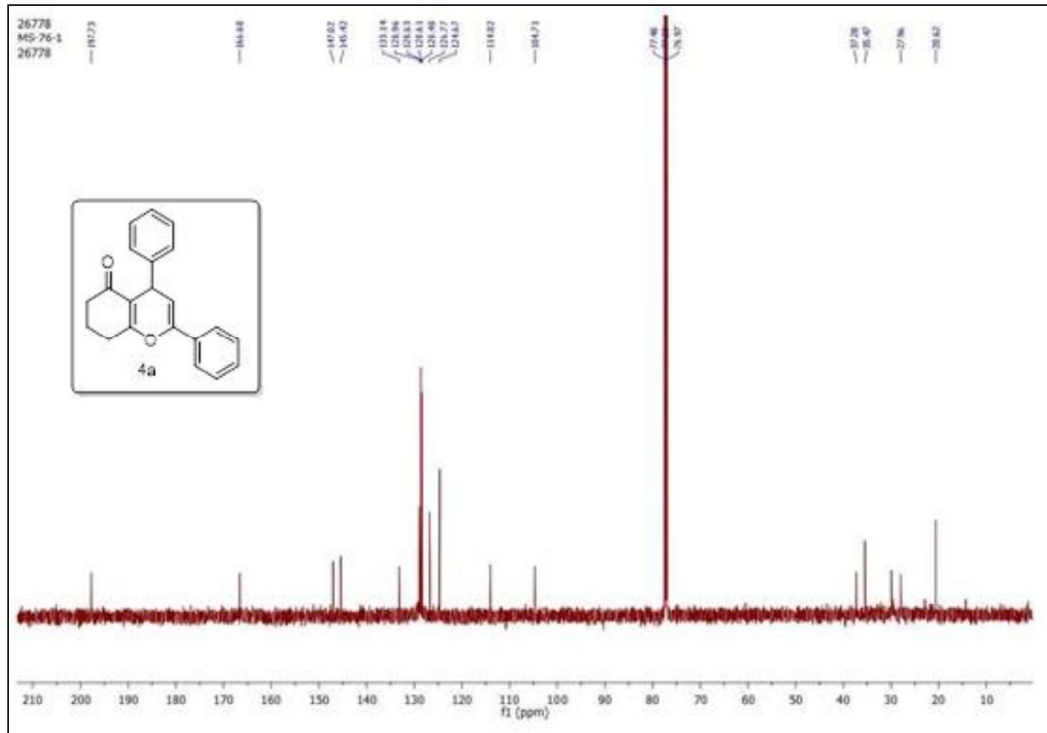
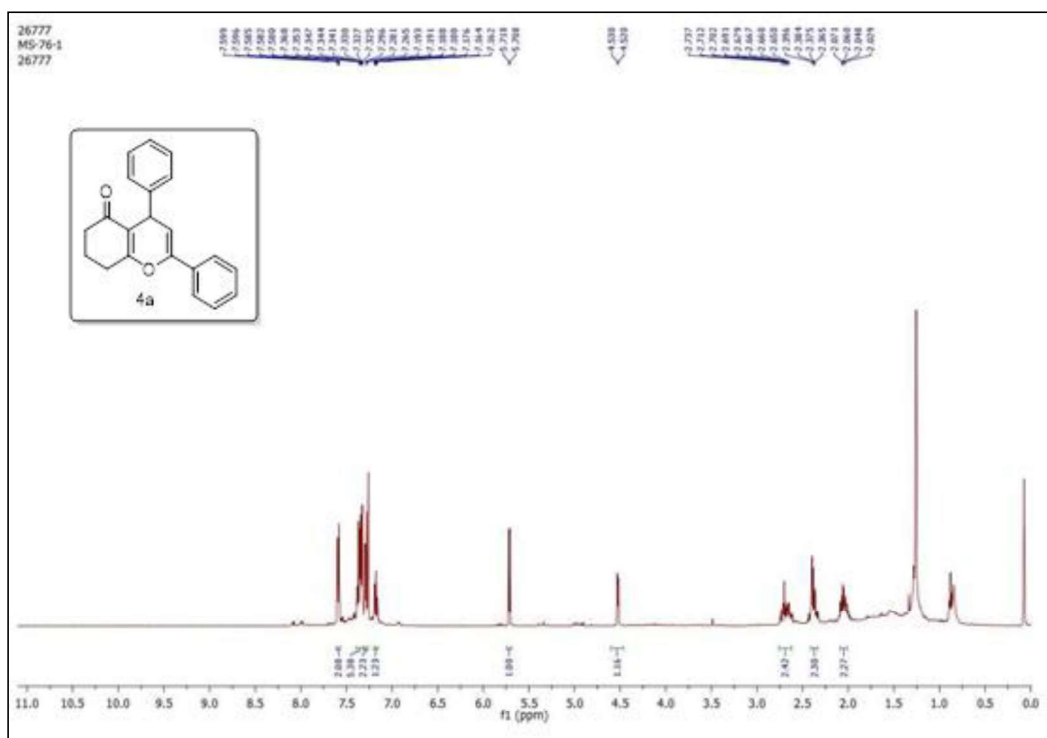
34. A. Kundu, S. Mukherjee and A. Pramanik, *RSC Adv.* 2015, **5**, 107847.

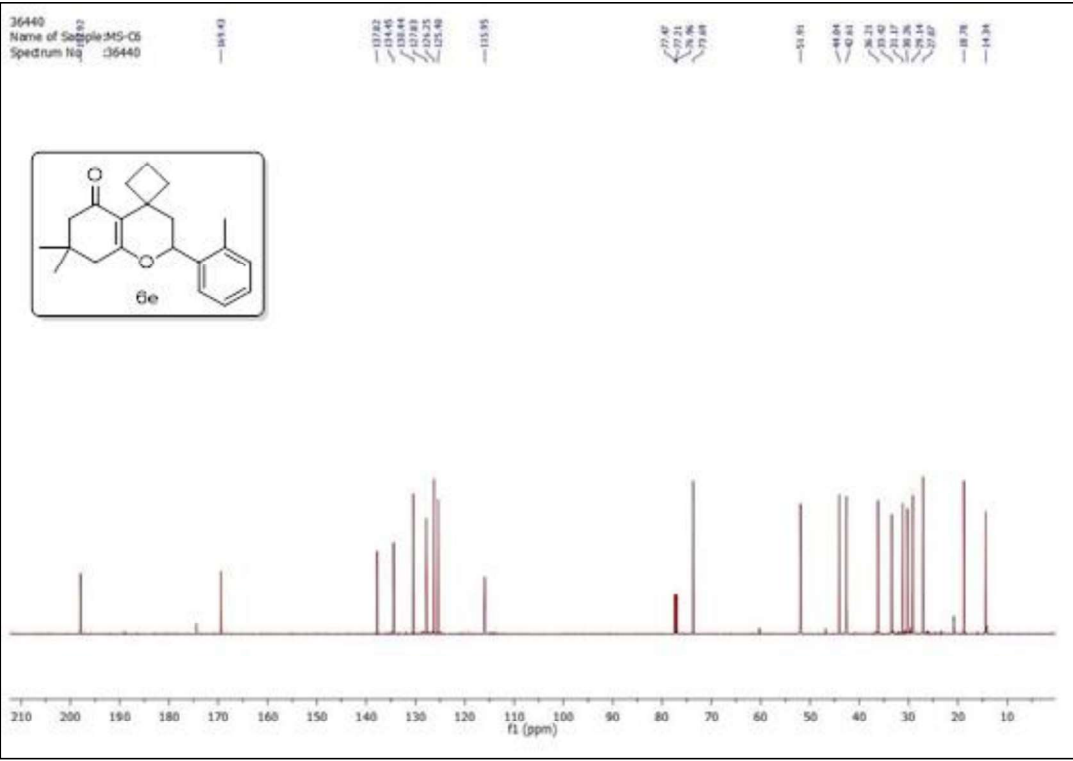
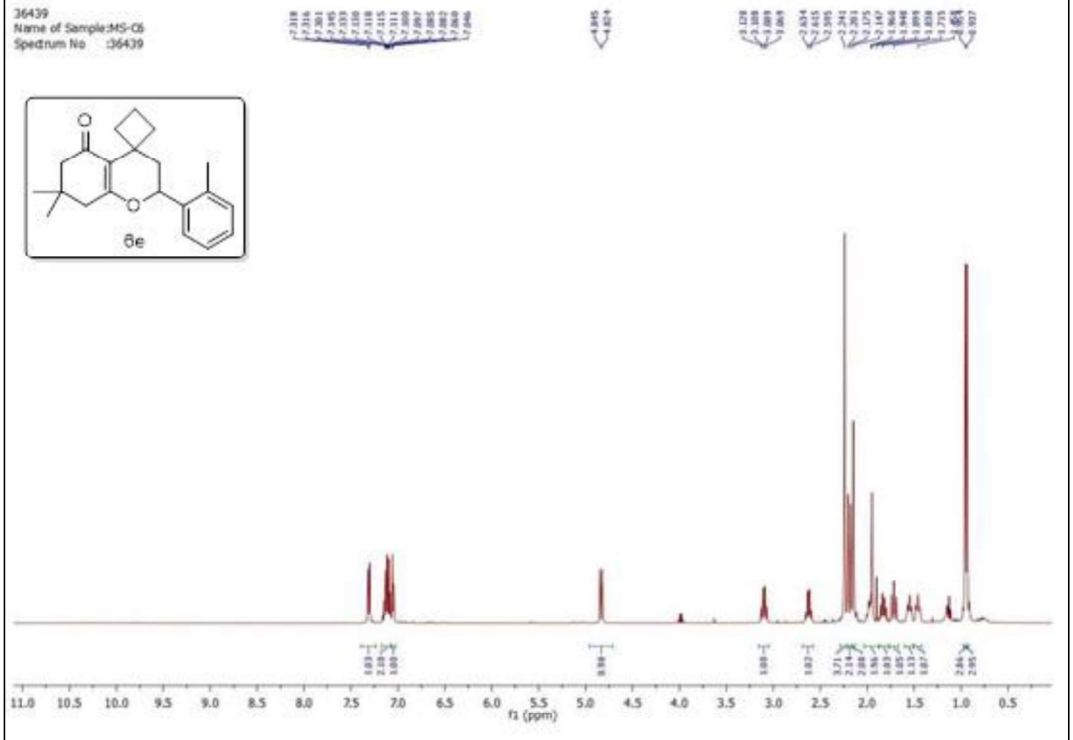
35. J. Safari and Z. Zarnegar, *RSC Adv.* 2015, **5**, 17738.

36. M. Kazemnejadi, S. A. Alavi G., Z. Rezazadeh, M. A. Nasser, A.

Allahresani and M. Esmailpour, *Appl. Organometal. Chem.* 2019, **34**, 1.

3.7 NMR spectra of selected compounds





# **Chapter 4**

**Synthesis of cellulose-supported copper nanoparticles and its application in synthesis of 1,2,3-triazole**

---

## 4.1 Introduction

The chemistry of 1,2,3-triazoles have attracted tremendous research interest owing to their application in polymer chemistry, organic synthesis and material chemistry.<sup>1</sup> The discovery of alkyne-azide cycloaddition (AAC) by Huisgen, Sharpless and Meldal paved the way for the synthesis and application of 1,2,3-triazoles and their complex counterparts.<sup>2</sup> The first report on the synthesis of 1,2,3-triazoles via cycloaddition reaction between an azide and alkyne was given by Dimorth in 1902 but the first in-depth study of the mechanism was conducted by Huisgen in the year 1965, thus giving rise to Huisgen 1,3-dipolar cycloaddition reaction.<sup>3</sup> In this method, a mixture of 1,4- and 1,5-disubstituted triazole regioisomers were obtained. Later on, Sharpless and Meldal independently, carried out copper catalyzed AAC reaction which led to the formation of a single regioisomer. The AAC reaction discovered by Sharpless has several advantages over 1,3-dipolar cycloaddition reaction discovered by Huisgen. These include mild reaction conditions, functional group tolerance, high reaction efficiency and enhanced regio- and chemoselectivities.<sup>4</sup> The term ‘Click Chemistry’ was first coined by Sharpless which defines an efficient approach for the combination of biocompatible functional groups in order to generate substances rapidly, thereby, eliminating the formation of by-products and purification steps. 1,2,3-triazoles are important motif in a number of therapeutics and possess striking pharmacological properties such as antifungal, antituberculosis, antibacterial, anticancer and HIV

protease inhibitors.<sup>5</sup> Rufinamide (**1**) is an approved drug containing 1,2,3-triazole core and is used as an antiepileptic, while molidustat (**2**) is a drug candidate used for the treatment of renal anaemia (Figure 1).<sup>6,7</sup> Fluconazole (**3**) (marketed as Diflucan) and ravuconazole (**4**) are used as antifungal agents (Figure 1).<sup>8,9</sup> Fluconazole is capable of curing fungal infections like cryptococcal meningitis, candidiasis, histoplasmosis and aspergillosis. It is also used in the prevention of yeast infection in cancer patients.<sup>8</sup>

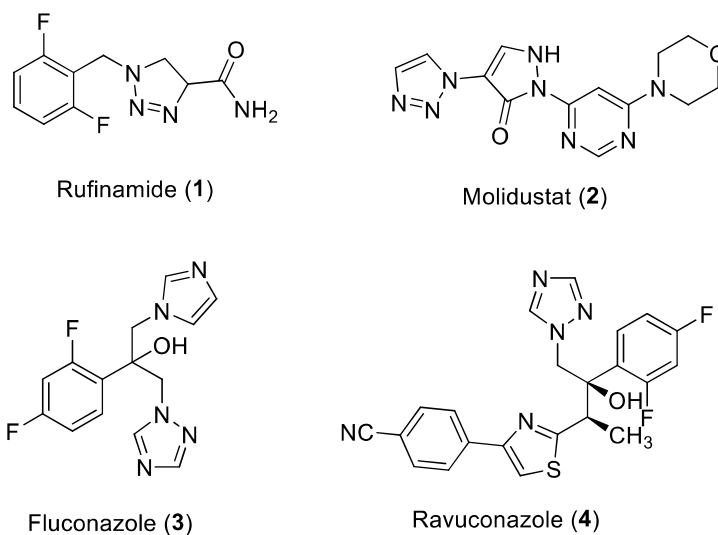


**Figure 1.** Representatives of some biologically active compounds containing 1,2,3-triazole backbone

The *N*-substitution of 1,2,3-triazoles is an important but challenging task from biological point of view. *N*-substituted 1,2,3-triazoles are important motifs in medicinal chemistry, carbene precursors, auxiliaries in C-H activation and ligand



chemistry.<sup>10-13</sup> Generally, *N*-substituted 1,2,3-triazoles are prepared by transition metal-catalyzed click reaction between azides and alkynes.<sup>14</sup> Organic azides used as starting materials suffer from limited availability and complications in their synthesis.<sup>15</sup> On the other hand, the use of commercially available sodium azide or *p*-toluenesulfonyl azide produces simply *NH*- or *N*-sulfonyl 1,2,3-triazoles.<sup>16</sup> The cycloaddition reaction between organic azides and carbonyl compounds in the presence of an organocatalyst producing *N*-substituted 1,2,3-triazoles has only been recently developed.<sup>17</sup> Other such methods include, *N*-alkylation of *NH*-1,2,3-triazoles formed, in situ, by reacting with alkyl halides, multicomponent reactions and reaction of organic azides with alkenes.<sup>18</sup>

Regitz diazo transfer process is the most commonly employed method for the synthesis of diazo compounds and has gained immense attention in recent decades. The process involves the transfer of a diazo group from an azide to a compound containing active methylene group.<sup>19</sup> Several diazo transfer agents have been used so far, which includes tosyl azide, polymer-supported sulfonyl azides, *p*-acetamidobenzenesulfonyl azide, ionic liquid sulfonyl azides, *p*-dodecylbenzenesulfonyl azide etc.<sup>20</sup> The diazo transfer process is environmentally benign and produces high yield of the desired product.

Different strategies giving access to 1,2,3-triazoles have evolved in the recent decades, which includes, metal-free AAC, metal-catalyzed AAC and azide-free synthesis.<sup>21</sup> Recently, Wan et al. prepared 1,4-disubstituted 1,2,3-triazoles by

transamination of enaminone with an amine catalyzed by ferric chloride, followed by Regitz diazo transfer with tosyl azide in the presence of a base.<sup>22</sup> In another report, Wang et al. exhibited the synthesis of 1,4-disubstituted 1,2,3-triazole disulfides catalyzed by copper iodide and a base, lithium tertiary butoxide.<sup>23</sup> Fazeli and co-workers reported the microwave-assisted multicomponent click reaction of  $\alpha$ -bromoketone with sodium azide and alkyne catalyzed by Cu/Cu(OTf)<sub>2</sub>.<sup>24</sup> Recently, Konwar and co-workers carried out an azide-alkyne cycloaddition catalyzed by an in situ generated copper ascorbate complex, leading to the formation of 1,2,3-triazoles.<sup>25</sup> Chetia et al. reported an efficient synthesis of 1,2,3-triazoles via azide-alkyne click reaction catalyzed by hydrotalcite-supported copper nanoparticles.<sup>26</sup> In a recent report, Dafin and co-workers developed a sulfonyl azide-free protocol for the Regitz diazo transfer reaction.<sup>27</sup> Resende and co-workers recently prepared 1,2,3-triazole derivatives *via* click reaction and screened the products for anticorrosive activity against carbon steel.<sup>28</sup> Tripathi and group prepared triazoles *via* reaction between azides and aldehydes/ketones in the presence of a phase transfer catalyst and a base.<sup>29</sup> In another report, Asemanipoor and co-workers prepared benzimidazole-1,2,3-triazole derivatives by click reaction and evaluated the synthesized compounds for their  $\alpha$ -glucosidase inhibitory property.<sup>30</sup> Pokhodylo et al. prepared triazole derivatives *via* base-catalyzed click reaction of azides with dihydro-2*H*-thiopyran-3(4*H*)-one 1,1-dioxide.<sup>31</sup> 1,3-dipolar cycloaddition reaction between azides and

enaminones leading to the formation of 1,2,3-triazoles was also reported by Nino et al.<sup>32</sup>

Cellulose is one of the organic polymers distributed abundantly in nature.<sup>33</sup> It is a widely studied renewable and biodegradable material and is blessed with properties such as thermal stability, high porosity, large specific surface area, excellent mechanical stability and biocompatibility. This material exhibits extraordinary properties of enhanced metal adsorption and drug loading.<sup>34</sup> The surface of cellulose contains abundant hydroxyl groups which can be modified with functional groups such as  $-\text{SO}_3\text{H}$ ,  $-\text{COOH}$ ,  $-\text{NH}_2$  etc. and this in turn improves the reusability of the material.<sup>35</sup> Cellulose sulfuric acid has emerged as an efficient solid support for acid catalyzed reactions. Kuarm et al. prepared cellulose sulfuric acid and used it for the synthesis of 1-oxo-hexahydroxanthene.<sup>36</sup> In another report, Shaabani and co-workers presented the efficient synthesis of quinolones via cellulose sulfuric acid.<sup>37</sup> Madhav and co-workers employed cellulose sulfuric acid for the synthesis of aryl-14*H*-dibenzo[*a,j*]xanthenes.<sup>38</sup> Sadeghi et al. prepared cellulose sulfuric acid and used it for the efficient synthesis of pyrano[2,3-*d*]pyrimidines.<sup>39</sup> Another report by Nasser and co-workers revealed the preparation of cellulose sulfuric acid and its application as solid acid catalyst for the synthesis of pyrazoles.<sup>40</sup> Cellulose-supported copper(0) nanoparticles have been extensively used for the synthesis of 1,2,3-triazoles *via* click chemistry. In a report, Bahsis et al. immobilized copper(II) and copper(I) ions on cellulose and efficiently used it for the synthesis of 1,4-disubstituted-1,2,3-triazoles

in aqueous medium.<sup>41</sup> Chavan and co-workers prepared cellulose-supported copper iodide heterogeneous catalyst and used it for the one-pot multicomponent reaction leading to the synthesis of spirochromenocarbazole tethered 1,2,3-triazoles.<sup>42</sup> Sarkar and co-workers prepared surface modified cellulose-supported copper(II) complex and applied it for the synthesis of triazoles via click reaction.<sup>43</sup> In another report, Yu et al. synthesized triazole derivatives via cellulose-supported copper(0) catalyst.<sup>44</sup> Although the existing methods are efficient and provide good yield of the product, but most of these processes are associated with certain disadvantages such as the requirement of a base, high temperature and prolonged reaction time. Also, none of these catalytic processes have so far been used for both the click and azide transfer click reaction together. Herein, we report the preparation of cellulose-sulfuric acid encapsulated copper(0) nanoparticles and its application in both click and diazo transfer click reaction for the synthesis of highly substituted 1,2,3-triazoles.

## **4.2 Results and discussion**

### **4.2.1 Preparation and characterization of cellulose-supported copper (Cell-Cu(0)) nanoparticles**

Cellulose-supported copper (Cell-Cu(0)) nanoparticles were prepared in two steps following a method already described in the literature.<sup>45</sup> Initially, after the preparation of Cell-Cu(0) NPs, the crystalline structure of the prepared nanoparticles was characterized by the powder XRD analysis (Figure 2). The diffraction peaks

observed at  $2\theta = 15.3^\circ$ ,  $22.6^\circ$  and  $34.5^\circ$  can be assigned to the (101), (002) and (040) planes of nanocellulose.<sup>46</sup> The appearance of diffraction peaks at  $2\theta$  values of  $43.2^\circ$ ,  $50.4^\circ$  and  $74.0^\circ$  corresponding to the planes (111), (200) and (220) reveals the formation of face centred cubic (FCC) copper nanoparticles on the surface of cellulose [JCPDS card no. 00-001-1241 and 85-1326]. The formation of any other secondary or amorphous phase was not observed. The average crystallite size has been calculated from XRD data based on Scherrer equation and was found to be in the range of 14.5 nm.

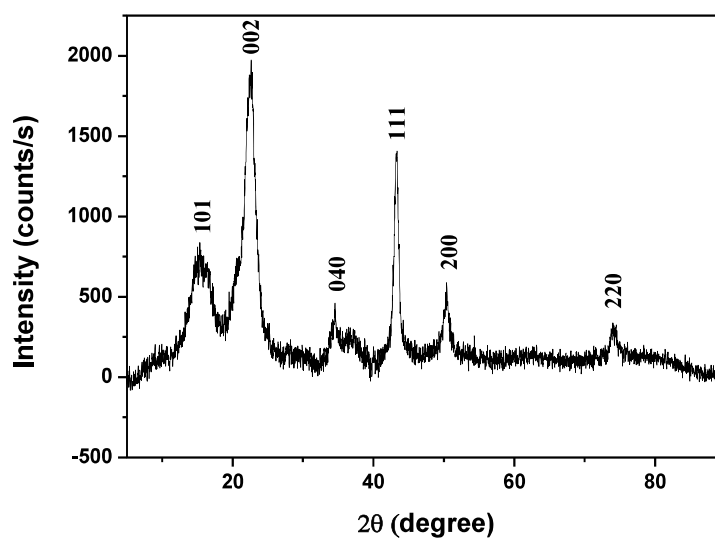


**Figure 2.** Powder XRD pattern of Cell-Cu(0)

The mode of bonding and functional groups present in Cell-Cu(0) were analyzed through FT-IR spectroscopy in the range of  $4000\text{-}400\text{ cm}^{-1}$  (Figure 3). The

absorption bands observed in the regions of 3346, 2900 and 1430  $\text{cm}^{-1}$  could be attributed to the  $-\text{OH}$  stretching,  $-\text{CH}$  stretching,  $\text{H}-\text{C}-\text{H}$  and  $\text{O}-\text{C}-\text{H}$  bending vibrations of cellulose, respectively.<sup>46</sup> The peak positioned at 1638  $\text{cm}^{-1}$  could be assigned to  $\text{H}-\text{O}-\text{H}$  bending vibration of the adsorbed water molecules.

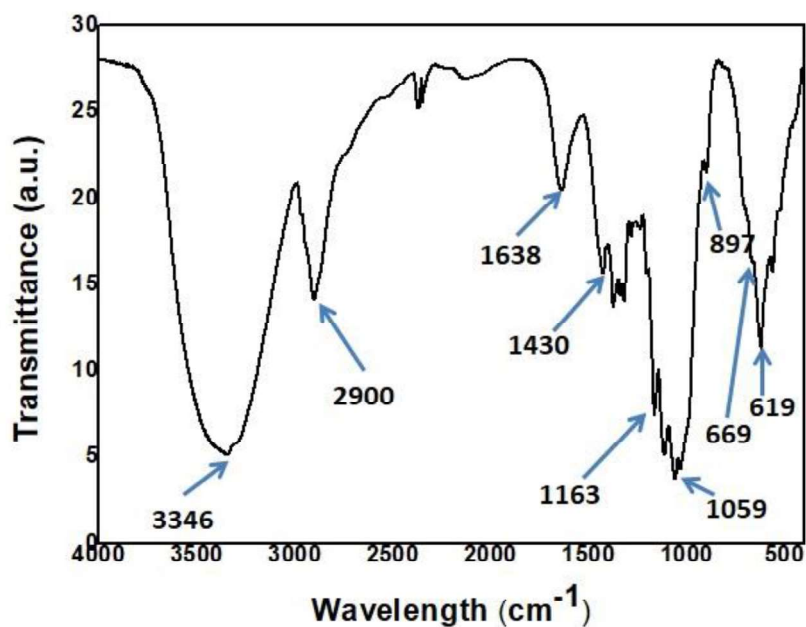


**Figure 3.** FT-IR spectra of Cell-Cu(0)

The absorption bands observed in the regions of 1163, 1059 and 897  $\text{cm}^{-1}$  could be attributed to the  $\text{C}-\text{O}$  stretching,  $\text{C}-\text{C}$  skeletal vibrations and  $\text{C}_1-\text{H}$  ring stretching of glucose unit of cellulose.<sup>47</sup> The peaks at 1163 and 1059  $\text{cm}^{-1}$  for the  $\text{O}=\text{S}=\text{O}$  group could be attributed to the asymmetric and symmetric stretching which merged with the  $\text{C}-\text{O}$  stretching and  $\text{C}-\text{C}$  skeletal vibrations of cellulose. The peak positioned at around 669  $\text{cm}^{-1}$  could be assigned to the  $\text{S}-\text{O}$  stretching vibrations and the band at

619  $\text{cm}^{-1}$  demonstrates the encapsulation of copper nanoparticles by the support (Figure 3).<sup>47,48</sup>

The particle distribution and microstructure of the synthesized Cell-Cu(0) was characterized by TEM and HRTEM analysis. The low resolution TEM image showed the homogeneous distribution of the nanoparticles on the surface of the support and the particle size distribution was found to be in the range of 8-13 nm with number-average diameter of 11.3 nm (standard deviation (SD) = 1.10) (Figure 4a,4b). The calculation of surface-weighted diameter ( $D_s = 11.47$  nm) and volume-weighted diameter ( $D_v = 11.56$  nm) revealed narrow-size distribution of the prepared nanoparticles as shown by the standard deviation value.

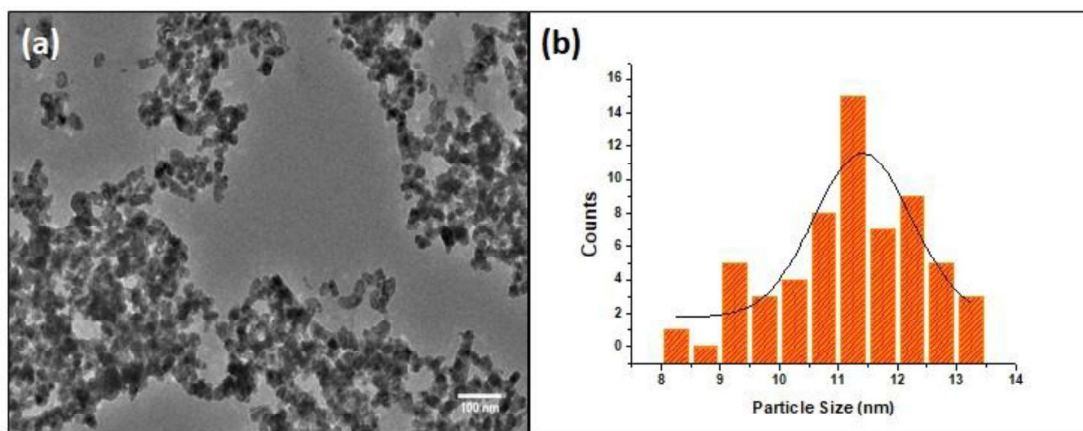


**Figure 4.** (a) TEM image of Cell-Cu(0) and (b) Particle size distribution histogram of Cell-Cu(0)

The selected area electron diffraction (SAED) pattern further confirmed the crystalline nature of the sample as indicated by the (111) crystalline plane (Figure

5a). The HRTEM image indicates the formation of highly crystalline nanoparticles with inter-planar lattice-fringe spacing of 0.25 nm which corresponds to the (111) plane of face centred cubic (FCC) copper nanoparticles (Figure 5b).

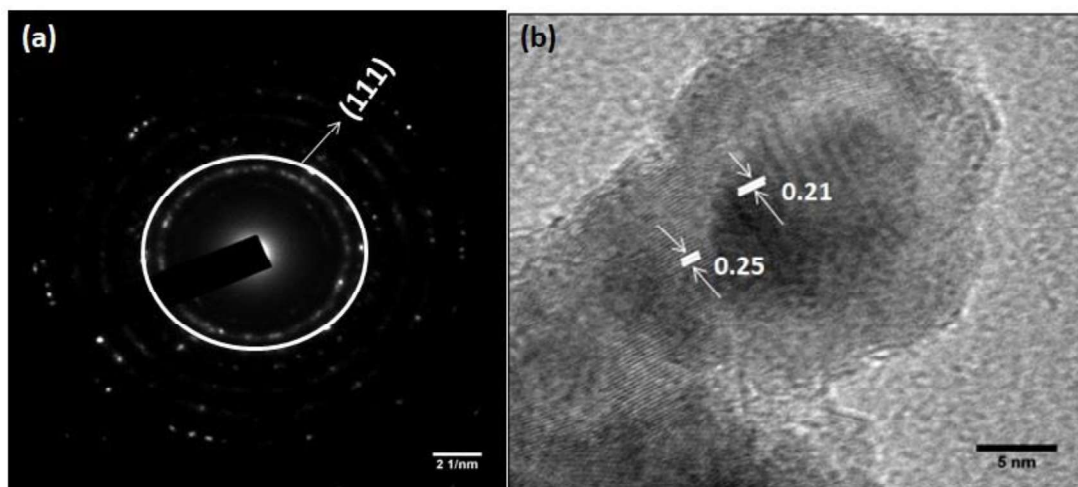


**Figure 5.** (a) SAED pattern of Cell-Cu(0) and (b) HRTEM image with fringe spacing of Cell-Cu(0)

The specific surface area of the synthesized Cell-Cu(0) NPs has been determined by the nitrogen gas adsorption study in the Brunauer-Emmett-Teller (BET) analyser (Table 1). An increase in the BET surface area and pore volume was observed after impregnation of metal nanoparticles as compared to that of the support and this may be attributed to the suppression of packing of lamellar structures in Cell-Cu(0) NPs.<sup>49</sup> An increase in the pore radius was also observed in Cell-Cu(0) NPs might be due to rupture of some of the pore walls during the synthesis process.<sup>50</sup>



**Table 1.** Comparison of surface area, pore radius and pore volume of support and freshly prepared catalyst

Sample	BET Surface Area (m <sup>2</sup> /g)	Pore Radius (nm)	Pore Volume (cm <sup>3</sup> /g)
Cellulose sulfuric acid support	8.599	1.75	0.03
Fresh Cell-Cu(0)	20.765	1.76	0.06

#### 4.2.2 Catalytic activity of the prepared Cell-Cu(0) nanoparticles towards the azide-alkyne click reaction

In our initial effort, the study commenced with a reaction between an azide and an alkyne catalysed by Cell-Cu(0) NPs leading to the formation of 1,2,3-triazole. *p*-Toluenesulfonylazide (**5a**) and phenylacetylene (**6a**) were chosen as model substrates and were subjected to optimisation studies with respect to variation of solvents, temperature, reaction time and catalyst loading (Table 2). Initially when the reaction was carried out at room temperature in H<sub>2</sub>O solvent, the formation of 1,2,3-triazole product was observed with 80% yield (Table 2, entry 1). Study was carried out by running the reaction with different solvents and acetonitrile was proved to be the most effective solvent with 91% yield (Table 2, entry 5). However, the formation of the product was not observed when DCM, DMF and toluene were used as the

solvent (Table 2, entries 2-4). Further study was also performed with variation of reaction time and catalyst loading (Table 2, entries 7-12). When the reaction was allowed to proceed in the absence of the catalyst, no product formation could be observed (Table 2, entry 13). The role of the catalyst was further confirmed by performing the reaction in the presence of only cellulose sulfuric acid,  $\text{CuSO}_4$  and  $\text{Cu}(\text{OAc})_2$  separately, when any product formation was not observed (Table 2, entries 14-16).

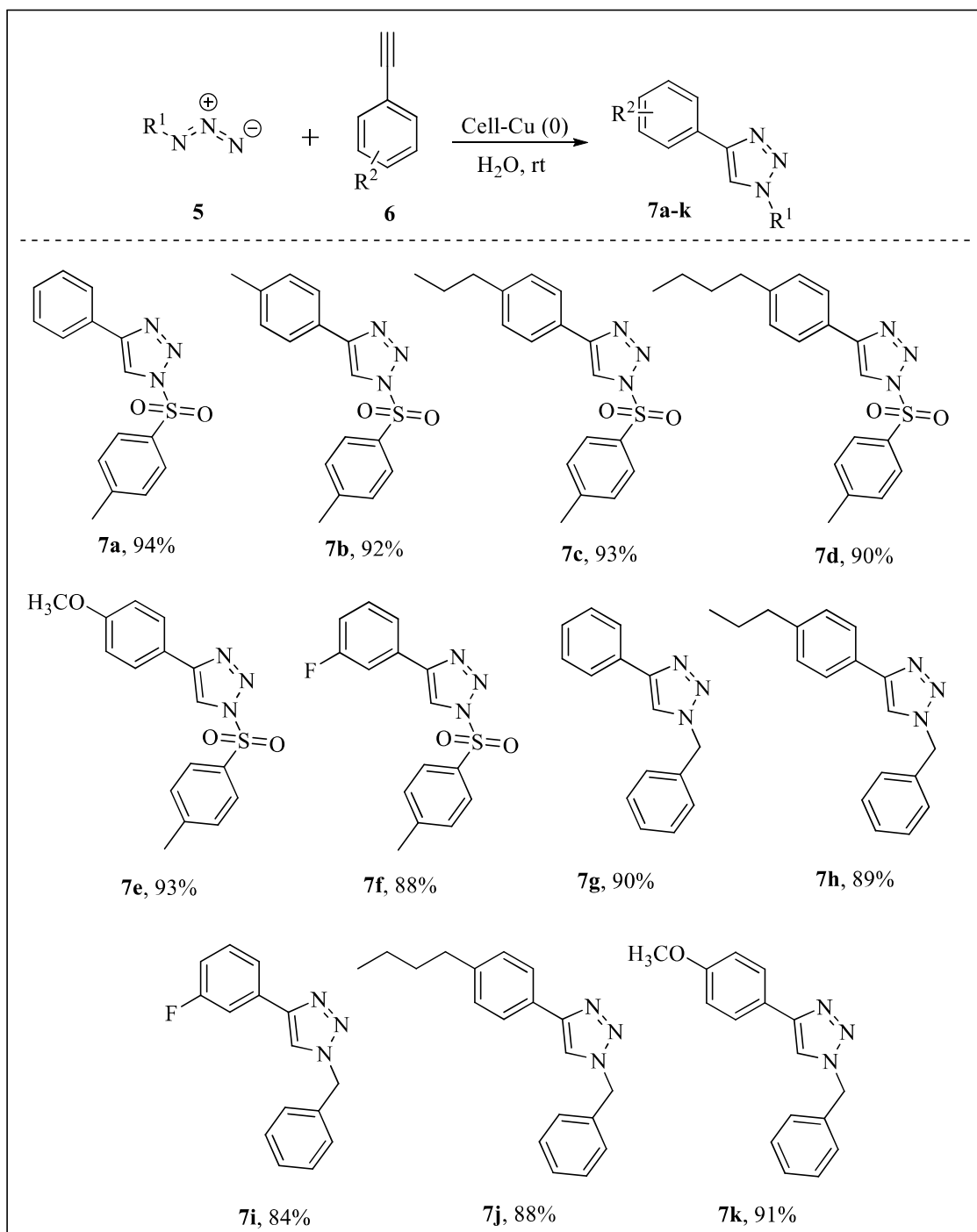
**Table 2.** Synthesis of 1,2,3-triazole and optimization of the reaction condition<sup>a</sup>

Entry	Catalyst	Solvent	Catalyst loading (wt%)	Time (h)	Yield (%) <sup>b</sup>
1	Cell-Cu(0)	H <sub>2</sub> O	20	3	80
2	Cell-Cu(0)	DCM	20	6	0
3	Cell-Cu(0)	DMF	20	6	0
4	Cell-Cu(0)	toluene	20	6	0
5	Cell-Cu(0)	CH <sub>3</sub> CN	20	2	91
6	Cell-Cu(0)	CH <sub>3</sub> CN	20	1	90
7	Cell-Cu(0)	CH <sub>3</sub> CN	15	1	90
8	Cell-Cu(0)	CH <sub>3</sub> CN	10	4	94
<b>9</b>	<b>Cell-Cu(0)</b>	<b>CH<sub>3</sub>CN</b>	<b>10</b>	<b>3</b>	<b>94</b>
10	Cell-Cu(0)	CH <sub>3</sub> CN	10	2	89
11	Cell-Cu(0)	CH <sub>3</sub> CN	5	1	86
12	Cell-Cu(0)	CH <sub>3</sub> CN	10	0.5	82

13	No catalyst	CH <sub>3</sub> CN	10	3	0
14	Only cellulose	CH <sub>3</sub> CN	10	3	0
15	CuSO <sub>4</sub>	CH <sub>3</sub> CN	10	3	0
16	Cu(OAc) <sub>2</sub>	CH <sub>3</sub> CN	10	3	0
<p>Bold values indicate the best experimental result. <sup>a</sup>All the reactions were carried out using <i>p</i>-toluenesulfonylazide <b>5a</b> (0.5 mmol) and phenylacetylene <b>6a</b> (0.5 mmol) in 5 mL of solvent in a round-bottomed flask under N<sub>2</sub> atmosphere. <sup>b</sup>Isolated yields.</p>					

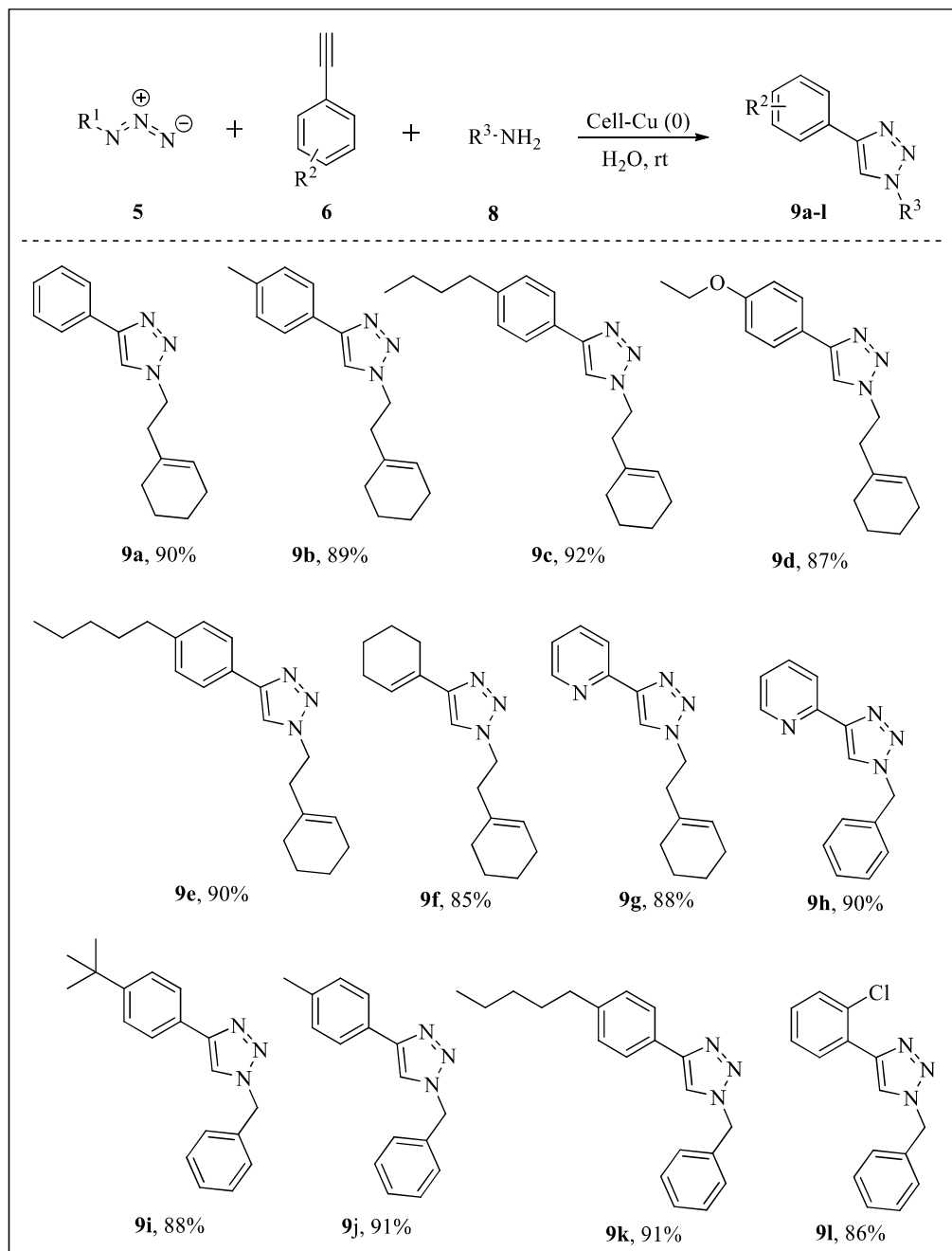
Following the optimization studies, we further explored the substrate scope by reacting *p*-toluenesulfonylazide with different terminal alkynes (Table 3). It was observed that terminal alkynes bearing both electron withdrawing and donating groups gave good yield of the corresponding 1,2,3-triazoles under the given set of reaction conditions **7(b-f)**. Other azides such as benzyl azide were also treated with terminal alkynes to give the corresponding triazoles **7(g-k)** with good yield. When benzyl azide was treated with trimethyl(phenylethynyl)silane under the given reaction conditions, 1-benzyl-4-phenyl-1*H*-1,2,3-triazole **7g** was produced *via* desilylation of alkyne. Any other disubstituted alkyne did not take part in the reaction.

Table 3. Synthesis of 1,2,3-triazoles by copper catalyzed azide-alkyne reaction

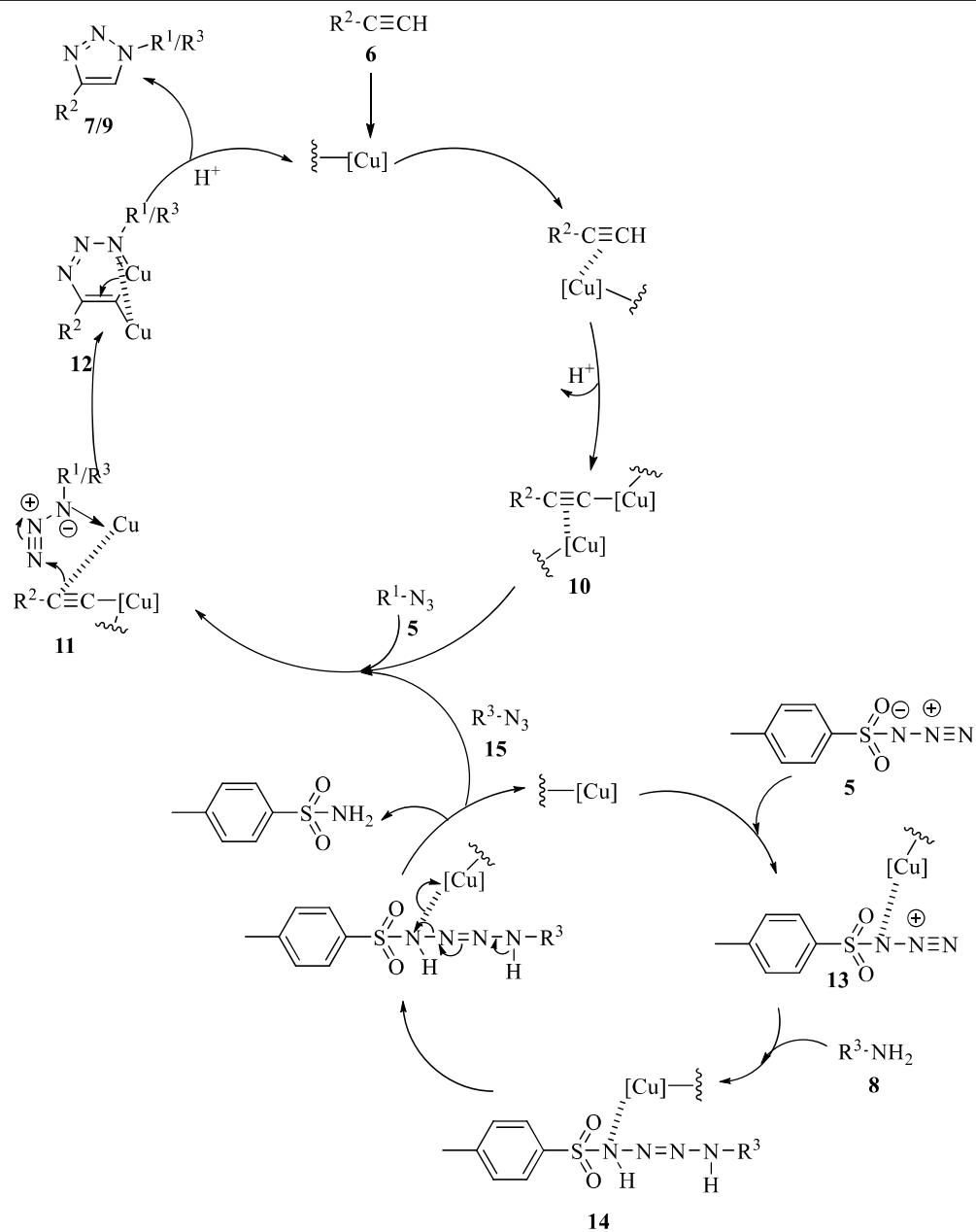


All the compounds were characterized with the help of  $^1\text{H}$  NMR and  $^{13}\text{C}$  NMR. The molecular formula was confirmed from HRMS data and the melting point data of the reported compounds were matched with the literature.

After the success in the click reaction, our study was further stretched towards a variation of the click reaction using diazo transfer process of a primary amine. It was observed that when *p*-toluenesulfonylazide was reacted with a terminal alkyne and a primary amine under the earlier mentioned reaction condition in the presence of the catalyst, diazo-transfer-click reaction occurred leading to the formation of 1-substituted triazoles **9(a-l)** (Table 4). When 2-(cyclohex-1-en-1-yl)ethan-1-amine and benzylamine was treated with tosyl azide and terminal alkynes, the corresponding *N*-substituted 1,2,3-triazoles **9(a-g)** and **9(h-l)** were obtained. Alkynes like 1-ethynylcyclohex-1-ene and 2-ethynylpyridine also produced the desired products **9(f-h)** in good yield. All the prepared compounds were duly characterized with the help of NMR and Mass spectral data.

**Table 4.** Synthesis of *N*-substituted 1,2,3-triazoles by copper catalyzed diazo transfer click reaction

Based on the earlier literature reports, a plausible mechanism has been discussed for both the reaction (Scheme 1).<sup>51</sup> Initially, the alkyne **6** forms a dinuclear copper acetylide **10**. The acetylide is then attacked by an azide **5** forming an intermediate **11**. The carbon atom in acetylide intermediate then attacks the azide nitrogen leading to the formation of intermediate **12**. Finally, ring contraction of intermediate **12** followed by protonation releases the desired product 1,2,3-triazole **7**. During the azide transfer click protocol, copper complexes with *p*-toluenesulfonylazide **5** and forms an intermediate **13**. The primary amine **8** then attacks the azide nitrogen in intermediate **13**, forming a tetrazine intermediate **14**. This intermediate then undergoes bond rearrangement to give the corresponding azide **15** *via* a diazo transfer route. The azide formed, then further undergoes reaction with dinuclear copper acetylide **10** and forms the desired product **9**.



**Scheme 1.** A plausible mechanism for both the click reaction and diazo transfer click reaction



### 4.2.3 Study of catalyst recyclability

The study of recyclability of a heterogeneous catalyst is an important aspect to be considered. In this case, initially the catalyst was recovered simply by filtration, followed by washing with distilled water, and drying under vacuum. The recovered catalyst was then used for the next reaction. It was observed that the same catalyst could be reused up to six times with minimum loss of activity (Figure 6). The physical characteristics of the recovered catalyst after 6<sup>th</sup> cycle were also studied by TEM and BET. The TEM image of the recovered catalyst did not show any significant change in the morphology (Figure 7).

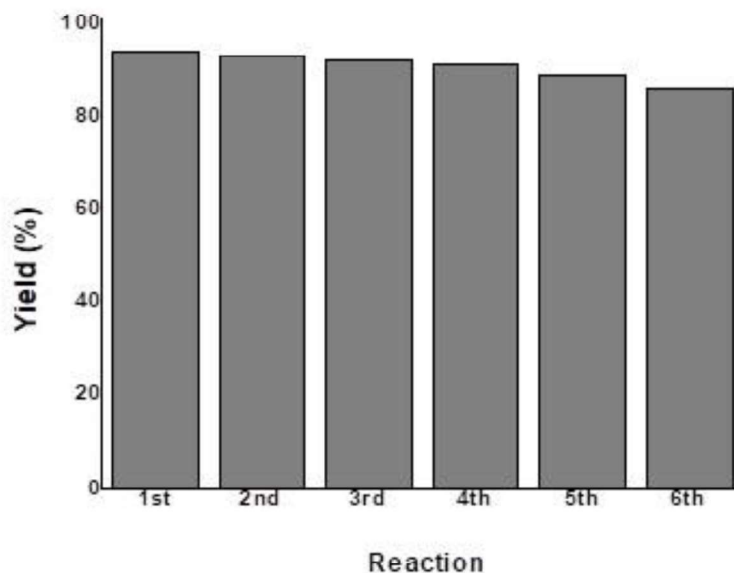


**Figure 6.** Study of recyclability of the catalyst

The BET surface area of the recovered catalyst was found to be 7.906 which are somehow lower as compared to the fresh one. This may be attributed to the blocking of the pores by different organic/inorganic by-products/impurities formed during the reaction. A pore radius of 1.76 nm and pore volume of 0.05 cm<sup>3</sup>/g was observed for the recovered catalyst which was quite similar to that of the fresh one. These observations prove that the catalyst did not undergo any change during the reaction.

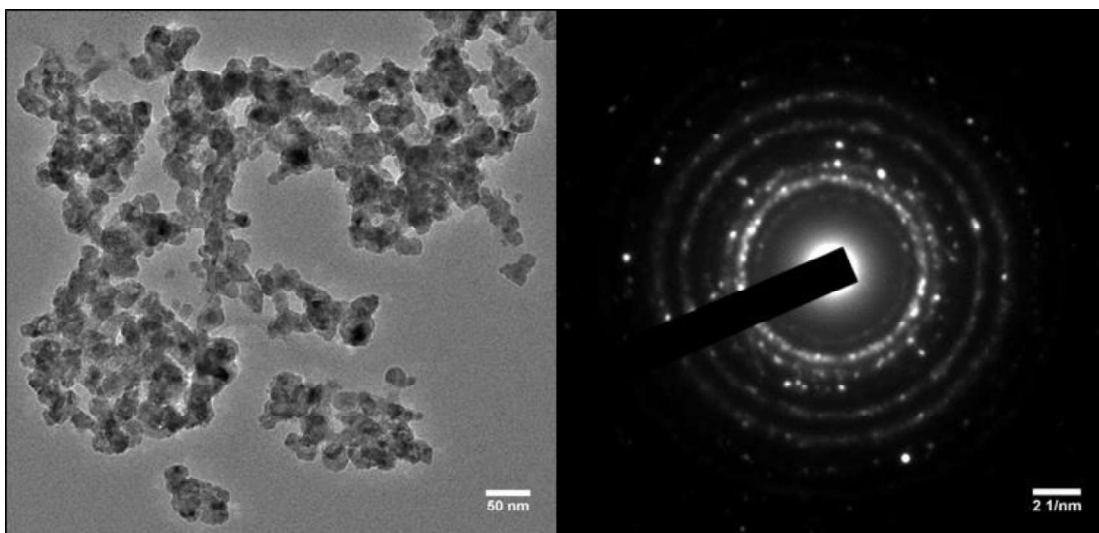


**Figure 7.** HRTEM and SAED images of the recovered catalyst

---

### 4.3 Conclusion

In summary, we have developed a mild cellulose sulfuric acid supported copper catalyst and characterized its physical and chemical properties by different analytical techniques such as HRTEM, FT-IR and BET. The applicability of the prepared catalyst was then studied through azide-alkyne click reaction leading to the formation of 1,2,3-triazoles. A similar reaction was also carried out by reacting an azide and an alkyne with a primary amine *via* a diazo transfer click pathway. Twelve different 1,2,3-triazoles with varied substituents were obtained through azide-alkyne click strategy. Twelve different *N*-substituted 1,2,3-triazoles have also been prepared *via* diazo transfer pathway. The recyclability of the catalyst has also been studied upto six consecutive cycles.

### 4.4 Experimental

#### 4.4.1 Preparation of cellulose-supported copper (Cell-Cu(0)) nanoparticles

##### 4.4.1.1 Preparation of cellulose sulfuric acid

Cellulose-supported copper (Cell-Cu(0)) catalyst was prepared in two steps. In the first step, cellulose sulfuric acid was prepared by using a method described in the literature employing cellulose and chlorosulfonic acid.<sup>45</sup> To a magnetically stirred solution of 5.00 g of cellulose dispersed in 30 mL of chloroform at 0 °C, 1.00 g of chlorosulfonic acid (9 mmol) was added dropwise. After the addition of chlorosulfonic acid was completed, the mixture was allowed to stir for another 2 h

when all the HCl gas was removed from the vessel. The mixture was then filtered, washed with 30 mL CHCl<sub>3</sub> and dried under vacuum to get a white powder of cellulose sulfuric acid.

#### **4.4.1.2 Preparation of cellulose-supported copper(0) nanoparticles (Cell-Cu(0) NPs)**

In the second step, 4.00 g (11.6 mmol) of cellulose sulfuric acid was homogeneously dispersed in 60 mL of distilled water. Copper(II) acetate monohydrate (6.2 mmol, 1.25 g) was dissolved in 40 mL of distilled water and added dropwise to the cellulose sulfuric acid solution under N<sub>2</sub> atmosphere. The mixture was allowed to stir for 1h and then NaBH<sub>4</sub> (50 mg) was added portionwise to the mixture at 0 °C when a black precipitate of nanoparticles was obtained. The mixture was further stirred for another 2 h. The solution was then filtered and the precipitate was washed with distilled water and dried under vacuum.

#### **4.4.2 General procedure for the synthesis of 1,2,3-triazoles *via* azide-alkyne click reaction**

To a solution of *p*-toluenesulfonylazide (0.5 mmol, 100 mg) and phenylacetylene (0.5 mmol, 52 mg) in acetonitrile (5 mL), Cell-Cu(0) (10 wt%, 10 mg) was added and the mixture was allowed to stir at room temperature under N<sub>2</sub> atmosphere. The progress of the reaction was monitored by using thin layer chromatography (TLC). After the completion of the reaction, the catalyst was

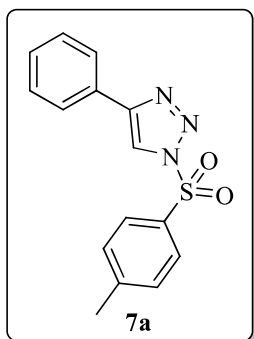
recovered by filtration and washed with acetonitrile. Combined acetonitrile was then removed under reduced pressure and the organics were extracted with ethyl acetate (2 x 30 mL). The combined organic extracts were washed with water (2 x 30 mL) and brine (10 mL). Drying over  $\text{Na}_2\text{SO}_4$  and removal of the solvent under reduced pressure provided the crude mixture which was then purified by column chromatography by using ethyl acetate/hexane (10%-30% ethyl acetate in hexane) as eluent. For further recyclability experiments, the recovered catalyst was dried under vacuum and then reused.

#### **4.4.3 General procedure for the synthesis of 1,2,3-triazoles *via* diazo transfer click reaction**

To a solution of *p*-toluenesulfonylazide (0.5 mmol, 100 mg), phenylacetylene (0.5 mmol, 52 mg) and 2-(1-cyclohexenyl)ethylamine (0.5 mmol, 63 mg) in acetonitrile (5 mL) under  $\text{N}_2$  atmosphere, Cell-Cu(0) (10 wt%, 10 mg) was added and the mixture was allowed to stir at room temperature. The progress of the reaction was monitored by using thin layer chromatography (TLC). After the completion of the reaction, the catalyst was recovered by filtration and washed with acetonitrile. Combined acetonitrile was then removed under reduced pressure and the remaining organics were extracted with ethyl acetate (2 x 30 mL) followed by washing with water (2 x 30 mL) and brine (10 mL). Drying over  $\text{Na}_2\text{SO}_4$  and removal of the solvent under reduced pressure, produced the crude mixture which was purified by column chromatography by using ethyl acetate/hexane (10%-30% ethyl acetate in

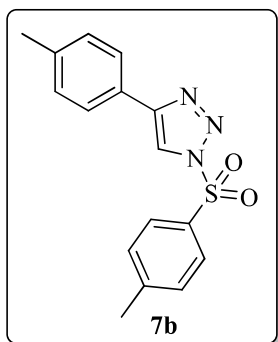
hexane) as eluent. For further study of recyclability experiments, the recovered catalyst was dried under vacuum before the next run.

#### 4.5 Characterization data of the synthesized compounds



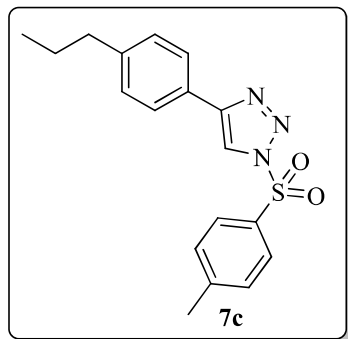
#### 4-Phenyl-1-tosyl-1H-1,2,3-triazole (7a)

White solid; Mp: 106-107 °C (Lit.<sup>52a</sup> 107-108 °C); Yield: 94%; <sup>1</sup>H NMR (500 MHz, CDCl<sub>3</sub>): δ 8.31 (s, 1H), 8.03 (d, 2H, *J* = 8.5 Hz), 7.82 (d, 2H, *J* = 8.5 Hz), 7.46 – 7.36 (m, 5 H), 2.45 (s, 3H); <sup>13</sup>C NMR (125 MHz, CDCl<sub>3</sub>): δ 147.2 (C), 132.9 (C), 130.1 (CH), 129.0 (CH), 128.9 (CH), 128.7 (C), 128.6 (CH), 125.9 (CH), 118.8 (CH), 21.7 (CH<sub>3</sub>); HRMS (ESI) *m/z* 300.0806 ([M+H]<sup>+</sup> C<sub>15</sub>H<sub>14</sub>N<sub>3</sub>O<sub>2</sub>S, requires 300.0807).

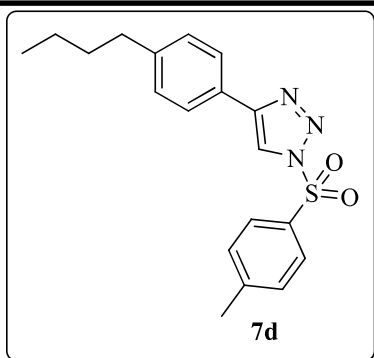


**4-(*p*-Tolyl)-1-tosyl-1*H*-1,2,3-triazole (7b)**

Yellow solid; Mp: 153-154 °C (Lit.<sup>52b</sup> 158-159 °C); Yield: 92%; <sup>1</sup>H NMR (500 MHz, CDCl<sub>3</sub>): δ 8.20 (s, 1H), 7.95 (d, 2H, *J* = 8.5 Hz), 7.64 (d, 2H, *J* = 8.5 Hz), 7.32 (d, 2H, *J* = 8.5 Hz), 7.16 (d, 2H, *J* = 8.5 Hz), 2.38 (s, 3H), 2.31 (s, 3H); <sup>13</sup>C NMR (125 MHz, CDCl<sub>3</sub>): δ 147.4 (C), 147.2 (C), 139.0 (C), 133.0 (C), 130.3 (CH), 129.6 (CH), 128.6 (CH), 127.0 (C), 125.9 (CH), 118.4 (CH), 21.7 (CH<sub>3</sub>), 21.2 (CH<sub>3</sub>); HRMS (ESI) *m/z* 314.0958 ([M+H]<sup>+</sup> C<sub>16</sub>H<sub>16</sub>N<sub>3</sub>O<sub>2</sub>S, requires 314.0963).

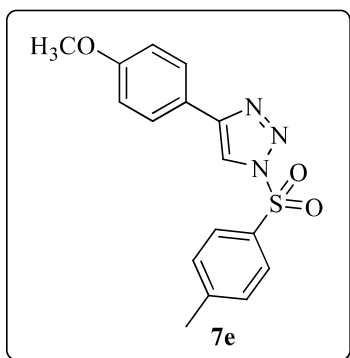
**4-(4-Propylphenyl)-1-tosyl-1*H*-1,2,3-triazole (7c)**

White solid; Mp: 135-137 °C; Yield: 93%; <sup>1</sup>H NMR (500 MHz, CDCl<sub>3</sub>): δ 8.20 (s, 1H), 7.94 (d, 2H, *J* = 8.5 Hz), 7.65 (d, 2H, *J* = 8.5 Hz), 7.30 (d, 2H, *J* = 8.5 Hz), 7.16 (d, 2H, *J* = 8.5 Hz), 2.53 (t, 2H, *J* = 7.5 Hz), 2.36 (s, 3H), 1.60 – 1.54 (m, 2H), 0.86 (t, 3H, *J* = 7.5 Hz); <sup>13</sup>C NMR (125 MHz, CDCl<sub>3</sub>): δ 147.4 (C), 147.2 (C), 143.8 (C), 133.0 (C), 130.3 (CH), 129.0 (CH), 128.5 (CH), 126.1 (C), 125.9 (CH), 118.4 (CH), 37.7 (CH<sub>2</sub>), 24.3 (CH<sub>3</sub>), 21.7 (CH<sub>2</sub>), 13.6 (CH<sub>3</sub>); HRMS (ESI) *m/z* 342.1283 ([M+H]<sup>+</sup> C<sub>18</sub>H<sub>20</sub>N<sub>3</sub>O<sub>2</sub>S, requires 342.1276).



#### 4-(4-Butylphenyl)-1-tosyl-1H-1,2,3-triazole (7d)

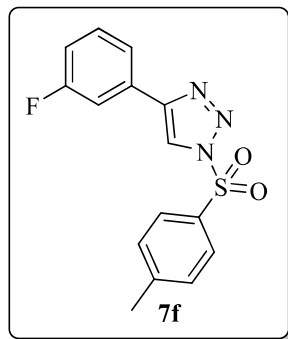
White solid; Mp: 121-124 °C; Yield: 90%;  $^1\text{H}$  NMR (500 MHz,  $\text{CDCl}_3$ ):  $\delta$  8.25 (s, 1H), 8.00 (d, 2H,  $J = 8.5$  Hz), 7.70 (d, 2H,  $J = 8.5$  Hz), 7.36 (d, 2H,  $J = 8.5$  Hz), 7.22 (d, 2H,  $J = 8.5$  Hz), 2.61 (t, 2H,  $J = 7.5$  Hz), 2.42 (s, 3H), 1.60 – 1.57 (m, 4H), 0.90 (t, 3H,  $J = 7.5$  Hz);  $^{13}\text{C}$  NMR (125 MHz,  $\text{CDCl}_3$ ):  $\delta$  147.7 (C), 147.5 (C), 144.4 (C), 133.3 (C), 130.6 (CH), 129.2 (CH), 128.9 (CH), 126.4 (C), 126.2 (CH), 118.7 (CH), 35.6 ( $\text{CH}_2$ ), 33.7 ( $\text{CH}_2$ ), 22.5 ( $\text{CH}_3$ ), 22.1 ( $\text{CH}_2$ ), 14.1 ( $\text{CH}_3$ ); HRMS (ESI)  $m/z$  356.1430 ( $[\text{M}+\text{H}]^+$   $\text{C}_{19}\text{H}_{22}\text{N}_3\text{O}_2\text{S}$ , requires 356.1433).



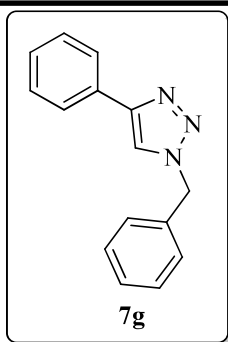


**4-(4-Methoxyphenyl)-1-tosyl-1H-1,2,3-triazole (7e)**

Pale yellow solid; Mp: 131-132 °C (Lit.<sup>52c</sup> 100-101 °C); Yield: 93%; <sup>1</sup>H NMR (500 MHz, CDCl<sub>3</sub>): δ 8.15 (s, 1H), 7.95 (d, 2H, *J* = 8.5 Hz), 7.68 (d, 2H, *J* = 8.5 Hz), 7.32 (d, 2H, *J* = 8.5 Hz), 6.89 (d, 2H, *J* = 8.5 Hz), 3.77 (s, 3H), 2.38 (s, 3H); <sup>13</sup>C NMR (125 MHz, CDCl<sub>3</sub>): δ 160.1 (C), 147.2 (C), 133.0 (C), 130.3 (CH), 128.6 (CH), 127.6 (C), 127.3 (CH), 121.3 (C), 117.8 (CH), 114.3 (CH), 55.2 (CH<sub>3</sub>), 21.7 (CH<sub>3</sub>); HRMS (ESI) *m/z* 330.0916 ([M+H]<sup>+</sup> C<sub>16</sub>H<sub>16</sub>N<sub>3</sub>O<sub>3</sub>S, requires 330.0912).

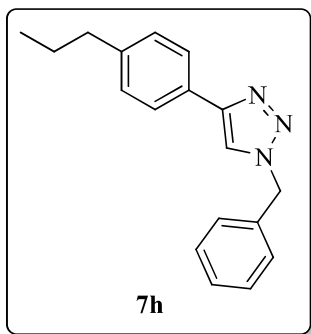
**4-(3-Fluorophenyl)-1-tosyl-1H-1,2,3-triazole (7f)**

Pale yellow solid; Mp: 137-138 °C (Lit.<sup>52b</sup> 140-141 °C); Yield: 88%; <sup>1</sup>H NMR (500 MHz, CDCl<sub>3</sub>): δ 8.26 (s, 1H), 7.96 (d, 2H, *J* = 8.5 Hz), 7.54 – 7.46 (m, 2H), 7.36 – 7.30 (m, 3H), 7.02 – 6.97 (m, 1H), 2.38 (s, 3H); <sup>13</sup>C NMR (125 MHz, CDCl<sub>3</sub>): δ 163.0 (d, C, *J* = 245.0 Hz), 147.4 (CH), 146.1 (C), 132.7 (C), 130.4 (CH), 129.6 (C), 128.7 (CH), 127.0 (C), 121.6 (CH), 119.3 (CH), 115.9 (d, CH, *J* = 21.25 Hz), 113.0 (d, CH, *J* = 22.5 Hz), 21.8 (CH<sub>3</sub>); HRMS (ESI) *m/z* 318.0711 ([M+H]<sup>+</sup> C<sub>15</sub>H<sub>13</sub>FN<sub>3</sub>O<sub>2</sub>S, requires 318.0713).



### 1-Benzyl-4-phenyl-1H-1,2,3-triazole (7g)

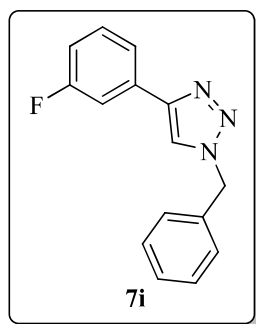
Brown solid; Mp: 119-121 °C (Lit.<sup>52d</sup> 120-122 °C); Yield: 90%; <sup>1</sup>H NMR (500 MHz, CDCl<sub>3</sub>): δ 7.80 – 7.76 (m, 2H), 7.64 (s, 1H), 7.40 – 7.35 (m, 5H), 7.32 – 7.27 (m, 3H), 5.56 (s, 2H); <sup>13</sup>C NMR (125 MHz, CDCl<sub>3</sub>): δ 148.4 (C), 134.8 (C), 130.7 (C), 129.4 (CH), 129.0 (C), 128.4 (CH), 128.3 (CH), 125.9 (CH), 119.7 (CH), 54.4 (CH<sub>2</sub>); HRMS (ESI) *m/z* 236.1194 ([M+H]<sup>+</sup> C<sub>15</sub>H<sub>14</sub>N<sub>3</sub>, requires 236.1188).



### 1-Benzyl-4-(4-propylphenyl)-1H-1,2,3-triazole (7h)

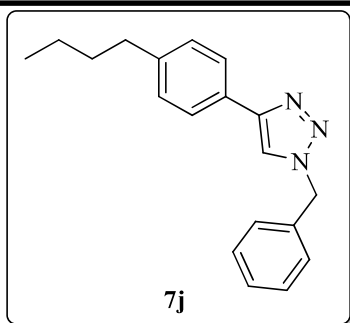
Yellow solid; Mp: 96-97 °C; Yield: 89%; <sup>1</sup>H NMR (500 MHz, CDCl<sub>3</sub>): δ 7.68 (d, 2H, *J* = 8.5 Hz), 7.60 (s, 1H), 7.38 – 7.33 (m, 3H), 7.30 – 7.26 (m, 2H), 7.20 (d, 2H,

$J = 8.5$  Hz), 5.54 (s, 2H), 2.57 (t, 2H,  $J = 7.5$  Hz), 1.66 – 1.59 (m, 2H), 0.92 (t, 3H,  $J = 7.5$  Hz);  $^{13}\text{C}$  NMR (125 MHz,  $\text{CDCl}_3$ ):  $\delta$  148.5 (C), 143.0 (C), 134.9 (C), 129.3 (CH), 129.1 (CH), 128.9 (CH), 128.2 (CH), 128.1 (C), 125.8 (CH), 119.4 (CH), 54.4 (CH<sub>2</sub>), 38.0 (CH<sub>2</sub>), 24.7 (CH<sub>2</sub>), 14.0 (CH<sub>3</sub>); HRMS (ESI)  $m/z$  278.1650 ( $[\text{M}+\text{H}]^+$  C<sub>18</sub>H<sub>20</sub>N<sub>3</sub>, requires 278.1657).

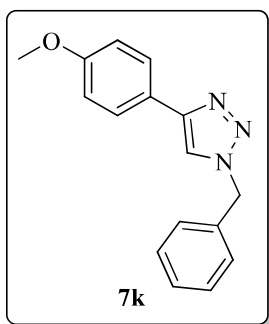


### 1-Benzyl-4-(3-fluorophenyl)-1H-1,2,3-triazole (7i)

Brown solid; Mp: 102-103 °C (Lit.<sup>52e</sup> 109-110 °C); Yield: 84%;  $^1\text{H}$  NMR (500 MHz,  $\text{CDCl}_3$ ):  $\delta$  7.59 (s, 1H), 7.51 – 7.43 (m, 2H), 7.35 – 7.30 (m, 3H), 7.30 – 7.23 (m, 3H), 6.97 – 6.91 (m, 1H), 5.52 (s, 2H);  $^{13}\text{C}$  NMR (125 MHz,  $\text{CDCl}_3$ ):  $\delta$  163.0 (d, C,  $J = 243.75$ ), 147.1 (C), 134.3 (C), 132.5 (C), 130.3 (CH), 129.1 (CH), 128.8 (CH), 128.0 (CH), 121.2 (CH), 119.7 (CH), 114.9 (d, CH,  $J = 21.25$  Hz), 112.5 (d, CH,  $J = 23.75$  Hz), 54.2 (CH<sub>2</sub>); HRMS (ESI)  $m/z$  254.1102 ( $[\text{M}+\text{H}]^+$  C<sub>15</sub>H<sub>13</sub>FN<sub>3</sub>, requires 254.1094).

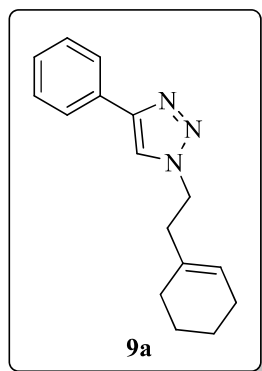
**1-Benzyl-4-(4-butylphenyl)-1H-1,2,3-triazole (7j)**

White solid; Mp: 110-111 °C; Yield: 88%;  $^1\text{H}$  NMR (500 MHz,  $\text{CDCl}_3$ ):  $\delta$  7.70 (d, 2H,  $J = 8.5$  Hz), 7.62 (s, 1H), 7.40 – 7.36 (m, 3H), 7.32 – 7.29 (m, 2H), 7.21 (d, 2H,  $J = 8.5$  Hz), 5.57 (s, 2H), 2.62 (t, 2H,  $J = 7.5$  Hz), 1.64 – 1.57 (m, 2H), 1.38 – 1.32 (m, 2H), 0.92 (t, 3H,  $J = 7.5$  Hz);  $^{13}\text{C}$  NMR (125 MHz,  $\text{CDCl}_3$ ):  $\delta$  148.2 (C), 143.0 (C), 134.6 (C), 129.0 (CH), 128.8 (CH), 128.6 (CH), 127.9 (CH), 127.7 (C), 125.5 (CH), 119.1 (CH); HRMS (ESI)  $m/z$  292.1820 ( $[\text{M}+\text{H}]^+$   $\text{C}_{19}\text{H}_{22}\text{N}_3$ , requires 292.1814).



**1-Benzyl-4-(4-methoxyphenyl)-1*H*-1,2,3-triazole (7k)**

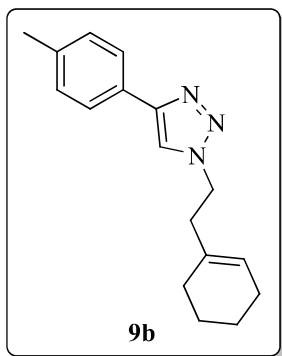
White solid; Mp: 126-127 °C; Yield: 91%; <sup>1</sup>H NMR (500 MHz, CDCl<sub>3</sub>): δ 7.69 – 7.63 (m, 2H), 7.51 (s, 1H), 7.33 – 7.28 (m, 3H), 7.30 – 7.22 (m, 2H), 6.86 (d, 2H, *J* = 9.0 Hz), 5.49 (2H), 3.76 (s, 3H); <sup>13</sup>C NMR (125 MHz, CDCl<sub>3</sub>): δ 159.5 (C), 148.0 (C), 134.6 (C), 129.0 (CH), 128.6 (CH), 127.9 (CH), 126.9 (CH), 123.1 (C), 118.6 (CH), 114.1 (CH), 55.2 (CH<sub>3</sub>), 54.1 (CH<sub>2</sub>); HRMS (ESI) *m/z* 266.1300 ([M+H]<sup>+</sup> C<sub>16</sub>H<sub>16</sub>N<sub>3</sub>O, requires 266.1293).

**1-(2-(Cyclohex-1-en-1-yl)ethyl)-4-phenyl-1*H*-1,2,3-triazole (9a)**

White solid; Mp: 83-84 °C; Yield: 90%; <sup>1</sup>H NMR (500 MHz, CDCl<sub>3</sub>): δ 7.84 (d, 2H, *J* = 8.5 Hz), 7.74 (s, 1H), 7.46 – 7.41 (m, 2H), 7.37 – 7.33 (m, 1H), 5.45 (s, 1H), 4.51 – 4.46 (m, 2H), 2.56 (t, 2H, *J* = 7.0 Hz), 2.0 – 1.97 (m, 4H), 1.67 – 1.64 (m, 2H), 1.58 – 1.54 (m, 2H); <sup>13</sup>C NMR (125 MHz, CDCl<sub>3</sub>): δ 147.7 (C), 133.1 (C), 130.9 (C), 129.0 (CH), 128.2 (CH), 125.8 (CH), 125.0 (CH), 119.7 (CH), 49.1 (CH<sub>2</sub>), 38.9

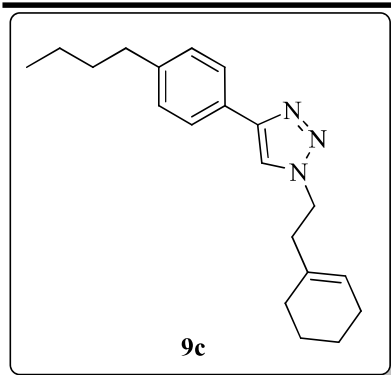
(CH<sub>2</sub>), 28.2 (CH<sub>2</sub>), 25.3 (CH<sub>2</sub>), 22.9 (CH<sub>2</sub>), 22.3 (CH<sub>2</sub>); HRMS (ESI) *m/z* 254.1655

([M+H]<sup>+</sup> C<sub>16</sub>H<sub>20</sub>N<sub>3</sub>, requires 254.1657).

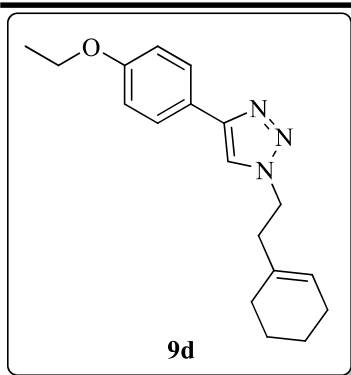


#### 1-(2-(Cyclohex-1-en-1-yl)ethyl)-4-(*p*-tolyl)-1*H*-1,2,3-triazole (9b)

Brown solid; Mp: 101-102 °C; Yield: 89%; <sup>1</sup>H NMR (500 MHz, CDCl<sub>3</sub>): δ 7.64 (d, 2H, *J* = 8.5 Hz), 7.61 (s, 1H), 7.16 (d, 2H, *J* = 8.5 Hz), 5.36 (s, 1H), 4.39 (t, 2H, *J* = 7.5 Hz), 2.47 (t, 2H, *J* = 7.5 Hz), 2.31 (s, 3H), 1.91 – 1.86 (m, 4H), 1.59 – 1.55 (m, 2H), 1.49 – 1.45 (m, 2H); <sup>13</sup>C NMR (125 MHz, CDCl<sub>3</sub>): δ 147.1 (C), 138.1 (C), 133.1 (C), 129.7 (CH), 128.1 (C), 125.8 (CH), 125.0 (CH), 119.4 (CH), 49.1 (CH<sub>2</sub>), 38.9 (CH<sub>2</sub>), 28.3 (CH<sub>2</sub>), 25.4 (CH<sub>2</sub>), 22.9 (CH<sub>2</sub>), 22.3 (CH<sub>2</sub>), 21.5 (CH<sub>3</sub>); HRMS (ESI) *m/z* 268.1815 ([M+H]<sup>+</sup> C<sub>17</sub>H<sub>22</sub>N<sub>3</sub>, requires 268.1814).

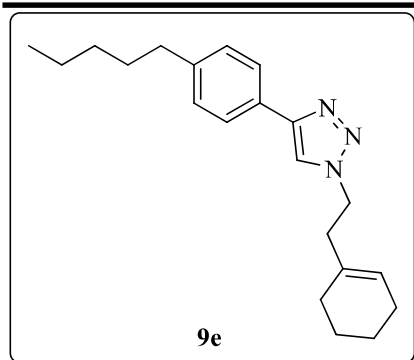
**4-(4-Butylphenyl)-1-(2-(cyclohex-1-en-1-yl)ethyl)-1H-1,2,3-triazole (9c)**

White solid; Mp: 77-78 °C; Yield: 92%; <sup>1</sup>H NMR (500 MHz, CDCl<sub>3</sub>): δ 7.70 (d, 2H, *J* = 8.0 Hz), 7.65 (s, 1H), 7.21 (d, 2H, *J* = 8.0 Hz), 5.40 (s, 1H), 4.44 (t, 2H, *J* = 7.5 Hz), 2.61 (t, 2H, *J* = 7.5 Hz), 2.52 (t, 2H, *J* = 7.5 Hz), 1.95 – 1.91 (m, 4H), 1.63 – 1.57 (m, 4H), 1.54 – 1.49 (m, 2H), 1.38 – 1.31 (m, 2H), 0.91 (t, 3H, *J* = 7.5 Hz); <sup>13</sup>C NMR (125 MHz, CDCl<sub>3</sub>): δ 147.8 (C), 143.1 (C), 133.1 (C), 129.1 (CH), 128.3 (C), 125.8 (CH), 125.0 (CH), 119.4 (CH), 49.1 (CH<sub>2</sub>), 38.9 (CH<sub>2</sub>), 35.6 (CH<sub>2</sub>), 33.8 (CH<sub>2</sub>), 28.2 (CH<sub>2</sub>), 25.4 (CH<sub>2</sub>), 22.9 (CH<sub>2</sub>), 22.5 (CH<sub>2</sub>), 22.3 (CH<sub>2</sub>), 14.2 (CH<sub>3</sub>); HRMS (ESI) *m/z* 310.2289 ([M+H]<sup>+</sup> C<sub>20</sub>H<sub>28</sub>N<sub>3</sub>, requires 310.2283).

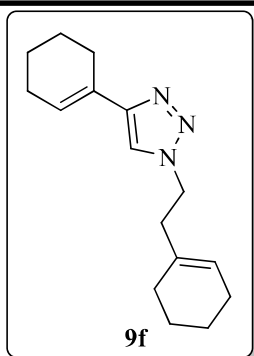
**1-(2-(Cyclohex-1-en-1-yl)ethyl)-4-(4-ethoxyphenyl)-1H-1,2,3-triazole (9d)**

Pale yellow solid; Mp: 90-91 °C; Yield: 87%;  $^1\text{H}$  NMR (500 MHz,  $\text{CDCl}_3$ ):  $\delta$  7.70 (d, 2H,  $J = 8.5$  Hz), 7.60 (s, 1H), 6.92 (d, 2H,  $J = 8.5$  Hz), 5.41 (s, 1H), 4.43 (t, 2H,  $J = 7.0$  Hz), 4.04 (q, 2H,  $J = 7.0$  Hz), 2.52 (t, 2H,  $J = 7.0$  Hz), 1.96 – 1.92 (m, 4H), 1.64 – 1.59 (m, 2H), 1.54 – 1.50 (m, 2H), 1.41 (t, 3H,  $J = 7.0$  Hz);  $^{13}\text{C}$  NMR (125 MHz,  $\text{CDCl}_3$ ):  $\delta$  159.1 (C), 147.7 (C), 133.1 (C), 127.1 (CH), 125.0 (CH), 123.5 (C), 118.9 (CH), 114.9 (CH), 63.7 ( $\text{CH}_2$ ), 49.1 ( $\text{CH}_2$ ), 38.9 ( $\text{CH}_2$ ), 28.3 ( $\text{CH}_2$ ), 25.4 ( $\text{CH}_2$ ), 22.9 ( $\text{CH}_2$ ), 22.3 ( $\text{CH}_2$ ), 15.0 ( $\text{CH}_3$ ); HRMS (ESI)  $m/z$  298.1927 ( $[\text{M}+\text{H}]^+$   $\text{C}_{18}\text{H}_{24}\text{N}_3\text{O}$ , requires 298.1919).



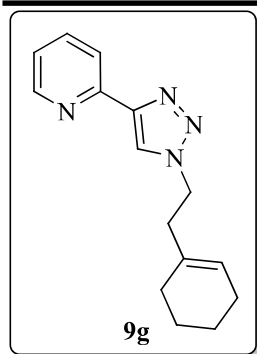
**1-(2-(Cyclohex-1-en-1-yl)ethyl)-4-(4-pentylphenyl)-1H-1,2,3-triazole (9e)**

Yellow solid; Mp: 80-82 °C; Yield: 90%;  $^1\text{H}$  NMR (500 MHz,  $\text{CDCl}_3$ ):  $\delta$  7.70 (d, 2H,  $J = 8.0$  Hz), 7.65 (s, 1H), 7.21 (d, 2H,  $J = 8.0$  Hz), 5.40 (s, 1H), 4.436 (t, 2H,  $J = 7.5$  Hz), 2.59 (t, 2H,  $J = 7.5$  Hz), 2.52 (t, 2H,  $J = 7.5$  Hz), 1.95 – 1.92 (m, 4H), 1.64 – 1.58 (m, 4H), 1.55 – 1.50 (m, 2H), 1.33 – 1.29 (m, 4H), 0.87 (t, 3H,  $J = 7.5$  Hz);  $^{13}\text{C}$  NMR (125 MHz,  $\text{CDCl}_3$ ):  $\delta$  147.9 (C), 143.2 (C), 133.1 (C), 129.1 (CH), 128.3 (C), 125.8 (CH), 125.0 (CH), 119.4 (CH), 49.1 ( $\text{CH}_2$ ), 38.9 ( $\text{CH}_2$ ), 35.9 ( $\text{CH}_2$ ), 31.7 ( $\text{CH}_2$ ), 31.3 ( $\text{CH}_2$ ), 28.3 ( $\text{CH}_2$ ), 25.4 ( $\text{CH}_2$ ), 23.0 ( $\text{CH}_2$ ), 22.7 ( $\text{CH}_2$ ), 22.3 ( $\text{CH}_2$ ), 14.2 ( $\text{CH}_3$ ); HRMS (ESI)  $m/z$  303.1394 ( $[\text{M}+\text{H}]^+$   $\text{C}_{21}\text{H}_{30}\text{N}_3$ , requires 324.2443).

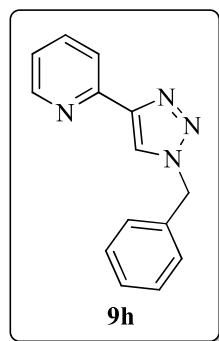


#### 4-(Cyclohex-1-en-1-yl)-1-(2-(cyclohex-1-en-1-yl)ethyl)-1H-1,2,3-triazole (9f)

Yellow low melting solid; Yield: 85%;  $^1\text{H}$  NMR (500 MHz,  $\text{CDCl}_3$ ):  $\delta$  7.31 (s, 1H), 6.48 – 6.45 (m, 1H), 5.38 (s, 1H), 4.37 (t, 2H,  $J = 7.5$  Hz), 2.46 (t, 2H,  $J = 7.5$  Hz), 2.36 – 2.33 (m, 2H), 2.2 – 2.14 (m, 2H), 1.94 – 1.90 (m, 4H), 1.76 – 1.71 (m, 2H), 1.67 – 1.62 (m, 2H), 1.62 – 1.58 (m, 2H), 1.53 – 1.49 (m, 2H);  $^{13}\text{C}$  NMR (125 MHz,  $\text{CDCl}_3$ ):  $\delta$  149.5 (C), 133.2 (C), 127.5 (C), 125.0 (CH), 124.9 (CH), 118.4 (CH), 49.0 ( $\text{CH}_2$ ), 38.9 ( $\text{CH}_2$ ), 28.3 ( $\text{CH}_2$ ), 26.6 ( $\text{CH}_2$ ), 25.5 ( $\text{CH}_2$ ), 25.4 ( $\text{CH}_2$ ), 23.0 ( $\text{CH}_2$ ), 22.7 ( $\text{CH}_2$ ), 22.4 ( $\text{CH}_2$ ), 22.4 ( $\text{CH}_2$ ); HRMS (ESI)  $m/z$  258.1966 ( $[\text{M}+\text{H}]^+$   $\text{C}_{16}\text{H}_{24}\text{N}_3$ , requires 258.1970).

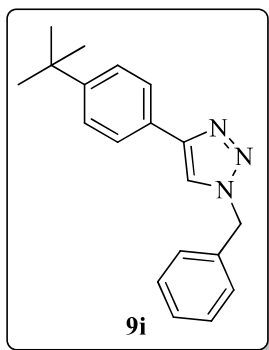
**2-(1-(2-(Cyclohex-1-en-1-yl)ethyl)-1H-1,2,3-triazol-4-yl)pyridine (9g)**

Brown low melting solid; Yield: 88%;  $^1\text{H}$  NMR (500 MHz,  $\text{CDCl}_3$ ):  $\delta$  8.50 (d, 1H,  $J = 4.0$  Hz), 8.11 (d, 1H,  $J = 8.0$  Hz), 8.05 (s, 1H), 7.73 – 7.69 (m, 1H), 7.18 – 7.13 (m, 1H), 5.37 (s, 1H), 4.42 (t, 2H,  $J = 7.5$  Hz), 2.49 (t, 2H,  $J = 7.5$  Hz), 1.91 – 1.86 (m, 4H), 1.59 – 1.53 (m, 2H), 1.50 – 1.44 (m, 2H);  $^{13}\text{C}$  NMR (125 MHz,  $\text{CDCl}_3$ ):  $\delta$  150.3 (C), 149.2 (CH), 148.0 (C), 136.8 (CH), 132.7 (C), 124.7 (CH), 122.7 (CH), 121.8 (CH), 120.1 (CH), 48.9 ( $\text{CH}_2$ ), 38.5 ( $\text{CH}_2$ ), 27.9 ( $\text{CH}_2$ ), 25.0 ( $\text{CH}_2$ ), 22.6 ( $\text{CH}_2$ ), 22.0 ( $\text{CH}_2$ ); HRMS (ESI)  $m/z$  255.1609 ( $[\text{M}+\text{H}]^+$   $\text{C}_{15}\text{H}_{19}\text{N}_4$ , requires 255.1610).

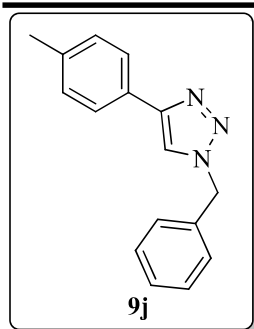


**2-(1-Benzyl-1*H*-1,2,3-triazol-4-yl)pyridine (9h)**

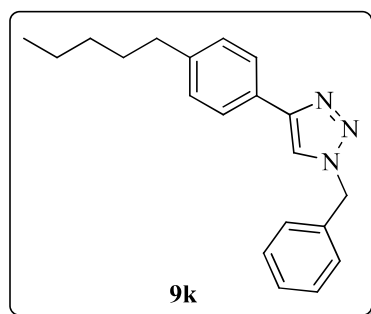
Brown solid; Mp: 110-111 °C (Lit.<sup>52f</sup> 114-115 °C); Yield: 90%. <sup>1</sup>H NMR (500 MHz, CDCl<sub>3</sub>): δ 8.43 (d, 1H, *J* = 4.0 Hz), 8.08 (d, 1H, *J* = 8.0 Hz), 7.99 (s, 1H), 7.70 – 7.64 (m, 1H), 7.30 – 7.25 (m, 3H), 7.25 – 7.22 (m, 2H), 7.14 – 7.09 (m, 1H), 5.49 (s, 2H); <sup>13</sup>C NMR (125 MHz, CDCl<sub>3</sub>): δ 150.4 (C), 149.5 (CH), 148.9 (C), 137.3 (CH), 134.5 (C), 129.4 (CH), 129.1 (CH), 128.5 (CH), 123.1 (CH), 122.1 (CH), 120.5 (CH), 54.6 (CH<sub>2</sub>); HRMS (ESI) *m/z* 273.1137 ([*M*+*H*]<sup>+</sup> C<sub>14</sub>H<sub>13</sub>N<sub>4</sub>, requires 237.1140).

**1-Benzyl-4-(4-(*tert*-butyl)phenyl)-1*H*-1,2,3-triazole (9i)**

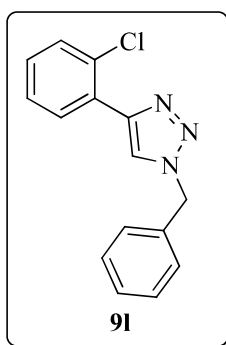
Yellow low melting solid; Yield: 88%; <sup>1</sup>H NMR (500 MHz, CDCl<sub>3</sub>): δ 7.74 (d, 2H, *J* = 8.5 Hz), 7.65 (s, 1H), 7.44 (d, 2H, *J* = 8.5 Hz), 7.41 – 7.37 (m, 3H), 7.33 – 7.29 (m, 2H), 5.59 (s, 2H), 1.34 (s, 9H); <sup>13</sup>C NMR (125 MHz, CDCl<sub>3</sub>): δ 151.5 (C), 148.4 (C), 135.0 (C), 129.3 (CH), 128.9 (CH), 128.2 (CH), 127.9 (C), 125.9 (CH), 125.6 (CH), 119.4 (CH), 54.5 (CH<sub>2</sub>), 34.9 (C), 31.5 (CH<sub>3</sub>); HRMS (ESI) *m/z* 292.1809 ([*M*+*H*]<sup>+</sup> C<sub>19</sub>H<sub>22</sub>N<sub>3</sub>, requires 292.1814).

**1-Benzyl-4-(*p*-tolyl)-1*H*-1,2,3-triazole (9j)**

Yellow solid; Mp: 147-148 °C (Lit.<sup>52g</sup> 151-153 °C); Yield: 91%; <sup>1</sup>H NMR (500 MHz, CDCl<sub>3</sub>): δ 7.66 (d, 2H, *J* = 8.5 Hz), 7.60 (s, 1H), 7.38 – 7.32 (m, 3H), 7.31 – 7.27 (m, 2H), 7.18 (d, 2H, *J* = 8.5 Hz), 5.55 (s, 2H), 2.34 (s, 3H); <sup>13</sup>C NMR (125 MHz, CDCl<sub>3</sub>): δ 148.5 (C), 138.2 (C), 134.9 (C), 129.7 (CH), 129.4 (CH), 129.0 (CH), 128.3 (CH), 127.8 (C), 125.8 (CH), 119.3 (CH), 54.4 (CH<sub>2</sub>), 21.5 (CH<sub>3</sub>); HRMS (ESI) *m/z* 250.1343 ([*M*+*H*]<sup>+</sup> C<sub>16</sub>H<sub>16</sub>N<sub>3</sub>, requires 250.1344).

**1-Benzyl-4-(4-pentylphenyl)-1*H*-1,2,3-triazole (9k)**

White solid; Mp: 82-83 °C; Yield: 91%;  $^1\text{H}$  NMR (500 MHz,  $\text{CDCl}_3$ ):  $\delta$  7.68 (d, 2H,  $J = 8.0$  Hz), 7.60 (s, 1H), 7.38 – 7.34 (m, 3H), 7.30 – 7.26 (m, 2H), 7.19 (d, 2H,  $J = 8.0$  Hz), 5.55 (s, 2H), 2.58 (t, 2H,  $J = 7.5$  Hz), 1.63 – 1.55 (m, 2H), 1.32 – 1.27 (m, 4H), 0.86 (t, 3H,  $J = 7.5$  Hz);  $^{13}\text{C}$  NMR (125 MHz,  $\text{CDCl}_3$ ):  $\delta$  143.3 (C), 134.9 (C), 131.0 (C), 129.3 (CH), 129.0 (CH), 128.9 (CH), 128.2 (CH), 128.1 (CH), 125.8 (CH), 119.4 (C), 54.4 ( $\text{CH}_2$ ), 35.89 ( $\text{CH}_2$ ), 31.6 ( $\text{CH}_2$ ), 31.2 ( $\text{CH}_2$ ), 22.7 ( $\text{CH}_2$ ), 14.2 ( $\text{CH}_3$ ); HRMS (ESI)  $m/z$  306.1968 ( $[\text{M}+\text{H}]^+$   $\text{C}_{20}\text{H}_{24}\text{N}_3$ , requires 306.1970).



### 1-Benzyl-4-(2-chlorophenyl)-1H-1,2,3-triazole (91)

White solid; Mp: 71-72 °C (Lit.<sup>52h</sup> 75-77 °C); Yield: 86%;  $^1\text{H}$  NMR (500 MHz,  $\text{CDCl}_3$ ):  $\delta$  8.17 (dd, 1H,  $J = 2.0, 6.0$  Hz), 8.05 (s, 1H), 7.37 – 7.27 (m, 6H), 7.26 – 7.23 (m, 2H), 5.54 (s, 2H);  $^{13}\text{C}$  NMR (125 MHz,  $\text{CDCl}_3$ ):  $\delta$  143.4 (C), 133.6 (C), 129.9 (d, C,  $J = 40.0$  Hz), 129.1 (CH), 128.8 (CH), 128.1 (CH), 128.0 (CH), 127.7 (CH), 127.6 (d, C,  $J = 11.25$  Hz), 126.9 (CH), 126.1 (CH), 122.2 (CH), 53.2 ( $\text{CH}_2$ ); HRMS (ESI)  $m/z$  270.0800 ( $[\text{M}+\text{H}]^+$   $\text{C}_{15}\text{H}_{13}\text{ClN}_3$ , requires 270.0798).

---

**4.6 References**

1. (a) L. Liang and D. Astruc, *Coord. Chem. Rev.* 2011, **255**, 2933; (b) S. K. Mamidyala and M. G. Finn, *Chem. Soc. Rev.* 2010, **39**, 1252; (c) J. E. Hein and V. V. Fokin, *Chem. Soc. Rev.* 2010, **39**, 1302; (d) M. Meldal and C. W. Tornøe, *Chem. Rev.* 2008, **108**, 2952; (e) J. E. Moses and A. D. Moorhouse, *Chem. Soc. Rev.* 2007, **36**, 1249; (f) P. L. Golas and K. Matyjaszewski, *Chem. Soc. Rev.* 2010, **39**, 1338.
2. (a) R. Huisgen, *Angew. Chem., Int. Ed.* 1963, **2**, 633; (b) V. V. Rostovtsev, L. G. Green, V. V. Fokin and K. B. Sharpless, *Angew. Chem. Int. Ed.* 2002, **41**, 2596; (c) L. V. Lee, M. L. Mitchell, S. J. Huang, V. V. Fokin, K. B. Sharpless and C. H. Wong, *J. Am. Chem. Soc.* 2003, **125**, 9588; (d) C. W. Tornøe, C. Christensen and M. Meldal, *J. Org. Chem.* 2002, **67**, 3057.
3. F. R. Benson and W. L. Savell, *Chem. Rev.* 1950, **46**, 1.
4. (a) H. C. Kolb, M. G. Finn and K. B. Sharpless, *Angew. Chem. Int. Ed.* 2001, **40**, 2004; (b) H. C. Kolb and K. B. Sharpless, *Drug Discov. Today* 2003, **8**, 1128.
5. (a) B. F. Abdel-Wahab, H. A. Mohamed and G. E. A. Awad, *Eur. Chem. Bull.* 2015, **4**, 106; (b) I. Fichtali, M. Chraibi, F. E. Aroussi, A. Ben-Tama, E. M. E. Hadrami, K. F. Benbrahim and S. E. Stiriba, *Der. Pharma. Chem.* 2016, **8**, 236; (c) M. Nahrwold, T. Bogner, S. Eissler, S.

- Verma and N. Sewald, *Org. Lett.* 2010, **12**, 1064; (d) J. Doiron, A. H. Saultan, R. Richard, M. M. Touré, N. Picot, R. Richard, M. Cuperlović-Culf, G. A. Robichaud and M. Touaibia, *Eur. J. Med. Chem.* 2011, **46**, 4010; (e) S. Deswal, Naveen, R. K. Tittal, D. G. Vikas, and A. Kumar, *J. Mol. Struct.* 2020, **1209**, 127982.
6. J. W. Wheless and B. Vazquez, *Epilepsy Curr.* 2010, **10**, 1.
  7. T. Akizawa, M. Taguchi, Y. Matsuda, K. Iekushi, T. Yamada and H. Yamamoto, *BMJ Open* 2019, **9**, 26602.
  8. (a) L. R. Ferreira, A. S. Sousa, L. H. Alvarenga, A. M. Deana, M. E. O. S. de Santi, I. T. Kato, C. R. L. Leal, M. S. Ribeiro and R. A. Prates, *Photodiagn. Photodyn. Ther.* 2016, **15**, 25; (b) S. Sungkanuparph, C. Savetamornkul and W. Pattanapongpaiboon, *Clin. Infect. Dis.* 2017, **64**, 967.
  9. H. Mikamo, X. H. Yin, Y. Hayasaki, Y. Shimamura, K. Uesugi, N. Fukayama, M. Satoh and T. Tamaya, *Chemotherapy* 2002, **48**, 7.
  10. (a) P. Thirumurugan, D. Matosiuk and K. Jozwiak, *Chem. Rev.* 2013, **113**, 4905; (b) S. G. Agalave, S. R. Maujan and V. S. Pore, *Chem. Asian J.* 2011, **6**, 2696.
  11. (a) A. V. Gulevich and V. Gevorgyan, *Angew. Chem. Int. Ed.* 2013, **52**, 1371; (b) M. Jia and S. Ma, *Angew. Chem. Int. Ed.* 2016, **55**, 9134; (c) H.



- 
- M. L. Davies and J. S. Alford, *Chem. Soc. Rev.* 2014, **43**, 5151; (d) B. Chattopadhyay and V. Gevorgyan, *Angew. Chem. Int. Ed.* 2012, **51**, 862.
12. (a) A. Irastorza, J. M. Aizpurua and A. Correa, *Org. Lett.* 2016, **18**, 1080; (b) Q. Gu, H. H. A. Mamari, K. Graczyk, E. Diers and L. Ackermann, *Angew. Chem. Int. Ed.* 2014, **53**, 3868; (c) Z. Wang, Q. Tian, X. Yu and C. Kuang, *Adv. Synth. Catal.* 2014, **356**, 961; (d) S. Shi and C. Kuang, *J. Org. Chem.* 2014, **79**, 6105; (e) X. Ye, Z. He, T. Ahmed, K. Weise, N. G. Akhmedov, J. L. Petersen and X. Shi, *Chem. Sci.* 2013, **4**, 3712.
13. (a) H. Duan, S. Sengupta, J. L. Petersen, N. G. Akhmedov and X. Shi, *J. Am. Chem. Soc.* 2009, **131**, 12100; (b) S. Jabeen, R. A. Khera, J. Iqbal, M. Asgher, *J. Mol. Struct.* 2020, **1206**, 127753.
14. (a) L. Liang and D. Astruc, *Coord. Chem. Rev.* 2011, **255**, 2933; (b) J. E. Hein and V. V. Fokin, *Chem. Soc. Rev.* 2010, **39**, 1302; (c) M. Meldal and C. W. Tornøe, *Chem. Rev.* 2008, **108**, 2952; (d) P. Wu and V. V. Fokin, *Aldrichimica Acta*, 2007, **40**, 7; (e) J. L. Mascarenas, P. Destito, J. R. Couceiro, H. Faustin and F. López, *Angew. Chem. Int. Ed.* 2017, **56**, 10766; (f) J. R. Johansson, T. Beke-Somfai, A. S. Stalsmeden and N. Kann, *Chem. Rev.* 2016, **116**, 14726 (g) J. McNulty and K. Keskar, *Eur. J. Org. Chem.* 2012, **28**, 5462; (h) J. McNulty, K. Keskar and R. Vemula, *Chem. Eur. J.* 2011, **17**, 14727; (i) S. Ding, G. Jia and J. Sun, *Angew. Chem. Int. Ed.* 2014, **53**, 1877; (j) E. Rasolofonjatovo, S.
-

- Theeramunkong, A. Bouriaud, S. Kolodych, M. Chaumontet and F. Taran, *Org. Lett.* 2013, **15**, 4698.
15. (a) E. F. V. Scriven and K. Turnbull, *Chem. Rev.* 1988, **88**, 297; (b) S. Bräse, C. Gil, K. Knepper and V. Zimmermann, *Angew. Chem. Int. Ed.* 2005, **44**, 5188.
16. (a) E. Y. Yoo, M. Ahlquist, S. H. Kim, I. Bae, V. V. Fokin, K. B. Sharpless and S. Chang, *Angew. Chem. Int. Ed.* 2007, **46**, 1730; (b) J. Raushel and V. V. Fokin, *Org. Lett.* 2010, **12**, 4952; (c) D. B. Ramachary, K. Ramakumar and V. V. Narayana, *Chem. Eur. J.* 2008, **14**, 9143; (d) D. Amantini, F. O. Fringuelli, Piermatti, F. Pizzo, E. Zunino and L. Vaccaro, *J. Org. Chem.* 2005, **70**, 6526; (e) J. Barluenga, C. Valdés, G. Beltrán, M. Escribano and F. Aznar, *Angew. Chem. Int. Ed.* 2006, **45**, 6893; (f) X. -J. Quan, Z. -H. Ren, Y. -Y. Wang and Z. -H. Guan, *Org. Lett.* 2014, **16**, 5728.
17. (a) D. B. Ramachary, G. S. Reddy, S. Peraka and J. Gujral, *ChemCatChem* 2017, **9**, 263; (b) J. Thomas, S. Jana, S. Liekens and W. Dehaen, *Chem. Commun.* 2016, **52**, 9236; (c) D. B. Ramachary, P. M. Krishna, J. Gujral and G. S. Reddy, *Chem. Eur. J.* 2015, **21**, 16775; (d) D. B. Ramachary, A. B. Shashank and S. Karthik, *Angew. Chem. Int. Ed.* 2014, **53**, 10420; (e) W. Li, Z. Du, J. Huang, Q. Jia, K. Zhang and J. Wang, *Green Chem.* 2014, **16**, 3003; (f) L. Wang, S. Peng, L. J. Danence,
-

- Y. Gao and J. Wang, *Chem. Eur. J.* 2012, **18**, 6088; (g) M. Belkheira, D. E. Abed, J. -M. Pons and C. Bressy, *Chem. Eur. J.* 2011, **17**, 12917; (h) L. J. T. Danence, Y. Gao, M. Li, Y. Huang and J. Wang, *Chem. Eur. J.* 2011, **17**, 3584.
18. (a) P. Appukkuttan, W. Dehaen, V. V. Fokin and E. Van der Eycken, *Org. Lett.* 2004, **6**, 4223; (b) H. Sharghi, R. Khalifeh and M. M. Doroodmand, *Adv. Synth. Catal.* 2009, **351**, 207; (c) M. Tavassoli, A. Landarani-Isfahani, M. Moghadam, S. Tangestaninejad, V. Mirkhani and I. Mohammadpoor-Baltork, *ACS Sustainable Chem. Eng.* 2016, **4**, 1454; (d) J. R. Johansson, P. Lincoln, B. Nordén and N. Kann, *J. Org. Chem.* 2011, **76**, 2355; (e) Z. Chen, Z. Liu, G. Cao, H. Li and H. Rena, *Adv. Synth. Catal.* 2017, **359**, 202; (f) F. Wei, W. Wang, Y. Ma, C. -H. Tunga and Z. Xu, *Chem. Commun.* 2016, **52**, 14188; (g) S. Hassan and T. J. J. Müller, *Adv. Synth. Catal.* 2015, **357**, 617; (h) W. Li, Q. Jia, Z. Du and J. Wang, *Chem. Commun.* 2013, **49**, 10187; (i) Y. Chen, G. Nie, Q. Zhang, S. Ma, H. Li and Q. Hu, *Org. Lett.* 2015, **17**, 1118; (j) W. Li, Z. Du, K. Zhang and J. Wang, *Green Chem.* 2015, **17**, 781; (k) W. Li and J. Wang, *Angew. Chem. Int. Ed.* 2014, **53**, 14186; (l) D. Janreddy, V. Kavala, C. W. Kuo, C. W. Chen, C. Ramesh, T. Kotipalli, T. S. Kuo, M. L. Chen, C. H. He and C. F. Yao, *Adv. Synth. Catal.* 2013, **355**, 2918.
19. W. Regitz, *Angew. Chem. Int. Ed.* 1967, **6**, 733.

20. (a) T. J. Curphey, *Org. Prep. Proced. Int.* 1981, **13**, 112; (b) E. Tarrant, C. V. O'Brien and S. G. Collins, *RSC Adv.* 2016, **6**, 31202; (c) J. S. Baum, D. A. Shook, H. M. L. Davies and H. D. Smith, *Synth. Commun.* 1987, **17**, 1709; (d) M. K. Muthyala, S. Choudhary and A. Kumar, *J. Org. Chem.* 2012, **77**, 8787; (e) F. W. B. G. G. Hazen, F. E. Roberts, W. K. Russ, J. J. Seman and S. Staskiewicz, *Org. Synth.* 1996, **73**, 144.
21. (a) S. S. V. Ramasastry, *Angew. Chem. Int. Ed.* 2014, **53**, 14310; (b) W. Li and J. Wang, *Angew. Chem. Int. Ed.* 2014, **53**, 14186; (c) J. Thomas, J. John, N. Parekh and W. Dehaen, *Angew. Chem. Int. Ed.* 2014, **53**, 10155; (d) J. -P. Wan, S. Cao and Y. Liu, *J. Org. Chem.* 2015, **80**, 9028; (e) W. Li, Z. Du, K. Zhang and J. Wang, *Green Chem.* 2015, **17**, 781; (f) H. -W. Bai, Z. -J. Cai, S. -Y. Wang and S. -J. Ji, *Org. Lett.* 2015, **17**, 2898; (g) Q. Hu, Y. Liu, X. Deng, Y. Li and Y. Chen, *Adv. Synth. Catal.* 2016, **358**, 1689; (h) N. J. Agard, J. A. Prescher and C. R. Bertozzi, *J. Am. Chem. Soc.* 2004, **126**, 15046; (i) K. Yamamoto, T. Bruun, J. Y. Kim, L. Zhang and M. Lautens, *Org. Lett.* 2016, **18**, 2644; (j) M. K. Barman, A. K. Sinha and S. Nembenna, *Green Chem.* 2016, **18**, 2534; (k) S. Chassaing, V. Benéteau and P. Pale, *Catal. Sci. Technol.* 2016, **6**, 923; (l) S. Hassan, T. J. Muller, *Adv. Synth. Catal.* 2015, **357**, 617; (m) E. Tasca, G. L. Sorella, L. Sporni, G. Strukul and A. Scarso, *Green Chem.* 2015, **17**, 1414; (n) X. Xiong, L. Cai, Y. Jiang and H. Han, *ACS Sustainable Chem. Eng.* 2014,
-

- 2, 765; (o) S. Roy, T. Chatterjee and S. M. Islam, *Green Chem.* 2013, **15**, 2532; (p) S. C. Sau, S. R. Roy, T. K. Sen, D. Mullangi and S. K. Mandal, *Adv. Synth. Catal.* 2013, **355**, 2982; (q) T. Song, L. Li, W. Zhou, Z. -J. Zhang, Y. Deng, Z. Xu and L. -W. Xu, *Chem. Eur. J.* 2015, **21**, 554; (r) Z. Chen, Q. Yan, Z. Liu, Y. Xu and Y. Zhang, *Angew. Chem. Int. Ed.* 2013, **52**, 13324; (s) Y. -J. Li, X. Li, S. -X. Zhang, Y. -L. Zhao and Q. Liu, *Chem. Commun.* 2015, **51**, 11564; (t) S. Ahamad, R. Kant and K. Mohanan, *Org. Lett.* 2016, **18**, 280; (u) J. -P. Wan, D. Hu, Y. Liu and S. Sheng, *ChemCatChem* 2015, **7**, 901.
22. J.-P. Wan, S. Cao, and Y. Liu, *Org. Lett.* 2016, **18**, 6034.
23. W. Wang, Y. Lin, Y. Ma, C. -H. Tung and Z. Xu, *Org. Lett.* 2018, **20**, 2956.
24. A. Fazeli, H. A. Oskooie, Y. S. Beheshtiha, M. M. Heravi, F. M. Moghaddam and B. K. Foroushani, *Z. Naturforsch.* 2013, **68**, 391.
25. M. Konwar, R. Hazarika, A. A. Ali, M. Chetia, N. D. Khupse, P. J. Saikia and D. Sarma, *Appl. Organomet. Chem.* 2018, **32**, 4425.
26. M. Chetia, P. S. Gehlot, A. Kumar and D. Sarma, *Tetrahedron Lett.* 2018, **59**, 397.
27. D. Dařin, G. Kantin and M. Krasavin, *Chem. Commun.* 2019, **55**, 5239.

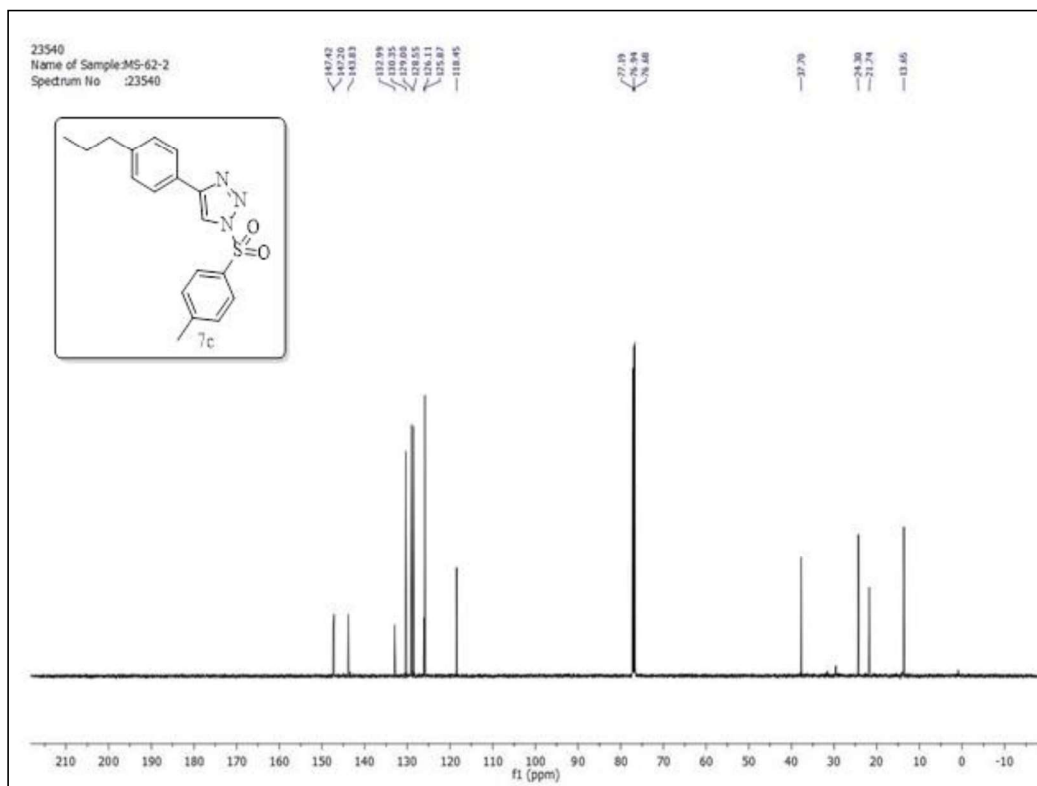
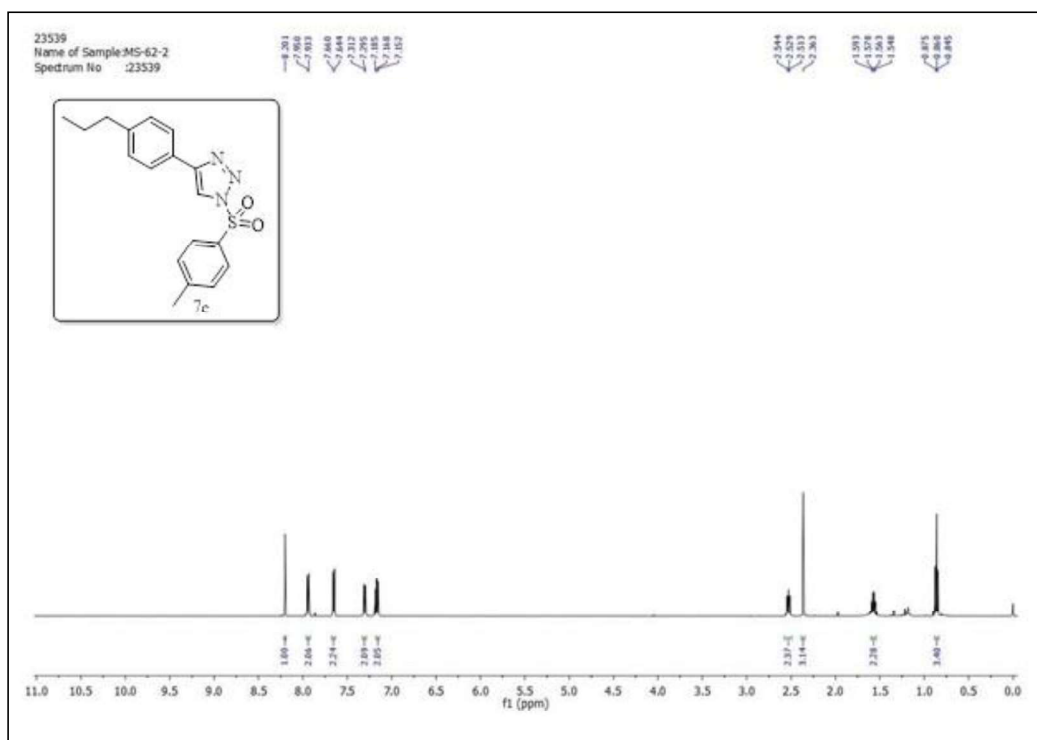
28. G. O. Resende, S. F. Teixeira, I. F. Figueiredo, A. A. Godoy, D. J. F. Lougon, B. A. Cotrim, and F. C. de Souza, *Int. J. Electrochem.* 2019, **67**, 59478.
29. A. Tripathi, C. V. Rode, J. Llop, S. P. Chavan and S. M. Joshi, *Tetrahedron Lett.* 2020, **61**, 151662.
30. N. Asemanipoor, M. Mohammadi-Khanaposhtani, S. Moradi, M. Vahidi, M. Asadi, M. A. Faramarzi, M. Mahdavi, M. Biglar, B. Larijani, H. Hamedifar, M. H. Hajimiri, *Bioorg. Chem.* 2020, **95**, 103482.
31. N. T. Pokhodylo, M. A. Tupyshak and V. A. Palchykov, *Synth. Commun.* 2020, **50**, 1835.
32. A. D. Nino, V. Algieri, M. A. Tallarida, P. Constanzo, M. Pedrón, T. Tejero, P. Merino and L. Maiuolo, *Eur. J. Org. Chem.* 2019, **33**, 5725.
33. G. C. Sahu, A. Garg, T. Majozi and S. Bandyopadhyay, *Ind. Eng. Chem. Res.* 2013, **52**, 5161.
34. (a) D. W. O'Connell, C. Birkinshaw and T. F. O'Dwyer, *Bioresour. Technol.* 2008, **99**, 6709; (b) F. Podczeck, P. E. Knight and J. M. Newton, *Int. J. Pharm.* 2008, **350**, 145.
35. M. U. Dural, L. Cavas, S. K. Papageorgiou and F. K. Katsaros, *Chem. Eng. J.* 2011, **168**, 77; (b) D. W. O'Connell, C. Birkinshaw and T. F. O'Dwyer, *Bioresour. Technol.* 2008, **99**, 6709.

36. B. S. Kuarm, J. V. Madhav, S. V. Laxmi, B. Rajitha, Y. T. Reddy, P. N. Reddy and P. A. Crooks, *Synth. Commun.* 2011, **41**, 1719.
37. A. Shaabani, A. Rahmati and Z. Badri, *Catal. Commun.* 2008, **9**, 13.
38. J. V. Madhav, Y. T. Reddy, P. N. Reddy, M. N. Reddy, S. Kuarm, Peter. A. Crooks and B. Rajitha, *J. Mol. Catal. A- Chem.* 2009, **304**, 85.
39. B. Sadeghi, A. Moradgholi and E. Akbarzadeh, *Bulg. Chem. Commun.* 2018, **50**, 63.
40. M. A. Nasser, M. Salimi and A. A. Esmaili, *RSC Adv.* 2014, **4**, 61193.
41. L. Bahsis, H. B. E. Ayouchia, H. Anane, K. Benhamou, H. Kaddami, M. Julve, S.-E. Stiriba, *Int. J. Biol. Macromol.* 2018, **119**, 849.
42. P. V. Chavan, U. V. Desai, P. P. Wadgaonkar, S. R. Tapase, K. M. Kodam, A. Choudhari and D. Sarkar, *Bioorg. Chem.* 2019, **85**, 475.
43. S. M. Sarkar and M. L. Rahman, *J. Clean. Prod.* 2017, **141**, 683.
44. W. Yu, L. Jiang, C. Shen, W. Xu and P. Zhang, *Catal. Commun.* 2016, **79**, 11.
45. S. C. Azimi, *Iran. J. Catal.* 2014, **4**, 113.
46. M. Goswami and A. M. Das, *Carbohydr. Polym.* 2019, **206**, 863.
47. Z. N. Siddiqui and T. Khan, *J. Braz. Chem. Soc.* 2014, **25**, 1002.
48. S. Haider, T. Kamal, S. B. Khan, M. Omer, A. Haider, F. U. Khan and A. M. Asiri, *Appl. Surf. Sci.* 2016, **387**, 1154.

49. X. Wu, Z. Shi, S. Fu, J. Chen, R. M. Berry and K. C. Tam, *ACS Sustain. Chem. Eng.* 2016, **4**, 5929.
50. T. Tsoncheva, G. Issa, T. Blasco, M. Dimitrov, M. Popova, S. Hernandez, D. Kovacheva, G. Atanasova and J. M. L. Nieto, *Appl. Catal. A-Gen.* 2013, **453**, 1.
51. (a) H. B. E. Ayouchia, H E. Mouli, L. Bahsis, H. Anane, R. Laamari, C. J. Gomez-García, M. Julve and S.-E. Stiriba, *J. Organomet. Chem.* 2019, **898**, 120881; (b) M. Y. Stevens, R. T. Sawant and L. R. Odell, *J. Org. Chem.* 2014, **79**, 4826.
52. (a) E. J. Yoo, M. Ahlquist, S. H. Kim, I. Bae, V. V. Fokin, K. B. Sharpless and S. Chang, *Angew. Chem. Int. Ed.* 2007, **46**, 1730; (b) K. Wang, X. Bi, S. Xing, P. Liao, Z. Fang, X. Meng, Q. Zhang, Q. Liu and Y. Ji, *Green Chem.* 2011, **13**, 562; (c) Y. Liu, X. Wang, J. Xu, Q. Zhang, Y. Zhao and Y. Hu, *Tetrahedron* 2011, **67**, 6294; (d) Z. -X. Wang and Z. -G. Zhao, *J. Heterocyclic Chem.* 2007, **44**, 89; (e) C. Shao, X. Wang, J. Xu, J. Zhao, Q. Zhang and Y. Hu, *J. Org. Chem.* 2010, **75**, 7002; (f) D. Wang, N. Li, M. Zhao, W. Shi, C. Ma and B. Chen, *Green Chem.* 2010, **12**, 2120; (g) X. Meng, X. Xu, T. Gao and B. Chen, *Eur. J. Org. Chem.* 2010, **28**, 5409; (h) J. R. Suárez, B. Trastoy, M. E. Pérez-Ojeda, R. Marín-Barrios and J. L. Chiara, *Adv. Synth. Catal.* 2010, **352**, 2515.



4.7 NMR spectra of selected compounds





# **Chapter 5**

## **Conclusion and Future scope**

---

## 5. Conclusion and future scope

### 5.1 Conclusion

In summary, the thesis describes the preparation of three different silica and cellulose supported copper and iron nanoparticles by using simple synthetic procedure followed by their characterization using sophisticated analytical and spectroscopic techniques like, XRD, HRTEM, FT-IR, BET, TGA and XPS. The catalytic activities of the prepared materials were then studied in various important organic reactions which led to the synthesis of dihydroquinazolines, 5-hydroxymethylfurfural, chromenones, and 1,2,3-triazoles. Additionally, a few of the synthesized compounds were evaluated for their potential antibacterial property. All the catalyst could be reused up to 5-8 consecutive catalytic cycles without any significant loss in the activity. The reactions were performed under comparatively mild condition and the prepared compounds were duly characterized with the help of NMR and Mass spectral data. A brief summary of the work and general conclusion from the work are presented below.

**Chapter 1:** This chapter describes an overview of the basic idea behind the development of heterogeneous nanosized acidic catalysts. Detailed literature reports on the preparation procedures as well as the application of these solid acidic catalysts in different fields are discussed. The role of various supports used in the preparation

and exhibition of catalytic behavior of acid catalysts has also been described. Finally the objective of the thesis is outlined briefly.

**Chapter 2:** This chapter describes the preparation of a copper oxide nanoparticle supported on silica using a simple reduction precipitation method. The prepared material was extensively characterized using XRD, HRTEM, FT-IR, BET and XPS. The catalytic activity of the prepared material was studied in a three-component reaction between 2-aminobenzophenone, aromatic aldehyde and ammonium hydroxide leading to the formation of 1,2-dihydroquinazoline at room temperature. The synthesized 1,2-dihydroquinazolines were screened for their possible antibacterial activity against three different bacterial strains namely, *Mycobacterium abscessus*, *Escheria fergusonil*, and *Staphylococcus aureus*. In a different experiment, the activity of the catalyst was studied towards the conversion of carbohydrates such as fructose, glucose, sucrose, cellulose etc. into 5-hydroxymethylfurfural (HMF). The recyclability of the catalyst has also been studied. Mechanism of both the reaction has been discussed.

**Chapter 3:** In this chapter, magnetically active silica was prepared by encapsulating magnetic iron oxide on silica. The prepared material was characterized by different analytical tools such as XRD, FT-IR, HRTEM, XPS, BET and TGA. The magnetic property of the catalyst was studied using Vibrating Sample Magnetometer. The material was found to act as a solid acid catalyst for a three component domino-Knoevenagel-hetero-Diels-Alder (DKHDA) reaction between 1,3-cyclohexanedione,

benzaldehyde/ketone and alkene/alkyne under solvent-free condition. The reaction produced a series of chromenone/dihydrochromenone/spirochromenone derivatives. It was also observed that the catalyst could be reused upto five catalytic cycles without any significant loss in activity.

**Chapter 4:** This chapter describes the preparation of a cellulose sulfuric acid supported copper catalyst and its characterization using analytical techniques such as XRD, FT-IR, HRTEM and BET. The applicability of the catalyst was studied towards azide-alkyne click reaction at room temperature leading to the formation of 1,2,3-triazoles. A similar reaction of tosyl azide with an alkyne in the presence of a primary amine was also studied which resulted in one-pot diazo-transfer-click reaction leading to *N*-substituted 1,2,3-triazoles. Substituent scope for both the reaction was studied. Based on earlier reports, mechanism of both the reactions was discussed. The catalyst could be recycled upto six times without any loss of activity. Physical characteristics of the recycled catalyst were also studied.

## **5.2 Future Scope**

There are high scopes for the development and expansion in the field of nanosized solid acid catalysts, particularly, control over their size, acidity and selectivity in reactions. The nanosized solid acid catalysts possess the combinatorial advantages of both solid acids and nanoparticles. Some of the future scopes of the investigations are highlighted below.

- We have developed simple and efficient methods for the preparation of three different heterogeneous acidic catalysts. The supports used are thermally very stable and possess large surface area. However, alternative natural sources can also be used as supports. Also, the process for the preparation of the nanoparticles can be used for the preparation of other more advanced nanoparticles especially, multi-metallic one with broad spectrum application.
- Due to the simple preparation methodologies, environmental friendliness, high thermal stability and good recyclability, the prepared catalysts can find widespread applications in chemical and pharmaceutical industries as well as in greener organic transformations.

# **Appendix I**

## **List of Publications**



---

## List of Publications

### A. Papers published in journals:

1. Magnetically recoverable silica catalysed solvent-free domino Knoevenagel-hetero-Diels-Alder reaction to access divergent chromenones; **Mrinaly Suri**, Farhaz Liaquat Hussain, Chinu Gogoi, Pankaj Das, Pallab Pahari; *Organic & Biomolecular Chemistry*, 2020, 18, 2058-2062.
  2. A mild aerobic oxidation of benzyl alcohols and oxidative decarboxylation of phenyl acetic acids by cellulose-supported Ag-Ag<sub>2</sub>S nanoparticles; Farhaz Liaquat Hussain, **Mrinaly Suri**, Ashutosh Namdeo, Geetika Borah, Dipanka Dutta, Tridip Goswami, Pallab Pahari; *Catalysis Communication*, 2019, 124, 76-80.
  3. Biological approach for the production of vanillin from lignocellulosic biomass (*Bambusa tulda*); Kumar Harshvardhan, **Mrinaly Suri**, Amrit Goswami, Tridip Goswami; *Journal of Cleaner Production*, 2017, 149, 485-490.
  4. Bi (NO<sub>3</sub>)<sub>3</sub>·5H<sub>2</sub>O and cellulose mediated Cu-NPs - A highly efficient and novel catalytic system for aerobic oxidation of alcohols to carbonyls and synthesis of DFF from HMF; Diganta Baruah, Farhaz L. Hussain, **Mrinaly Suri**, Ujwal Pratim
-

---

Saikia, Pinaki Sengupta, Dipak K. Dutta, Dilip Konwar; *Catalysis Communications*, 2016, 77, 9–12.

5. Selective N-acetylation of aromatic amines using acetonitrile as acylating agent; Ujwal Pratim Saikia, Farhaz L. Hussain, **Mrinaly Suri**, Pallab Pahari; *Tetrahedron Letters*, 2016, 57, 1158–1160.

---

---

**B. Research Paper/Poster Presented in the Seminar/Symposium**

1. Presented a poster entitled '*A domino-Knoevenagel-hetero-Diels-Alder reaction using  $Fe_3O_4@SiO_2$  nanoparticle as an efficient and magnetically recoverable catalyst*' at International Conference on Engineering Sciences & Technologies for Environmental Care (ESTEC-2020) organized by CSIR-North-East Institute of Science and Technology Jorhat on 20-22<sup>nd</sup> February, 2020.
  2. Presented a poster entitled '*Development of silica supported iron oxide nanoparticle and its application towards the synthesis of chromen-5-one derivatives*' at 25<sup>th</sup> CRSI National Symposium in Chemistry (CRSI-2019) organized by IIT, Kanpur on 19-21<sup>st</sup> July, 2019.
  3. Presented a poster entitled '*A Green Protocol for The Development of Cellulose Supported Copper Catalyst and Its Application Towards The Synthesis of 1,2,3-triazole Derivatives*' at International Conference on Emerging Trends in Chemical Sciences (ETCS-2018) organized by Department of Chemistry, Dibrugarh University on 26-28<sup>th</sup> February, 2018.
  4. Presented a paper entitled '*Microwave assisted one pot dehydration of carbohydrates to HMF catalysed by novel silica supported tin catalyst*' at Departmental annual seminar, Department of Chemistry, Dibrugarh University on 5<sup>th</sup> December, 2017.
  5. Presented a poster entitled '*Development of Silica Based Copper Oxide Catalyst and Its Application towards Synthesis of Quinazoline Derivatives*' at National
-

---

Symposium on Recent Trends in Chemical Sciences (RTCS-2017) organized by Department of Chemistry, National Institute of Technology, Meghalaya, Shillong on 12-13<sup>th</sup> October, 2017.

6. Presented a poster entitled '*Development of Silica Supported Solid Acid Catalyst for the Conversion of Cellulose to HMF*' at National Seminar on Recent Developments in Synthesis and Catalysis (RDSC-2017) organized by Department of Chemistry, Dibrugarh University on 10-11<sup>th</sup> March, 2017.

---

# **Appendix II**

**Reprints of published paper**

**(First page)**



Cite this: *Org. Biomol. Chem.*, 2020, 18, 2058

Received 8th February 2020,  
Accepted 3rd March 2020

DOI: 10.1039/d0ob00284d

rsc.li/obc

## Magnetically recoverable silica catalysed solvent-free domino Knoevenagel-hetero-Diels–Alder reaction to access divergent chromenones†

Mrinaly Suri,<sup>a</sup> Farhaz Liaquat Hussain,<sup>a</sup> Chinu Gogoi,<sup>a</sup> Pankaj Das<sup>b</sup> and Pallab Pahari<sup>id</sup> \*<sup>a,c</sup>

A three-component domino Knoevenagel-hetero-Diels–Alder (DKHDA) reaction between 1,3-dicarbonyl, aldehydes/ketones, and alkenes/alkynes leading to the divergent synthesis of chromenones, dihydrochromenones, and spirocyclic chromenones is reported. The reaction was carried out under solvent-free conditions using a magnetically separable silica ( $\text{Fe}_3\text{O}_4@\text{SiO}_2$ ) catalyst. While two component DKHDA reactions are known, this is the first example of a three component DKHDA reaction involving 1,3-dicarbonyl, ketones, and alkynes producing spirocyclic pyranone derivatives. Twenty-six different highly substituted chromenones were synthesized using this methodology. A wide substrate scope due to the multicomponent nature of the reaction, high atom economy, the use of inexpensive and non-toxic recyclable silica as the catalyst, and solvent free reaction conditions make it an advantageous process. The catalyst was characterized using different analytical techniques such as XRD, IR, HRTEM, VSM, and TGA. Based on the earlier reports a mechanism has also been proposed.

### Introduction

The chromene core is exemplified as a privileged moiety in a variety of natural products such as flavonoids, alkaloids and anthrocyanins and is known to possess fascinating therapeutic properties.<sup>1</sup> For example, calanolide A and B show prominent HIV-1 inhibitory activity (Fig. 1).<sup>2</sup> Ethuliacoumarion A and its derivatives show anticancer, molluscicidal and anthelmintic activities.<sup>3</sup> Ferprenin is a specific inhibitor of the enzyme VKORC1 which is responsible for the recycling of vitamin K, a

vitamin essential for blood clotting,<sup>4</sup> and trigolutes show AChE inhibitory activity.<sup>5</sup> Synthetic chromene derivatives also show antioxidant,<sup>6</sup> anticancer,<sup>7</sup> antimicrobial,<sup>8</sup> and molluscicidal activities.<sup>9</sup>

In recent years, the domino Knoevenagel-hetero-Diels–Alder (DKHDA) reaction has gained immense interest due to its application in the construction of synthetic drugs,<sup>10</sup> natural products<sup>11</sup> and poly-heterocyclic compounds<sup>12</sup> incorporating pyran-based frameworks with high atom economy. Following the pioneering works by Tietze,<sup>12a–c</sup> several methods have been reported in the literature employing the DKHDA strategy leading to the construction of a vast array of highly diverse pyran-fused carbocycles.<sup>13</sup> Although intramolecular or two component DKHDA reactions between various aromatic and aliphatic aldehydes and 1,3-dicarbonyl compounds have been widely reported,<sup>10,13</sup> examples of intermolecular three component reactions involving 1,3-dicarbonyl, aldehydes/ketones, and alkenes/alkynes are comparatively less.<sup>14</sup> Moreover, reactions with non-activated terminal alkynes are limited compared to alkenes. To our knowledge there are no reports on DKHDA reactions involving 1,3-

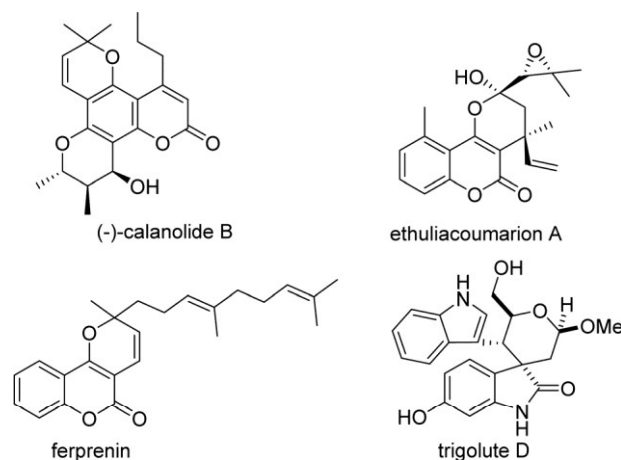


Fig. 1 Biologically active natural products containing chromenones.

<sup>a</sup>Chemical Science and Technology Division, CSIR-North East Institute of Science and Technology, Jorhat-785006, Assam, India. E-mail: ppahari@gmail.com, pallab@neist.res.in

<sup>b</sup>Department of Chemistry, Dibrugarh University, Dibrugarh-786004, Assam, India

<sup>c</sup>Academy of Scientific and Innovative Research, CSIR-NEIST Campus, Jorhat-785006, Assam, India

† Electronic supplementary information (ESI) available: Experimental details, catalyst characterization and spectra of all new products. See DOI: 10.1039/d0ob00284d